

Common Borders. Common Solutions.

**A Scientific Network
for Earthquake, Landslide & Flood Hazard Prevention**



**Pilot Implementation of Seismic Hazard
Assessment at Regional and Local Scales
Deliverable No.: D.03.01, Vol. 1**

**GA3. Earthquake, Landslide and Flood Hazard Assessment: Implementation
at Regional and Local scales, Activities A.3.3 & A.3.6**

**OVERALL RESPONSIBLE for GA.3: Democritus University of Thrace (P.1)
RESPONSIBLE for A.3.3 & A.3.6: P2 (EPPO –ITSAK)
INVOLVED PARTNERS: ALL**



Project funded by the
EUROPEAN UNION



Project Details

Programme

Black Sea JOP

Priority and Measure

Priority 2 (Sharing resources and competencies for environmental protection and conservation), Measure 2.1. (Strengthening the joint knowledge and information base needed to address common challenges in the environmental protection of river and maritime systems)

Objective

Development of a Scientific Network

Project Title

A Scientific Network for Earthquake, Landslide and Flood Hazard Prevention

Project Acronym

SCInet NatHaz

Contract No

MIS-ETC 2614

Lead Partner

TEI OF KENTRIKI MAKEDONIA, GREECE

Total Budget

700.000,00 Euro (€)

Time Frame

Start Date – End Date

01/05/2013 – 30/11/2015

Book Captain:
Contributing
Authors:

K. PAPTAEODOROU (TEI KENTRIKI MAKEDONIA)



Document Release Sheet

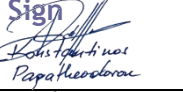
Book captain:	K. PAPTAEODOROU (TEI KENTRIKIS MAKEDONIAS)	Sign 	Date 04.02.2016
Approval	K. PAPTAEODOROU (TEI KENTRIKIS MAKEDONIAS)	Sign 	Date 04.02.2016
Approval	ATTILA ANSAL (KOERI/BOGAZICI UNIVERSI) UNIVERSITY)	Sign  M. Atilla Ansal	Date 04.02.2016
Approval	N. KLIMIS (DEMOCRITUS UNIVERSITY of THRAKI)	Sign  Nikolaos Klimis	Date 04.02.2016
Approval	B. MARGARIS (EPP0/ITS AK)	Sign  Basil N. Margaritis	Date 04.02.2016
Approval	V. NENOV ("ASSEN ZLATAROV" UNIVERSITY)	Sign 	Date 04.02.2016
Approval	L. TOFAN ("OVIDIUS" UNIVERSITY)	Sign 	Date 04.02.2016
Approval	A. SIDORENKO ("Dr. GHITU" INSTITUTE ACAD. of SCIENCES)	Sign 	Date 04.02.2016
Approval	K. STEPANOVA (BSB UEAS)	Sign 	Date 04.02.2016



TABLE OF CONTENTS

1	<u>BACKGROUND OF THE DOCUMENT</u>	13
1.1	GENERAL NOTE	13
1.2	SCOPE AND OBJECTIVES	13
1.3	RELATED DOCUMENTS	13
1.3.1	INPUT	13
1.3.2	OUTPUT	13
2	<u>INTRODUCTION</u>	14
3	<u>SEISMIC HAZARD ASSESSMENT</u>	15
3.1	METHODOLOGY	15
3.1.1	PROBABILISTIC SEISMIC HAZARD ASSESSMENT	18
3.1.2	DETERMINISTIC SEISMIC HAZARD ASSESSMENT	21
4	<u>REGIONAL AND LOCAL SCALE SEISMIC HAZARD APPLICATIONS</u>	22
4.1	GREECE	22
4.1.1	BACKGROUND INFORMATION ON SEISMIC HAZARD MAPS IN GREECE	22
4.1.2	SEISMICITY & SEISMOTECTONICS OF THE AREA.	29
4.1.3	EMPIRICAL PREDICTIVE RELATIONS OF MACROSEISMIC INTENSITIES	34
4.1.4	DISTRIBUTION OF MAXIMUM MACROSEISMIC INTENSITIES IN THE STUDY AREA	41
4.1.5	INFORMATION OF EMPIRICAL PREDICTIVE RELATIONS OF HORIZONTAL PEAK GROUND ACCELERATION	42
4.1.6	REGIONAL SEISMIC HAZARD ASSESSMENT	49
4.1.7	DISTRIBUTION OF MAXIMUM VALUES OF GROUND PARAMETERS	57
4.1.8	COMPARISON FOR SITE SPECIFIC ON STATISTICAL TREATMENT OF OBSERVED INTENSITIES	61
4.1.9	LOCAL SEISMIC HAZARD ASSESSMENT	63
	REFERENCES	71
	APPENDIX 1	77
4.2	TURKEY	83
4.2.1	INTRODUCTION	84
4.2.2	SEISMICITY	85
4.2.3	TECTONICS OF THE REGION	86
4.2.4	TECTONIC SETTING OF THE MARMARA REGION	88
4.2.5	TECTONIC SETTING OF BLACK SEA REGION	90
4.2.6	SEISMIC SOURCE ZONATION	94
4.2.7	SEISMIC SOURCE ZONATION FOR ISTANBUL AND TEKIRDAG (MARMARA REGION)	94
4.2.8	SEISMIC SOURCE ZONATION FOR SAMSUN PROVINCE (TURKEY)	95



Project funded by the
EUROPEAN UNION



4.2.9	METHODOLOGY OF PROBABILISTIC SEISMIC HAZARD ASSESSMENT	96
4.2.10	TIME-DEPENDENT APPROACH USED FOR MARMARA REGION	97
4.2.11	THE TIME-INDEPENDENT (POISSON) APPROACH USED FOR SAMSUN PROVINCE (TURKEY)	99
4.2.12	EARTHQUAKE RECURRENCE MODELS FOR MARMARA REGION	100
4.2.13	EARTHQUAKE RECURRENCE MODEL FOR TURKEY	101
4.2.14	GROUND MOTION PREDICTION EQUATIONS	102
4.2.15	HAZARD MAPS FOR MARMARA REGION	104
4.2.16	HAZARD MAPS FOR THE SAMSUN PROVINCE (TURKEY)	108
	REFERENCES	110
4.3	BULGARIA	115
4.3.1	COUNTRY, PROJECT AREA IN THE COUNTRY	115
4.3.2	SEISMIC ACTIVITY, STRONG EARTHQUAKES NOW AND HISTORIC ONES	115
4.3.3	SEISMIC MONITORING NETWORK	122
4.3.4	PROBABILISTIC SEISMIC HAZARD ASSESSMENT (PSHA)	124
4.3.5	TREATMENT OF UNCERTAINTIES (RANDOM & EPISTEMIC)	127
4.3.6	DE-AGGREGATION OF PSHA	128
4.3.7	PSHA RESULTS FOR ELIGIBLE AREA	129
4.3.8	DE-AGGREGATION OF PROBABILISTIC SEISMIC HAZARD ASSESSMENT FOR BULGARIAN ELIGIBLE AREA (MAIN DISTRICT TOWNS)	132
4.3.9	DETERMINISTIC HAZARD	136
	REFERENCES	140
4.4	UKRAINE	143
4.4.1	SEISMIC HAZARD	143
4.4.2	SEISMIC EVENTS IN ODESSA REGION	146
4.4.3	SEISMIC MICROZONING	149
4.4.4	MAPS OF GENERAL SEISMIC ZONING	157
4.4.5	POTENTIAL LOSSES	164
	REFERENCES	168
4.5	ROMANIA	170
4.5.1	SEISMIC ZONATION	170
4.5.2	THE ASSESSMENT OF SEISMIC HAZARD USING THE PROBABILISTIC APPROACH	184
	REFERENCES	199
4.6	MOLDOVA	201
4.6.1	PAST EVENTS AND THEIR CONSEQUENCES	201
4.6.2	EXISTING LEGISLATION FRAMEWORK	202
	REFERENCES	209
5	CONCLUDING REMARKS	216



LIST OF FIGURES

FIG.1. SEISMIC RISK IS THE OUTPUT OF CONVOLUTION OF SEISMIC HAZARD AND VULNERABILITY. TYPICAL GRAPHS DEPICTING EACH QUANTITY ARE SHOWN. (COBURN AND SPENCE, 2002).	17
FIG.2. FLOW CHART FOR SEISMIC HAZARD ASSESSMENT STUDY BASED ON PROBABILISTIC (LEFT) OR DETERMINISTIC (RIGHT) APPROACH. (REITER, 1990).	18
FIG.3. THE FIRST SEISMIC HAZARD MAP OF GREECE.	23
FIG 4. SEISMIC HAZARD MAP OF GREECE IN THE SEISMIC CODE OF 1992 (PAPAZACHOS ET AL., 1992).	25
FIG 5. HYBRID MODEL OF FAULT AND AREA SOURCES IN THE AEGEAN AND SURROUNDING AREA (PAPAIOANNOU, 2001).	26
FIG 6. THE MAIN FAULTS OF SHALLOW STRONG ($M \geq 6.0$) EARTHQUAKES IN THE AGEGEAN AREAS (PAPAZACHOS ET AL., 2001).	26
FIG 7. SEISMIC SOURCES MODELS OF SHALLOW (BLACK) AND INTERMEDIATED DEPTH (RED) EARTHQUAKES (PAPAZACHOS, 1990).....	27
FIG 8. SEISMIC SOURCES MODELS OF SHALLOW (BLACK) AND INTERMEDIATED DEPTH (RED) EARTHQUAKES (PAPAZACHOS AND PAPAIOANNOU, 1993 REVISED).....	27
FIG 9. COMPARISON OF THE VARIOUS EMPIRICAL PREDICTIVE RELATIONS FOR THE PGA, USED IN THE PRESENT STUDY FOR $M=6.5$ AND SOIL CONDITIONS "ROCK"	28
FIG 10. GEOGRAPHICAL DISTRIBUTION OF THE MEAN VALUES OF THE PEAK GROUND ACCELERATION (CM/SEC ²) IN GREECE AND SURROUNDING AREA	28
FIG 11. GEOGRAPHICAL DISTRIBUTION OF THE STANDARD DEVIATION OF THE PEAK GROUND ACCELERATION VALUES (CM/SEC ²) IN GREECE AND SURROUNDING AREA.....	28
FIG 12. THE OFFICIAL CURRENT SEISMIC HAZARD MAP OF GREECE.....	29
FIG 13. THE MAIN FEATURES OF TECTONIC ORIGIN IN THE BROADER AEGEAN AREA. THE RECTANGULAR SHOWS THE INVESTIGATED AREA.	30
FIG 14. GEOGRAPHICAL DISTRIBUTION OF STRONG EARTHQUAKES WITHIN THE INVESTIGATED AREA. THE FAULTS ARE AFTER PAPAZACHOS ET AL. (2001).	31
FIG 15. GEOGRAPHICAL DISTRIBUTION OF MODERATE-TO-SMALL EARTHQUAKES WITHIN THE INVESTIGATED AREA SHOWN BY A RECTANGULAR. INFORMATION OF THE TIME PERIOD AND SIZE OF THE EVENTS ARE SHOWN IN THE LEGEND.	32
FIG 16. GEOGRAPHICAL DISTRIBUTION THE EPICENTERS OF THE KNOWN EARTHQUAKES AT THE BROADER AREA OF THE INVESTIGATED AREA (SHOWN BY PINK-HACHURED RECTANGULAR). THE BLUE POLYGONS SHOW THE SEISMIC SOURCES PROPOSED BY PAPAIOANNOU AND PAPAZACHOS (2000).	33
FIG 17. A HYBRID MODEL OF AREA-TYPE AND LINE-TYPE (FAULTS) IN THE AREA PAPAIO-ANNOU (2002). THE FAULTS ARE AFTER PAPAZACHOS ET AL. (2001). THE RED LINES REPRESENT NORMAL FAULTS WHILE THE GREY LINEAR SYMBOLS STAND FOR THE STRIKE SLIP FAULTS.	34
FIG 18. COMPARISON BETWEEN VARIOUS ATTENUATION RELATIONS HOLDING FOR DIFFERENT AREAS OF THE WORLD. THE CONTINUOUS BLACK LINE STANDS FOR THE AEGEAN AREA (PAPAZACHOS AND PAPAIOANNOU, 1997).	36
FIG 19. ISOSEISMAL MAP OF THE EARTHQUAKE OF 1752 IN THRACE (PAPAZACHOS ET AL., 1997A).	37
FIG 20. ISOSEISMAL MAP OF THE EARTHQUAKE OF MAY 5, 1829 $M=7.3$ (PAPAZACHOS ET AL., 1997A).	38
FIG 21. ISOSEISMAL MAP OF THE EARTHQUAKE OF AUGUST 9, 1912 $M7.6$ EARTHQUAKE (AMBRASEYS AND FINKEL 1987).	39
FIG 22. ISOSEISMAL MAP OF THE EARTHQUAKE OF APRIL 4, 1904 $M=7.7$ KRESNA MAINSHOCK. (PAPAZACHOS ET AL., 1997A).	39
FIG 23. ISOSEISMAL MAP OF THE EARTHQUAKE OF APRIL 14, 1928 $M=6.8$ PLOVDIV EARTHQUAKE. (PAPAZACHOS ET AL., 1997A).	40
FIG 24. ISOSEISMAL MAP OF THE EARTHQUAKE OF SEPTEMBER 26, 1932 $M=7.0$ IERISSOS EARTHQUAKE. (PAPAZACHOS ET AL., 1997A).....	41



FIG 25. MAP DEPICTING THE GEOGRAPHICAL DISTRIBUTION OF THE MAXIMUM MACRO-SEISMIC INTENSITIES IN THE EXAMINED. THE MAIN FAULTS OF STRONG EARTHQUAKES (PAPAZACHOS ET AL., 2001) IN THE AREA ARE ALSO SHOWN.42

FIG 26. COMPARISON OF THE PGA EMPIRICAL RELATIONS, (11A) (GREY CONTINUOUS LINE) AND (B) (BLACK DASHED LINE) WITH THOSE PROPOSED BY AMBRASEYS ET AL (1996) (GREY DASHED LINE) FOR M=5.5 AND 6.5 AND ROCK SOIL CONDITIONS.44

FIG 27. COMPARISON OF THE PGA EMPIRICAL RELATIONS EQS. (A) (GREY CONTINUOUS LINE) AND (B) (BLACK DASHED LINE) WITH THOSE PROPOSED BY SABETTA AND PUGLIESE (1996), (GREY DASHED LINE) FOR M=5.5 AND 6.5 AND ROCK SOIL CONDITIONS.45

FIG 28. COMPARISON OF THE PGA EMPIRICAL RELATIONS EQS. (A) (GREY CONTINUOUS LINE) AND (B) (BLACK DASHED LINE) WITH THOSE PROPOSED BY SPUDICH ET AL (1993), (GREY DASHED LINE) FOR M=5.5 AND 6.5 AND ROCK SOIL CONDITIONS.45

FIG 29. COMPARISON OF THE PGA EMPIRICAL RELATIONS (BLACK CONTINUOUS LINE), WITH THOSE PROPOSED BY CAMPBELL (1989) (RED DASHED LINE), THEODULIDIS AND PAPAZACHOS (1992) (LIGHT GREEN DASHED) AND SKARLATOUDIS ET AL (2003) (LIGHT BLUE CONTINUOUS LINE) FOR EPICENTRAL DISTANCE R=20 KM.46

FIG 30. GEOGRAPHICAL DISTRIBUTION OF THE NETWORK OF BROADBAND ACCELEROGRAPHS (RED SQUARES) AND STRONG MOTION INSTRUMENTS (OTHER SYMBOLS AS IN LEGEND) WITHIN THE STUDIED AREA. THE CYAN STAR STANDS FOR THE LOCATION OF THE EURO-SEISTEST ARRAY.47

FIG 31. GEOGRAPHICAL DISTRIBUTION OF THE NETWORK OF THE ACCELEROGRAPHS AND STRONG MOTION INSTRUMENTS, EPICENTERS OF EARTHQUAKES WITH M>3.0 AND FAULT PLANE SOLUTIONS OF THE STRONGEST EVENTS (M>5.0) SINCE 2009.49

FIG 32. DISTRIBUTION OF THE PGA VALUES (IN CM/SEC²) USING THE HYBRID MODEL OF FAULTS AND AREA SOURCES (UPPER MAP) AND THE AREA-TYPE MODEL OF SOURCES PAPAIOANNOU AND PAPAZACHOS (2000) (BOTTOM) FOR MEAN RETURN PERIOD OF 476 YEARS.52

FIG. 33. DISTRIBUTION OF THE PGA VALUES (IN CM/SEC²) USING THE HYBRID MODEL OF FAULTS AND AREA SOURCES (UPPER MAP) AND THE AREA-TYPE MODEL OF SOURCES PAPAIOANNOU AND PAPAZACHOS (2000) (BOTTOM) FOR MEAN RETURN PERIOD OF 952 YEARS.53

FIG 34. DISTRIBUTION OF THE MEAN PGA AND STANDARD DEVIATION VALUES FOR TM=476 YEARS.54

FIG 35. DISTRIBUTION OF THE MEAN PGA AND STANDARD DEVIATION VALUES FOR TM=952 YEARS.54

FIG 36. GEOGRAPHICAL DISTRIBUTION OF HORIZONTAL PGA BASED ON MERGING RESULTS PROVIDED BY ALL THE PARTNERS FOR 100 YRS MEAN RETURN PERIOD.55

FIG 37. GEOGRAPHICAL DISTRIBUTION OF HORIZONTAL PGA BASED ON MERGING RESULTS PROVIDED BY ALL THE PARTNERS FOR 100 YRS MEAN RETURN PERIOD.56

FIG 38. DISTRIBUTION OF INTENSITIES AND SEISMIC HAZARD CURVE BASED ON PROBABILISTIC APPROACH OF MCGUIRE AND STATISTICAL TREATMENT OF OBSERVED INTENSITIES.57

FIG 39. GEOGRAPHICAL DISTRIBUTION OF MEAN AND MEAN+1 σ MAXIMUM PGA VALUES FROM THE CONVERSION OF KNOWN MAXIMUM INTENSITIES.59

FIG 40. GEOGRAPHICAL DISTRIBUTION OF MEAN AND MEAN+1 σ MAXIMUM PGV VALUES USING SCALING RELATIONS FOR THE CONVERSION OF KNOWN MAXIMUM INTENSITIES.60

FIG 41. INTENSITY RATES FOR ALEXANDROUPOLIS.61

FIG 42. DISTRIBUTION OF INTENSITIES AND SEISMIC HAZARD CURVE BASED ON PROBABILISTIC APPROACH OF MCGUIRE AND STATISTICAL TREATMENT OF OBSERVED INTENSITIES.62

FIG 43. SEISMIC HAZARD CURVES FOR FOUR CITIES WITHIN THE ELIGIBLE AREAS. THE PARAMETER USED IS THE MACROSEISMIC INTENSITY.63

FIG 44. THE CONTRIBUTION OF THE SEISMIC ACTIVITY RATE IN PSHA FOR THE SITE OF SERRES CITY COMBINING THE CORRESPONDING CALCULATIONS WITHOUT INCLUDING THIS FAULT.64

FIG 45. STOCHASTIC STRONG MOTION TIME HISTORY AND RESPONSE SPECTRUM (z=5%) FOR THE AREA OF SERRES WITH DESIGN MAGNITUDE M6.1 AND DISTANCE D=15KM.67

FIG 46. STOCHASTIC STRONG MOTION TIME HISTORY AND RESPONSE SPECTRUM (z=5%) FOR THE AREA OF SERRES WITH DESIGN MAGNITUDE M6.2 AND DISTANCE D=3KM.68



FIG 47. STOCHASTIC STRONG MOTION TIME HISTORY AND RESPONSE SPECTRUM ($z=5\%$) FOR THE AREA OF KOMOTINI WITH DESIGN MAGNITUDE $M6.3$ AND DISTANCE $D=5\text{KM}$	69
FIG 48. STOCHASTIC STRONG MOTION TIME HISTORY AND RESPONSE SPECTRUM ($z=5\%$) FOR THE AREA OF KOMOTINI WITH DESIGN MAGNITUDE $M6.7$ AND DISTANCE $D=5\text{KM}$	70
FIG 49. LOCATION OF SAMSUN.....	83
FIG 50. LOCATION OF TEKIRDAĞ, AND ISTANBUL.....	84
FIG 51. BASIC STEPS OF A PROBABILISTIC SEISMIC HAZARD ANALYSIS.....	85
FIG 52. INSTRUMENTAL SEISMICITY DISTRIBUTION FOR TURKEY.....	86
FIG 53. PLATE TECTONICS OF THE EASTERN MEDITERRANEAN AND CAUCASUS REGIONS (AFTER MCKENZIE, 1970).....	87
FIG 54. THE RELATIVE MOTION BETWEEN EURASIAN AND ARABIAN PLATES AND THE WESTWARD MOTION OF THE ANATOLIAN AND AEGEAN BLOCKS (ARMIJO ET AL., 1999).....	88
FIG 55. DISTRIBUTION OF ACOUSTIC ANOMALIES, SUPERIMPOSED ON THE BATHYMETRIC MAP (RANGIN ET AL., 2001, ARMIJO ET AL., 2002; 2005; IMREN ET AL., 2001, LE PICHON ET AL., 2001) OF THE DEEPER PARTS OF THE MARMARA SEA.....	89
FIG 56. TECTONIC SETTING OF THE BLACK SEA BASIN (NIKISHIN ET AL., 2003).....	91
FIG 57. TECTONICS OF THE BLACK SEA (FROM BARKA AND REILINGER, 1997).....	92
FIG 58. TECTONIC FRAMEWORK OF THE BLACK SEA REGION (AFTER TEMEL AND CIFTCI, 2002).....	93
FIG 59. MAP OF THE BLACK SEA REGION AND SEISMIC ZONES (AFTER CHEKUNOV, 1994).....	93
FIG 60. OFFSHORE FAULTING ASSOCIATED WITH THE BLACK SEA ESCARPMENT (AFTER DONDURUR, 2009).....	94
FIG 61. FAULT SEGMENTATION MODEL PROPOSED FOR THE MARMARA REGION (ERDIK ET AL., 2004).....	95
FIG 62. A SEISMIC SOURCE ZONATION FOR SAMSUN PROVINCE (TURKEY).....	96
FIG 63. THE LONG-TERM SEISMICITY OF THE MARMARA REGION (SEISMICITY BETWEEN 32 AD –1983 TAKEN FROM AMBRASEYS AND FINKEL, 1991).....	98
FIG 64. THE SEQUENCE OF EARTHQUAKES IN THE 18TH CENTURY AROUND MARMARA REGION (AFTER HUBERT-FERRARI, 2000).....	99
FIG 65. PGA MAP AT NEHRP B/C BOUNDARY SITE CLASS FOR 40% PROBABILITY OF EXCEEDENCE IN 50 YR (POISSON MODEL).....	104
FIG 66. PGA MAP AT NEHRP B/C BOUNDARY SITE CLASS FOR 40% PROBABILITY OF EXCEEDENCE IN 50 YR (RENEWAL MODEL).....	105
FIG 67. PGA MAP AT NEHRP B/C BOUNDARY SITE CLASS FOR 10% PROBABILITY OF EXCEEDENCE IN 50 YR (POISSON MODEL).....	105
FIG 68. PGA MAP AT NEHRP B/C BOUNDARY SITE CLASS FOR 10% PROBABILITY OF EXCEEDENCE IN 50 YR (RENEWAL MODEL).....	106
FIG 69. PGA MAP AT NEHRP B/C BOUNDARY SITE CLASS FOR 5% PROBABILITY OF EXCEEDENCE IN 50 YR (POISSON MODEL).....	106
FIG 70. PGA MAP AT NEHRP B/C BOUNDARY SITE CLASS FOR 5% PROBABILITY OF EXCEEDENCE IN 50 YR (RENEWAL MODEL).....	107
FIG 71. PGA MAP AT NEHRP B/C BOUNDARY SITE CLASS FOR 2% PROBABILITY OF EXCEEDENCE IN 50 YR (POISSON MODEL).....	107
FIG 72. PGA MAP AT NEHRP B/C BOUNDARY SITE CLASS FOR 2% PROBABILITY OF EXCEEDENCE IN 50 YR (RENEWAL MODEL).....	108
FIG 73. PGA MAP AT NEHRP B/C BOUNDARY SITE CLASS FOR 40% PROBABILITY OF EXCEEDENCE IN 50 YR (POISSON MODEL).....	109
FIG 74. PGA MAP AT NEHRP B/C BOUNDARY SITE CLASS FOR 10% PROBABILITY OF EXCEEDENCE IN 50 YR (POISSON MODEL).....	109
FIG 75. PGA MAP AT NEHRP B/C BOUNDARY SITE CLASS FOR 5% PROBABILITY OF EXCEEDENCE IN 50 YR (POISSON MODEL).....	110
FIG 76. PGA MAP AT NEHRP B/C BOUNDARY SITE CLASS FOR 2% PROBABILITY OF EXCEEDENCE IN 50 YR (POISSON MODEL).....	110



FIG 77. BULGARIAN ELIGIBLE AREA	116
FIG 78. EPICENTRAL MAP FOR BULGARIA AND SURROUNDINGS ($M \geq 3.0$)	119
FIG 79. EPICENTRAL MAP FOR BULGARIA AND SURROUNDINGS (AFTER 1980, ALL RECORDED EVENTS)	120
FIG 80. BULGARIAN SEISMIC NETWORK AND FOREIGN STATIONS USED IN EPICENTER LOCATION	123
FIG 81. FLOW CHART FOR SEISMIC HAZARD ASSESSMENT	125
FIG 82. MAP OF SEISMIC SOURCES USED FOR SEISMIC HAZARD ASSESSMENT	130
FIG 83. PROPOSED MAP FOR SEISMIC CODE (ELIGIBLE AREA)	131
FIG 84. INFLUENCE OF THE INTERMEDIATE VRANCEA EARTHQUAKES ON THE SEISMIC HAZARD	132
FIG 85. UNIMODAL DISTRIBUTION OF EARTHQUAKE MAGNITUDE AND DISTANCE TO GROUND MOTION EXCEEDANCE FREQUENCY - THE STRONGEST CONTRIBUTOR TO THE HAZARD FOR THE CITIES IS THE NEAR REGIONAL SEISMICITY	134
FIG 86. SLIGHT BIMODAL DISTRIBUTION OF EARTHQUAKE MAGNITUDE AND DISTANCE - STRONGER CONTRIBUTOR TO THE HAZARD FOR THE CITIES IS THE NEAR REGIONAL SEISMICITY	134
FIG 87. SLIGHT BIMODAL DISTRIBUTION OF EARTHQUAKE MAGNITUDE AND DISTANCE - STRONGER CONTRIBUTOR TO THE HAZARD FOR THE CITIES IS THE VRANCEA INTERMEDIATE SOURCE	135
FIG 88. A BIMODAL DISTRIBUTION OF EARTHQUAKE MAGNITUDE AND DISTANCE TO GROUND MOTION EXCEEDANCE FREQUENCY	136
FIG 89. ACTIVE FAULTS	138
FIG 90. 5% DAMPED MEAN AND MEAN +1 σ HAZARD SPECTRA	139
FIG 91. MAP OF EARTHQUAKE EPICENTERS IN ODESSA REGION AND SURROUNDING AREAS (B. PUSTOVITENKO, 2004)	143
FIG 92. THE FAULT STRUCTURE AND POCKETS OF HISTORICAL EARTHQUAKES NEAR ODESSA [2].	144
FIG 93. SCHEMATIC MAP ISOSEISMALS VRANCEA EARTHQUAKE IN 1802 (A) [3] AND 1940. (B) [4].	144
THE NUMBERS NEAR THE NAME MEANS THE OBSERVED SEISMIC RATING.....	144
FIG 94. A SCHEMATIC MAP OF THE EARTHQUAKE ISOSEISMALS DOBROGEA REGION OCTOBER 14, 1892. LEGEND: 1 - 2-3 POINTS, 2 - 3 POINTS, 3 - 3-4 SCORE 4 - 4 POINTS, 5 - 4-5, 6 - 5 POINTS, 7 - 5-6, 8 - 6 POINTS, 9 - 6- 7, 10 - 7 POINTS, 11 7-8, 12 FIELD ISOSEISMALS (FROM [11]).	145
FIG 95. THE VERTICAL COMPONENT OF OSCILLATIONS CALCULATED BY RECORDING THE EARTHQUAKE 06.10.2013, OF THE VRANCEA ZONE, REGISTERED BY THE SEISMIC STATION "ODESSA-CITY": A - ACCELERATION, B - SPEED C - OFFSET. (MAG 4.7)	147
FIG 96. THE HORIZONTAL OF OSCILLATIONS CALCULATED BY RECORDING THE EARTHQUAKE 22.11.2014, OF THE VRANCEA ZONE, REGISTERED BY THE SEISMIC STATION "ODESSA-CITY": A - ACCELERATION, B - SPEED C - OFFSET. (MAG 6.3)	147
FIG 97. SEISMIC LAYOUT IN THE BASEMENT HOUSING OF ODESSA ACADEMY OF CIVIL ENGINEERING AND ARCHITECTURE.	148
FIG 98. EXAMPLE OF THE THREE-COMPONENT RATED ACCELEROGRAMS, MODELLING RATED EARTHQUAKE OF LOCAL FOCAL ZONE ON THE FREE SURFACE OF THE GROUND ONE OF THE SITES IN THE CITY OF ODESSA. .	150
FIG 99. DIRECTION OF VECTOR COMPONENTS OF THE TOTAL SEISMIC VIBRATIONS.	151
FIG 100. LINEAR RESPONSE SPECTRA OF INDIVIDUAL OSCILLATORS ACCELEROGRAM SHOWN IN FIGURE 4. FIGURES 1, 2, 3 CORRESPOND WITH INTRINSIC ATTENUATION OF SINGLE OSCILLATORS: 2, 5 AND 10 PERCENT OF CRITICAL, F - THE ANGULAR FREQUENCY AND $T = 1 / F$	152
FIG 101- GENERAL SEISMIC ZONING MAP GSZ-2004-A IN UKRAINE	158
FIG 102- GENERAL SEISMIC ZONING MAP GSZ-2004-B IN UKRAINE	159
FIG 103- GENERAL SEISMIC ZONING MAP GSZ-2004-C IN UKRAINE	160
FIG 105- DETAIL MAPS GSZ-2004-A.	161
ODESSA REGION	161
FIG 104- DETAIL MAPS GSZ-2004-A0.	161
ODESSA REGION	161
FIG 107- DETAIL MAPS GSZ-2004-C.	162



ODESSA REGION	162
FIG 106– DETAIL MAPS GSZ-2004-B.....	162
ODESSA REGION	162
FIG 108. THE SEISMIC ZONATION OF THE EASTERN PART OF ROMANIA AND THE BLACK SEA AREA	172
FIG 109 SEISMIC SOURCES SELECTED FOR THIS STUDY TOGETHER WITH THE ASSOCIATED SEISMICITY. WE PLOTTED EPICENTERS FOR $M_w > 3.5$ FOR THE INLAND SOURCES AND $M_w > 3.0$ FOR THE MARINE SOURCES.	174
FIG 110. THE SciNetNATHAZ IMPLEMENTATION AREA FOR THE ROMANIAN PARTNER IS MARKED WITH A BLACK RECTANGLE	175
FIG 111. THE FREQUENCY-MAGNITUDE DISTRIBUTION FOR VI ZONE: A) NON-CUMULATIVE; B) CUMULATIVE; $M_w \geq 2.8$ - BLUE LINE, $M_w \geq 5.0$ -RED LINE.....	176
FIG 112. THE FREQUENCY-MAGNITUDE DISTRIBUTION FOR VN ZONE: A) NON-CUMULATIVE; B) CUMULATIVE	178
FIG 113. THE FREQUENCY-MAGNITUDE DISTRIBUTION FOR BD ZONE: (A) NON-CUMULATIVE; (B) CUMULATIVE	179
FIG 114. THE FREQUENCY-MAGNITUDE DISTRIBUTION FOR PD ZONE: (A) NON-CUMULATIVE; (B) CUMULATIVE	180
FIG 115. THE FREQUENCY-MAGNITUDE DISTRIBUTION FOR IMF AND DUL ZONE: (A) NON-CUMULATIVE; (B) CUMULATIVE.....	182
FIG 116. THE FREQUENCY-MAGNITUDE RELATIONS FOR BS2 WITH $M_w \geq 3.0$; A) NON-CUMULATIVE; B) CUMULATIVE	183
FIG 117. THE FREQUENCY-MAGNITUDE DISTRIBUTION FOR BS3 ZONE. THE FREQUENCY-MAGNITUDE RELATIONS FOR WITH $M_w \geq 3.0$; A) NON-CUMULATIVE; B) CUMULATIVE	184
FIG 118. SEISMIC HAZARD FOR $T_r=100$ YEARS FOR $I=V$ AND $I=VI$ (USING ONLY CRUSTAL SOURCES).....	188
FIG 119A. SEISMIC HAZARD FOR $T_r=475$ YEARS FOR $I=V/ A=0.012G \dots 0.025G$ AND $I=VI/ A=0.026G \dots 0.050G$ (USING ONLY CRUSTAL SOURCES).....	189
FIG 119B. SEISMIC HAZARD FOR $T_r=475$ YEARS FOR $I=VI/ A=0.026G \dots 0.050G$ AND $I=VII / A=0.051G \dots 0.100G$ (USING ONLY CRUSTAL SOURCES).....	190
FIG 120. SEISMIC HAZARD FOR $T_r=1000$ YEARS FOR $I=VI/ A=0.026G \dots 0.050G$ AND $I=VII / A=0.051G \dots 0.100G$ (USING ONLY CRUSTAL SOURCES).....	190
FIG 121. EXCEEDANCE PROBABILITY (%) OF $I=V$ AND $I=VI$ IN AN 100 YEARS RETURN PERIOD (USING ONLY CRUSTAL SOURCES).....	191
FIG 122. EXCEEDANCE PROBABILITY (%) OF $I=VI$ IN 475 YEARS RETURN PERIOD.....	191
(USING ONLY CRUSTAL SOURCES)	191
FIG 123. MACROSEISMIC INTENSITY CURVES FOR $T_r=50$ AND 100 YEARS (USING ONLY CRUSTAL SOURCES).....	193
FIG 124. MACROSEISMIC INTENSITY CURVES FOR $T_r=200$ AND 475 YEARS (USING ONLY CRUSTAL SOURCES) ..	193
FIG 125. MACROSEISMIC INTENSITY CURVES FOR $T_r=1000$ AND 2000 YEARS (USING ONLY CRUSTAL SOURCES)	194
FIG 126. MACROSEISMIC INTENSITY VALUES AND CURVES FOR $T_r=100$ YEARS (USING ONLY CRUSTAL SOURCES)	194
FIG 127. MACROSEISMIC INTENSITY VALUES AND CURVES FOR $T_r=475$ YEARS (USING ONLY CRUSTAL SOURCES)	195
FIG 128. ANNUAL SEISMIC HAZARD FOR $I=IV$ AND $I=V$ (USING BOTH CRUSTAL AND INTERMEDIATE DEPTH SOURCES)	195
FIG 129. SEISMIC HAZARD FOR $T_r=50$ YEARS FOR $I=VII$ AND $T_r=100$ YEARS $I=VIII$ (USING BOTH CRUSTAL AND INTERMEDIATE DEPTH SOURCES)	196
FIG 130. SEISMIC HAZARD FOR $T_r=475$ YEARS FOR $I=IX$ AND $I=X$ (USING BOTH CRUSTAL AND INTERMEDIATE DEPTH SOURCES).....	196
FIG 131. SEISMIC HAZARD FOR $T_r=1000$ YEARS FOR $I=IX$ AND $I=X$ (USING BOTH CRUSTAL AND INTERMEDIATE DEPTH SOURCES).....	197
FIG 132. MACROSEISMIC INTENSITY CURVES FOR $T_r=50$ AND 100 YEARS (USING BOTH CRUSTAL AND INTERMEDIATE DEPTH SOURCES)	197



FIG 133. MACROSEISMIC INTENSITY CURVES FOR TR=50 AND 100 YEARS (USING BOTH CRUSTAL AND INTERMEDIATE DEPTH SOURCES)	198
FIG 134. MACROSEISMIC INTENSITY CURVES FOR TR= 100 YEARS (USING BOTH CRUSTAL AND INTERMEDIATE DEPTH SOURCES).....	198
FIG 135. THE LOCATION OF THE SEISMIC STATIONS IN REPUBLIC OF MOLDOVA	203
FIG 136. THE NEW SEISMIC ZONING MAP OF MOLDOVA REPUBLIC.	204
FIG 137. THE NEW SEISMIC MICROZONATION MAP OF CHISINAU CITY.....	205
FIG 138. SEISMIC RISK MAP OF KISHINEV CITY.	206
FIG 139. SEISMIC RISK MAP OF MOLDOVA REPUBLIC.....	207
FIG 140. RELATIVE SEISMIC RISK MAP OF MOLDOVA REPUBLIC.....	208

LIST OF TABLES

TABLE 4.1.1 INFORMATION ON THE SEISMICITY PARAMETERS OF THE SOURCES WHICH INFLUENCE THE EXAMINED AREA (PAPAIOANNOU AND PAPAZACHOS (2000)).	32
TABLE 4.1.2 RESULTS ON THE ANALYSIS OF SELECTED RECORDS OF THE MAY 22, 2012 EARTHQUAKE IN BULGARIA.	48
TABLE 4.1.3 SEISMIC HAZARD DE- AGGREGATION RESULTS IN A LOCAL SCALE FOR THE 2 EXAMINE SITES (SERRES AND KOMOTINI) AND VARIOUS PGA'S VALUES CORRESPONDING IN DIFFERENT RETURN PERIODS (100, 200, 475, 950, 1890 YEARS)	65
TABLE 4.2.1 POISSON AND RENEWAL MODEL CHARACTERISTIC EARTHQUAKE PARAMETERS ASSOCIATED WITH THE SEGMENTS.....	100
TABLE 4.2.2 POISSON MODEL EARTHQUAKE PARAMETERS ASSOCIATED WITH THE SEGMENTS.....	102
TABLE 4.2.3 CHARACTERISTICS OF THE SELECTED GMPES FOR ACTIVE SHALLOW REGIONS (DELVAUD ET AL., 2012) ..	103
TABLE 4.3.1 STRONG AND DESTRUCTIVE EARTHQUAKES OCCURRED IN BULGARIA AFTER 1900 YEAR. (BOLD AND RED – EARTHQUAKES IN OR CLOSE TO ELIGIBLE AREA).....	117
TABLE 4.4.1 SEISMIC EVENTS WITH MAGNITUDE >4 OF 2008 TO 2014YEAR	148
TABLE 4.4.2 EXAMPLE OF THE BASIC PARAMETERS OF THE SYNTHESIZED TERNARY RATED ACCELEROGRAMS SHOWN IN FIGURE 98.	152
TABLE 4.4.3 LIST OF WORKS PERFORMED BY SEISMIC MICROZONING.	152
TABLE 4.4.4 PGA MODEL (46.617016, 31.099141).....	153
TABLE 4.4.5 PGA MODEL (46.471814, 30.706389).....	154
TABLE 4.4.6 PGA MODEL (46.556782, 30.767741).....	155
TABLE 4.4.7 DESTRUCTIVE EARTHQUAKES ROMANIAN CARPATHIANS (VRANCEA ZONE).....	164
TABLE 4.4.8 PREDICTION OF POSSIBLE LOSSES AMONG THE POPULATION OF THE ODESSA REGION IN THE RESIDENTIAL SECTOR IN THE EARTHQUAKE 01.01.2006.	166
TABLE 4.5.1 PARAMETERS NEEDED FOR A PROBABILISTIC HAZARD ASSESSMENT: GEOGRAPHICAL DISTRIBUTION, AVERAGE DEPTH, ACTIVITY RATE AND GUTENBERG RICHTER PARAMETERS, ETC.	172
TABLE 4.5.2 MACROSEISMIC INTENSITY BASED ON INSTRUMENTAL RECORDINGS (STAS 3684-71)	186



1 BACKGROUND OF THE DOCUMENT

1.1 GENERAL NOTE

Pilot implementation on regional and on local scale actions, fall into the GA.3 “Pilot Implementation on Regional and on Local Scales”; started for all types of hazards on March 2014 and ended at the end of October 2015 (instead the end of August) in order to have time to evaluate the outputs and complete the respective reports.

Responsible for the Seismic Hazard Implementation activities was partner P2 (EPPO -ITSAK). All partners have contributed.

1.2 SCOPE AND OBJECTIVES

Pilot implementation for SHA were scheduled and implemented by all partners in their respective Pilot Implementation Areas (PIA), in order to evaluate the outputs of the selected methods and their adaptability to specific conditions. Evaluation is based on comparison of their outputs to actual facts and on assessing their dissemination potential in order to promote their use by the project’s stakeholders (administration staff members, scientific community, engineers, geologists, planners etc.).

1.3 RELATED DOCUMENTS

1.3.1 Input

List of former deliverables acting as inputs to this document

Document ID	Descriptor
-------------	------------

1.3.2 Output

List of other deliverables for which this document is an input.

Document ID	Descriptor
-------------	------------



2 INTRODUCTION

It has been identified by Seismological Society of America (1910) that three parts of the earthquake phenomenon should be studied: the event itself (time, location and mechanism), the associated ground motions and the effects on structures. These constitute the fundamental elements in evaluating earthquake risk. Mitigating the seismic risk requires a logical and consistent approach to evaluating the effects of future seismic loads (with the expected uncertainty) on people and their structures. To accomplish a complete earthquake risk assessment four basic steps are taken into account (McGuire 2004). First is the seismic hazard analysis probabilistically or deterministically which gives a probabilistic description (frequency of exceedance) or a seismic worst case scenario of earthquake characteristics such as ground motion values. Second is the estimation of earthquake damage, evaluating proper damage and loss functions. Third is the assessment of the seismic risk translating the seismic hazard results into seismic risk ones (frequencies of damage or loss by utilizing the selected functions. And fourth is the formal or informal analysis of earthquake mitigations decisions, wherein the options, uncertainties, costs, decision criteria and risk aversion of the decision maker are merged in the decision process. The main target of the application of the seismic hazard assessment and the seismic risk analysis is to propose the criteria that can be used to make rational decisions on seismic safety.

Virtually every important decision regarding the evaluation of earthquake effects on people and manmade facilities is made using some form of probabilistic seismic hazard. Sometime there analyses are conducted informally, with probabilities or likelihoods assessed intuitively with subjective expert opinion. In such instances our judgment, intuition, and experience are adequate to assess relative probabilities of occurrence and to make rational decision on the optimum course of action (or inaction) to take. Sometime the judgments made are so natural and intuitive that they are made largely unconsciously; our experience and confidence allows assurance that the results are nearly optimal.

In instances involving complicated assessments of effects derived from various geo- science and engineering disciplines, decision makers often prefer formal assessments of probabilities of earthquake occurrences and associated natural effects that may produce damage to facilities and injury or life-loss to people. Such formal assessments are usually most appropriate for recommendations on (1) regional or national seismic design requirements; (2) earthquake evaluation of important facilities whose loss would imply substantial financial hardship to owners; (3) estimation of earthquake damage and losses for emergency preparedness purposes; (4) decision making regarding seismic safety of critical facilities (whose damage might lead to substantial life loss, injury, monetary and property loss, or threat to national security).

In this report we mainly focus in regional seismic hazard assessment of the area studied within the framework of the project (e.g. Greece, Turkey, etc). The earthquake hazard analysis requires the use of



various scientific branches other than seismology. Geological and Geophysical sciences are demanded for defining the location and the geometrical shape of the potential seismic sources of known or unknown seismic faults as well as the radiation pattern of the generating seismic arrays of the aforementioned seismic foci. Mathematics, especially an understanding of probability and statistics, is significant in the increasingly prevalent probabilistic evaluations. Geotechnical engineering is extremely indispensable in estimating the effects of local soil conditions of the ground motions. Structural and earthquake engineering determine the way of parameterization of the most seismic hazard results.

3 SEISMIC HAZARD ASSESSMENT

3.1 METHODOLOGY

The purpose of seismic hazard analysis is to evaluate the hazard of seismic ground motion at a site by considering all possible earthquakes in the area, estimating the associated strong shaking at this site. There are two main approaches in seismic hazard analysis the deterministic and the probabilistic. In the Deterministic Seismic Hazard Analysis (DSHA), a single “maximum” earthquake is specified by magnitude and location with respect to a site of interest, and the associated ground motion is assessed and used to design or evaluate the safety of a facility. The deterministic approach may be justified, for example, for major earthquakes on a given segment of a plate boundary fault that is known to break repeatedly, generating similar size earthquakes characteristic to the fault segment. The DSHA selects one or more earthquakes as the target for designing an earthquake resistant structure. The target earthquake for a critical structure (usually the “maximum seismic event” or the “maximum credible earthquake”) is usually selected by consideration of the historical seismicity record and the physical characteristics of the seismic sources. The DSHA does not consider the likelihood of the occurrence of the target earthquake, nor does it offer any insight into the importance of the target earthquake relative to other possible seismic hazards, such as those due to smaller but closer earthquakes or larger but more distant seismic events.

On the other hand the Probabilistic Seismic Hazard Assessment (PSHA) may be used to calculate the probability that a range of small and large earthquakes may occur along a given fault and that various faults in a broader region might affect the site. The PSHA addresses the questions of how strongly and how often the ground will shake, by considering all possible earthquakes that might affect the site. The range of ground motions at a site resulting from earthquakes that might occur on a variety of seismic sources is estimated by using an empirical predictive relationship to translate to the site through distance the ground motions associated with earthquakes that are considered. The rate of earthquake occurrence on each seismic source is also considered. Thus, PSHA combines information on earthquake size, origin location, probability of occurrence, and resulting ground motion to give results in terms of ground motion and associated annual probability of occurrence (or exceedance). An important issue for PSHA is which ground motion measures will meet the needs of various users (e.g. pga, 5%-response spectra, etc).



When seismic hazard must be quantified in the face of uncertainty in the locations of seismic sources, magnitude distributions, and ground motion estimates, PSHA can incorporate and display the range of scientific opinion regarding these issues. One way to do this is to identify various hypotheses and models to describe each science phenomena involved. When this is done, the range of uncertainty in the PSHA corresponding to the range of hypotheses can and should be explicitly displayed, so that the decision maker will be aware of the uncertainties and will not have a false impression of accuracy that might be associated with a single valued hazard estimate. Expert judgment can be employed to assign subjective probabilities to each hypothesis and thus identify to the decision makers where, in the range of uncertainty, the prevailing weight of opinion would assign the risk. When the uncertainties in the PSHA results is too large to be useful for decision making, a consensus could still be sought among experts who may capture by an in depth DSHA analysis, subtle but crucial details of earth science information which escaped the quantification procedure in PSHA.

The design of structures considering the potential seismic actions at a given site is, for the time being, the only way for the minimization of loss of lives due to earthquakes. We can define as *seismic hazard* at a site, where a structure (building, bridge, etc) exists or will be constructed, a quantity, H , which is measured by the expected (with given probability of occurrence) *intensity of strong seismic ground motion* in this. This intensity can be measured by the expected ground acceleration, a , (peak value, spectral values, etc), the ground velocity, v , by the ground displacement, s , or by the expected macroseismic intensity, I .

The mathematical formulation of the seismic hazard can be given by the following relation:

$$Y_t = \frac{\ln N_0 t}{\beta} - \frac{\ln[-\ln(1 - P_t)]}{\beta} \quad (1)$$

where Y_t is the seismic hazard parameter, that has P_t probability to be exceeded within a given time window of t years and N_0 , β are constants determined using the distribution of the seismic intensities (peak ground values, macroseismic intensities or spectral values)..

The expected final result of the seismic motion at a site (damage in structures, deaths of people, etc) can be called *seismic risk*, R , and depends on the seismic hazard, H , at this site and on the properties and dynamic features of the technical structure (quality, natural period, damping, plasticity, etc). The measure of these properties of the structure is called *vulnerability*, V , of the structure. For this reason, the seismic risk, R , is considered as the convolution of seismic hazard, H , and of vulnerability, V . That is,

$$R = H * V \quad (2)$$

which in graphical form is given in figure (Fig.1)

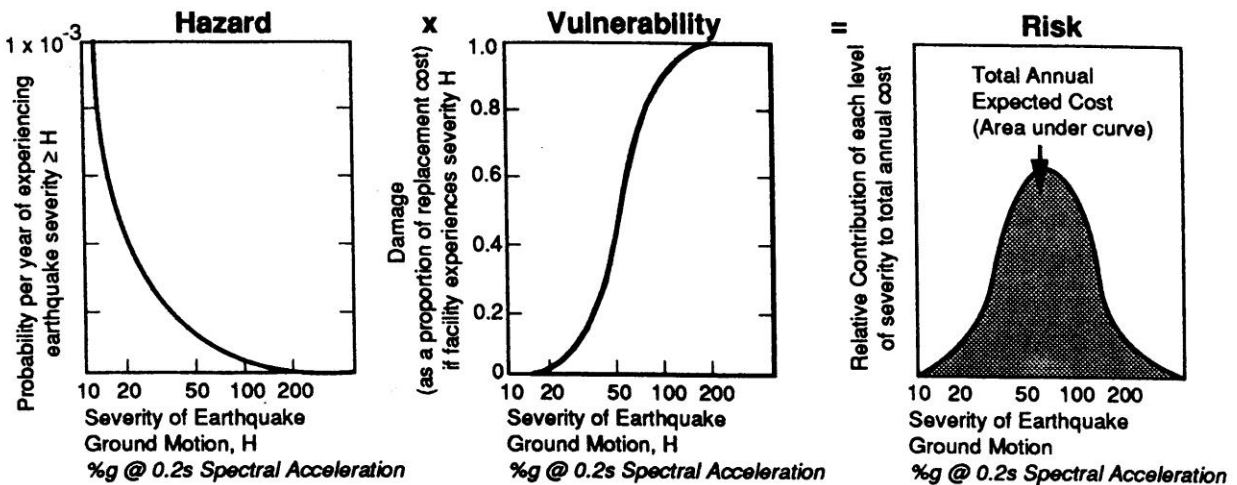


Fig.1. Seismic Risk is the output of convolution of seismic hazard and vulnerability. Typical graphs depicting each quantity are shown. (Coburn and Spence, 2002).

The main aim of the relative sciences and technology today is the reduction of the consequences of the earthquakes, that is, the decrease of seismic risk, R . Theoretically, this can be obtained by decreasing both V and H , according to the previous relation. In practice, however, we can decrease only V , not H , because the seismic hazard at a site depends on physical factors (seismicity, source and wave path properties, properties of foundation soil, etc), which cannot be controlled by the human beings. These physical factors can be studied and their effects on the seismic hazard can be understood. Vulnerability is a topic studied by Earthquake Engineering and civil engineers are mainly responsible to propose methods for reducing the vulnerability of a structure without excessive cost. This can be done successfully if accurate knowledge on the seismic hazard at the site of the structure exists. Seismic hazard is a subject studied by Engineering Seismology and seismologists are mainly responsible for its estimation.

Usually, the following two main objectives of seismic risk reduction are sought:

- a) The technical structure not to suffer any damage or to suffer slight damage (easily repaired) by the *most probable* expected seismic motion during the lifetime of the structure (e.g. 50 years).
- b) The technical structure to suffer some damage but not collapse by the *maximum expected* seismic motion at the site of the structure.

The aim of any seismic hazard either on small or large scale is the robust determination of the constants of relation (1) which is achieved through the following main steps depending on the procedure (probabilistic or deterministic):

1. A seismic source model, based on the adoption of a reliable seismotectonic model, which best describes the active tectonics of the study area. With the term active tectonics we mean the kinematic and dynamic processes of the lithosphere that take place in the area (e.g. motion of the lithospheric plates, deformation),
2. The accurate determination of the seismicity parameters using complete and homogeneous catalogues,
3. Compilation and adoption of reliable predictive relation for the attenuation of the strong ground parameters
4. Finally the selection of a methodology for the statistical analysis of the distribution of seismic intensities in time and space.

The entire list of steps in the hazard analysis is of crucial importance and their uncertainties must be considering in any hazard analysis (Fig. 2).

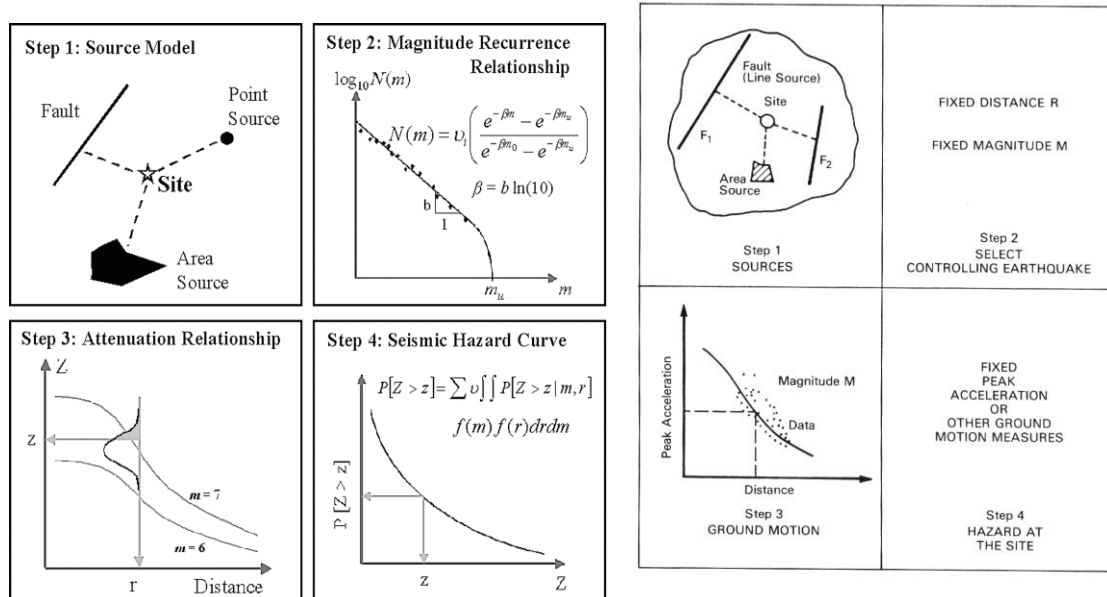


Fig.2. Flow chart for seismic hazard assessment study based on probabilistic (left) or deterministic (right) approach. (Reiter,1990).



3.1.1 Probabilistic Seismic Hazard Assessment

This part of project examines a formal probabilistic seismic hazard analysis (PSHA), evaluates its strengths and weaknesses, and suggests those elements of the PSHA that are considered necessary for a reasonable statement of seismic hazard. When the probabilities calculated cannot be correlated directly with observed statistics, or the consequences of earthquake damage are significant, or the uncertainties in physical interpretation for one or more scientific fields are large, formal procedures for PSHA are generally preferred. PSHA evaluates the seismic hazard of seismic ground motion at a site considering all possible earthquakes in the area studied, estimating the associated shaking at the site, and calculating the probabilities of these occurrences. While this project focuses on the seismic hazard of ground shaking, similar probabilistic techniques can be applied to the assessment of hazard from fault movement, liquefaction, floods and landslides. PSHA procedures have several advances over less formal, more subjective evaluations.

PSHA studies typically include the following:

1. A database consisting of potentially damaging earthquake sources, including known active faults and historic seismic source zones, their activity rates, and distances from the project site. This should include a comparison with developed slip rates for faults considered. Differences in slip rates should be documented and the reasons for them explained (for example, revised slip rates or new paleoseismic information from recent studies). Use of published maximum moment magnitudes for earthquake sources, or estimates that are justified, well-documented, and based on published procedures;
2. Use of published curves for empirical predictive relations of PGA with distance from earthquake source, as a function of earthquake magnitude and travel path.
3. An evaluation of the likely effects of site-specific response characteristics (e.g., amplification due to soft soils, deep sedimentary basins, topography, near-source effects, etc.).
4. Characterization of the ground motion at the site in terms of PGA with a certain number of probability of exceedance in specific return period, taking into account historical seismicity, available paleoseismic data, the geological slip rate of regional active faults, and site-specific response characteristics.

The objective of seismic hazard analysis is to provide a formal estimate of the earthquake threat as a specific site. Typically the threat is presented in terms of the amplitude of seismic shaking (e.g. pga, pgv, 5%-psa, etc). The time span of these PSHA calculations is a time period of 30-50 years approximately the economic lifetime of engineered structures and facilities. Application to critical facilities implies much longer time periods and the uncertainties inherent in such calculations require special consideration. The



hazard estimate is a function of available information relevant to earthquake activity in the region. A typical PSHA seeks to estimate the annual probabilities of exceedance as a function of a single amplitude of strong ground shaking e.g. Four steps are considered to assess PSHA.

- A. Seismic source (zones or faults within which future earthquakes will occur) are delineated. From this a distribution of possible distances, $f_R(r)$, is derived.
- B. A rate of earthquake occurrence v_i and a magnitude distribution, $f_M(m)$, are derived for each source.
- C. A ground-motion model is derived that, for any specified magnitude m and distance d , allows calculation of the probability that a ground - motion amplitude is exceeded.
- D. An estimation is accomplished of the rate v , with which amplitude is exceeded, using inputs A through C, by integrating overall possible magnitudes and distances and any accounting for their relative probabilities.

The third input is an "empirical predictive relation" that permits estimation of the distribution of ground-motion amplitudes as a function of magnitude and distance. The probability analysis integrates overall earthquakes sizes and distances, and sums over all seismic sources, to estimate the expected number of exceedances of amplitude per unit time, which is an accurate estimate of the annual probability of exceedance of amplitude for a low value of probability.

Use of the expected number of events v (instead of the probability of one or more such events) greatly simplifies the formulation and makes the model more robust. As usual, in probabilistic analysis, it is easier to calculate expectations than probabilities. In PSHA, one calculates the expected number of occurrences as the sum of expected occurrences caused by many diverse earthquakes. The expectation of that sum will always be the sum (integral) of those expectations, even if future events are correlated in time, space and size. There need not be any implicit or explicit assumption of Poissonian behavior, either in space or time in the analysis. Virtually any model of future earthquake occurrence, including spatial, temporal, and size dependence, can be accommodated as (eg memoryless - poissonian or time dependent model).

3.1.1.1 Statistical Earthquake -Occurrence Models

Several earthquake-occurrence models have been proposed, showing various degrees of sophistication and incorporating different physical concepts. Anyone may consider a variety of probabilistic dependencies and memory patterns involving earthquake times, locations and sizes. Examples are time-predictable and slip-predictable, Markov, characteristic earthquake, self-exciting or double-stochastic or clustering point processes, and renewal models, all of which have been suggested as possible representations of seismic sequences. In practice, a random, memoryless (Poisson) process has been generally assumed in PSHA because of ease of application. Models with memory (time dependent)



require more detailed knowledge and understanding of earthquake processes, which is often not available. The impact of non-poissonian behavior on seismic hazard may or may not be significant.

Characteristics of seismicity for which only a few modeling alternatives and estimation procedures exist are the variations of seismic rates in space (nonhomogeneity) and in time (nonstationary). Spatial variations are especially important and difficult to estimate in regions where the stress-generating process and the causative geologic features are not well known. This includes areas where a lack of a thorough understanding of the physical processes that control earthquake occurrence rates and hence nonhomogeneity. A typical approach in this instance is to define seismogenic provinces as geographical regions within which the seismicity is assumed to be homogeneous. Models of this type are popular because of their simplicity. However, hazard results are sometimes sensitive to the configuration of the seismogenic provinces and to the assumption of homogeneous activity within each province.

Temporal variations of seismicity ranging from long term (hundreds or thousands years) to short term (weeks or months) are currently ignored, but understanding these variations will provide a basis for more credible hazard estimates in the future. An important example, which is handled at an intuitive level in the process of defining homogeneous seismogenic provinces, is that regions that have been quiescent in the recent past - say during at least the period of the historical record - may suddenly become active in the next few decades.

An often influential modeling choice is that of the type of probability distribution of earthquake magnitude, including numerous variations on the distribution of one or several characteristic values. In practice, simple models such as the truncated exponential law should be preferred, unless such models are overshadowed by clear physical or statistical evidence. Significant work on statistical earthquake occurrence has concentrated on model formulation and parameter estimation. New models, with spatial and temporal variation of seismicity and with various types of probabilistic dependences, should continue to be developed, but priority should perhaps be given to studying procedures for the validation and comparison of models on the basis of available data.

3.1.2 Deterministic Seismic Hazard Assessment

The essential feature of deterministic seismic hazard analysis (DSHA) is that one or more earthquakes are selected with only implicit consideration of their probabilities of occurrence. One example is the tectonic province procedure currently used for critical facilities sites, in which the largest Macroseismic intensity in the province is identified, and then assumed to occur at the site. A second example is the assignment of a maximum credible earthquake with specified magnitude and at a specified distance. A third example is the identification of a “characteristic earthquake” on a fault segment with specified source parameters, which enables seismologists to predict strong ground-motion. Ground-motions obtained by analysis range in sophistication from peak values obtained from empirical predictive relations, to complete seismograms that may be either synthetic or selected from prior recordings under similar conditions. Probabilistic



concepts enter in this analysis only in a simple form, such as scatter about a mean ground motion estimation curve.

Deterministic evaluation of seismic hazard can also be performed, and the results of correctly performed and suitably comprehensive DSHA studies can also supersede values of PGA. DSHA studies typically include the following:

1. Evaluation of potentially damaging earthquake sources, and deterministic selection of one or more suitable "controlling" sources and seismic events. The deterministic earthquake event magnitude for any fault should be a *maximum* value that is specific to that seismic source. Maximum earthquakes may be assessed by estimating rupture dimensions of the fault.
2. Use of published curves for the effects of seismic travel path using the shortest distance from the source(s) to the site (e.g., see special issue of Seismological Research Letters, v. 68, n.1, 1997);
3. Evaluation of the effects of site-specific response characteristics on either (a) site accelerations, or (b) cyclic shear stresses within the site soils of interest.

REFERENCE

McGuire R., Seismic hazard and risk analysis, Eqk. Eng. Res. Inst. Monograph, MNO-10, pp221.

4 REGIONAL AND LOCAL SCALE SEISMIC HAZARD APPLICATIONS

4.1 GREECE

In the present chapter, seismic hazard assessment at regional scale is presented for the broader area of Eastern Macedonia and Greek-part of Thrace, based on the selected methodology from GA1. The selected area E-Macedonia and Thrace area is located on the North-Eastern part of Greece bounded by Bulgaria (to the North), Turkey (to the East), North Aegean Sea (to the South) and Central Macedonia district (to the West). The population of the examined area is almost 600,000 (census 2010).

4.1.1 Background Information on Seismic Hazard Maps in Greece

The seismic hazard maps appeared in the various seismic codes of Greece since 50's were based on the valid seismological knowledge during the corresponding period of compilation. The area under study was always considered as low seismicity and low hazard area.

Until the end of fifty's several regulations were issued after disastrous earthquakes for the rehabilitation of the damaged structures (Corinthos 1926, Chalkidiki 1932, Thessaloniki 1932, Ionian Island 1953 Thessalia 1954-1957).



In the first seismic hazard map of Greece with the title “*Engineering Seismic Map of Greece*” the area of Greece was divided in 5 classes of seismic hazard (Technical Chronicles, no 184, 1939) and was compiled by Roussopoulos (1956). The classification was based on a proposed value corresponding to fraction of the horizontal acceleration which was considered as design acceleration. In the revision of 1956 (2nd edition) the area of the Dodecanese islands was considered in the zonation and the new map included five seismic hazard classes with a division each of them in three subclasses depending to the soil classification. The coefficient was varied between 0.01g and 0.16g. The map is shown in figure (Fig.3).

This map was based on the macroseismic effects of the earthquakes during the 19th and early of the 20th century reflecting the geographical distribution of the maximum intensities. No statistics was used.

The first Greek seismic code was adopted in 1959 (Royal Decree 19/26.2.1959, Gov. Gazet. 36A) and included a list of 144 sites which were grouped in 3 classes. The classification was based on the maximum observed intensity and its frequency without any scientific treatment.

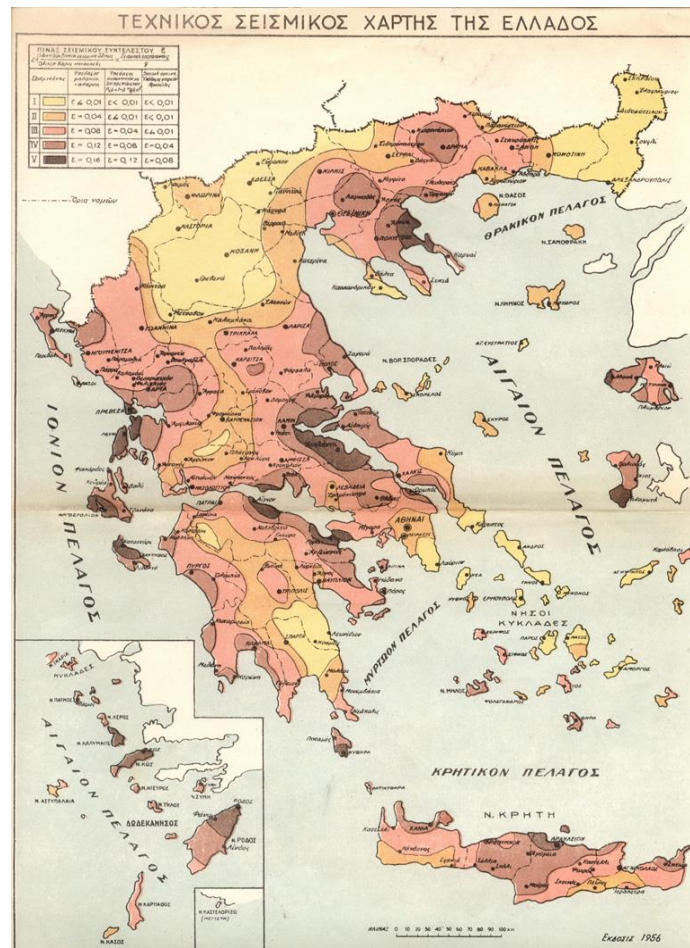


Fig.3. The first seismic hazard map of Greece.

Discussions of the revision of the seismic code of Greece started after the 1978 M=6.5 Thessaloniki earthquake, which caused extended damage to reinforced concrete structures, which were built according to the seismic code of 1959. These discussions were densified after the strong earthquakes of 1981-1986 which caused high degree damage including collapses at several regions.

Until that period many research papers and PhD theses were published aiming in reliable assessment of seismic hazard. These scientific efforts started on the basis of point source approximation for seismic hazard studies with the application of the probabilistic methods of mean values and the Gumbell I and III asymptotic distributions. The paper by Galanopoulos and Delibasis (1972) was the first attempt on seismic hazard even at elementary level of data statistical treatment. The first trusted attempt was made by Algermissen et al (1972). The publications of Makropoulos (1978), Papaioannou (1984), Papoulia (1988) and the papers by Drakopoulos and Makropoulos (1983), Papaioannou (1986), Makropoulos and



Burton (1989), were based on the Gumbell's (1958) first and third asymptotic distributions. Following, the more detailed zonation by Hatzidimitriou (1984), the Cornell's (1968) method and its modification due to McGuire (1976) was applied by Papazachos et al (1985) using the area-type seismic sources model by Hatzidimitriou (1984) which was based on the pioneering work for the compilation of an area-type seismic sources model by Papazachos (1980). In the paper by Papazachos et al (1985) the authors adopt the opinion expressed by Cornell (1968), that the use of seismic hazard recurrence curves is more useful than ill-defined single numbers as the "probable maximum" or the "maximum credible" intensity. This is due to the fact that even well-defined single numbers, as the "expected lifetime maximum" are insufficient to give the engineers an understanding of how quickly the hazard (annual probability of exceedence) decreases as the ground motion intensity increases. Papazachos et al. (1990) attempted to perform a statistical elaboration of the macroseismic observation for selected sites in Greece and compare the results with probabilistic seismic hazard.

Improvements and contribution to the credibility of the results were made by Margaris (1994), who took into account the azimuthal variation of the seismic intensity in the calculations.

Given the proposal for the empirical predictive relation for the peak ground values by Theodulidis (1991), the seismic sources model for the shallow and intermediate depth earthquakes (Papazachos, 1990) and the compilation of the catalogue of historical earthquakes by Papazachos and Papazachou (1989), seismic hazard maps were compiled using the McGuire (1976) code and also the mean values and Gumbell (1958) probabilistic methods. These individual maps were considered as the basis of the revised version of seismic hazard zonation of Greece (Papazachos et al., 1989). In this map the area of Greece was divided into four zones of seismic hazard with design values for the ground acceleration (seismic design coefficient) equals to 0.12g, 0.16g, 0.24g and 0.36g and is shown in figure (Fig 4). Following the earthquake of 1995 in Kozani there was a modification for the area of W. Macedonia due to increase level of the seismic hazard.

Even though the background work for the seismic hazard map of Greece was accomplished in 1989 the seismic code of Greece was published in the Government Gazette in 1992 being valid in parallel with the 1950 code. In 1995 two disastrous earthquakes occurred in Greece (Kozani, M6.6 and Aigio M6.2). In July-August 1996 two earthquakes of magnitude M 5.2 and 5.6 occurred in NW Greece with recorded peak accelerations 0.39g at the town of Konitsa (zone II) were a partial collapse of a reinforced concrete 4 stories building was observed. In September 1999 a magnitude M5.9 earthquake caused great damage in the metropolitan area of Athens. This was the trigger effect for the government to request for a new updated seismic hazard map of Greece on the basis of the new scientific information gained during the period 1989-1999.

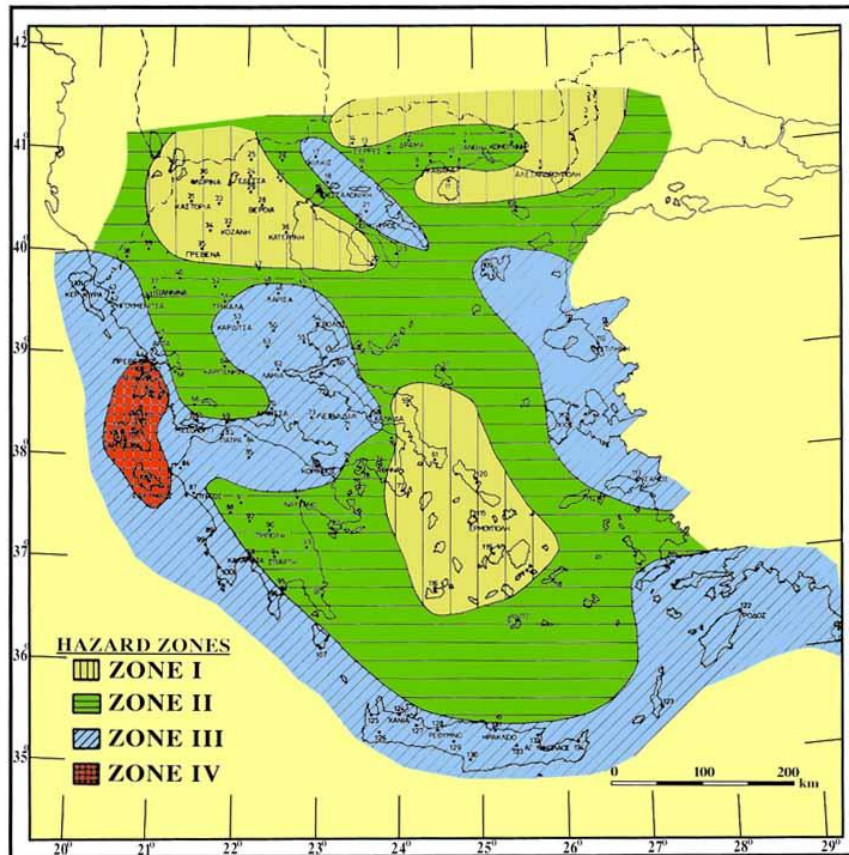


Fig 4. Seismic Hazard map of Greece in the seismic code of 1992 (Papazachos et al., 1992).

Therefore the Institute of Engineering Seismology & Earthquake Engineering (ITSAK), the Laboratory of Geophysics of the Thessaloniki University (GLAUTH), the Geodynamic Institute of Athens (GI.NOA) and the Laboratories of Seismology of Athens (NKUA) and Patras Universities (UP) merged their results obtained by using various input data and procedures (seismotectonic models, seismic sources models, empirical predictive relations, parameters describing the measures of seismic hazard and software) for the compilation of their individual seismic hazard maps.

In order to accomplish its role ITSAK used the seismic sources model of area type sources by Papaioannou and Papazachos (2000) and the hybrid model of area type sources and faults proposed by Papaioannou (2002) and the empirical predictive relations by (Margaris et. al., 2002). The zonation proposed by Papaioannou (2002) took into account the paper by Papazachos et al. (2001) on the geometrical and seismological parameters of the main faults in the broader Aegean area proposed by Papazachos et al., (2001). Both are shown in the maps of figures (Fig 5.) and (Fig 6.).

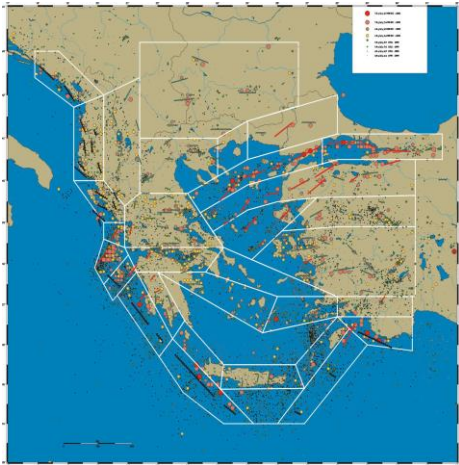


Fig 5. Hybrid model of fault and area sources in the Aegean and surrounding area (Papaioannou, 2001).

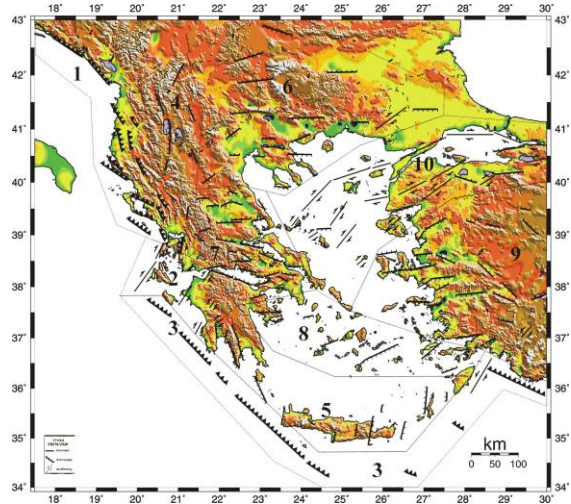


Fig 6. The main faults of shallow strong ($M \geq 6.0$) earthquakes in the Aegean areas (Papazachos et al., 2001).

The two models of shallow and intermediate depth earthquakes compiled by Papazachos (1990) and Papazachos and Papaioannou (1993) which were used by G.I.NOA, NKUA and UPatras are shown in figures (Fig 7) and (Fig 8).

Several empirical predictive relations for the peak ground values were used in Greece which include the publications of Makropoulos (1978), Theodulidis (1991), Theodulidis and Papazachos (1992), Ambraseys (1995), Ambraseys et al, (1996) and Margaris et al. (2001, 2002). A comparison of these relations for a magnitude $M_w=6.5$ earthquake and site conditions “ROCK” are shown in the graph of figure (Fig 9).



Project funded by the
EUROPEAN UNION

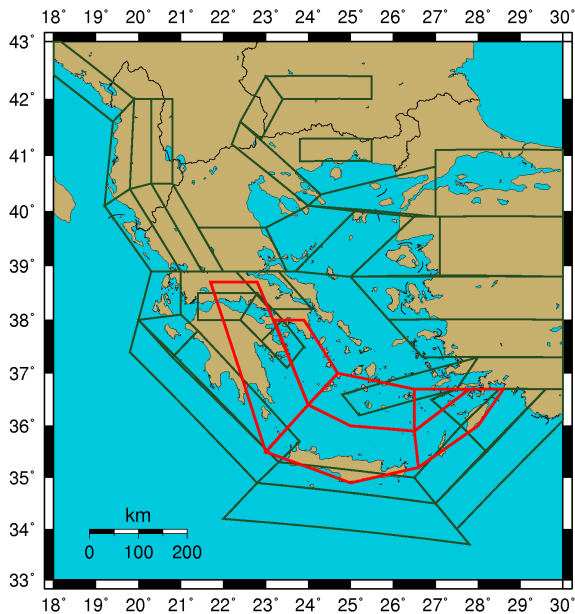


Fig 7. Seismic sources models of shallow (black) and intermediate depth (red) earthquakes (Papazachos, 1990)

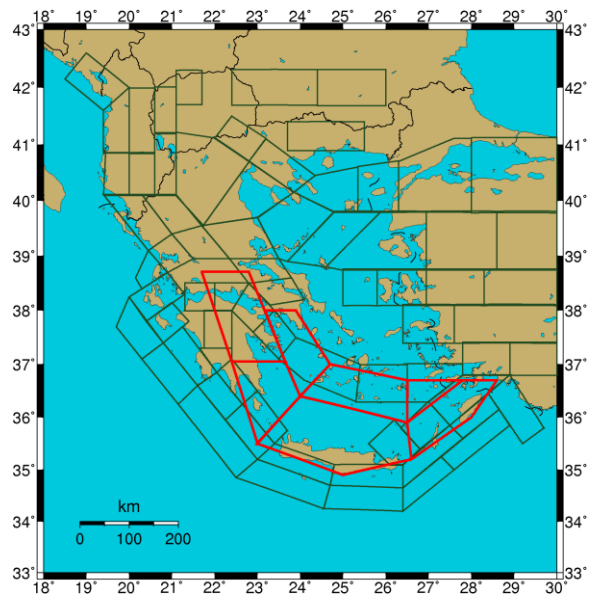


Fig 8. Seismic sources models of shallow (black) and intermediate depth (red) earthquakes (Papazachos and Papaioannou, 1993 revised).

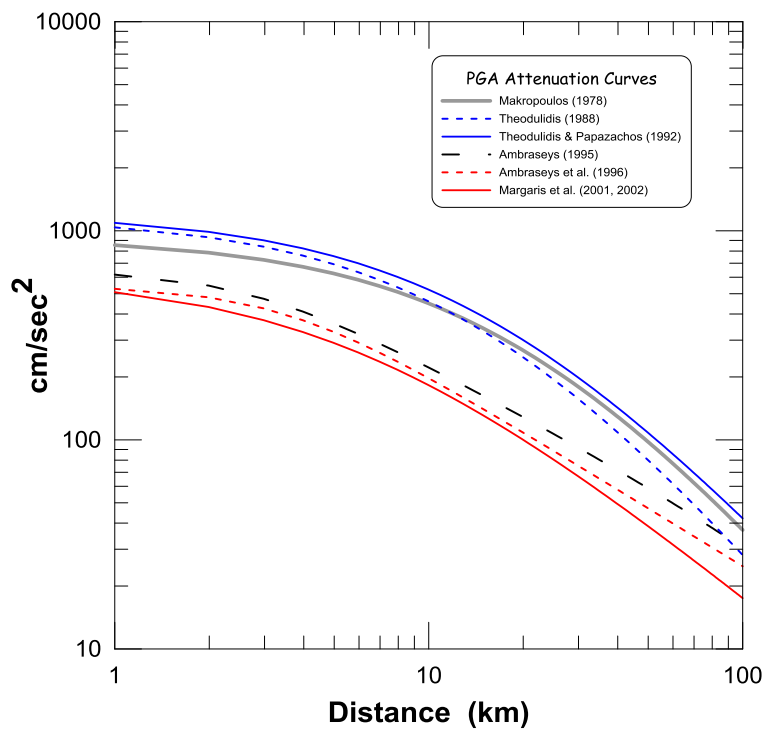




Fig 9. Comparison of the various empirical predictive relations for the PGA, used in the present study for $M=6.5$ and soil conditions “rock”

A scientific committee was established by the Earthquake Planning and Protection Organization for the compilation of the official hazard map based on the results of the five seismological organizations. The committee decided to consider the hazard values of the five partners get the mean value remove the outliers and adopt the remaining values for the compilation of the final hazard map. The geographical distribution of the mean values and the standard deviation values of the peak ground acceleration are shown in the figure (Fig 10) and (Fig 11).

The final seismic hazard map which was included in the revision of the Greek seismic code, it was published in the Government Gazette (Φ.Ε.Κ. Β' 1154/12-8-2003) and is shown in the map of figure (Fig 12). In this map the area of Greece is divided in three zones with design values of the horizontal ground acceleration equals to 0.16g, 0.24 and 0.36g. Practically the geographic areas corresponding to the zones I and II of the previous map were merged into zone I of the new map. It must be pointed out that this map and the seismic code are valid only for ordinary structures of engineering interest. For the construction of special structures which are of significant importance and high levels of security special seismic hazard studies are required.

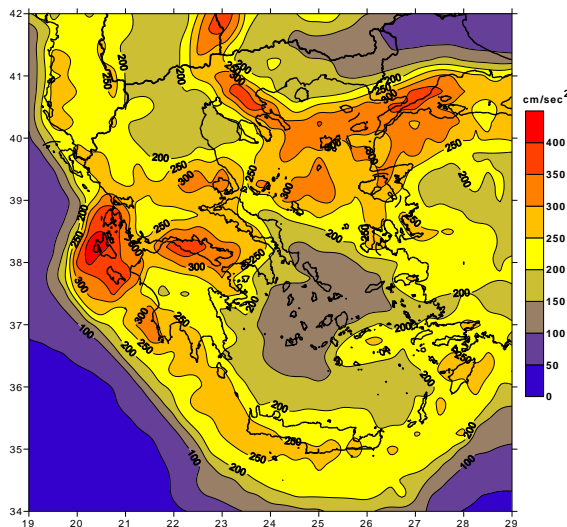


Fig 10. Geographical distribution of the mean values of the peak ground acceleration (cm/sec²) in Greece and surrounding area

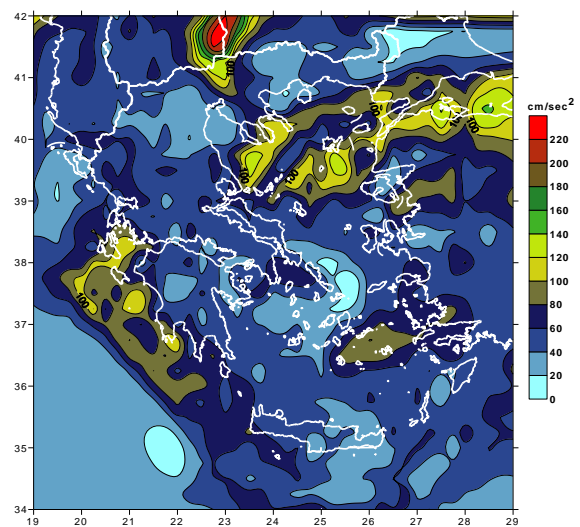


Fig 11. Geographical distribution of the standard deviation of the peak ground acceleration values (cm/sec²) in Greece and surrounding area

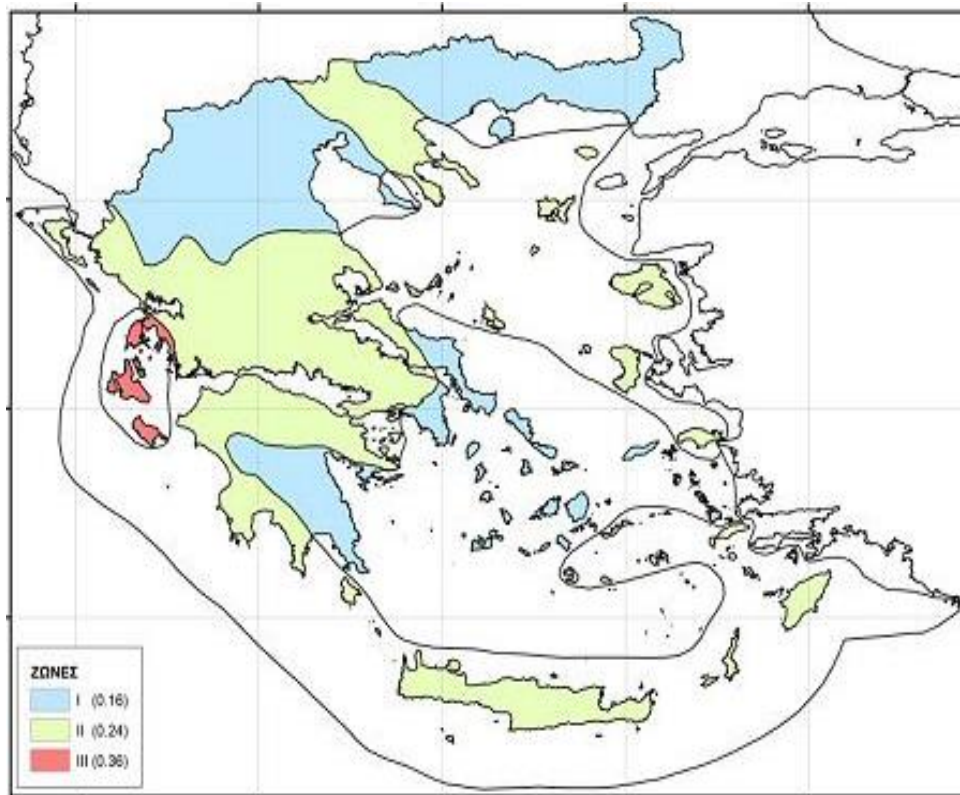


Fig 12. The official current seismic hazard map of Greece

The comparison between the maps appeared in figures (Fig 3.), (Fig 4.), and (Fig 12) shows clearly that the examined area covers low hazard zones.

4.1.2 Seismicity & Seismotectonics of the Area.

The area under study is located in the northern part of the broader Aegean area. The map in figure (Fig. 13) shows the main features of tectonic origin of the Aegean area. The black rectangular denotes the area of the present study. The most important tectonic feature in the broader area is the branch of the North Anatolian Fault with its termination in the North Aegean, located at the southern border of the examined area.

An effective way to study the spatial distribution of seismicity in a certain area is to divide this area into seismic zones or seismogenic regions, that is, into regions with uniform seismo-tectonic features, and to define seismicity parameters in each one of them. Such efforts have been made by several authors



Project funded by the
EUROPEAN UNION



(Papazachos, 1980; 1990; Papazachos and Papaioannou, 1993; Papaioannou and Papazachos, 2000 among others).

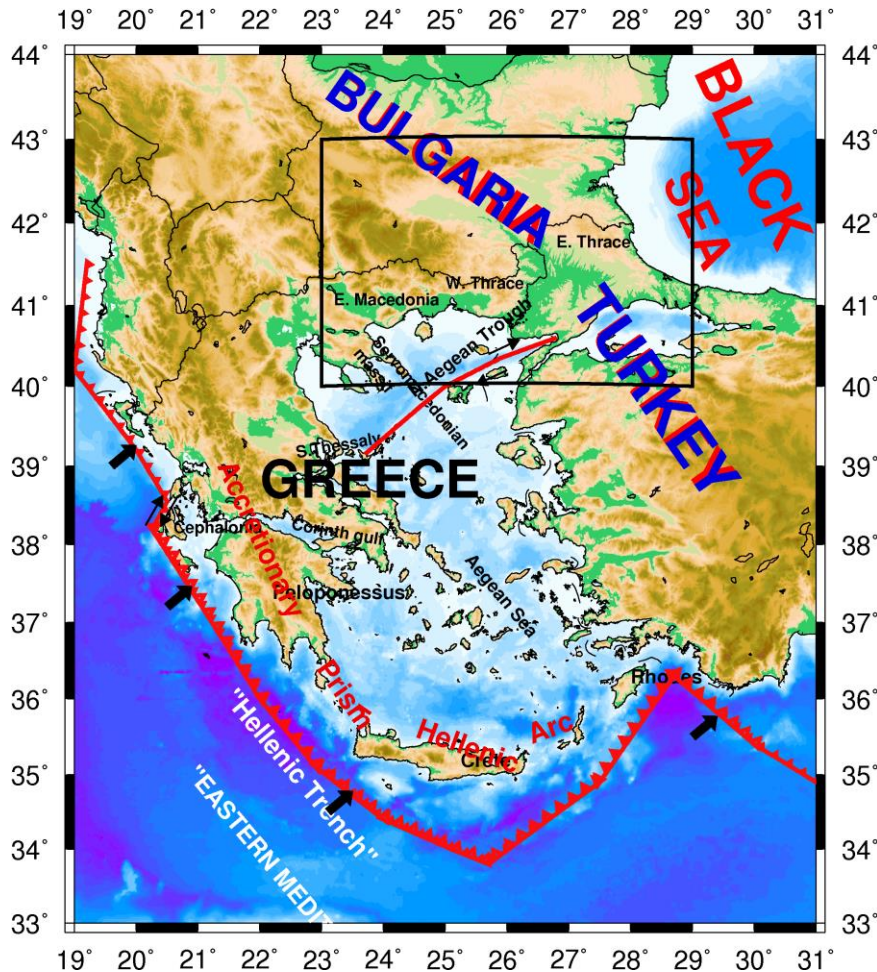


Fig 13. The main features of tectonic origin in the broader Aegean area. The rectangular shows the investigated area.

Using information on seismicity, active tectonics, attenuation pattern of seismic intensities, location of active faults Papazachos and Papaioannou (2000) and Papaioannou (2002) proposed seismotectonic models for the area. The reliability of these models can be proved on the basis of research and applied work numerous publications, which made use of these models.

The map in figure (Fig. 14) shows the location of epicenters of strong $M_w \geq 6.0$ earthquakes since the historical times and the earthquake with $M_w \geq 5.5$ during the instrumental era (1911-2013). The source of the historical earthquakes is the catalogues of Papazachos and Papazachou (2003), while the data for the

period 1900-2013 are from the updated catalogue of Papazachos et al. (2012). Different size and color circles were used to denote the various magnitudes of earthquakes and time period as in legend.

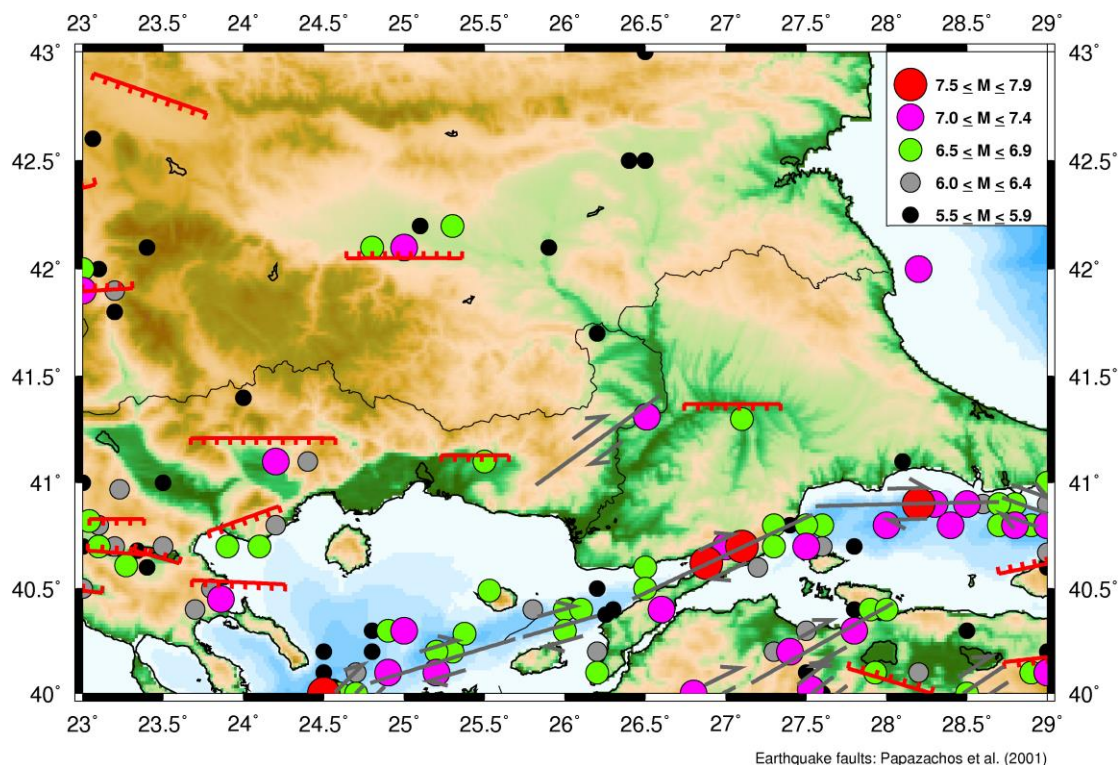


Fig 14. Geographical distribution of strong earthquakes within the investigated area. The faults are after Papazachos et al. (2001).

The map in figure (Fig 15) shows the distribution of the moderate-to-small magnitude ($3.5 \leq M_w \leq 5.4$) earthquakes during the instrumental era according to the legend.

From the maps in figures (Fig 14) and (Fig 15.) one can conclude that the area is a low seismicity region with considerable activity of moderate magnitude events and nucleation of strong earthquakes mainly at the borders. The highest activity is related to the Servomacedonian zone, the north Aegean trough and the north Anatolia fault, the Kresna and Plovdiv fault areas. The activity at the area of the July 29, 1752 Havsa earthquake (41.41N 26.61E, $M=7.5$) and the November 6, 1784 Komotini earthquake (41.10N 25.30E, $M6.7$) is very low.

EARTHQUAKES 1911 – 2014, $M \leq 5.9$

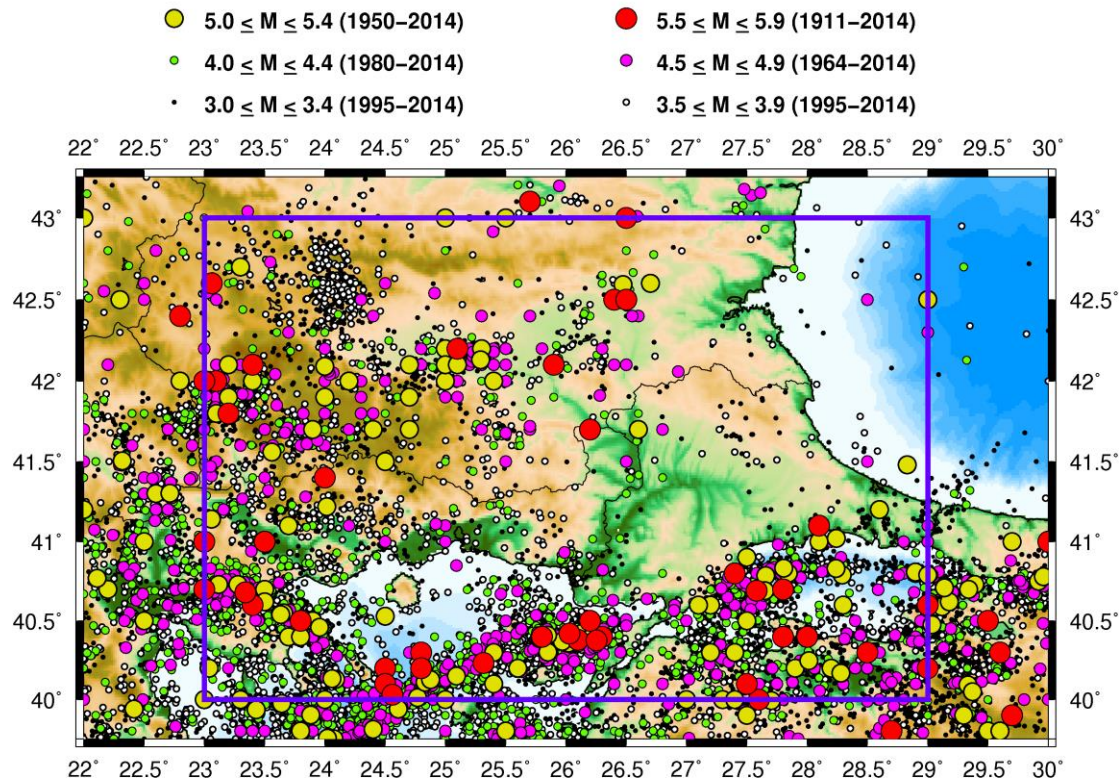


Fig 15. Geographical distribution of moderate-to-small earthquakes within the investigated area shown by a rectangular. Information of the time period and size of the events are shown in the legend.

The map in figure (Fig 16) shows the location of the area type sources proposed by Papaioannou and Papazachos (2000) (blue polygons) and the epicenters of the earthquakes. The table (table 4.1) includes information on the seismicity parameters of the sources which mostly influences the results of the seismic hazard in the area.

Table 4.1.1 Information on the seismicity parameters of the sources which influence the examined area (Papaioannou and Papazachos (2000)).

Name	b	a	Area Km ²	M_{\max}	Rate $M \geq 5.0$
Philipoupolis	0.79	3.23	14315	6.9	0.187
Kresna	0.83	3.44	20078	7.2	0.196
Drama	0.81	3.22	17305	7.0	0.158



Serres	0.82	3.54	9271	7.0	0.271
Athos	0.83	3.92	5249	7.3	0.595
Samothrace	0.82	3.76	10088	7.1	0.467
Hellispontos	0.80	3.74	19181	7.5	0.527

The map in figure (Fig 17) shows a hybrid model of line-type and area-type sources, which was proposed for the broader area (Papaioannou, 2002). In this model the strong ($M \geq 6.0$) earthquakes are associated with faults and the smaller events were considered that are located within the sources. This model takes into account the modern opinion on the distribution of strong events which is that the association of strong events with faults is more realistic than the view of having the same probability for the occurrence of a large magnitude event at every place within a seismic source. The faults are after Papazachos et al. (2001).

Area Sources Model (BSSA 2000)
with distribution of strong & moderate events

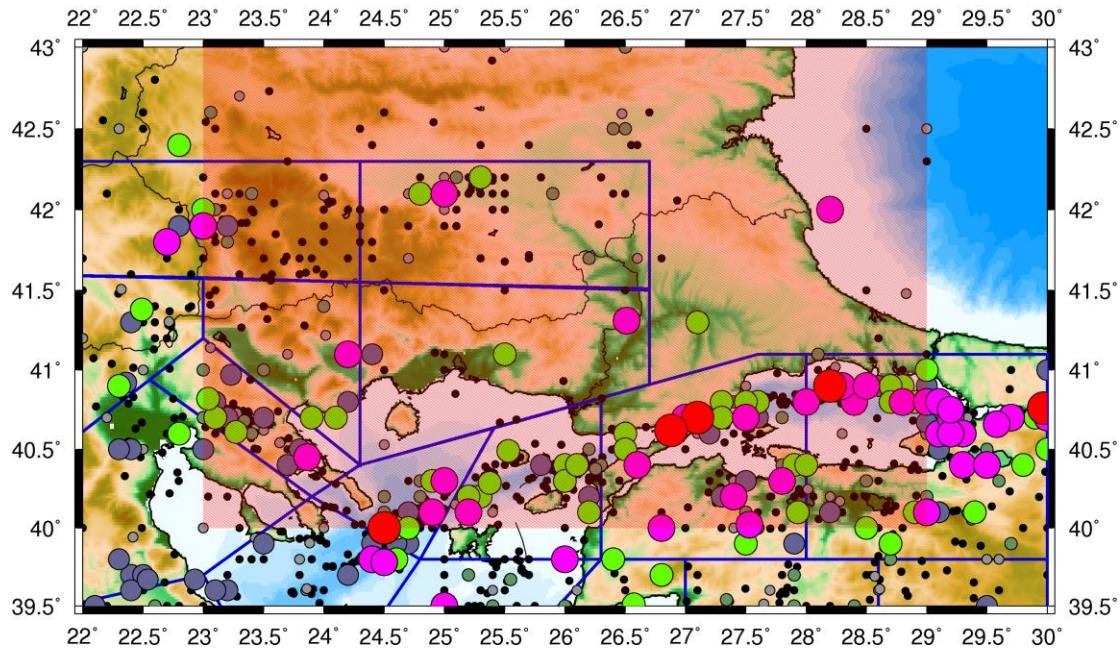


Fig 16. Geographical distribution the epicenters of the known earthquakes at the broader area of the investigated area (shown by pink-hatched rectangular). The blue polygons show the seismic sources proposed by Papaioannou and Papazachos (2000).

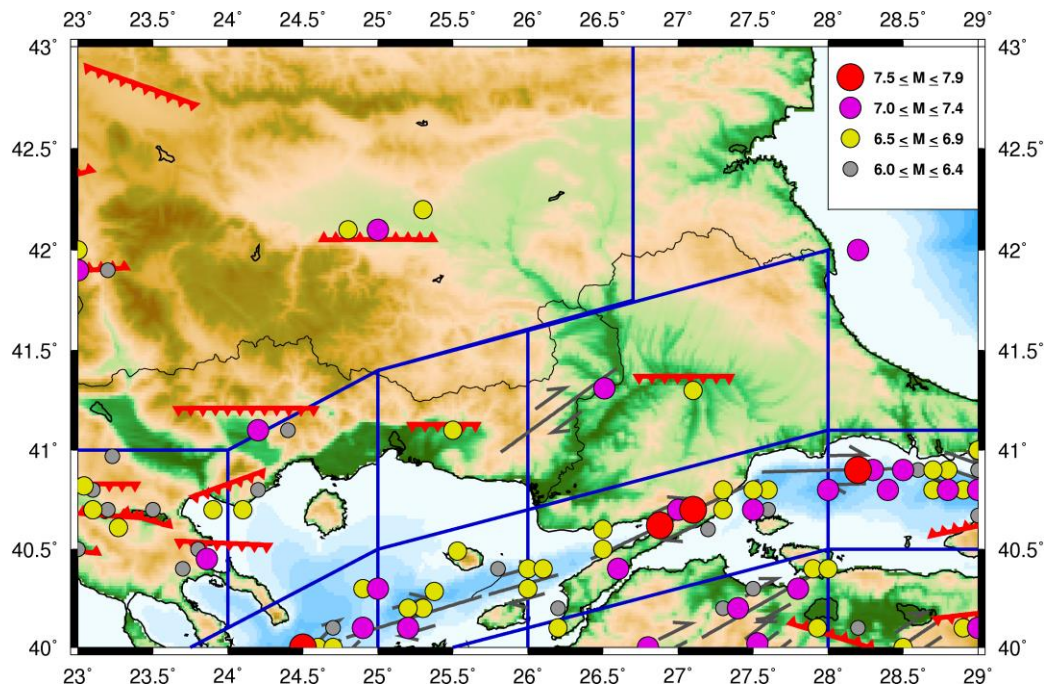


Fig 17. A hybrid model of area-type and line-type (faults) in the area Papaio-annou (2002). The faults are after Papazachos et al. (2001). The red lines represent normal faults while the grey linear symbols stand for the strike slip faults.

4.1.3 Empirical Predictive Relations of Macroseismic Intensities

In order to assess the seismic hazard at a site, it is necessary to adopt reliable relations describing the dependence of the seismic intensity measures as a function of the distance and source properties of the earthquakes in the area. The parameters which are usually used for these purposes are the macroseismic intensity and the peak values of the ground motion. In the present study the empirical relations for the macroseismic intensity and the peak ground acceleration were used.

The macroseismic intensities were used because the macroseismic intensity, effect of the earthquake, is the only procedure to investigate historical events and link them with the current situation. Furthermore using scaling relations holding between the macroseismic intensity and instrumental parameters of the



ground motion, we can define with acceptable uncertainties the distribution of the maximum values of instrumentally determined parameters as pga, pgv or pgd.

Several attenuation relations of macroseismic intensity as a function of magnitude and distance have been proposed for the Balkan area. Due to their simplicity such relations are used in seismic hazard assessment especially in the Cornell's (1968) method. During the last thirty years 356 macroseismic maps with more than 30.000 macroseismic intensity data points of shallow earthquakes in the Balkan area have been compiled (Papazachos and Papaioannou, 1997). Based on this large number of macroseismic observations a new attenuation relation has been proposed. This relations is,

$$I - I_0 = -3.59 \log (\Delta + 6) + 3.19 \quad (1)$$

where I_0 is the epicentral intensity. The aforementioned authors have also proposed relations between epicentral intensity I_0 and magnitude M , applicable separately for every Balkan country independently. For Greece the proposed relation (Papazachos and Papaioannou, 1997) is,

$$I_o = 1.43M - 0.93 \quad (2)$$

From the relations (1) and (2) the average macroseismic attenuation relation for the area of Greece is,

$$I_i = 2.26 + 1.45M - 3.59 * \log(\Delta + 6) \quad (3)$$

Relation (3) was used for the seismic hazard assessment calculations considering the macroseismic intensity as a parameter of the seismic hazard.

Figure (Fig 18) shows a comparison of attenuation relations as a function of the macroseismic intensity for various areas of the world (Papazachos and Papaioannou, 1997). It is clear that regions with high seismic activity (Balkans, W. USA, and Italy) show high attenuation compared with less active areas as E.USA, NW Europe and Scandinavia.

Poardi firstly used Macroseismic data in 1627 in an attempt to measure the size of the earthquakes. Since the beginning of the 19th century macroseismic observations were routinely reported in the bulletins of the Observatory of Athens. Until 1934 the Rossi-Forell intensity scale was used, while since 1950 an intensity scale equivalent to the Modified Mercalli scale has been being used (Shebalin, 1974).

In Greece, macroseismic observations were firstly used for the definition of isoseismals of shallow and intermediate depth earthquakes by several authors. It has to be mentioned that substantial work has been done during the time period 1936-1949 when no bulletins were published by the Observatory of Athens (Galanopoulos, 1941, 1944, 1949, 1950, 1953, 1954; Ambraseys, 1988; Ambraseys and Jackson, 1990).



Moreover, the study of individual earthquakes included, among other topics, the study of their macroseismic fields.

The Geophysical Laboratory of the Aristotle University of Thessaloniki, recognizing the importance of the study of the macroseismic observations for Earthquake Engineering, started to collect macroseismic data in the beginning of '80. Papazachos and Papazachou (1989) presented a catalogue of strong ($M \geq 6.0$) earthquakes, which occurred in the Aegean and surrounding area during 550BC-1986. Papazachos et al. (1997a, b), used an updated and more complete catalogue of strong earthquakes occurred in the Aegean area during 550BC-1996 (Papazachos and Papazachou, 1997), and after extracting macroseismic data from the bulletins of the Observatory of Athens (1900-1939 and 1950-1996), compiled a data base consisting of 37,000 macroseismic observations of 900 earthquakes, which occurred in this area. This data base can be used for the determination of attenuation relations for every site in Greece, for the compilation of synthetic isoseismals and the definition of rupture zones. It can also be used to test the results of probabilistic seismic hazard studies (Papazachos and Papaioannou, 1998; Papazachos et al., 1998).

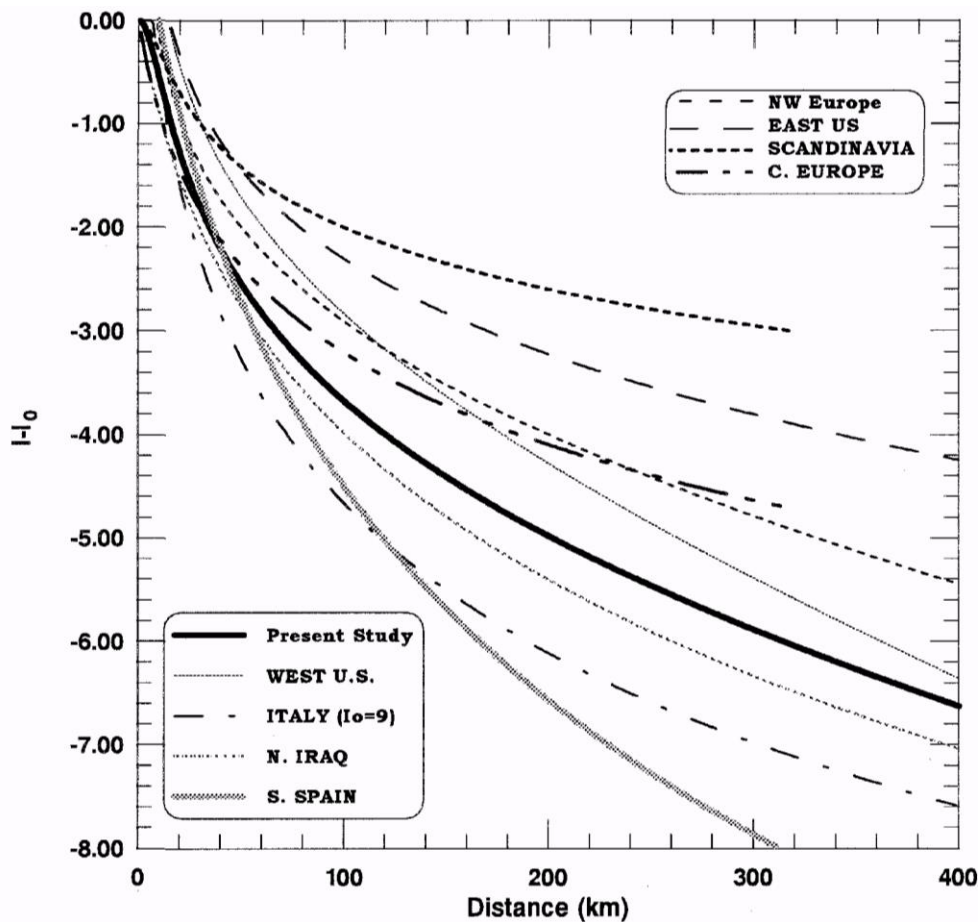


Fig 18. Comparison between various attenuation relations holding for different areas of the world. The continuous black line stands for the Aegean area (Papazachos and Papaioannou, 1997).

The maps in figures (Fig 19), (Fig 20), (Fig 21), (Fig 22), (Fig 23) and (Fig 24) show the macroseismic field of strong earthquakes in the examined area.

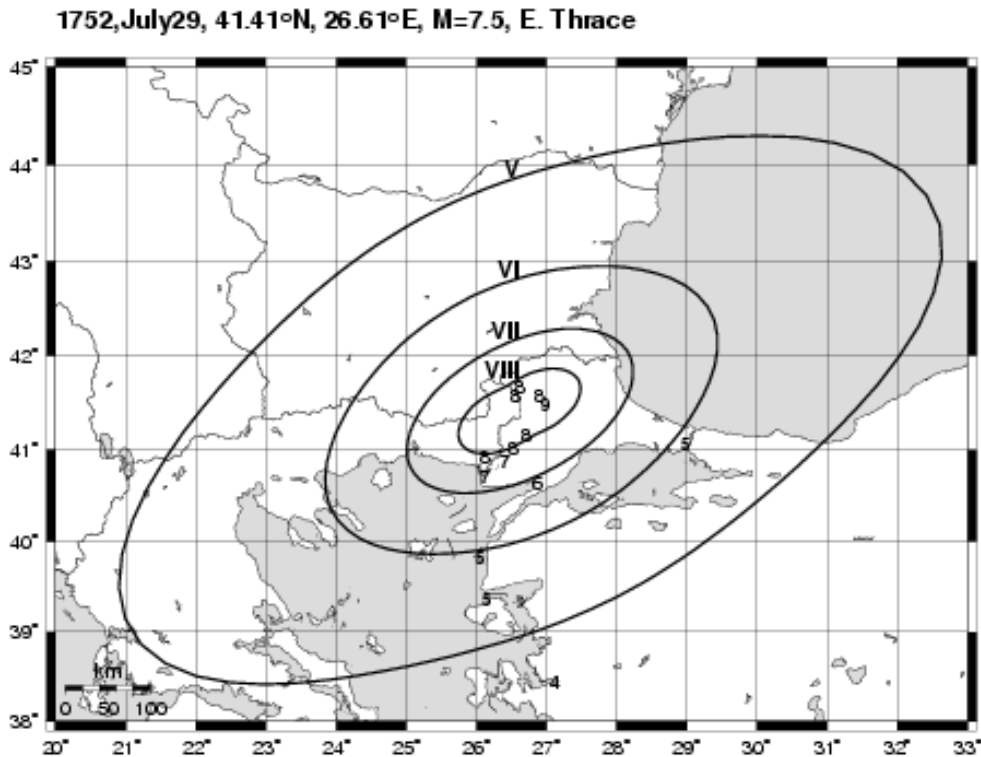


Fig 19. Isoseismal map of the earthquake of 1752 in Thrace (Papazachos et al., 1997a).



Project funded by the
EUROPEAN UNION



1829, May 5, 41.10°N, 24.50°E, M=7.3, Drama

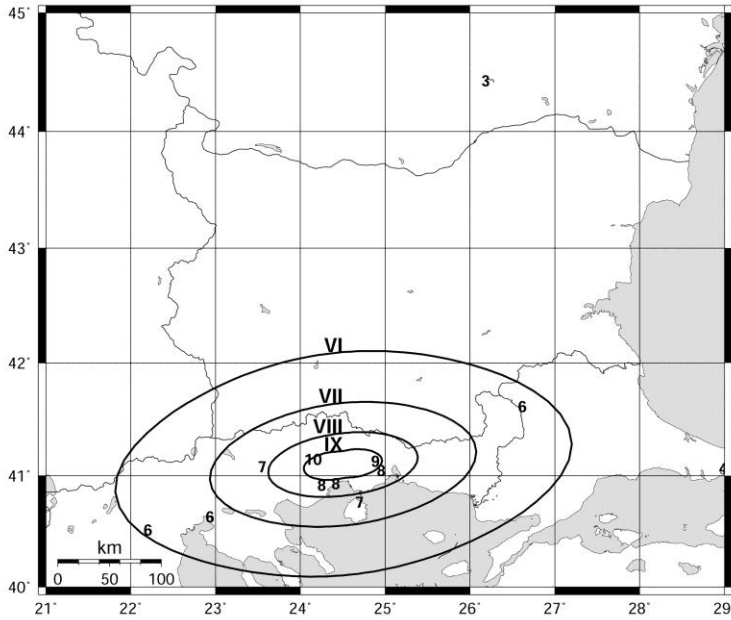


Fig 20. Isoseismal map of the earthquake of May 5, 1829 M=7.3 (Papazachos et al., 1997a).

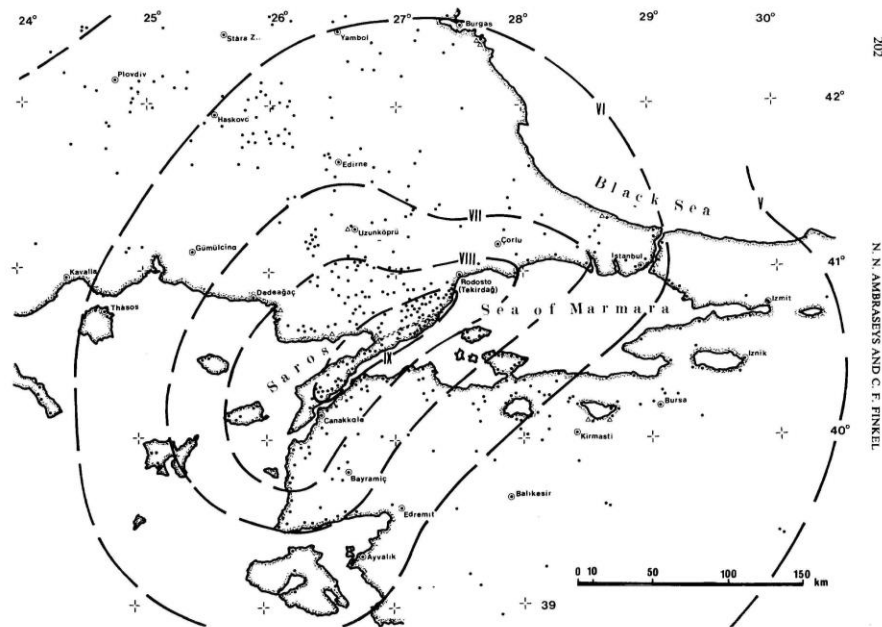


Fig 21. Isoseismal map of the earthquake of August 9, 1912 M7.6 earthquake (Ambraseys and Finkel 1987).

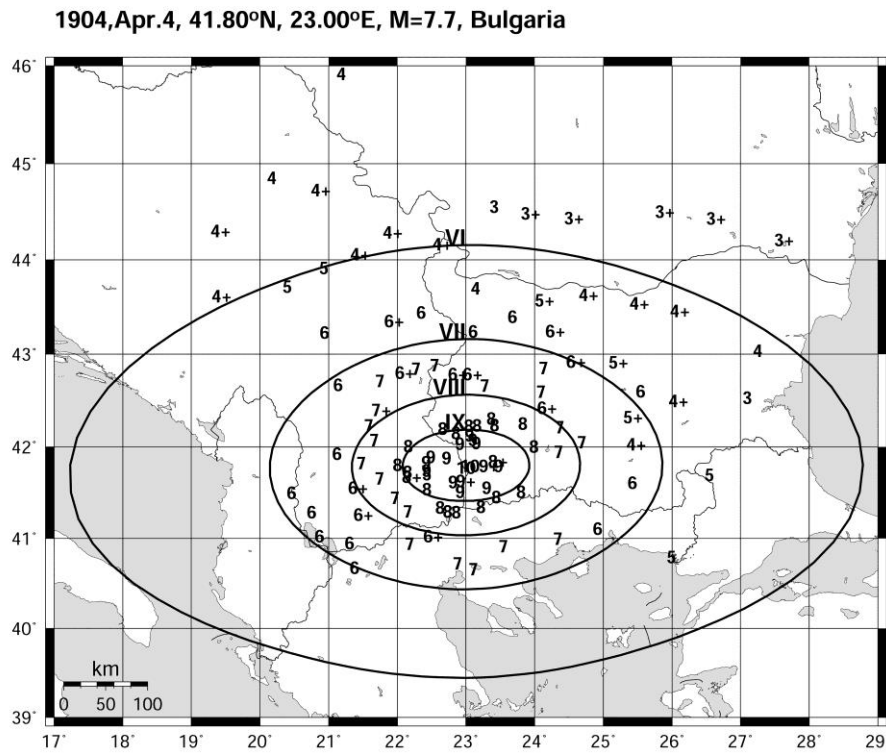


Fig 22. Isoseismal map of the earthquake of April 4, 1904 M=7.7 Kresna mainshock. (Papazachos et al., 1997a).



Project funded by the
EUROPEAN UNION



1928, Apr.14, 42.15°N, 25.28°E, M=6.8, Bulgaria

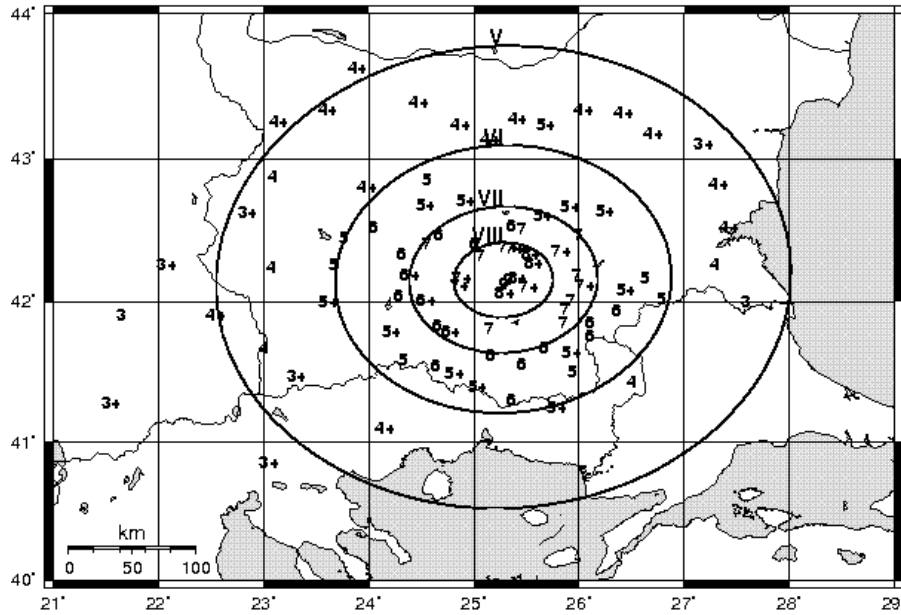


Fig 23. Isosismal map of the earthquake of April 14, 1928 M=6.8 Plovdiv earthquake. (Papazachos et al., 1997a).

1932, Sep.26, 40.45°N, 23.76°E, M=7.0, Hierissos

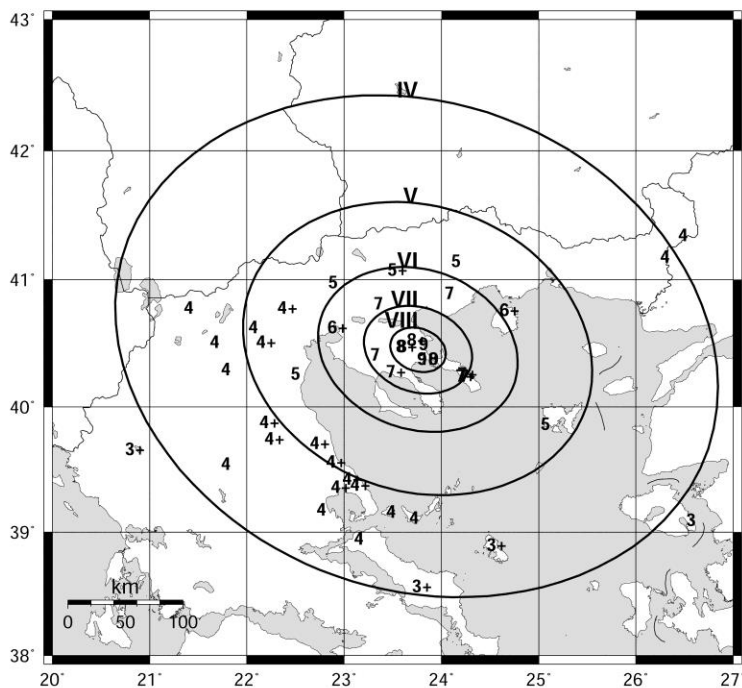




Fig 24. Isoseismal map of the earthquake of September 26, 1932 M=7.0 Ierissos earthquake. (Papazachos et al., 1997a).

It is obvious the influence of the NE-SW striking strike slip strong earthquakes at the eastern part and the EW striking normal faults on the pattern of macroseismic field in the area.

4.1.4 Distribution of Maximum Macroseismic Intensities in the Study Area

For the estimation of the maximum macroseismic intensities that have been observed at the area of study, it is necessary to have a set of macroseismic observations for the study area covering a long time window. Although a large number of observations is available for the study area, the use only of observed macroseismic intensity values is problematic. The main limitation of the observed intensity data set is that frequently no observations are available for the site under study, either due to the absence of important cities or towns, or due to the lack of information concerning the damage distribution from certain large events. For this reason, it was initially considered appropriate to use deterministically computed macroseismic intensities for the broader study area.

For these estimations, the earthquakes that had the most significant impact on the broader area of the study were used.

For the modeling of the macroseismic field of the previous earthquakes the formulation of Papazachos (1992) was used. This formulation assumes that the main energy source for each event can be represented by a point source and therefore the Kovesligethy relation can be used:

$$I - I_0 = n \log \sqrt{1 + \frac{\Delta^2}{h^2}} + c(\sqrt{\Delta^2 + h^2} - h) \quad (4)$$

where I_0 is the epicentral intensity, I is the observed intensity at distance Δ , h is the source depth, n is the geometrical spreading factor and c is the anelastic attenuation coefficient. The main modification in the applied formulation is that the isoseismals are assumed to have an elliptical shape, due to the anisotropic radiation of the seismic energy at the source. Therefore, equation (6) is modified to:

$$I - I_{0_{\min}} = n \log \left(S^{1/2} \sqrt{1 + \frac{\Delta^2}{h^2}} \right) + c(\sqrt{\Delta^2 + h^2} - h) \quad (5)$$

where $I_{0_{\min}}$ defines the apparent epicentral intensity at the direction of the minimum energy radiation (small axis of the elliptical isoseismals), and S is a factor which determines the azimuthal variation of the intensity and which is given by:

$$S = 1 - \varepsilon^2 \cos^2(\zeta - \phi) \quad (6)$$

where ε is the ellipticity of the isoseismals, ζ is the azimuth of the major axis of the elliptical isoseismals and ϕ is the azimuth of each site/direction we are studying. It can be shown (Papazachos, 1992) that at each direction equation (6) still applies with an “equivalent” epicentral intensity at each direction which is given by:

$$I_0(\phi) = I_{0_{\min}} + \frac{n}{2} \log S \quad (7)$$

Using the previous methodology and the values $n=-3.227$ and $c=-0.0033$ estimated by Papazachos and Papaioannou (1997), we computed the intensity values for the earthquakes using a grid with a spacing of 2 km which covered the broader study area. For every point we combined the results that are based on estimations, with the observed macroseismic intensities, which were extracted from the data bank of macroseismic information (Papazachos et al., 1998). The final results (in MM scale) are presented in the map of figure (Fig 25), which shows the distribution of the maximum intensities based on the overlapping of the above mentioned results.

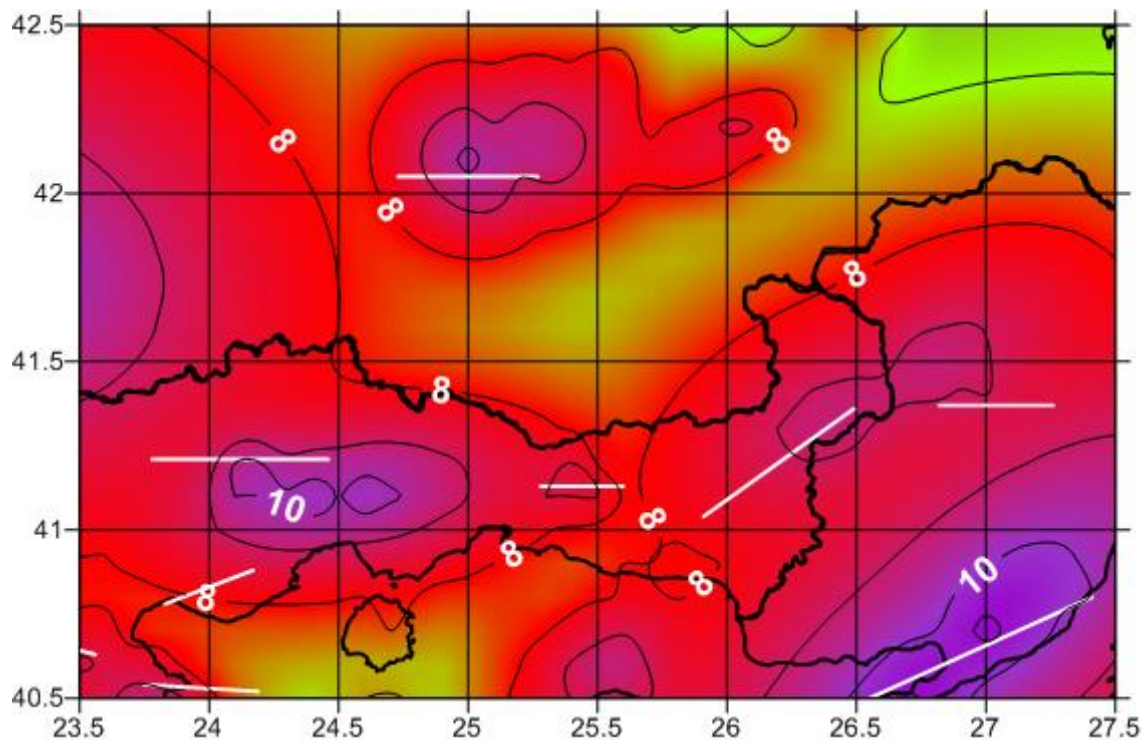


Fig 25. Map depicting the geographical distribution of the maximum macro-seismic intensities in the examined. The main faults of strong earthquakes (Papazachos et al., 2001) in the area are also shown.



4.1.5 Information of Empirical Predictive Relations of Horizontal Peak Ground Acceleration

Seismic hazard assessment is commonly based on empirical predictive attenuation relations. Such relations are generally expressed as mathematical functions relating a dependent variable to parameters characterising the earthquake source, propagation path and local site conditions. To date many attenuation relations for peak ground acceleration, velocity and displacement have been published based on ever increasing number strong motion data from the Circum Pacific region as well as from Europe and Middle East region.

Attenuation of strong ground motion in Greece in terms of peak ground acceleration, velocity and spectral pseudovelocity has been studied and relevant empirical models have been proposed for shallow earthquakes (Theodulidis and Papazachos 1992, 1994; Margaritis et al. 2001, 2002, Tselentis and Danciu, 2008, 2010).

Recently, Skarlatoudis et al. (2003) proposed predictive relations for the attenuation of peak ground acceleration (PGA in cm/sec²), velocity (PGV in cm/sec) and displacement (PGD in cm) for shallow earthquakes in Greece of the general type:

$$\log Y = c_0 + c_1 M_w + c_2 \log(R^2 + h^2)^{1/2} + c_3 F + c_5 S \quad (8)$$

$$\log Y = c_0 + c_1 M_w + c_2 \log(R + c_4) + c_3 F + c_5 S \quad (9)$$

where Y is the strong motion parameter to be predicted, M is the moment magnitude, R is the epicentral distance, h is the focal depth of each earthquake, S is the variable accounting for the local site conditions and F is the variable referring to the effect of the faulting mechanism of the earthquakes in the predicting relations. Scaling coefficients c₀, c₁, c₂, c₃ and c₅ are to be determined from regression analysis. Coefficient c₄ in equation (11) accounts for saturation in the near field and is difficult to be determined directly by regression analysis on the available data given its strong correlation with scaling coefficient c₂, as it was shown using appropriate Monte-Carlo simulations (Papazachos and Papaioannou, 1997, 1998). For this reason value of c₄=6km was adopted from Margaritis et al. (2002), that roughly corresponds to the average focal depth of the events used in the present study.

$$\ln Y = c_0 + c_1 M_w + c_2 \ln(R + r_0) + c_3 S + c_4 * F \quad (10)$$

and

$$\ln Y = c_0 + c_1 M_w + c_2 \ln \sqrt{(R^2 + h_0^2)} + c_3 S + c_4 * F$$

where Y is the strong motion parameter to be predicted, M_w is the moment magnitude, R is the epicentral distance, S is a variable which takes the value 0 for the soil category B, 1 for the C and 2 for the D and F is a variable which is related to the faulting mechanism. Scaling coefficients c₀, c₁, c₂, c₃, c₄ are to be determined from regression analysis. Coefficient r₀ accounts for saturation in the near field, while h₀ is



known as “effective” depth of an event, that is, depth where seismic energy is released. Both equations are practically similar apart from the fact that the first has a simple term for distance and in the near field they give slightly different results.

The following pairs of attenuation relations were defined for horizontal PGA (cm/sec^2) and PGV (cm/sec):

$$\ln \text{PGA} = 4.16 + 0.69M_w - 1.24 \ln(R+6) + 0.12 * S \pm 0.70 \quad (11a)$$

$$\ln \text{PGA} = 3.52 + 0.70M_w - 1.14 \ln(R^2 + 7^2)^{1/2} + 0.12 * S \pm 0.70 \quad (11b)$$

The last term gives the ± 1 standard deviation of each relation.

The data set used consist of 1000 strong motion recordings, corresponding to 225, mainly normal and strike-slip faulting, shallow earthquakes in Greece. This data set was selected from the entire database of the available accelerograms in Greece (ITSAK: www.itsak.gr and NOA: www.noa.gr) that spans the period 1973-1999. The selected records satisfy at least one of the following criteria: (a) The earthquake which triggered the instrument should have a moment magnitude of $M \geq 4.5$, (b) The strong motion record should have a peak ground acceleration $\text{PGA} \geq 0.05g$, independent of the earthquake magnitude or, (c) The record can have $\text{PGA} < 0.05g$ but another record with $\text{PGA} \geq 0.05g$ should be available from the same earthquake.

In Figure (Fig 26) comparison of the horizontal PGA relations with those proposed by Ambraseys et al., (1996), for “rock” ($S=0$) soil conditions, is shown. For distances up to about 30km a good agreement is observed whereas for longer distances the latter relations give higher PGA values. Such a deviation may be due to different data sets used in regression analyses. For instance, Ambraseys used data from various seismotectonic environments that extend to long site-to-source distances.

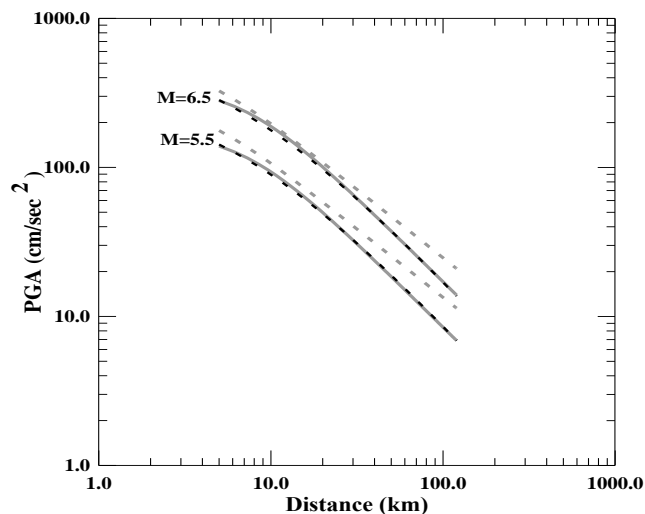


Fig 26. Comparison of the PGA empirical relations, (11a) (grey continuous line) and (B) (black dashed line) with those proposed by Ambraseys et al (1996) (grey dashed line) for $M=5.5$ and 6.5 and rock soil conditions.

Sabetta and Pugliese (1996) based on strong motion data from normal and thrust faulting-type earthquakes occurred in Italy, proposed horizontal PGA and PGV attenuation relations. In Figure (Fig 27) comparison of their horizontal PGA attenuation relation with those presented in this study, for “rock”(S=0) soil conditions, shows systematically higher values of the former. This difference may be due to the fact that Italian data come from both normal and thrust faulting events while the Greek data mainly from normal faulting. Spudich et al (1993) based on strong motion data from normal faulting earthquakes proposed horizontal PGA attenuation relation, that is compared with PGA attenuation relation of this study, for “rock”(S=0) soil conditions (Fig 28). For magnitude $M_w=6.5$ there is good agreement between the two relations while for $M_w=5.5$ divergence mainly in long distances is observed.

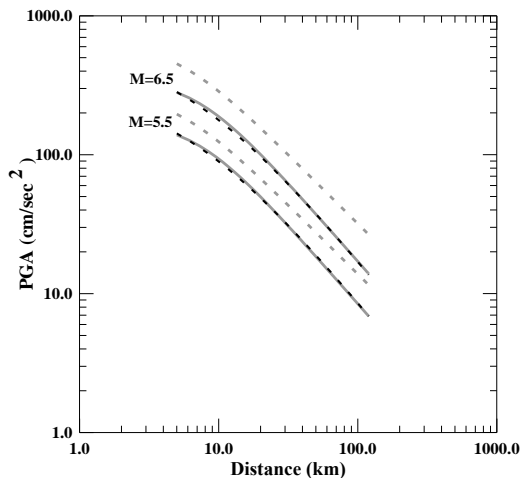


Fig 27. Comparison of the PGA empirical relations Eqs. (A) (grey continuous line) and (B) (black dashed line) with those proposed by Sabetta and Pugliese (1996), (grey dashed line) for $M=5.5$ and 6.5 and rock soil conditions.

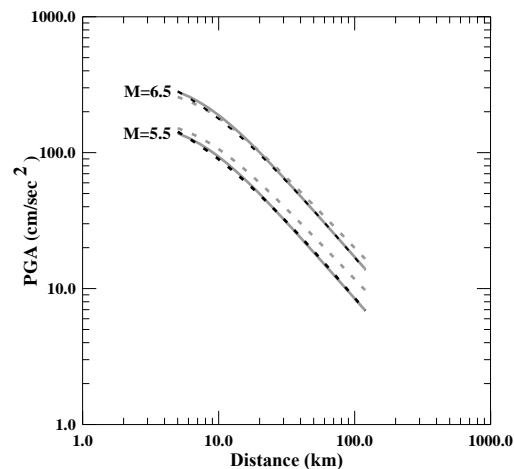


Fig 28. Comparison of the PGA empirical relations Eqs. (A) (grey continuous line) and (B) (black dashed line) with those proposed by Spudich et al (1993), (grey dashed line) for $M=5.5$ and 6.5 and rock soil conditions.

Recently Skarlatoudis et al (2004) found that the attenuation of the small-to-moderate magnitude earthquakes in Greece show different pattern in comparison with the strong earthquakes. This observation must be taken into account especially in seismic hazard studies for areas affected by strong earthquakes with large mean return periods, where the adoption of one attenuation relation may result in overestimation of the results.



Figure (Fig 29) shows a comparison of the predictive relations defined by Skarlatoudis et al (2004), with those proposed by Campbell (1989), Theodulidis and Papazachos (1992).and Skarlatoudis et al. (2003). All relations are scaled at the epicentral distance of 20 Km and plotted against magnitude. Skarlatoudis (2004) relation is plotted for site category C, using the classification proposed by NEHRP and UBC. Plotting against magnitude would reveal a proper definition of the scaling law that rules the predictive relations in low magnitude range. The expected results from this kind of comparison would be continuous curves for the entire range of magnitudes. On the contrary, they observed the existence of a “step” in the predicted levels of PGA around the magnitude of $M=4.5$, as can be seen in figure (Fig 29).

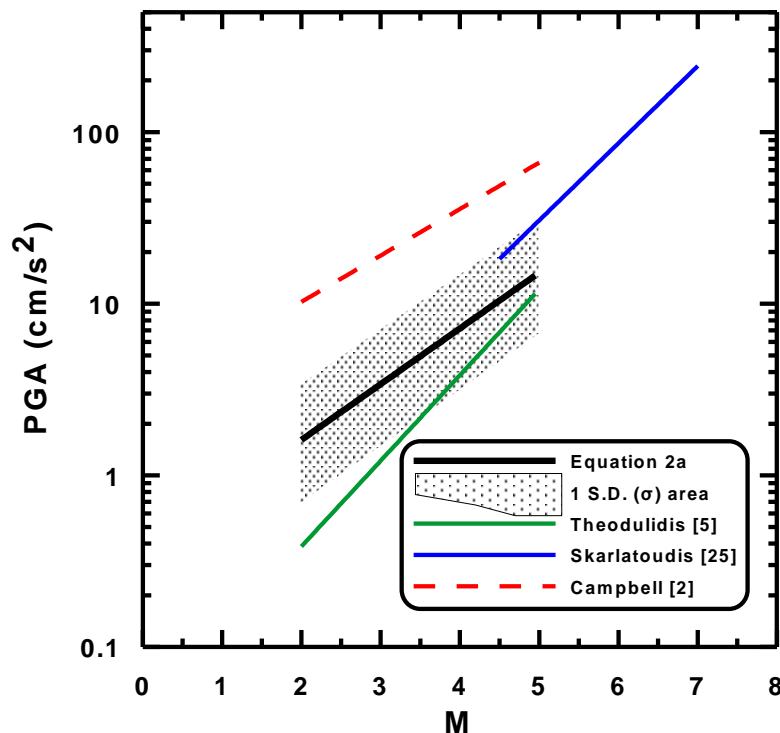


Fig 29. Comparison of the PGA empirical relations (black continuous line), with those proposed by Campbell (1989) (red dashed line), Theodulidis and Papazachos (1992) (light green dashed) and Skarlatoudis et al (2003) (light blue continuous line) for epicentral distance $R=20$ Km.

This observation was taken into account in the calculations of the present work by modification of the computer codes used.

ITSAK during the last years upgraded its network of accelerographs with the installation in the territory of Greece of a dense network of continuous recording accelerographs. These instruments are of CMG-5TDE type of Guralp Systems Ltd (<http://www.guralp.com/product-range/5t-accelerometers/>) and are equipped with broadband accelerometers, recording unit with 24 bits resolution, GPS timing system and transfer the data in real time at the premises of ITSAK in Thessaloniki using the network SYZEFXIS of the public sector of the Hellenic Republic. The red triangles in the map in figure (Fig 30) show the geographical distribution of the CMG-5TDE accelerographs in the investigated area. The inverted triangles and the black circles represent additional instruments of lower resolution which work in trigger mode.

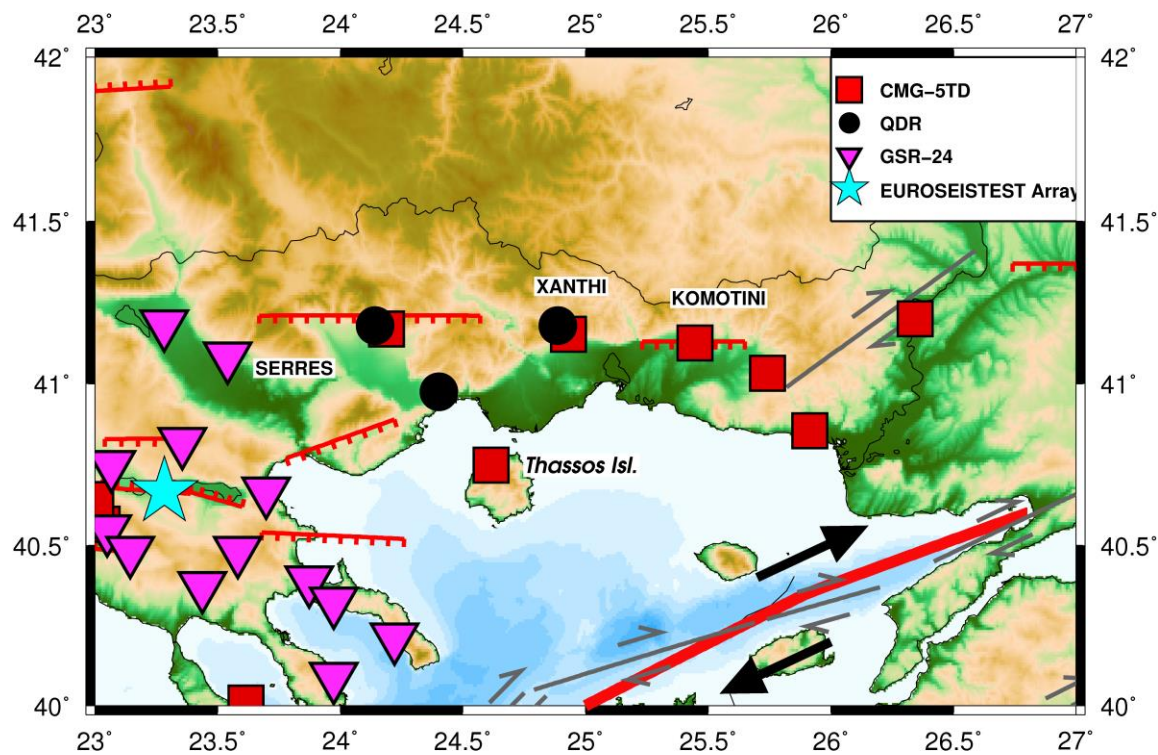


Fig 30. Geographical distribution of the network of broadband accelerographs (red squares) and strong motion instruments (other symbols as in legend) within the studied area. The cyan star stands for the location of the Euro-SeistTest array



During the last years two moderate magnitude events took place and triggered the network. The map in the figure (Fig.31) shows the accelerographic network of ITSAK and the location of the epicenters of these two earthquakes and the fault plane solution after global CMT project. Different colored symbols were used for the reorientation of the various types of instruments as it is explained in the legend. The two blue stars depict the location of the two ETNA strong motion instruments in the area of Sofia.

Table (4.2) summarizes the results of the recorded acceleration values by the two stations in Sofia and the stations located at the Greek eligible area.

Table 4.1.2 Results on the analysis of selected records of the May 22, 2012 earthquake in Bulgaria.

HORIZONTAL COMPONENTS

Component	Distance	PGA	PGV/PGA
KMT_N	260	8.2	0.12
KMT_E	260	7.88	0.12
THS_E	246	3.25	0.07
THS_N	246	5.99	0.06
SAP_E	285	4.27	0.16
SAP_N	285	5.09	0.13
SFL_N	316	12.62	0.07
SFL_E	316	10.97	0.08
XAN_N	226	6.47	0.14
XAN_E	226	10.56	0.09
SBO_E	32	91.6	0.065175
SBO_N	32	98.2	0.130957
SGF_E	41	38.1	0.12126
SGF_N	41	29.88	0.163655

VERTIOCAL COMPONENTS

KMT_Z	260	2.87	0.2
THS_Z	246	2.72	0.06



SAP_Z	285	3.17	0.12
SFL_Z	316	5.37	0.07
XAN_Z	226	10.78	0.103
SBO_Z	32	47.4	0.068143
SGF_Z	41	18.2	0.091758

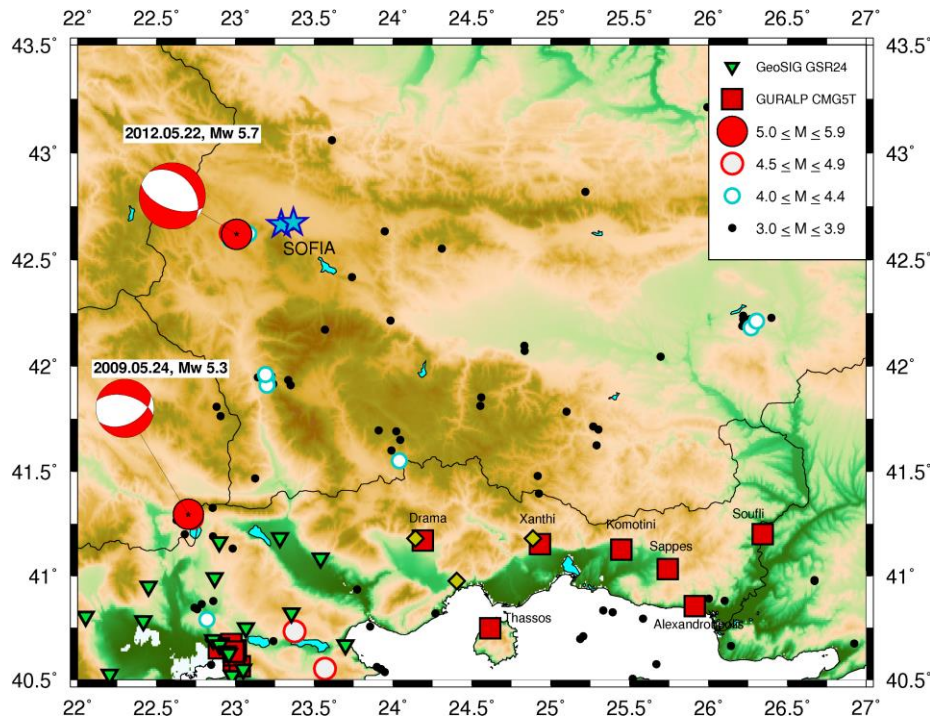


Fig 31. Geographical distribution of the network of the accelerographs and strong motion instruments, epicenters of earthquakes with $M > 3.0$ and fault plane solutions of the strongest events ($M > 5.0$) since 2009.

4.1.6 Regional Seismic Hazard Assessment

Every important decision concerning the evaluation of seismic loads imposed on manmade facilities is made using some form of seismic hazard analysis. In some cases, these analyses are informally conducted, with probability and likelihood assessed intuitively with subjective expert opinion. In instances involving complicated assessments of effects derived from various geo-science and engineering disciplines, decision makers often prefer formal assessments of probabilities of earthquake occurrences



and associated natural effects that may produce damage to facilities and injury or life-loss to people. Such formal assessments are usually most appropriate for recommendations on regional or national seismic design requirements, earthquake evaluation of important facilities whose loss would imply substantial financial hardship to owners, estimation of earthquake damage and losses for emergency preparedness purposes and decision making regarding seismic safety of critical facilities.

There are two main approaches to assess seismic hazard, the deterministic and the probabilistic one. Recent efforts have considered five types of analyses that reflect the current usage. In the *type I, purely deterministic seismic hazard analysis*, one or more earthquakes are selected with only implicit consideration of their probabilities of occurrence. As example, it could be mentioned, the assignment of a maximum credible earthquake with specified magnitude and distance or the identification of a “characteristic” earthquake on a specified fault segment with specified source parameters. Probabilistic concepts enter in this analysis only in a simple form, such as scatter about an average ground-motion estimation curve. The *type II analysis, a semi-probabilistic seismic hazard analysis* takes into account one or more specific earthquakes, but, however the probability of occurrence is an explicit consideration in the selection of the earthquake. The *type III analysis, a single model of probabilistic seismic hazard assessment (PSHA)*, differs sharply from type I and type II analysis techniques because in this case no specific earthquake is identified. In this case, a seismic hazard curve is produced that presents the annual probability that given levels of a ground-motion parameter will be exceeded at the site of structure. The *type III is called single model PSHA* because it employs only one model for the distribution of earthquake locations and magnitudes, and one attenuation model of the ground-motion parameter (Algermissen et al., 1982). Due to the uncertainty concerning the appropriate model to use for the spatial distribution and occurrence rates of earthquakes and for the attenuation of ground-motion with distance, an appropriate procedure is to consider alternative models and to calculate the hazard curve for each of these models. The variability of results illustrates the range of uncertainty on the hazard and this is the *type IV, multiple model of PSHA* (EPRI, 1986; Bernreuter et al., 1985a, b). Combinations of techniques might be desirable in a given situation. A hybrid method uses a type III and/or IV PSHA to characterize ground-motion probabilities and identify individual earthquakes that contribute the most to the seismic hazard. Then uses deterministic procedures to derive more detailed characteristics of the seismic hazard, including time histories of ground motion, that are available from a typical PSHA. This hybrid procedure can more effectively take advantage of recent advances in geological and seismological observations and physical modelling of the seismic source, wave propagation and site effects.

The results of PSHA are used by engineers, decision-makers, code-writers, risk managers and insurance entities, for a variety of purposes. To design and estimate damage to buildings, residences, and standard commercial facilities, a scalar characterization of ground motion and a minimum representation of uncertainty are often sufficient. A standard spectral shape can be anchored to the chosen scalar to obtain approximate, equivalent results for a range of structural periods of interest. Typically, ground motions with annual probabilities in the range of 10^{-1} to 10^{-3} are of interest to these facilities. For critical facilities



(nuclear power plants, large dams, tunnels, etc.), a vector representation of ground motion is often required, including ground motion energy characteristics (Koliopoulos et al., 1998) at multiple frequencies and duration of strong shaking (Margaris et al., 1990; Papazachos et al., 1992; Koutrakis et al., 1999). For these critical systems, nonlinear models of structures may be used; appropriate realistic input motions for these models are required, and the PSHA must give sufficient information so that realistic motions can be derived for annual probability levels of 10^{-3} to 10^{-4} or lower.

In order to accomplish the main target of this report which is a reliable seismic hazard assessment of the examined area. For this reason, an accurate definition of seismic sources is indispensable in order to estimate seismic hazard at the site, which is threatened by earthquakes generated in these seismic sources. Analytical works concerning seismicity and active tectonics have been accomplished in Greece and surrounding area that has been separated in seismogenic sources of shallow and intermediate depth earthquakes (Papazachos and Papaioannou, 1993; Papaioannou and Papazachos, 2000). Papazachos et al., (2001) defined the faults which are related to the nucleation of strong ($M \geq 6.0$) earthquakes since antiquity. Papaioannou (2001) proposed a hybrid model for the Aegean and surrounding area consisting of fault type sources according to Papazachos et al., (2001) and area type sources for the earthquakes with magnitude $4.0 \leq M \leq 5.9$. This model is useful for a reliable seismic hazard assessment at the examined site by the application of the method proposed by Cornell (1968) using the computer code FRISK88M (1996) properly modified. Using the aforementioned geographical distribution of the seismogenic sources in the area studied, the seismicity parameters of each source, the attenuation model of strong ground motion proposed the seismic hazard assessment was assessed for two mean return periods 476 and 952 years. The results are shown in figures (Fig 32) and (Fig 33) and were made for “ROCK” site conditions.

The relation holding between the lifetime of a structure, t and the probability P_t of occurrence of a given value of a seismic hazard parameter and the mean return period, T_m , is given by the relation:

$$T_m = -\frac{t}{\ln(1 - P_t)} \quad (12)$$

For the Greek Seismic Code the calculations were performed for $T_m = 475$ years (which corresponds to lifetime, $t=50$ years and probability of exceedance $P_t = 10\%$). This is valid also for the hazard maps of the EC8.

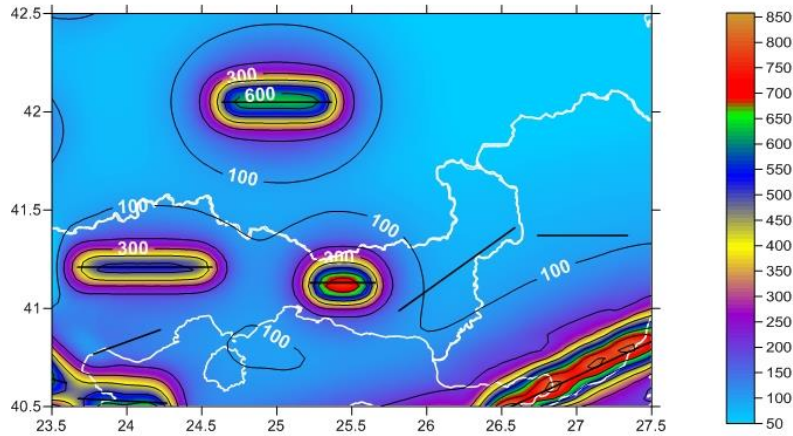
The maps in the figures (Fig 34) and (Fig 35) depict the geographical distribution of the mean PGA and the standard deviation values for the two return periods.



Project funded by the
EUROPEAN UNION



HYBRID MODEL OF AREA AND FAULT -TYPE SOURCES



MODEL OF AREA TYPE SOURCES (PAPAIOANNOU & PAPAZACHOS 2000)

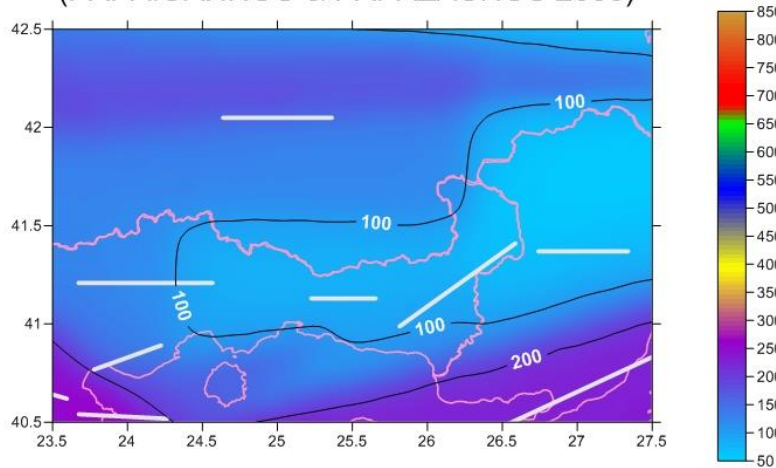


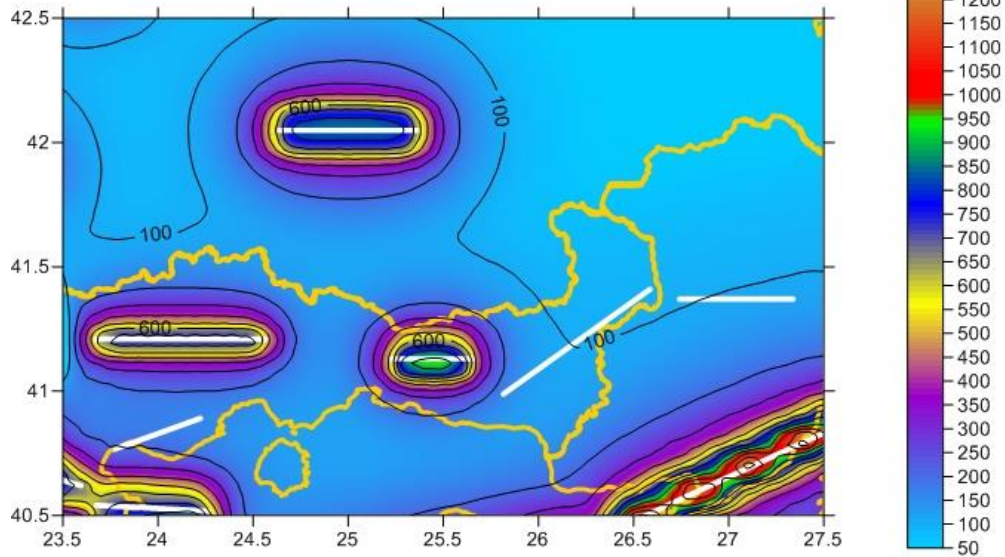
Fig 32. Distribution of the PGA values (in cm/sec²) using the hybrid model of faults and area sources (upper map) and the area-type model of sources Papaioannou and Papazachos (2000) (bottom) for mean return period of 476 years.



Project funded by the
EUROPEAN UNION



HYBRID MODEL OF AREA AND FAULT -TYPE SOURCES



MODEL OF AREA TYPE SOURCES (PAPAIOANNOU & PAPAZACHOS 2000)

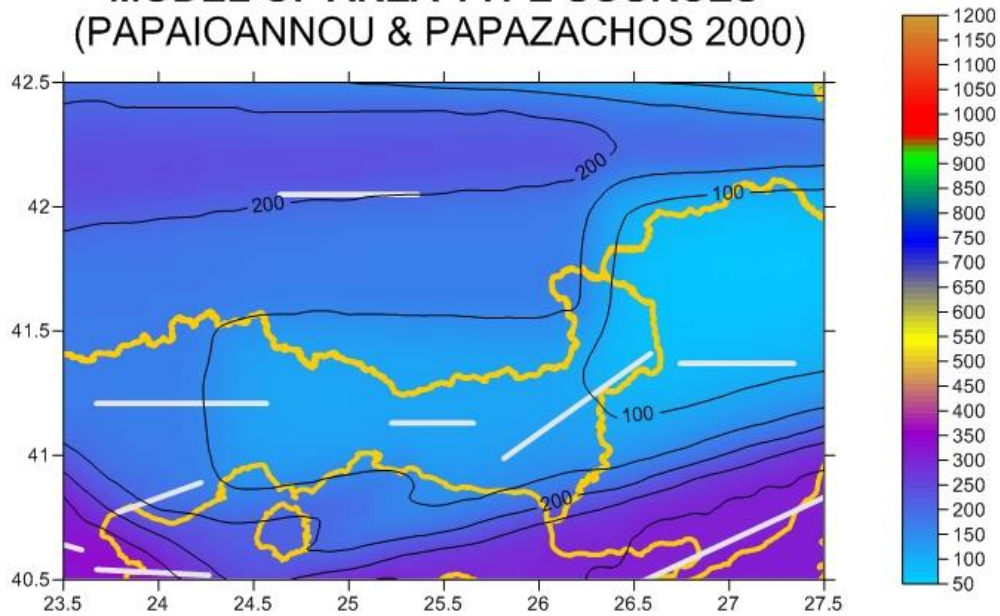




Fig. 33. Distribution of the PGA values (in cm/sec²) using the hybrid model of faults and area sources (upper map) and the area-type model of sources Papaioannou and Papazachos (2000) (bottom) for mean return period of 952 years.

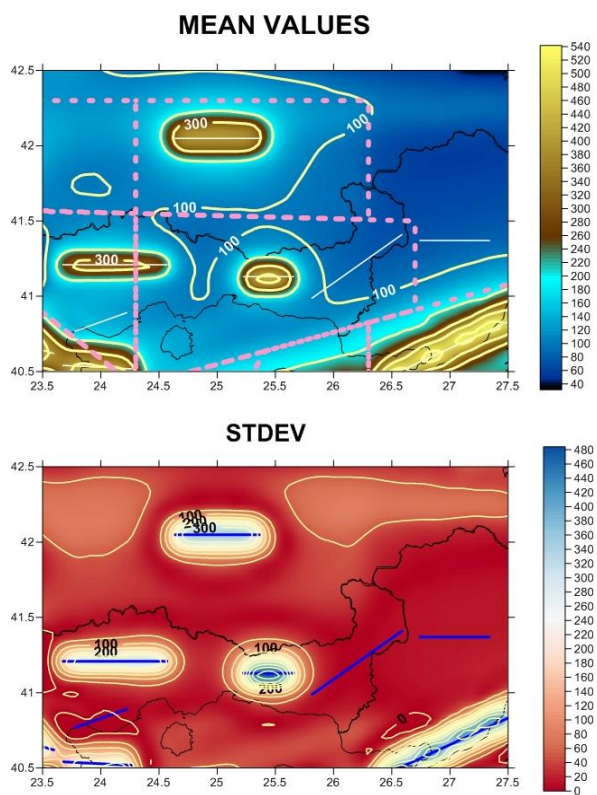


Fig 34. Distribution of the mean PGA and standard deviation values for TM=476 years.

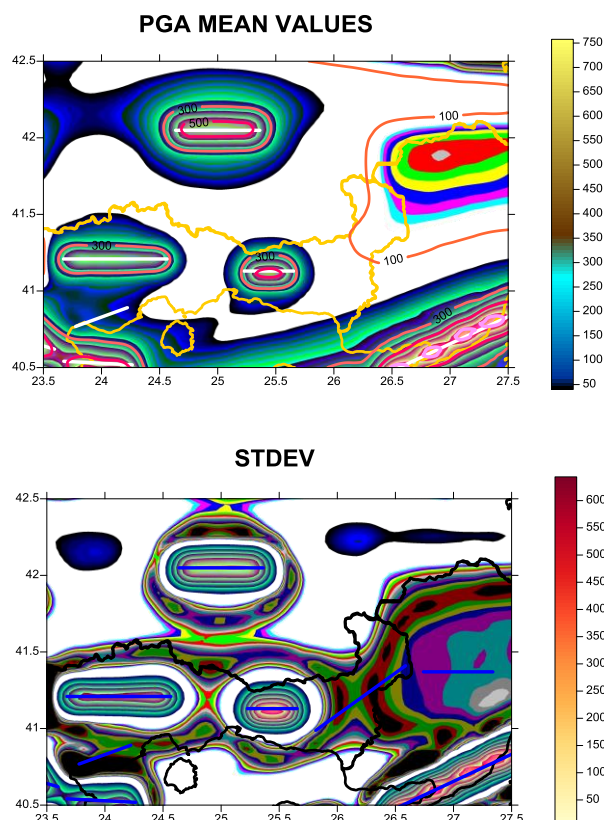


Fig 35. Distribution of the mean PGA and standard deviation values for TM=952 years

All the maps were compiled using the licenced software SURFER and applying the Modified Shepard's Method. The calculation were made on a grid of points spaced $0.025^{\circ} \times 0.025^{\circ}$ and considering a search radius of 0.50° . The Modified Shepard's Method uses an inverse distance weighted least squares method, which results in the elimination or reduction of "bull's-eye" appearance of the generated contours. Modified Shepard's Method may extrapolate values beyond initial data's Z range.

Even though the application of the Papaioannou and Papazachos (2000) model (: PP2000 model) results in smoothed results compared the application of the Papaioannou (2002) (: Pap2002 model), as it is clear from the maps in figures (Fig 32) and (Fig 33) however the latest seems to be more realistic. The high hazard values for sites located in the vicinity of faults influence the results appeared in the maps of figures



(Fig 34)and (Fig 35) depicting the geographical distribution of the mean results .

In an attempt to compare the results provided by the partners we attempted to merge the results and compile one seismic hazard map for the area. The results show that the region affected by the Vrancea zone intermediate depth earthquakes is very wide, while the influence of the shallow earthquakes associated with known faults define narrow areas. The results appeared in the maps may need further elaboration (Fig 36).

SEISMIC. HAZARD

RT : 100 yrs

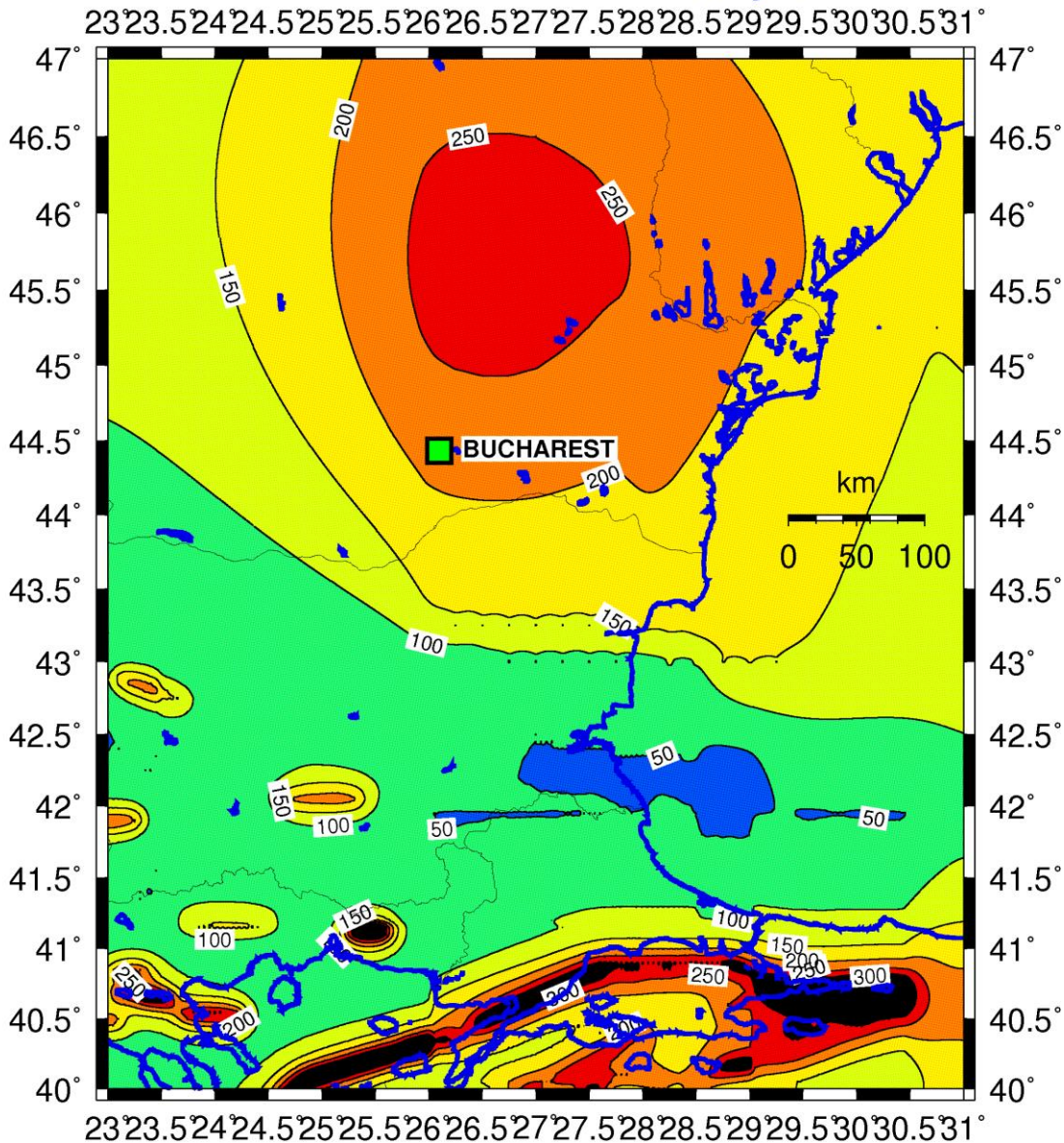


Fig 36. Geographical distribution of horizontal PGA based on merging results provided by all the partners for 100 yrs mean return period.

The same results for mean 10% probability of exceedance in 50yrs are shown in the map of figure (Fig 37).

SEISMIC. HAZARD

RT : 475 yrs

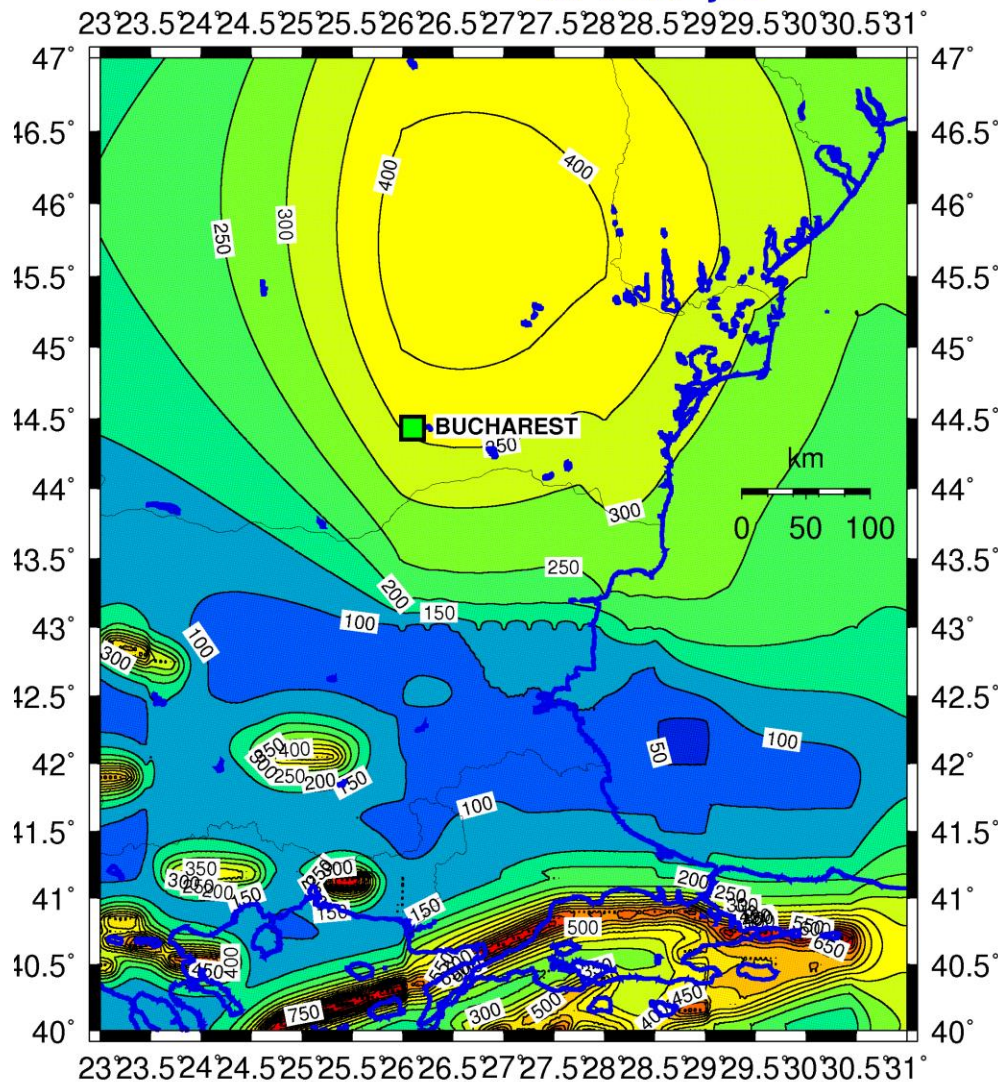
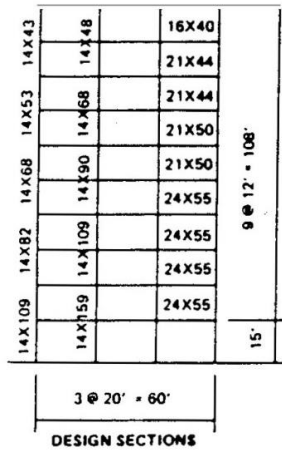


Fig 37. Geographical distribution of horizontal PGA based on merging results provided by all the partners for 100 yrs mean return period.

The idea of using macroseismic intensity as another measure of the seismic hazard results is based on the approximation that the *Macroseismic Intensity* reflects the result of the overall all content of the seismic motion. This is shown in figure (Fig 38) by Anderson and Naeim (1984). The displacement of the model structure found to be much larger due to the 1979 Imperial Valley record compared to that of the 1940 El



Centro record. The peak ground acceleration is the same 0.36g however the existence of a large pulse resulted in much greater displacements.



(a) Design Frame

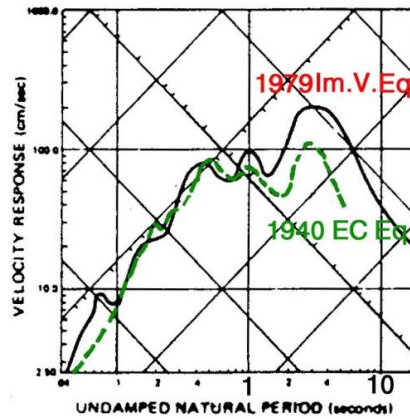
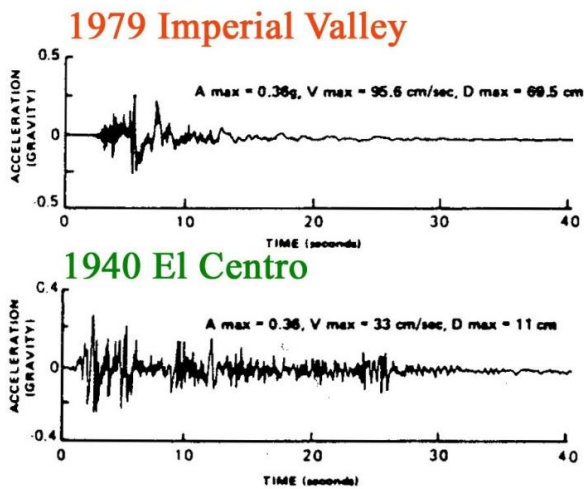
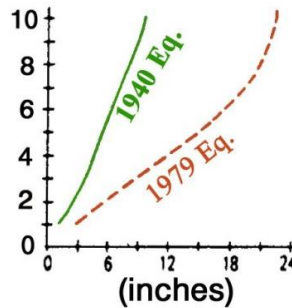


Fig 38. Distribution of intensities and seismic hazard curve based on probabilistic approach of McGuire and statistical treatment of observed intensities

4.1.7 Distribution of Maximum Values of Ground Parameters

Another use of the elaboration of the macroseismic data is the compilation of maps depicting the maximum values of PGA or PGV on the basis of scaling relations holding between the macroseismic intensity and these parameters. For Greece relation of the type :



$$\ln Y = c_1 + c_2 I_{MM} + c_3 S + \sigma_{\ln Y} P \quad (13)$$

where holding between the parameter Y of the strong ground motion (PGA, PGV, PGD), as a function of the macroseismic intensity, I_{MM} and the site effect factor, S . Relations of this type were proposed by Theodulidis (1991), Koliopoulos et al (1998) and Tselentis and Danciu (2008).

In order to compile these maps the scaling relations:

$$\begin{aligned} \ln a_g &= 0.28 + 0.67 I_{MM} + 0.42 S + 0.59 P \\ \ln v_g &= -3.02 + 0.79 I_{MM} - 0.04 S + 0.70 P \end{aligned} \quad (14)$$

proposed by Theodulidis (1991) were applied for PGA and PGV for the conversion of the values of the grid of map in figure (Fig 25) for “ROCK” type site conditions. The results for the mean values and the mean+1 σ are presented in the maps of figures (Fig 39) and (Fig 40).



Project funded by the
EUROPEAN UNION

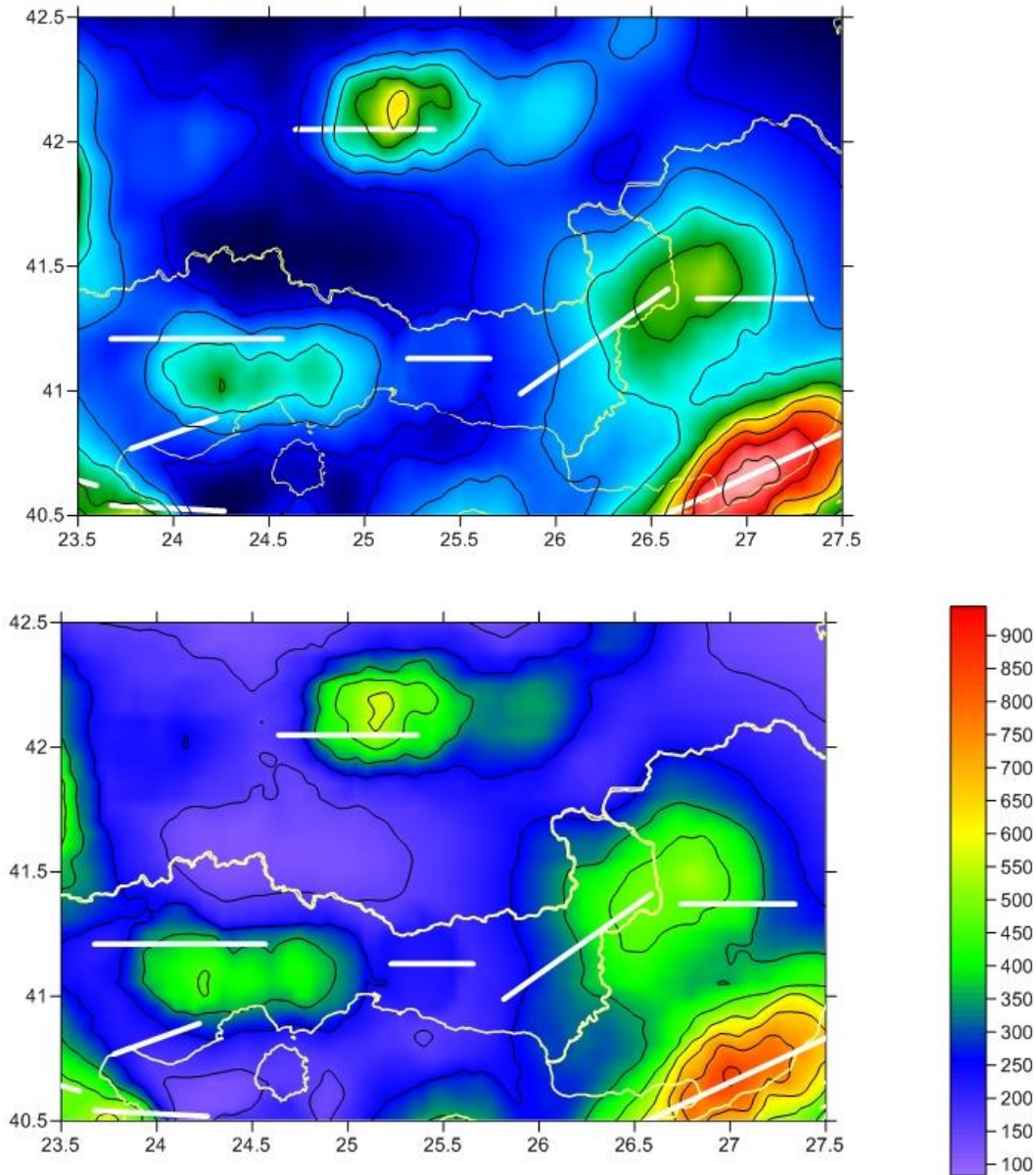


Fig 39. Geographical distribution of mean and mean+1 σ maximum PGA values from the conversion of known maximum intensities.

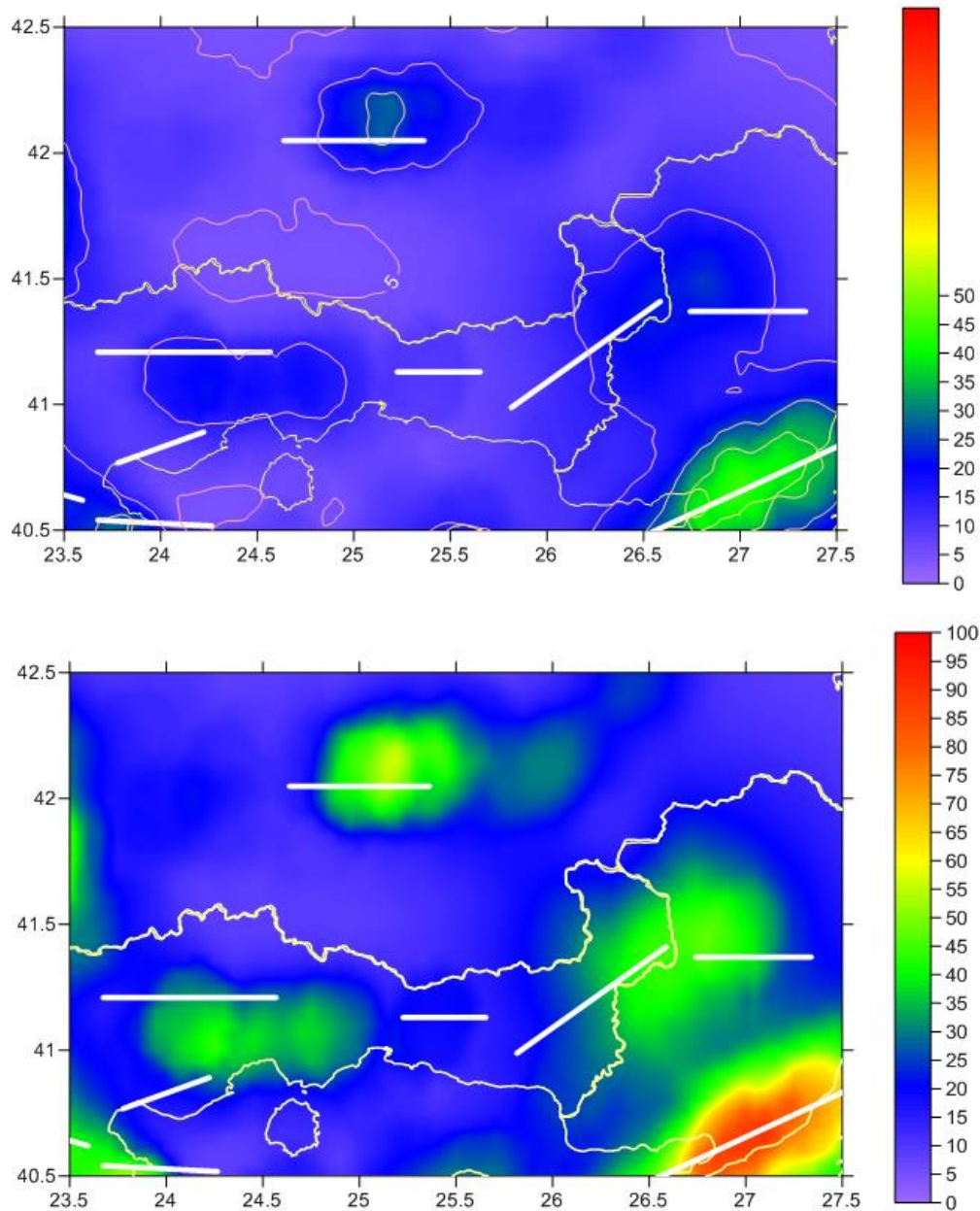


Fig 40. Geographical distribution of mean and mean+1 σ maximum PGV values using scaling relations for the conversion of known maximum intensities.



4.1.8 Comparison for Site Specific on Statistical Treatment of Observed Intensities

Another approach for the seismic hazard is based on the statistical treatment of observed intensities. An example of this approach for the area is shown for the town of Alexandroupolis.

In order to apply this procedure is necessary to use a complete sample of macroseismic intensities which cover a long time window. The graphs in figure (Fig 41) show the intensity rate for Alexandroupolis. We can assign various data completeness depending on the intensity level.

Using the complete sample of data we can examine the distribution of intensities as it is shown in figure (Fig 42)

The comparison of the two hazard curves in figure (Fig 42) supports the idea that if a good complete sample of intensity values is used the results have no significant differences and these are within the errors of the intensity values for the time period covered by the data/

However in order to examine the applicability of this procedure for longer mean return periods to various cities, we examine the comparison of the results for various places. The graphs in the figures (Fig 43) represent the seismic hazard curves using as parameter the macroseismic intensity for four cities in the eligible area of Greece.

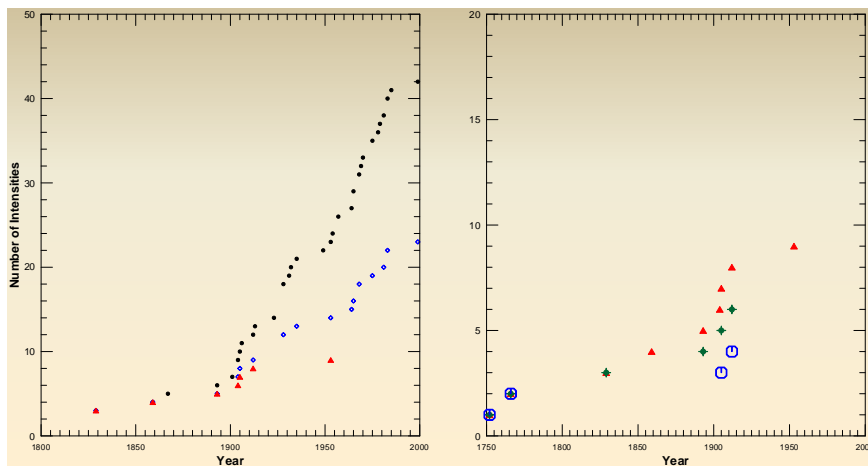


Fig 41. Intensity rates for Alexandroupolis.

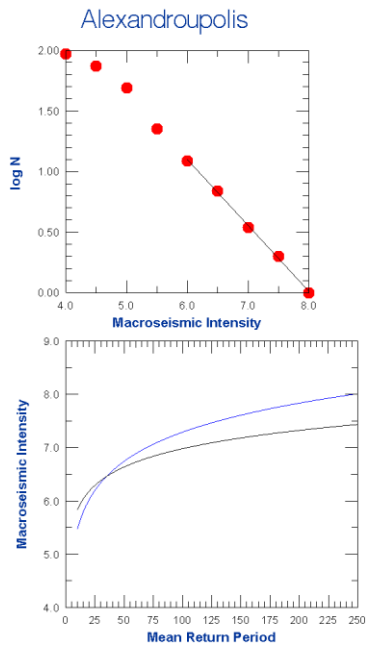


Fig 42. Distribution of intensities and seismic hazard curve based on probabilistic approach of McGuire and statistical treatment of observed intensities

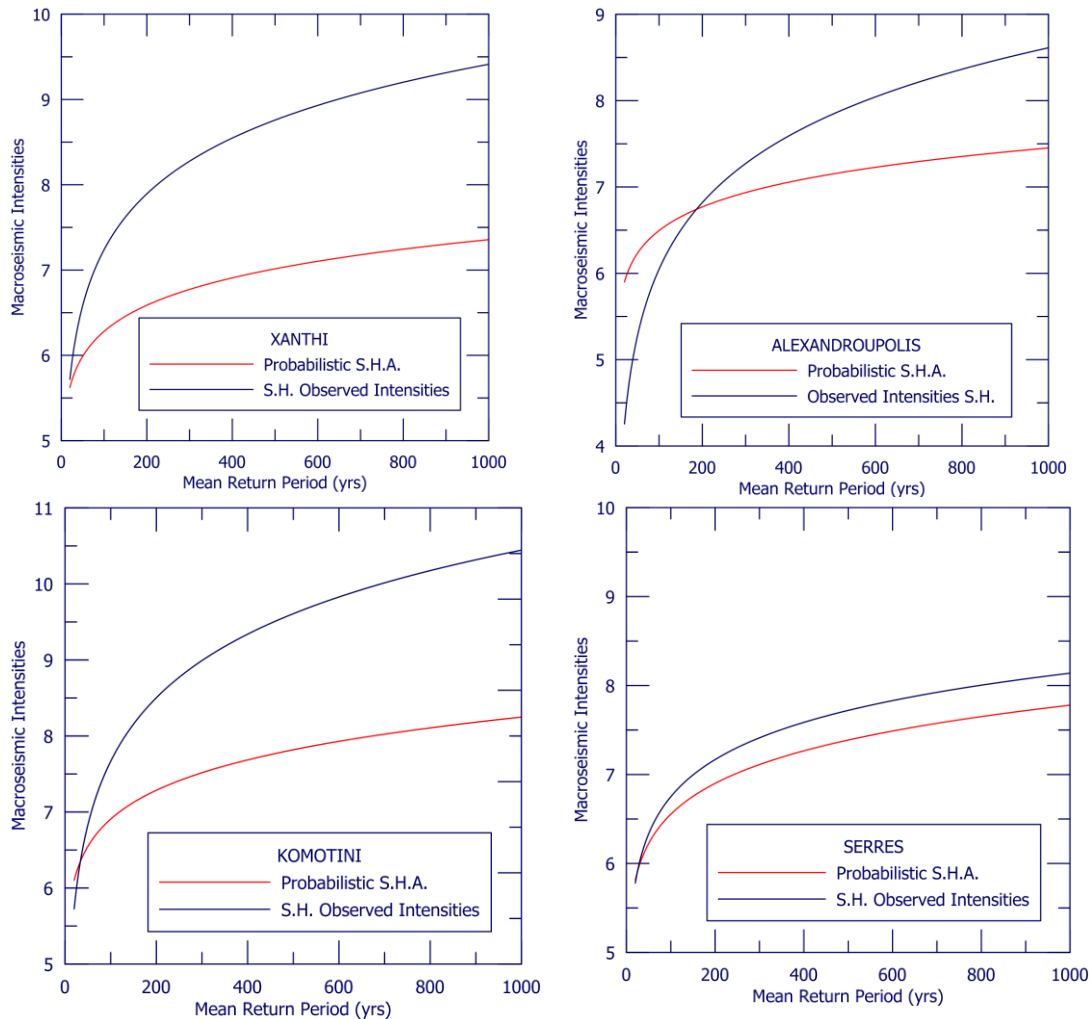


Fig 43. Seismic hazard curves for four cities within the eligible areas. The parameter used is the macroseismic intensity.

4.1.9 Local Seismic Hazard Assessment

In order to determine realistic earthquake scenarios for the eligible of the project surrounding areas of cities in Serres and Komotini utilizing them in the subsequent landslide hazard analysis, a Probabilistic Seismic Hazard Analysis (PSHA) is performed in a very dense geographical grid for various return periods (annual probabilities of exceedance). In addition to this the seismic hazard results are de-aggregated examining the contribution of seismic hazard as a function of magnitude and distance and the ground motion uncertainty ϵ . The purpose of Probabilistic Seismic Hazard Analysis (PSHA) is to assess the hazard of ground motion at a site taking into account all the possible seismic foci seriously affecting



the examined site, estimating the associated shaking, and calculating the probabilities of these occurrences. A PSHA has the ability to, and should, merge all necessary background about the seismic phenomenon relevant to the description of the hazard. This includes known or suspected behavior of the of seismic events in a "random" way in time, space and size hypothesized or proven models that describe the wave propagation in the earth crust, and empirical or theoretical means of estimating or determining the effects of the surficial geology on seismic waves. In fact, PSHA provides the best format for incorporating earthquake predictions into the decision-making process. A typical PSHA seeks to assess the annual probabilities of exceedance as a function of single amplitude of strong ground shaking e.g. peak ground acceleration (PGA). A general formulation of a PSHA which is ensued in this analysis has analytically described in previous section of this report (Cornel, 1968; McGuire, 1995).

A rate of seismic activity and a magnitude distribution are derived for each seismic source (Papazachos et al., 2001; Karakaisis and Koutrakis pers. comm. modified by Papaioannou and Papazachos, 2000). A ground motion predictive model is utilized for every magnitude M and distance D , allowing estimation of the probability that, the ground-motion amplitude is exceeded. For this reason a Ground Motion Predictive Equation (GMPE) proposed by Skarlatoudis et al. (2003) is applied. The PSHA for Serres and Komotini surrounding areas and the two grid sites are carried out by FRISK88M software (FRISK88M, 1995) for various return periods (probabilities of exceedances) $T_R=10, 25, 50, 100, 200, 475, 950$ and 1890 years respectively. The results of the PSHA for PGA (cm/sec^2), of various return periods T_R , and for rock site conditions for the Serres and Komotini grid sites are presented in Appendix 1 (A&B). It is noteworthy to mention, that an active neotectonic fault (Serres) in the nearby of Serres city is incorporated in the PSHA based on the Caputo et al., (2012; Fig.3) work. In order to adopt in our PSHA calculations the active neotectonic fault nearby the eligible area (city of Serres), we applied 3 different seismic activity rates ($r=0.002, 0.004, 0.006$) due to the fact no any calculated seismic rate value exists. The contribution of the seismic activity rates in PSHA for the site of Serres city combining the corresponding calculations without including this fault is presented in Figure (Fig 44). A significant amplification in the PSHA results varying the seismic activity rates of the Serres fault (Caputo et al., 2012) is shown up to return period of $T_R=950$ years, while the exclusion of this active fault in PSHA calculations gives systematically very low accepted peak ground values. Taking into account the rate values of the neighboring seismic faults we proposed as the most appropriate rate in our calculations $r=0.002$ for this particular active fault.

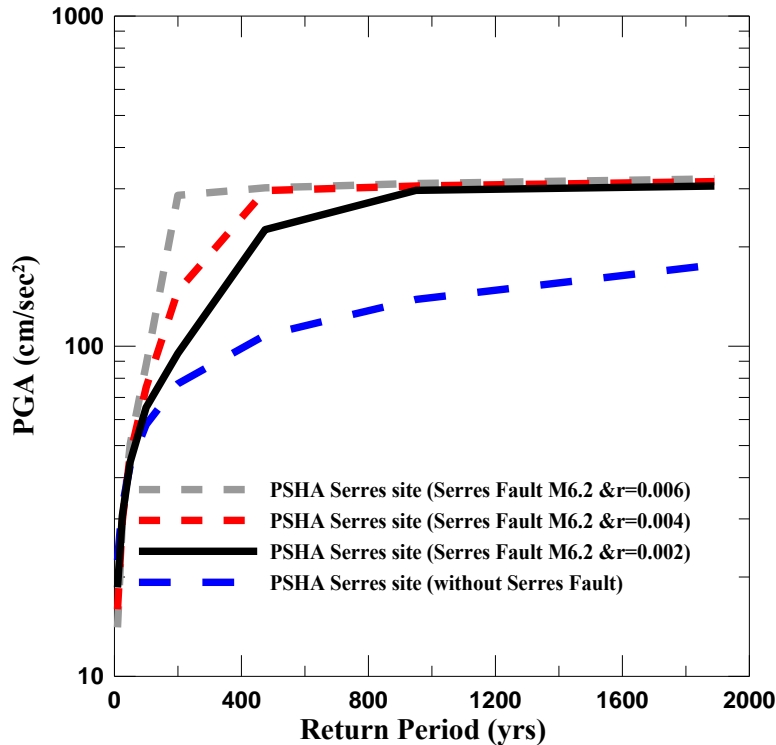


Fig 44. The contribution of the seismic activity rate in PSHA for the site of Serres city combining the corresponding calculations without including this fault.

The subsequent step was to perform a de-aggregation analysis of seismic hazard, which provided earthquake scenarios for the selected return periods on the nearby to the site of Xanthi. The basic advantage of the PSHA is that, it integrates the hazard to an examined site from all contributing seismic sources. However, this integration may restrain the PSHA use to the cases that demand earthquake scenarios such as those that require time series. The application of seismic hazard de-aggregation can allow to determine predominant sources in PSHA. Significant seismic hazard de-aggregation methods have been carried out by Stepp et al. (1993), Chapman (1996), McGuire (1995), Cramer and Petersen (1996), Harmsen and Frankel (2001) among others. This analysis follows the suggestions and principles of Bazzurro and Cornell (1999) seminal work.

The type of seismic hazard de-aggregation which includes magnitude, M , distance D and the ground motion uncertainty, ε , is performed. The results of the seismic hazard de-aggregation indicate the relative contribution of the seismic sources in the (D, M, ε) bin. The magnitude-bin width is 0.1 and the corresponding distance-bin width is 2km due to a limited area examined of this site-specific seismic hazard analysis. The applied software for this case is HAZ30 (Bazzurro P., and Abrahamson N., per. com.) As an input in this de-aggregation analysis, the output from FRISK88M code was adopted and for



the specific sites E.S. as referred in Appendix 1A & 1B. The de-aggregation results for the examined sites (Appendix 1A & 1B) are given in the Table (Table 4.1.3) for various return periods (100 to 1890 years) and PGA values ranging from 43 to 360 cm/sec². In this analysis we only used the larger Return Periods T_R , (≥ 100 years) emphasizing for the strong ground motion. Two different seismic scenarios are proposed per each examined site (Serres and Komotini) respectively.

Table 4.1.3 Seismic Hazard De- aggregation results in a Local Scale for the 2 examine Sites (Serres and Komotini) and various PGA's values corresponding in different return periods (100, 200, 475, 950, 1890 years)

SITE1 COORDINATES: 23.549 41.088 SERRES

AMP:	53.78	195.00	287.84	341.50	360.80
M	6.1	6.1	6.1	6.1	6.2
D (km)	15	15	15	15	3
Eps*	-0.625E-01	-0.625E-01	0.312E+00	0.687E+00	-0.625E-01

SITE COORDINATES: 25.448 41.188 KOMOTINI

AMP:	53.78	195.00	287.84	341.50	360.80
M	6.3	6.3	6.3	6.3	6.3
D (km)	5	5	5	5	5
Eps*	-0.625E-01	-0.625E-01	-0.625E-01	-0.625E-01	-0.625E-01

The de-aggregation analysis identified the earthquake scenarios with the largest contribution to the estimated hazard for the aforementioned areas are those presented in Table (Table 4.1.3) and for Serres area are M= 6.1 and R=15km, M=6.2 and R=3km. Correspondingly for the Komotini area the basic earthquake scenario could be M=6.3 and R=5 km and a possible threat could be from the seismic fault nearby of the area (Papazachos et al., 2001) with M=6.7 and keeping the same design distance R=5 km.

To investigate the seismic scenarios of various earthquakes, we chose to apply the stochastic method for finite faults. The stochastic method was originally proposed by Boore (1983) and lies amongst the most commonly used tools from engineers and seismologists when it comes to simulating strong ground motion from earthquakes. The original method was extended by Beresnev and Atkinson (1997) to incorporate the finite dimensions of seismic sources and more recently, Motazedian and Atkinson (2005) released the EXSIM code, which further advanced the stochastic method by replacing the static subfault corner frequency of previous implementations of the method by a dynamic corner frequency. This dynamic corner frequency is related to the dimensions of the area that experiences slip at a certain point in time during the rupture process of an earthquake. EXSIM also incorporated the analytical model of Mavroeidis and Papageorgiou (2002) that can simulate long-period pulses, often observed in the near-



field of an earthquake. The most recent version of EXSIM was based on the publication of Boore (2009) and is the one adopted for the herein presented stochastic simulations.

The stochastic method, either in its original form or after the modifications of Beresnev and Atkinson (1997) and Motazedian and Atkinson (2005), has been repetitively applied and validated in various seismotectonic environments around the globe (Boore, 2003 and references therein). It has also been adopted in several studies of earthquakes in the broader Aegean area (e.g., Margaris and Boore, 1998; Margaris and Hatzidimitriou, 2002) and is considered as an effective tool, especially in cases where the sparsity of seismotectonic and seismological data do not facilitate the application of more refined and physically sound methodologies. For a detailed description of the stochastic method, the reader is referred to the work of Boore (1983, 2003), Beresnev and Atkinson (1997) and Motazedian and Atkinson (2005).

The application of the stochastic method for finite faults requires the definition of certain parameters that describe the geometry of the considered seismic source, the seismic wave propagation path effect and the site effect at the observation point(s). For seismic sources the fault parameters proposed by Papazachos et al. (2001) and Caputo et al. (2012) are utilized. The propagation model includes parameters for the geometric spreading, the anelastic attenuation, and the near-surface attenuation, as well as site-amplification factors. For the geometric attenuation we applied a geometric spreading operator of $1/R$, and the anelastic attenuation was represented by a mean frequency-dependent quality factor, $Q(f)=100f^{0.8}$ (Hatzidimitriou, 1993, 1995), derived from studies of *S*-wave and coda-wave attenuation in northern Greece. The effect of the near-surface attenuation was also taken into account by diminishing the simulated spectra by the factor $\exp(-\pi\kappa_0f)$ (Anderson and Hough, 1984). The kappa operator (κ_0) was given the value 0.035 corresponding to rock site conditions (Margaris and Boore, 1998). In the next Figures (Fig 45 to Fig 48) the stochastic time histories and the corresponding response spectra for the aforementioned scenarios of the Serres and Komotini area are depicted.



Seismic Scenario SRS M6.1 R=15km
PGA= 214 cm/sec²

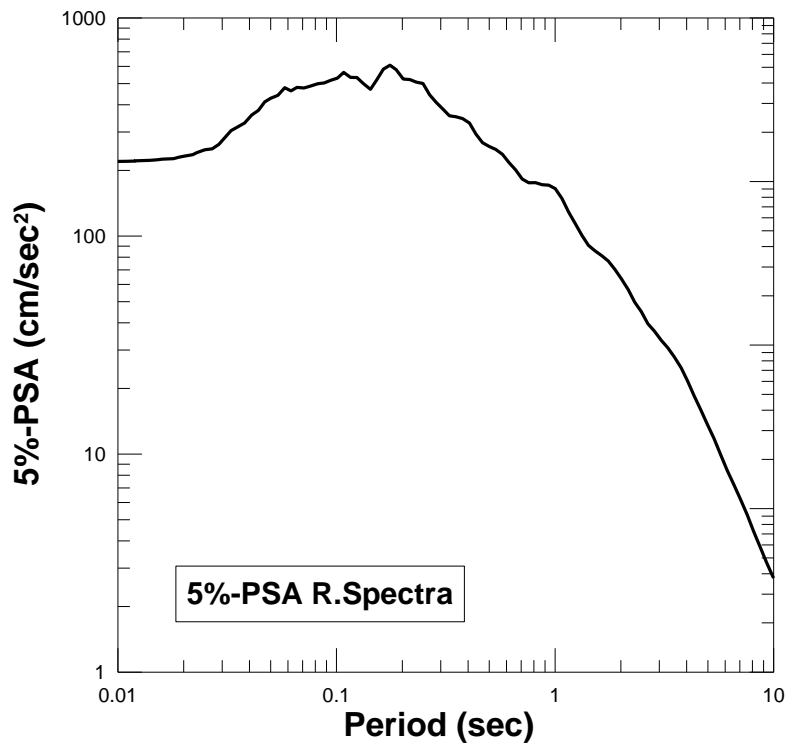
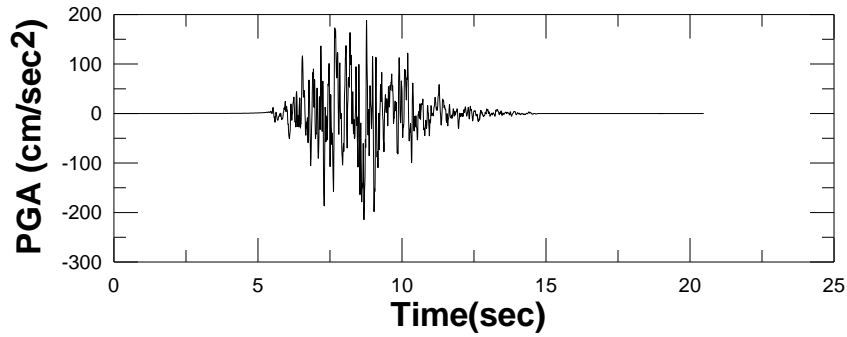


Fig 45. Stochastic strong motion time history and response spectrum ($\zeta=5\%$) for the area of Serres with design magnitude M6.1 and distance D=15km.



Seismic Scenario SRS M6.2 R=3km
 ———— PGA= 340 cm/sec²

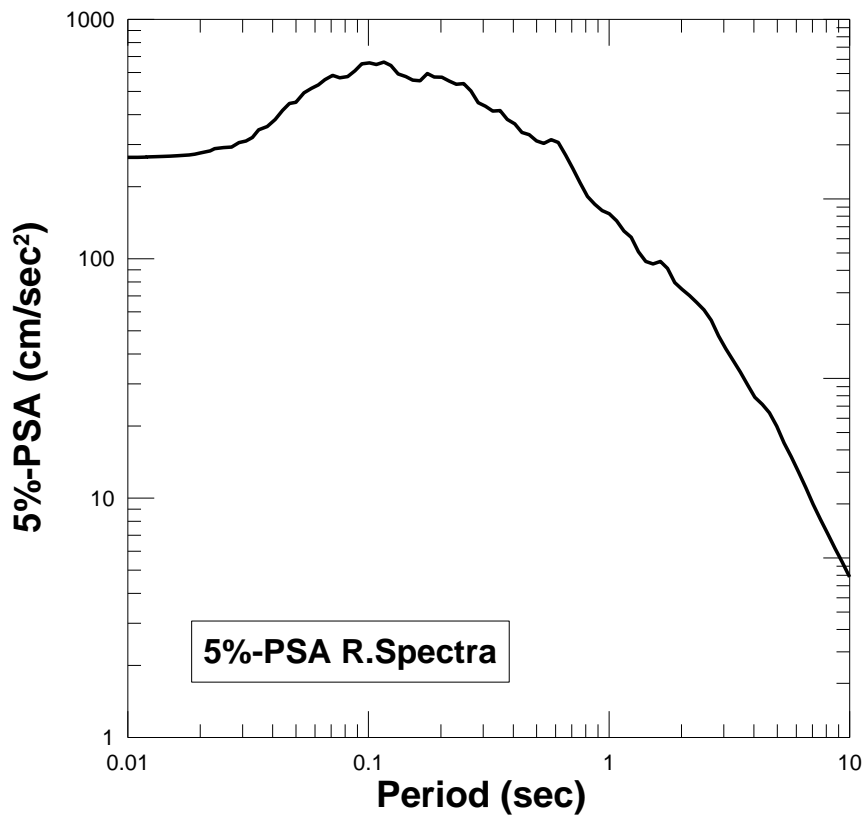
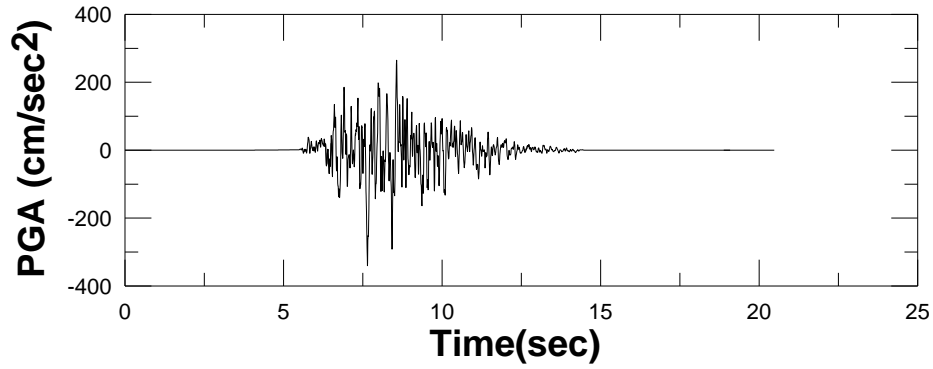


Fig 46. Stochastic strong motion time history and response spectrum ($\zeta=5\%$) for the area of Serres with design magnitude M6.2 and distance D=3km.

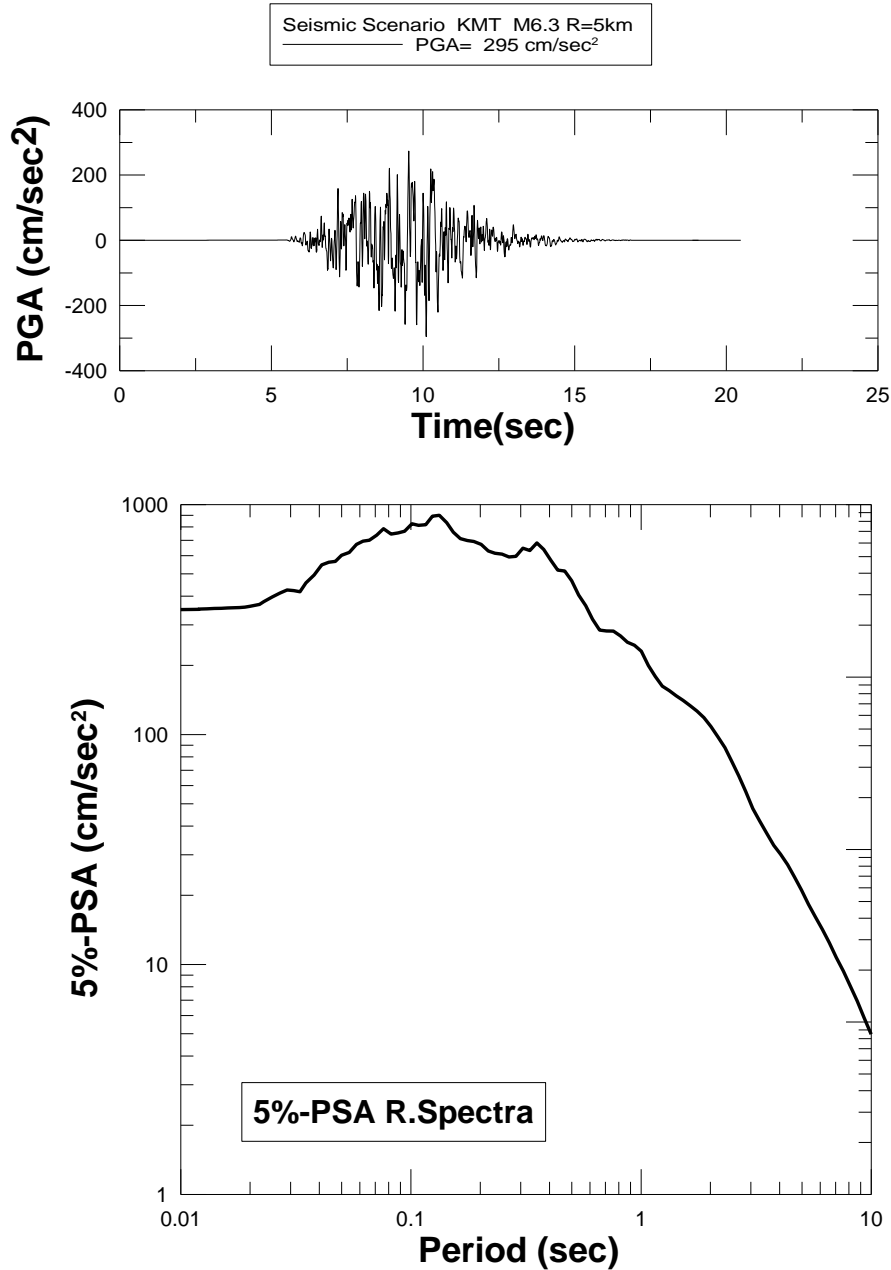


Fig 47. Stochastic strong motion time history and response spectrum ($\zeta=5\%$) for the area of Komotini with design magnitude M6.3 and distance D=5km.

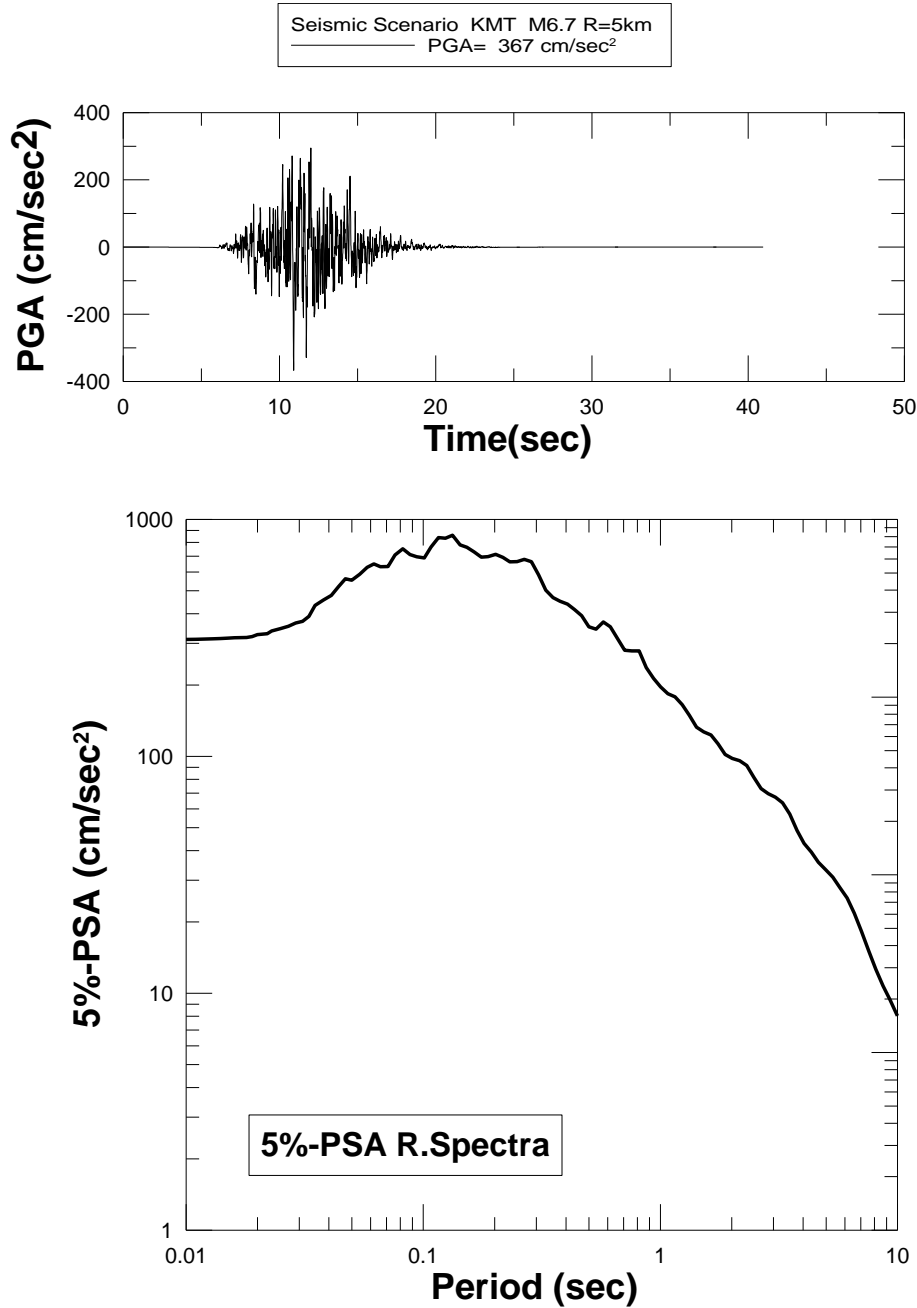


Fig 48. Stochastic strong motion time history and response spectrum ($\zeta=5\%$) for the area of Komotini with design magnitude M6.7 and distance D=5km.



REFERENCES

- Algermissen, S.T., D.M. Perkins, W. Isherwood, D. Gordon, G. Reagor and C. Howard (1976). Seismic risk evaluation of the Balkan region, *Proc. Sem. Seismic Zoning Maps, UNESCO, Skopje*, 2, 172-240.
- Algermissen, S.T., D.M. Perkins, P.C. Thenhaus, S.L. Hanson and B.L. Bender (1982): Probabilistic estimates of maximum acceleration and velocity in rock in the contiguous United States, *U.S. Geological Survey Open- Report 82-103*, 112pp.
- Ambraseys, N.N. (1995). The prediction of earthquake peak ground acceleration in Europe, *Earthq. Eng. Struct. Dyn.*, 24, 467-490.
- Ambraseys, N. N. (1988): Engineering Seismology. *Earthq. Engin. and Struct. Dyn.*, 17, 1-105.
- Ambraseys, N. N. and C.F. Finkel (1987): The Saros–Marmara earthquake of 9 August 1912 *Earthq. Eng. Struct. Dyn.*, 15, 189-211.
- Ambraseys, N. N. and J. A. Jackson (1990): Seismicity and associated strain of central Greece between 1890 and 1988. *Geophys. J. Int.*, 101, 663-708.
- Ambraseys, N.N., K.A. Simpson, and J.J. Bommer (1996). Prediction of horizontal response spectra in Europe, *Earthq. Eng. Struct. Dyn.*, 25, 371-400.
- Anderson, J and F. Naeim (1984): Design criteria and ground motion effects on the seismic response of multistory buildings. *In: Critical aspects of earthquake ground motion and building damage potential. ATC 10-1*, 259 pp.
- Bazzurro, P. And C. Allin Cornel (1999). Disaggregation of seismic hazard, *Bull. Seism. Soc. Am.*, **89**, 501-520.
- Beresnev, I. A. and G. M. Atkinson (1997). Modeling finite-fault radiation from the ω^n spectrum, *Bull. Seism. Soc. Am.* **87**, 67-84.
- Bernreuter, D. L., J.B. Savy, R. W. Mensing, J. C. Chen, and B. C. Davis (1985a): Seismic hazard characterization of the Eastern United States, Vol. 1, Methodology and results for ten sites; *UCID-20421*.
- Bernreuter, D. L., J.B. Savy, R. W. Mensing, J. C. Chen, and B. C. Davis (1985b): Seismic hazard characterization of the Eastern United States, Vol.2, *UCID-20421*.
- Boore, D. M. (2003). Simulation of ground motion using the stochastic method, *Pure Appl. Geophys.* **160**, 635-676.
- Boore (2009). Comparing stochastic point-source and finite-source ground-motion simulations: SMSIM to EXSIM, *Bull. Seism. Soc. Am.* **99(6)**, 3202-3216.



Boore, D. M. (1983). Stochastic simulation of high-frequency ground motions based on seismological models of the radiated spectra, *Bull. Seism. Soc. Am.* **73**, 1865-1894.

Campbell KW. (1989): The dependence of peak horizontal acceleration on magnitude, distance and site effects for small magnitude earthquakes in California and Eastern North America. *Bull. Seism. Soc. Am.* **79**, 1311-1338.

Chapman, M.C. (1995). A probabilistic approach of ground motion selection for engineering design., *Bull. Seism. Soc. Am.*, **85**, 937-942.

Coburn, A. and R. Spence (2002): Earthquake Protection. *J. Willey & Sons Ltd.*, 420 pp.

Cornell, C. A. (1968). Engineering seismic risk analysis. *Bull. Seism. Soc. Am.*, 58, 1503-1606.

Cramer, C.H. and M.D. Petersen (1996). Predominant seismic source distance and magnitude maps for Los Angeles, Orange and Ventura Counties, California, *Bull. Seism. Soc. Am.*, **86**, 1645-1649.

Drakopoulos, J. and K. Makropoulos (1983): Seismicity and seismic hazard studies in the area of Greece. *Publ. Univ. of Athens, Seism. Lab.*, 1, 126pp.

EPRI (1986): Seismic hazard methodology for the central and eastern United States, 10 volumes, *EPRI report NP-4726, Palo Alto, California.*

FRISK88M (1996): User's Manual, ver. 1.70. *Risk Engineering Inc., Boulder CO.*, 69pp, 2 Appendixes.

Galanopoulos, A.G. (1941): Das riesenbeben der Messenischen kust vom 27 August 1886. *Proc. Acad. Athens*, 16, 127-134. (in Greek).

Galanopoulos, A.G. (1944): The two damaging earthquakes of Larisa in 1892 and 1941. *Proc. Acad. Athens*, 15 and 17 June 1944, 222-224. (in Greek).

Galanopoulos, A.G. (1949): The Koroni, Messinia earthquake of October 6, 1947. *Bull. Seism. Soc. Am.*, 39, 33-39.

Galanopoulos, A.G (1950): Die beiden schadenbringenden beben von Larisa aus den Jahren 1892 and 1941. *Gerl. Beitz. zur Geophysik*, 62, 27-38.

Galanopoulos, A.G. (1953): Katalog der Erdbeben in Griechenland fur die Zeit von 1879 bis 1892. *Ann. Geol. Pays Hellen.*, 5, 144-229.

Galanopoulos, A.G. (1954): Die seismiztat der insel Chios. *Geitr. z. Geophys.*, 63, 253-264.

Galanopoulos, A. G. and N. Delibasis (1972): Map of maximum observed intensities in Greece, period 1800-1970, *Athens*, 1972.

Gumbell, J. (1958): Extreme value statistics. *Columbia Univ. Press, New York*, 375pp.



- Harmsen, S. and A. Frankel (2001). Geographical Deaggregation of seismic hazard in the United States, *Bull. Seism. Soc. Am.*, **91**, 13-26.
- Hatzidimitriou, P. M. (1993). Attenuation of coda waves in Northern Greece, *Pure and Appl. Geophys.* **140**, 63-78.
- Hatzidimitriou, P. M. (1995). S-wave attenuation in the crust in Northern Greece, *Bull. Seism. Soc. Am.* **85**, 1381-1387.
- Koliopoulos, P.K., B.N. Margaris, and N.S. Klimis (1998): Duration and energy characteristics of Greek strong motion records. *J. Earthq. Eng.*, 2, 391-417.
- Koutrakis, S.I, P.K. Koliopoulos, G.F. Karakaisis, B.N. Margaris and P.M. Hatzidimitriou (1999): Seismic hazard in Greece based on different strong ground motion parameters. *J. Earthq. Engin.*, 6, 75-109.
- Makropoulos, K.C. (1978) : The statistics of large earthquake magnitude and an evaluation of Greek seismicity. *Ph.D. thesis, Univ. of Endinburgh.*, 193pp.
- Makropoulos, K. C. and P. W. Burton (1985): Seismic hazard in Greece. II. Ground acceleration. *Tectonophysics*, 117, 259-294.
- Makropoulos, K.C., J. Drakopoulos and J.B. Latoussakis (1989): A revised and extended earthquake catalogue in Greece since 1900. *Geophys. J. Int.*, 98, 391-394.
- Margaris V. N. (1994) : Azimuthal variation of the seismic waves in Greece and contribution in the seismic hazard assessment. *Ph. D. Thesis, Univ. Thessaloniki*, 324pp (in Greek).
- Margaris, B. N. and D. M. Boore (1998). Determination of $\Delta\sigma$ and κ_0 from response spectra of large earthquakes in Greece, *Bull. Seism. Soc. Am.* **88**, 170-182.
- Margaris, B.N. and P.M. Hatzidimitriou (2002). Source spectral scaling and stress release estimates using strong-motion records in Greece, *Bull. Seism. Soc. Am.*, 92,1040-1059.
- Margaris, B.N., C. Papazachos, Ch. Papaioannou, N. Theodulidis, I. Kalogeras and A. Skarlatoudis (2001): Empirical relations for the attenuation of the horizontal strong ground motion of shallow earthquakes in Greece. *Proc. 2nd Hell. Congress of Earthq. Engin. and Eng. Seismology*, Vol.A, 27-36.
- Margaris, B.N., C. Papazachos, Ch. Papaioannou, N. Theodulidis, I. Kalogeras and A. Skarlatoudis (2002): Ground motion attenuation relations for shallow earthquakes in Greece. *Proc. 12th European Conference on Earthquake Engineering, London, September 2002*, Paper Ref.. 385.
- Mavroeidis, G. P. and A. S. Papageorgiou (2003). A mathematical representation of near-fault ground motions, *Bull. Seism. Soc. Am.* **93**, 1099-1131.



- McGuire, R.K. (1995). Probabilistic seismic hazard analysis and design earthquakes: closing the loop, *Bull. Seism. Soc. Am.*, **85**, 1275-1284.
- Motazedian, D. and G. M. Atkinson (2005). Stochastic Finite-Fault Modeling Based on a Dynamic Corner Frequency, *Bull. Seism. Soc. Am.* **95**, 995-1010.
- Papaoiannou, Ch.A. (1984): Attenuation of seismic intensities and seismic hazard in the area of Greece, *Ph. D. Thesis, Univ. Thessaloniki*, 200pp. (in Greek, with an English abstract).
- Papaoiannou, Ch. A. (1986): Seismic hazard assessment and long term earthquake prediction in Southern Balkan region, *Proc. 2nd Int. Sem. on Earthquake Prognostics*, A. Vogel and K. Brandes (Editors), Berlin, 223-241.
- Papaoiannou, Ch. A. (2002): A new Approach of Seismic Hazard Assessment in S. Balkan Area Based on a Hybrid Model of Area- and Fault Type Sources. *ESC, XXVIII Gen. Ass, September 1-6, 2002, Genova-ITALY*. (Abstracts volume).
- Papaoiannou, Ch. A. and B.C. Papazachos (2000): Time independent and time dependent seismic hazard in Greece based on seismogenic sources. *Bull. Seism. Soc. Am.*, **90**, 22-33.
- Papazachos, B.C. (1980): Seismicity rates and long-term prediction in the Aegean area, *Quat. Geod.* **3**, 171-190.
- Papazachos, B.C. (1990): Seismicity of the Aegean and surrounding area, *Tectonophysics*, **178**, 287-308.
- Papazachos, B. and K. Papazachou (1989): The earthquakes in Greece. *Ziti Publ. Co., Thessaloniki, Greece*, 356pp. (in Greek).
- Papazachos, B. and K. Papazachou (1997): The earthquakes in Greece. *Ziti Publ. Co., Thessaloniki, Greece*, 304 pp.
- Papazachos, B.C. and C.B. Papazachou (2003). The earthquakes of Greece 3rd Edition, *Ziti Editions*, Thessaloniki, Greece, 273pp (in Greek).
- Papazachos, B.C. and Ch.A. Papaoiannou (1993). Long-term earthquake prediction in the Aegean area based on a time and magnitude predictable model. *Pure Appl. Geophys.* **140**, 595–612.
- Papazachos, B.C., Kiratzi, A.A., Hatzidimitriou, P.M., Papaoiannou, Ch.A. and N.P. Theodulidis (1985): Regionalization of seismic hazard in Greece. *Proc. 12th Reg. Sem. on Earthq. Eng. EAEE-EPPO*, Halkidiki, Greece. 12 pp.
- Papazachos, B.C., Papaoiannou, Ch.A., Papastamatiou, D.J., Margaris, V.N. and N.P. Theodulidis (1990): On the reliability of different methods of the seismic hazard assessment in Greece. *Nat. Hazards* **3**, 141–151.
- Papazachos, B.C., K. Makropoulos, I. Latoussakis and N.P. Theodulidis (1989): Compilation of a seismic



hazard map for Greece. 2nd Proj. Rept. EPPO-GREECE, 24pp. and 24 figs (in Greek).

Papazachos, B.C., Papaioannou, Ch.A., 1993. Long-term earthquake prediction in the Aegean area based on a time and magnitude predictable model. *Pure Appl. Geophys.* 140, 595–612.

Papazachos, B. C., Ch. A. Papaioannou, C. B. Papazachos and A. A. Savvaidis (1997a): Atlas of isoseismal maps for strong ($M \geq 5.5$) shallow ($h < 60\text{km}$) earthquakes in Greece and surrounding area, 426BC-1995. *Publ. Geophysical Lab., Univ. Thessaloniki*, 4, 176pp.

Papazachos, B. C., Ch. A. Papaioannou, C. B. Papazachos and A. S. Savvaidis (1997b): A data bank of macroseismic information for shallow earthquakes in the southern Balkan area 550BC-1995AD. *Abstr. Vol. 29th IASPEI General Assembly*, Thessaloniki, 18-28 August, 1997.

Papazachos, B. C., Ch.A. Papaioannou, C.B. Papazachos and A.S. Savvaidis (1998): A data bank of macroseismic information for shallow and intermediate depth earthquakes in the southern Balkan area 550BC-1998AD. *Abstr. Vol. XXII IUGG General Assembly, Birmingham, July 19-30*.

Papazachos B.C., D.M. Mountrakis, C.B. Papazachos, M.D. Tranos, G.F. Karakaisis and A.S. Savvaidis (2001). The faults which have caused the known major earthquakes in Greece and surrounding area between the 5th century BC and today. *Proc. 2nd Hell. Congress of Earthq. Engin. and Eng. Seismology*, Vol. 1, 55-64.

Papazachos, B.C., E.M. Scordilis, Ch.A. Papaioannou, C.B. Papazachos and G.F. Karakaisis (2012). A homogeneous and complete earthquake catalogue for the Aegean area during the period 365-2012, *Publ. Geophys. Lab. Univ. of Thessaloniki*, Greece, 1, 160pp.

Papazachos, C. B. (1992): Anisotropic radiation modeling of macroseismic intensities for estimation of the attenuation structure of the upper crust in Greece. *Pure Appl. Geophys.*, 138, 445-469.

Papazachos, C. and Ch. Papaioannou (1997): The macroseismic field of the Balkan area. *J. of Seismology*, 1, 181-201.

Papazachos, C.B., and Ch. Papaioannou (1998): Further information on the macroseismic field in the Balkan area (Reply on the comment of M. D. Trifunac on the paper «The macroseismic field of the Balkan area»). *J. Seismology*, 2, 363-375.

Papoulia, I.E. (1988): Statistical and seismotectonic models for the assessment of seismic risk using as parameter the macroseismic intensity. *Ph.D. thesis, Univ. Athens*, 1-266.

Reiter, L. (1990): Earthquake hazard analysis: Issues and insights, *Columbia University Press (New York)*, 254 pp.

Roussopoulos, A. (1956): Antiseismic Structures, *V. Papaxrisanthemou Publ.*, 2nd, Athens, 431pp.



Sabetta, F. and A. Pugliese (1987): Attenuation of peak horizontal acceleration and velocity from Italian strong motion records, *Bull. Seism. Soc. Am.* **77**, 1491- 1513.

Shebalin, N.V. (1974): Atlas of isoseismal maps. Part III of the catalogue, UNESCO Scopje.

Skarlatoudis, A.A., C.B. Papazachos, B.N. Margaris, N. Theodulidis, Ch. Papaioannou, I. Kalogeras, E.M. Scordilis and V. Karakostas (2003): Empirical peak ground motion predictive relations for shallow earthquakes in Greece. *Bull. Seism. Soc. Am.*, 93, 2591-2603.

Skarlatoudis A., N. Theodulidis, Ch. Papaioannou and Z. Roumelioti ⁽²⁰⁰⁴⁾: The dependence of peak horizontal acceleration on magnitude and distance for small magnitude earthquakes in Greece. *Proc. 13WCEE*, Paper No. 1857, *Vancouver BC, August 1-6, 2004*, 12pp.

Spudich, P., Joyner, W.B., Lindh, A.G., Boore, D.M., Margaris, B.N. and Fletcher, J.B SEA99, (1999): A revised ground motion prediction for use in extensional tectonic regimes, *Bull. Seism. Soc. Am.* **89**, 1156-1170.

Thenhaus, P.C. and K.W. Campbell (2003): Seismic Hazard Analysis, in *W-F Chen & Ch. Scawthorn (:editors) Engineering Handbook*, CRC Press.

Theodulidis, N.P. (1991): Contribution to strong ground motion study in Greece. *PhD Thesis* (in Greek), 500pp.

Theodulidis N. and B. Papazachos (1992). Dependence of strong ground motion on magnitude-distance, site geology and macroseismic intensity for shallow earthquakes in Greece: I, Peak horizontal acceleration, velocity and displacement. *Soil Dyn. & Earth. Eng.*, 11, 387-402.

Tselentis, G-Akis and L. Danciu (2008). Empirical Relationships between Modified Mercalli Intensity and Engineering Ground-Motion Parameters in Greece, *Bull. Seism. Soc. Am.* 98, 1863–1875.

Tselentis, G-A. and L. Danciu, (2010): Probabilistic Seismic Hazard Assessment in Greece Part I:Engineering Ground Motion Parameters, *Natural Hazards and Earth Science Systems*, 10, 25-39.



APPENDIX 1

A. Local Seismic Hazard (in $PGAc_m/sec^2$) for a geographical grid surrounding of City of Serres and various Return Periods (10- 1890 years). E.S. is the examined site where disaggregation is carried out

Geogr. Coord.	10	25	50	100	200	475	950	1890	E.S.
23.5010 41.0761	22.92	34.86	47.87	65.75	90.29	196.69	234.38	279.00	
23.5410 41.0761	22.15	34.36	47.89	66.74	93.03	216.13	291.58	294.01	
23.5492 41.0878	18.58	30.61	44.66	65.17	95.08	225.38	296.20	305.51	Serres
23.5810 41.0761	18.44	30.69	45.12	66.34	98.34	277.75	345.06	360.90	
23.6210 41.0761	15.63	27.84	43.08	66.67	105.53	291.34	346.99	360.93	
23.6610 41.0761	13.10	25.14	41.17	67.43	113.35	294.07	350.16	360.99	
23.7010 41.0761	11.04	22.86	39.66	68.79	120.48	296.56	351.87	361.02	
23.7410 41.0761	8.97	20.40	37.98	70.69	127.68	298.01	346.63	360.88	
23.5010 41.1161	16.58	27.99	41.60	61.83	91.89	182.74	205.10	217.25	
23.5410 41.1161	15.03	26.66	41.14	63.48	98.62	203.69	244.48	290.72	
23.5810 41.1161	12.85	24.40	39.63	64.38	107.03	220.58	292.20	309.76	
23.6210 41.1161	11.05	22.50	38.52	65.93	116.08	231.28	295.95	318.00	
23.6610 41.1161	9.07	20.14	36.83	67.37	127.64	243.52	302.80	332.02	
23.7010 41.1161	6.86	17.32	34.89	70.28	141.90	256.91	310.43	345.18	
23.7410 41.1161	5.47	15.38	33.61	73.48	155.31	268.85	316.86	354.78	
23.5010 41.1561	13.69	24.74	38.71	60.58	94.79	160.23	173.94	188.72	
23.5410 41.1561	11.81	22.86	37.68	62.11	103.90	178.32	210.61	240.22	
23.5810 41.1561	10.16	21.05	36.51	63.34	112.97	190.69	228.23	270.94	
23.6210 41.1561	8.44	18.99	35.07	64.78	127.56	204.09	255.25	324.36	



Project funded by the
EUROPEAN UNION



23.6610	41.1561	6.31	16.30	33.42	68.53	147.30	222.84	290.13	389.99
23.7010	41.1561	5.35	15.06	32.95	72.10	160.33	241.66	328.77	444.87
23.7410	41.1561	5.01	14.72	33.26	75.14	171.98	265.21	372.19	496.38
23.5010	41.1961	10.35	20.55	34.53	58.02	96.53	121.96	147.07	185.91
23.5410	41.1961	9.54	19.78	34.35	59.64	99.17	133.28	172.67	228.38
23.5810	41.1961	8.50	18.76	34.15	62.16	103.87	148.58	211.59	293.13
23.6210	41.1961	6.51	16.37	32.88	66.06	111.40	173.65	270.10	376.98
23.6610	41.1961	5.86	15.61	32.79	68.85	118.04	218.02	347.92	484.91
23.7010	41.1961	5.29	14.96	32.87	72.19	125.94	291.13	420.57	583.76
23.7410	41.1961	4.48	13.85	32.50	76.29	134.46	332.06	477.60	673.72
23.5010	41.2361	14.86	25.27	37.76	56.43	84.32	117.83	147.02	187.47
23.5410	41.2361	13.64	24.22	37.40	57.76	89.19	130.11	173.64	228.50
23.5810	41.2361	11.44	22.16	36.55	60.27	98.26	149.32	215.96	293.47
23.6210	41.2361	10.08	20.81	36.01	62.29	104.28	176.88	278.06	383.55
23.6610	41.2361	9.11	19.83	35.72	64.34	111.28	223.88	359.26	495.17
23.7010	41.2361	8.26	18.96	35.54	66.64	120.07	294.93	446.36	589.99
23.7410	41.2361	7.41	18.07	35.47	69.60	130.27	352.93	503.91	683.46
23.5010	41.2761	18.77	28.84	39.92	55.25	76.47	111.08	144.92	189.40
23.5410	41.2761	16.15	26.64	38.90	56.81	82.95	127.24	175.22	229.66
23.5810	41.2761	14.95	25.71	38.75	58.41	88.03	147.45	216.66	293.49
23.6210	41.2761	13.46	24.41	38.29	60.07	94.24	176.88	279.22	383.55
23.6610	41.2761	12.31	23.39	38.00	61.73	101.22	224.30	359.28	496.84
23.7010	41.2761	11.33	22.50	37.81	63.53	110.62	294.93	446.37	589.99
23.7410	41.2761	10.25	21.47	37.58	65.76	122.83	353.47	503.92	684.66



B. Local Seismic Hazard (in $PGAc_m/sec^2$) for a geographical grid surrounding of City of Komotini and various Return Periods (10- 1890 years). E.S. is the examined site where disaggregation is carried out

Geogr. Coord.	10	25	50	100	200	475	950	1890	E.S
25.3682 41.1083	2.8187	8.8382	20.9803	49.8031	195.0051	423.2858	494.6844	531.8370	
25.3882 41.1083	2.7787	8.7575	20.8693	49.7320	195.0104	425.2623	494.6844	531.8370	
25.4082 41.1083	2.7773	8.7589	20.8830	49.7892	290.0008	426.3970	494.6844	531.8370	
25.4282 41.1083	2.7947	8.8003	20.9574	49.9091	290.0009	427.2125	494.6844	531.8370	
25.4482 41.1083	2.7915	8.7978	20.9654	49.9613	290.0009	427.2125	494.6844	531.8370	
25.4682 41.1083	2.7843	8.7870	20.9610	50.0011	290.0009	427.2027	494.6844	531.8370	
25.4882 41.1083	2.8074	8.8406	21.0542	50.1412	195.0104	425.3562	494.6844	531.8370	
25.5082 41.1083	2.8314	8.8961	21.1503	50.2843	195.0051	423.2874	494.6844	531.8370	
25.5282 41.1083	2.8864	9.0170	21.3448	50.5270	195.0025	418.3771	494.6844	531.8370	
25.3682 41.1283	4.5479	12.2056	25.7570	54.3541	195.0051	423.2860	494.6844	531.8370	
25.3882 41.1283	3.0526	9.3255	21.7053	50.5194	195.0104	425.2642	494.6844	531.8370	
25.4082 41.1283	2.7279	8.6470	20.6960	49.5345	290.0008	426.4029	494.6844	531.8370	
25.4282 41.1283	2.7230	8.6409	20.6983	49.5804	290.0009	427.2125	494.6844	531.8370	
25.4482 41.1283	2.7155	8.6291	20.6920	49.6179	290.0009	427.2125	494.6844	531.8370	
25.4682 41.1283	2.7084	8.6183	20.6873	49.6575	290.0009	427.2029	494.6844	531.8370	
25.4882 41.1283	2.7318	8.6729	20.7825	49.8003	195.0104	425.3562	494.6844	531.8370	
25.5082 41.1283	2.7859	8.7930	20.9773	50.0452	195.0051	423.2874	494.6844	531.8370	
25.5282 41.1283	2.8101	8.8491	21.0745	50.1900	195.0025	418.3771	494.6844	531.8370	



Project funded by the
EUROPEAN UNION



25.3682	41.1483	4.4909	12.0946	25.5899	54.1434	195.0051	387.3650	455.9715	520.5436	
25.3882	41.1483	4.5025	12.1208	25.6374	54.2271	195.0104	387.3650	455.9715	520.5436	
25.4082	41.1483	3.8338	10.8769	23.9380	52.6833	195.0105	387.3650	455.9715	520.5436	
25.4282	41.1483	2.6575	8.4937	20.4566	49.2684	290.0004	387.3650	455.9715	520.5436	
25.4482	41.1483	2.6408	8.4619	20.4194	49.2737	290.0004	387.3650	455.9715	520.5436	
25.4682	41.1483	2.6338	8.4511	20.4145	49.3131	290.0004	387.3650	455.9715	520.5436	
25.4882	41.1483	2.6851	8.5664	20.6034	49.5537	195.0104	387.3650	455.9715	520.5436	
25.5082	41.1483	2.7110	8.6266	20.7074	49.7062	195.0051	387.3650	455.9715	520.5436	
25.5282	41.1483	2.7348	8.6821	20.8042	49.8514	195.0025	384.0055	455.0213	520.5436	
25.3682	41.1683	4.3934	11.9091	25.3215	53.8393	195.0010	357.6268	404.0822	454.5201	
25.3882	41.1683	4.4249	11.9718	25.4186	53.9690	195.0011	357.7815	404.0822	454.5201	
25.4082	41.1683	4.3970	11.9260	25.3687	53.9637	195.0012	357.9125	404.0822	454.5201	
25.4282	41.1683	4.2920	11.7377	25.1247	53.7795	195.0012	357.9125	404.0822	454.5201	
25.4482	41.1683	2.7072	8.5992	20.6136	49.4141	195.0012	357.9125	404.0822	454.5201	
25.4682	41.1683	2.5695	8.3051	20.1729	48.9997	195.0012	357.9125	404.0822	454.5201	
25.4882	41.1683	2.6140	8.4065	20.3413	49.2204	195.0011	357.7815	404.0822	454.5201	
25.5082	41.1683	2.6371	8.4611	20.4374	49.3655	195.0010	357.6268	404.0822	454.5201	
25.5282	41.1683	2.6607	8.5167	20.5349	49.5122	158.0044	350.6672	401.7994	453.7051	
25.3682	41.1883	4.3335	11.7917	25.1449	53.6192	173.2538	287.7657	341.5022	360.8021	
25.3882	41.1883	4.3226	11.7768	25.1366	53.6517	191.9954	287.8357	341.5022	360.8021	
25.4082	41.1883	4.2949	11.7307	25.0858	53.6454	195.0004	287.8401	341.5022	360.8021	
25.4282	41.1883	4.3005	11.7462	25.1192	53.7174	195.0004	287.8401	341.5022	360.8021	
25.4482	41.1883	4.3000	11.7505	25.1375	53.7758	195.0004	287.8401	341.5022	360.8021	E.S.
25.4682	41.1883	3.1821	9.5903	22.0940	50.9000	195.0004	287.8401	341.5022	360.8021	
25.4882	41.1883	2.5424	8.2442	20.0744	48.8805	195.0004	287.8401	341.5022	360.8021	
25.5082	41.1883	2.5646	8.2972	20.1684	49.0242	158.0044	287.7657	341.5022	360.8021	
25.5282	41.1883	2.5880	8.3528	20.2664	49.1723	158.0022	287.6835	341.5022	360.8021	



Project funded by the
EUROPEAN UNION



25.3682	41.2083	4.2450	11.6212	24.8952	53.3308	155.1111	226.9725	273.4689	290.4854
25.3882	41.2083	4.2217	11.5831	24.8549	53.3335	160.5711	227.9177	273.7413	290.4854
25.4082	41.2083	4.1941	11.5368	24.8035	53.3262	160.6882	228.3229	273.8578	290.4854
25.4282	41.2083	4.1997	11.5523	24.8370	53.3986	159.3436	228.3229	273.8578	290.4854
25.4482	41.2083	4.2060	11.5692	24.8726	53.4733	158.0034	228.3229	273.8578	290.4854
25.4682	41.2083	4.2465	11.6495	24.9951	53.6291	158.0005	228.3229	273.8578	290.4854
25.4882	41.2083	3.8411	10.8904	23.9556	52.6952	158.0005	228.3229	273.8578	290.4854
25.5082	41.2083	2.5108	8.1735	19.9605	48.7457	146.6296	226.9726	273.4689	290.4854
25.5282	41.2083	2.5166	8.1905	19.9990	48.8318	138.6528	225.5073	273.0450	290.4854
25.3682	41.2283	4.1485	11.4349	24.6228	53.0202	115.2399	193.8882	195.8500	196.7193
25.3882	41.2283	4.1222	11.3906	24.5737	53.0144	117.2879	193.9495	195.8500	196.7193
25.4082	41.2283	4.0947	11.3441	24.5216	53.0061	117.4113	193.9498	195.8500	196.7193
25.4282	41.2283	4.1003	11.3597	24.5552	53.0789	117.5351	193.9502	195.8500	196.7193
25.4482	41.2283	4.1071	11.3775	24.5922	53.1552	117.3721	193.9428	195.8500	196.7193
25.4682	41.2283	4.1478	11.4588	24.7166	53.3137	116.1157	193.9007	195.8500	196.7193
25.4882	41.2283	4.1882	11.5395	24.8401	53.4712	116.1902	193.8996	195.8500	196.7193
25.5082	41.2283	4.1416	11.4576	24.7401	53.4206	114.6909	193.8366	195.8500	196.7193
25.5282	41.2283	2.5884	8.3421	20.2184	49.0026	114.6548	193.8304	195.8500	196.7193
25.3682	41.2483	4.0502	11.2442	24.3438	52.7047	103.8403	159.2736	185.7735	195.5996
25.3882	41.2483	4.0240	11.1995	24.2930	52.6944	103.8944	159.2885	185.7777	195.5996
25.4082	41.2483	3.9966	11.1528	24.2402	52.6852	103.9524	159.3034	185.7818	195.5996
25.4282	41.2483	4.0022	11.1684	24.2740	52.7584	104.0107	159.3185	185.7860	195.5996
25.4482	41.2483	4.0104	11.1889	24.3147	52.8385	104.0694	159.3336	185.7903	195.5996
25.4682	41.2483	4.0498	11.2682	24.4371	52.9959	104.1173	159.3050	185.7823	195.5996
25.4882	41.2483	4.0900	11.3489	24.5611	53.1548	103.7951	157.3168	185.3233	195.5996
25.5082	41.2483	4.1307	11.4305	24.6863	53.3147	103.7892	156.7543	185.2431	195.5996
25.5282	41.2483	4.1628	11.4958	24.7889	53.4536	103.8425	156.7558	185.2431	195.5996



Project funded by the
EUROPEAN UNION



25.3682	41.2683	3.2535	9.8453	22.7510	52.5738	102.9447	140.3678	167.0453	185.6715
25.3882	41.2683	3.9016	10.9670	23.9677	52.3800	101.6878	139.9158	167.0572	185.6757
25.4082	41.2683	3.9000	10.9629	23.9595	52.3635	101.6819	139.9372	167.0691	185.6798
25.4282	41.2683	3.9056	10.9786	23.9934	52.4371	101.7258	139.9778	167.0812	185.6841
25.4482	41.2683	3.9168	11.0049	24.0424	52.5254	101.7699	140.0186	167.0933	185.6883
25.4682	41.2683	3.9531	11.0788	24.1578	52.6770	101.8144	140.0597	167.1055	185.6927
25.4882	41.2683	3.9931	11.1597	24.2827	52.8377	101.8585	140.0954	167.1150	185.6960
25.5082	41.2683	4.0337	11.2416	24.4089	52.9994	101.7025	138.3943	166.2314	185.3844
25.5282	41.2683	4.5154	12.0342	25.2619	53.0291	100.8119	136.8699	165.5335	185.1374
25.3682	41.2883	6.8229	15.2625	28.0629	51.5988	94.8736	115.4399	134.1183	155.6753
25.3882	41.2883	6.7923	15.2200	28.0208	51.5877	94.9756	115.4774	134.1679	155.7396
25.4082	41.2883	7.5890	16.2582	28.9321	51.4859	91.6212	114.7919	133.7793	155.7606
25.4282	41.2883	7.8034	16.5372	29.1882	51.5173	90.9282	114.6451	133.7179	155.8162
25.4482	41.2883	7.8185	16.5659	29.2346	51.5914	91.0455	114.6884	133.7722	155.8838
25.4682	41.2883	7.8499	16.6190	29.3101	51.6927	91.1677	114.7321	133.8269	155.9518
25.4882	41.2883	7.8916	16.6872	29.4037	51.8107	91.2930	114.7761	133.8820	156.0204
25.5082	41.2883	7.9339	16.7563	29.4983	51.9298	91.4189	114.8202	133.9370	156.0887
25.5282	41.2883	7.9767	16.8261	29.5939	52.0498	91.5454	114.2792	132.7260	154.0085



4.2 TURKEY

Seismic hazard assessment at regional and local scales is evaluated for the broader area of Samsun (Turkey), Tekirdağ and Istanbul (Marmara Region, Turkey) based on the selected methodology from GA1.

Samsun (Fig 49) is located on the Black Sea coast of Turkey with a population of 1,252,693 (2010). Its adjacent provinces are Sinop on the northwest, Çorum on the west, Amasya on the south, Tokat on the southeast, and Ordu on the east.



Fig 49. Location of Samsun

Tekirdağ (Fig 50) is located at the northern shores of the Marmara Sea, and approximately 10 km NNE of a large and well-developed geological structure peculiar to the strike-slip faulting.



The Istanbul-Marmara region of northwestern Turkey with a population of more than 15 million faces a high probability of being exposed to an earthquake of magnitude 7 or more.



Fig 50. Location of Tekirdağ, and Istanbul

4.2.1 Introduction

Probabilistic seismic hazard analysis (PSHA) is a method used to evaluate seismic hazard by computing the probability of a specified level of ground motion being exceeded at a site or area of interest. In the most general sense, seismic hazard analysis aims to estimate the expected earthquake ground motion at a given site. These basic steps of PSHA are illustrated in figure (Fig 51) for the determination of design basis response spectrum in terms of peak ground acceleration (PGA) only, and in terms several spectral

acceleration amplitudes. For PSHA the latter case represents the so-called equi-hazard spectrum, where all the spectral acceleration amplitudes used in the construction of the spectrum have the same probability of exceedance.

The earthquake hazard assessment is generally conducted for the free-field reference soil sites, generally chosen as the so-called “engineering bedrock” where the average shear wave propagation velocity in the upper 30m is less than about 750m/s (in US practice NEHRP Site Class B/C boundary).

In this study, the probabilistic earthquake hazard assessment has been conducted in the bedrock level.

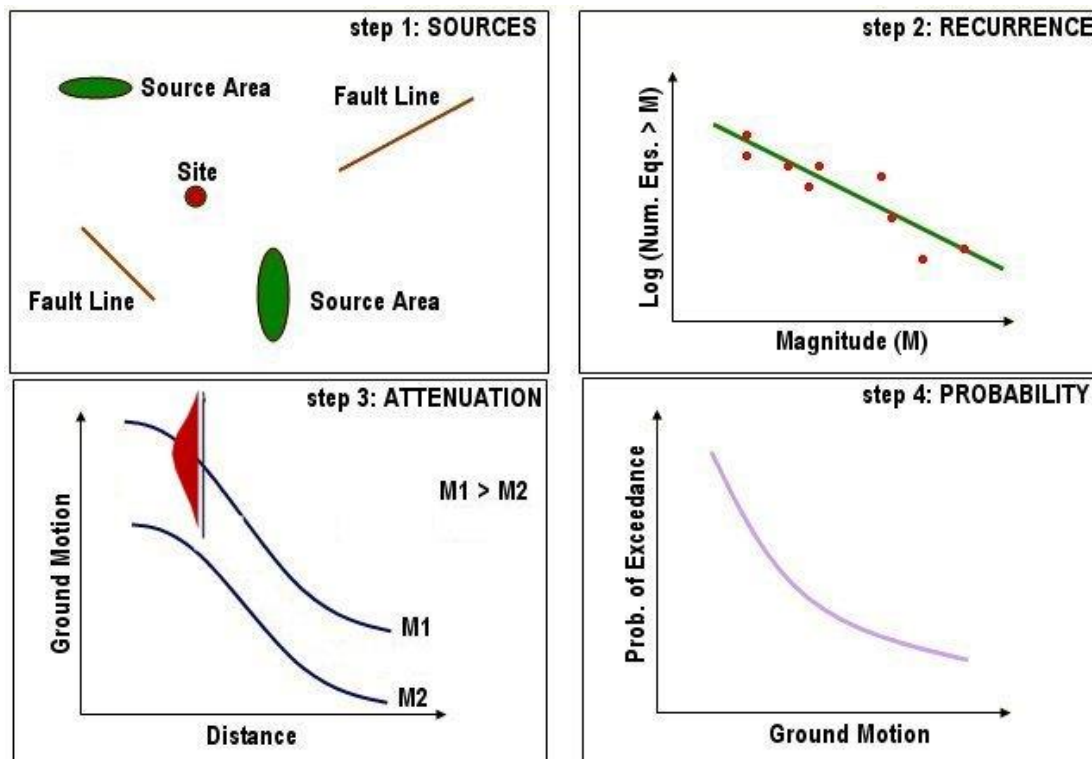


Fig 51. Basic steps of a probabilistic seismic hazard analysis

4.2.2 Seismicity

In the traditional probabilistic seismic hazard assessment (Cornell, 1968) only independent events are to be considered. To satisfy this requirement earthquakes in the study region needs to be de-clustered by

removing foreshocks and aftershocks from the seismicity databases in order to obtain a Poissonian distribution. The seismicity distribution (i.e. epicentral maps) between 1000 and 2007 years time period for Turkey is given in figure (Fig 52).

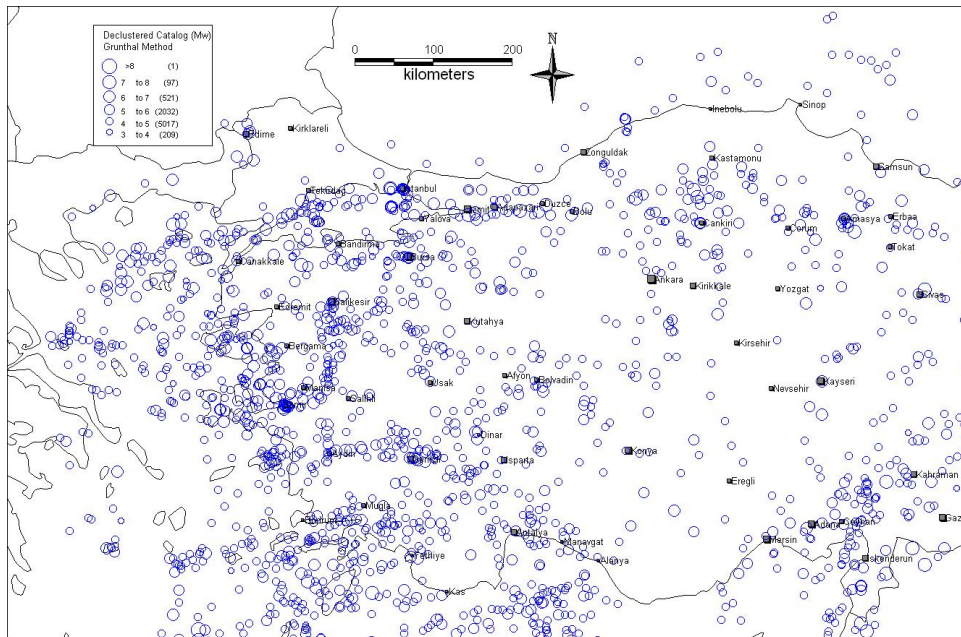


Fig 52. Instrumental seismicity distribution for Turkey

4.2.3 Tectonics of the Region

Turkey is a tectonically active region that experiences frequent destructive earthquakes. In a tectonic map, Turkey lies within the Mediterranean sector of the Alpine-Himalayan orogenic system, which runs west east from the Mediterranean to Asia. Turkey is surrounded by three major plates: African, Eurasian, and Arabian, and is located on two generally acknowledged minor plates: Aegean and Anatolian, as shown in Figure 53 (McKenzie, 1970). The relative motion between Eurasian, Arabian plates and the westward motion of the Anatolian-Aegean block is also illustrated in Figure 54 (Armijo et al., 1999).

GPS measurements carried out in Turkey during the period of 1988-1994 reveal valuable information about the rate of motion of the plates relative to one another in the region along major faults (Barka et. al., 1997; Barka & Reilinger, 1997). The results can be summarized as follows:

- Central Anatolia behaves as a rigid block and moves westward relative to Eurasia at about 15 mm/yr.
- Western Anatolia moves in a southwest direction at about 30 mm/yr.
- The Arabian plate moves northward with respect to Eurasia at a rate of 23 ± 1 mm/yr, 10 mm/yr of this rate is taken up by shortening in the Caucasus. The internal deformation in Eastern Anatolia caused by conjugate strike-slip faulting and E-W trending thrusts, including the Bitlis frontal thrust, accommodates approximately a 15 mm/yr slip rate.
- The Western Anatolian grabens take up a total of 15 mm/yr of the NE-SW extension.
- The African plate is moving in a northerly direction relative to Eurasia, at a rate of about 10 mm/yr.

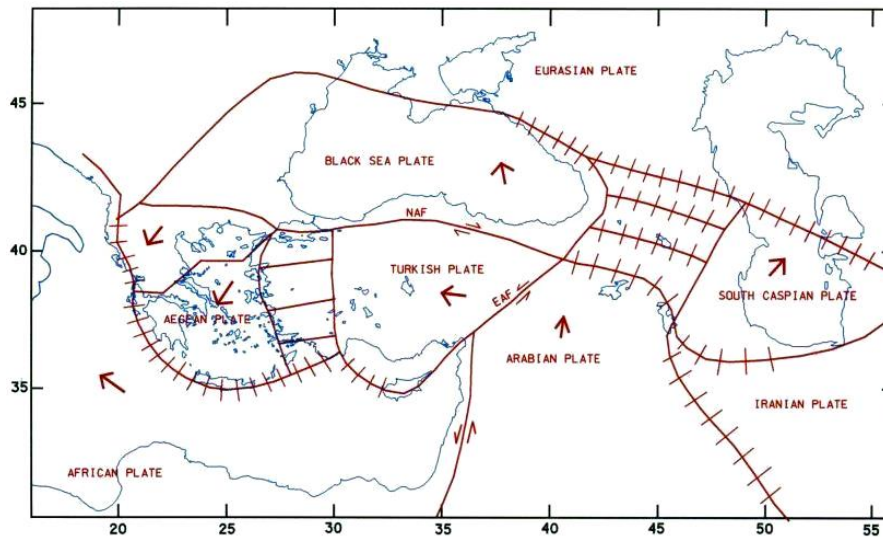


Fig 53. Plate tectonics of the Eastern Mediterranean and Caucasus regions (after McKenzie, 1970)

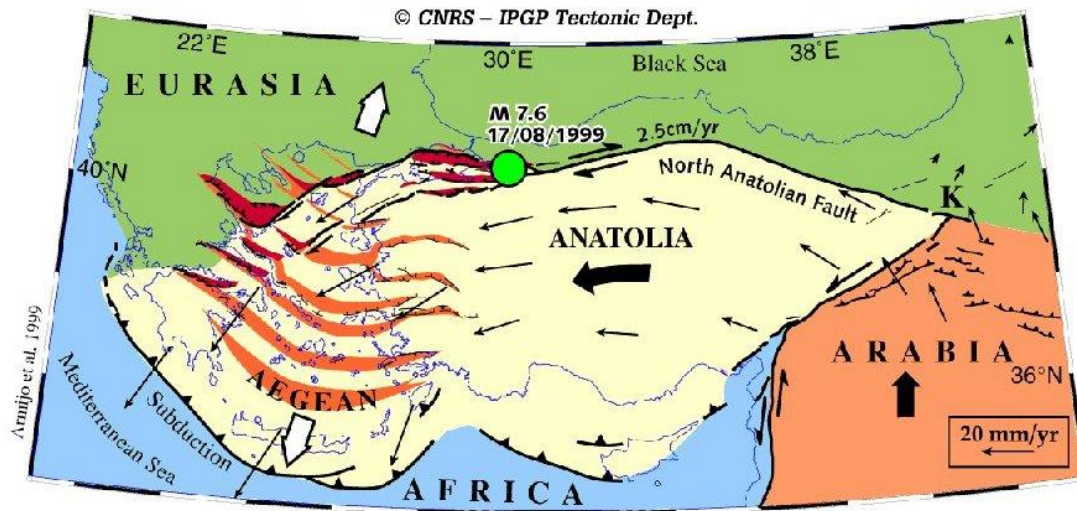


Fig 54. The relative motion between Eurasian and Arabian plates and the westward motion of the Anatolian and Aegean blocks (Armijo et al., 1999)

4.2.4 Tectonic Setting of the Marmara Region

North Anatolian Fault Zone (NAFZ) extending in the Sea of Marmara have a more complex structure. Several researches have developed different tectonic models for NAF Marmara Sea region.

Le Pichon *et al.* (2001, 2003), Aksu *et al.* (2000), Imren *et al.* (2001), Gokasan *et al.* (2001), Kuscu *et al.* (2002), Alpar and Yaltirak (2002), and Demirbag *et al.* (2003) proposed that the NAF was composed of a pure right-lateral fault system along the trough of the Northern Marmara Sea. However, Armijo *et al.* (1999, 2002), Barka and Kadinsky-Cade (1988), Barka (1992), Stein *et al.* (1997), Okay *et al.* (2004), Parke *et al.* (2002), Flerit *et al.* (2003) and Polonia *et al.* (2004) proposed that the Sea of Marmara was a pull-apart basin formed by the right step-over between the strike-slip faults of Ganos and Izmit, further the normal faults in the Cinarcik Basin and the Central Marmara Sea were also active. Another alternative structural model is defined that NAF was composed of a pull a part system produced by fault segmentation, oversteps and slip partitioning (Armijo *et al.*, 1999; Armijo *et al.*, 2002; Barka and Kadisky-Cade, 1988; Barka, 1992; Stein *et al.*, 1997; Okay *et al.*, 2000; Parke *et al.*, 2002; Flerit *et al.*, 2003; Polonia *et al.*, 2004).

The North Marmara Basin is located by the conspicuous 70-km-wide step-over between two strike-slip faults, well-known on land, which have ruptured with purely right-lateral motion during recent earthquakes, both with similar magnitude (M 7.4) and clear surface rupture. One is the 1912 Ganos Earthquake that ruptured the Dardanelles region to the west of the Marmara Sea; the second is the Izmit Earthquake that ruptured in 1999 east of the Marmara Sea. Pinar (1943) had previously drawn a single



fault, bisecting the Gulf of Izmit and the three Marmara deeps. Thus, this fault was named “the Main Marmara Fault”, which is located as an arc of great radius, going from Ganos to the entry of the Gulf of Izmit”. Based on the recent high resolution bathymetric and deep-tower seismic reflection data set acquired by the MARMARASCARPS CRUISE in 2000, Armijo *et al.* (2005) found out that the surface ruptures formed by the 1912 Ganos (Sarkoy-Murefte) Earthquake reached the eastern end of Central Basin, and also the fault scarps associated with the 1894 earthquake could be estimated in the southern edge of the Cinarcik Basin (Fig 55).

In this study, we have used the fault segmentation model for the Marmara Sea region as shown in Figure 61 (Erdik *et al.*, 2004). This model is based on the tectonic model of the Marmara Sea, defining the Main Marmara fault, a thoroughgoing dextral strike-slip fault system, as the most significant tectonic element in the region. The segmentation provided relies on Le Pichon *et al.* (2001)’s discussion of several portions of the Main Marmara Fault based on bathymetric, sparker and deep-towed seismic reflection data and interprets it in terms of fault segments identifiable for different structural, tectonic and geometrical features. From east to west the Main Marmara fault cuts through Çınarcık, Central and Tekirdağ basins, which are connected by higher lying elements. The fault follows the northern margin of the basin when going through the Çınarcık trough in the northwesterly sense, makes a sharp bend towards west to the south of Yesilkoy, entering central highs, cuts through the Central basin and alternates in this manner until it reaches the 1912 Murefte-Şarköy rupture. All these features are interpreted as different fault segments in the model. The remaining segments of the model (e.g. for the eastern and southern Marmara regions) are compiled from various studies (Barka and Kadinsky-Cade, 1988; Şaroğlu *et al.*, 1992; Akyuz *et al.*, 2000; Yaltirak, 2002).

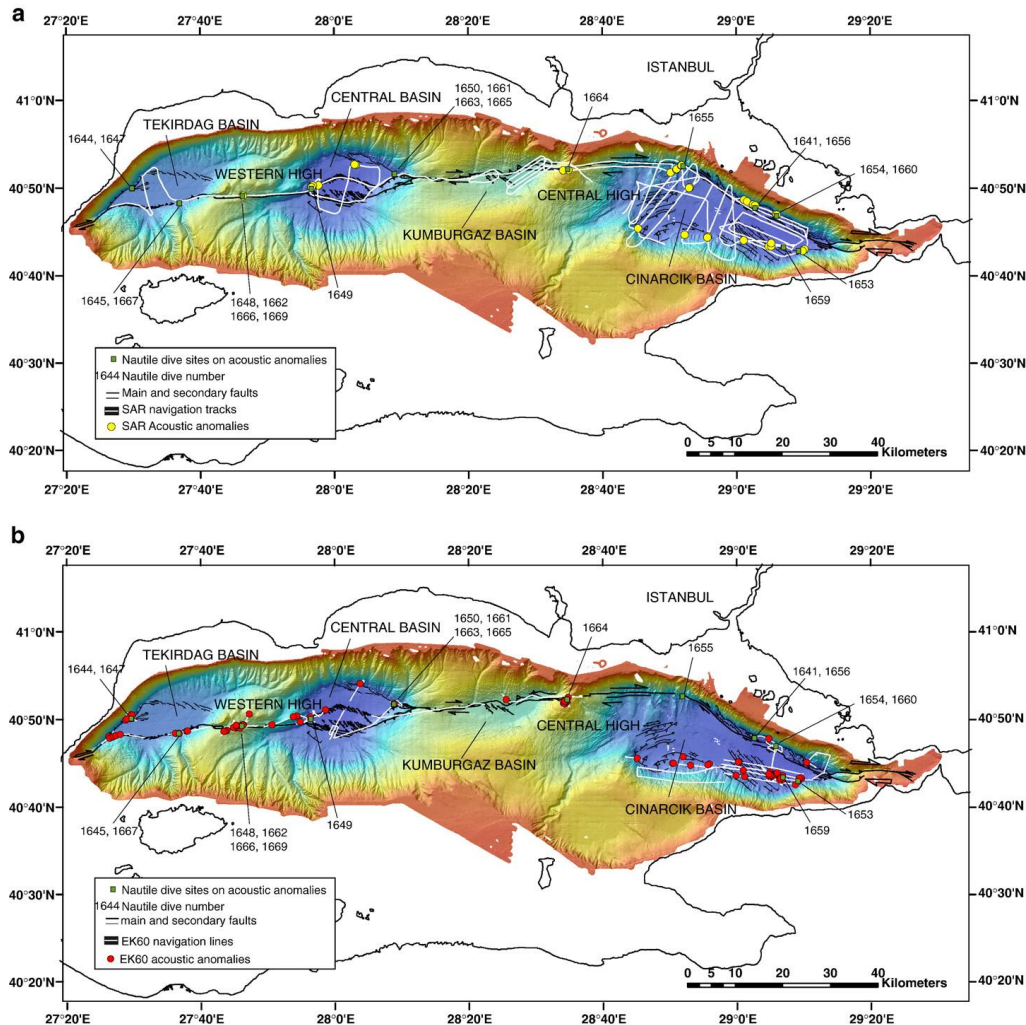


Fig 55. Distribution of acoustic anomalies, superimposed on the bathymetric map (Rangin et al., 2001, Armijo et al., 2002; 2005; Imren et al., 2001, Le Pichon et al., 2001) of the deeper parts of the Marmara Sea

4.2.5 Tectonic Setting of Black Sea Region

The Black Sea is located between Ukraine, Russia, Georgia, Turkey, Bulgaria and Romania. It is a semi-isolated extensional basin surrounded by thrust belts. The structure of the basin is known mainly through the acquisition and interpretation of seismic data (Tugolesov *et al.*, 1985; Finetti *et al.*, 1988; Belousov and Volvovsky, 1989). In terms of crustal structure, The Black Sea is formed of two deep basins (Fig 56). The western Black Sea Basin is underlain by oceanic to sub-oceanic crust and contains a sedimentary cover of up to 19 km thick. On the other side, the eastern Black Sea Basin is underlain by thinned



continental crust approximately 10 km in thickness and up to 12 km thickness of sediments (Nikishin *et al.*, 2003). These basins are separated by the Mid Black Sea Ridge which consists of the Andrusov Ridge in the north and the Archangelsky Ridge in the south (Fig 57 & Fig 58). The Andrusov Ridge is formed from continental crust and overlain by 5.–6. km thickness of sedimentary cover (Tugolesov *et al.*, 1985; Finetti *et al.*, 1988; Belousov and Volvovsky, 1989; Robinson, 1997). The Archangelsky Ridge is bound to the south by the eastern Pontide belt, a complex terrane formed by a sequence of orogenic events during the Mesozoic and Cenozoic.



Project funded by the
EUROPEAN UNION

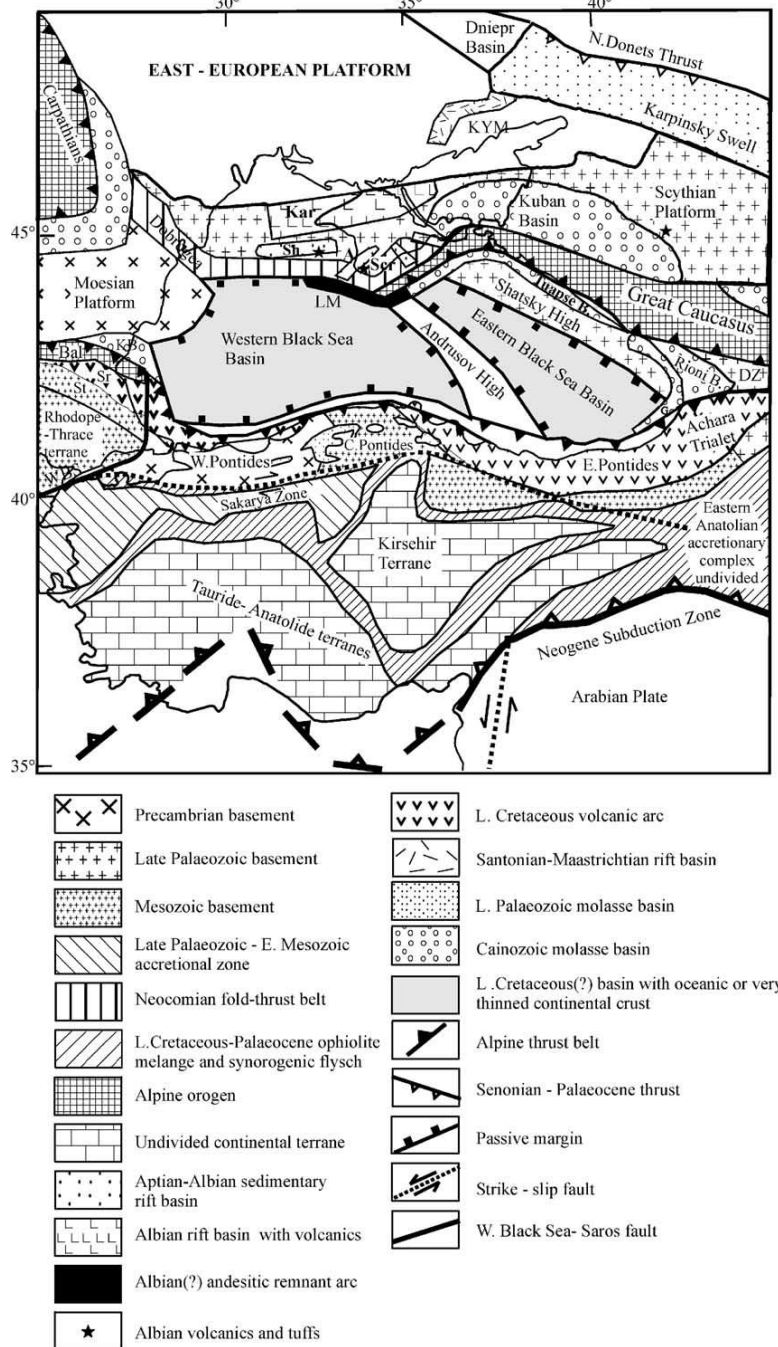


Fig 56. Tectonic setting of the Black Sea Basin (Nikishin et al., 2003)



Project funded by the
EUROPEAN UNION

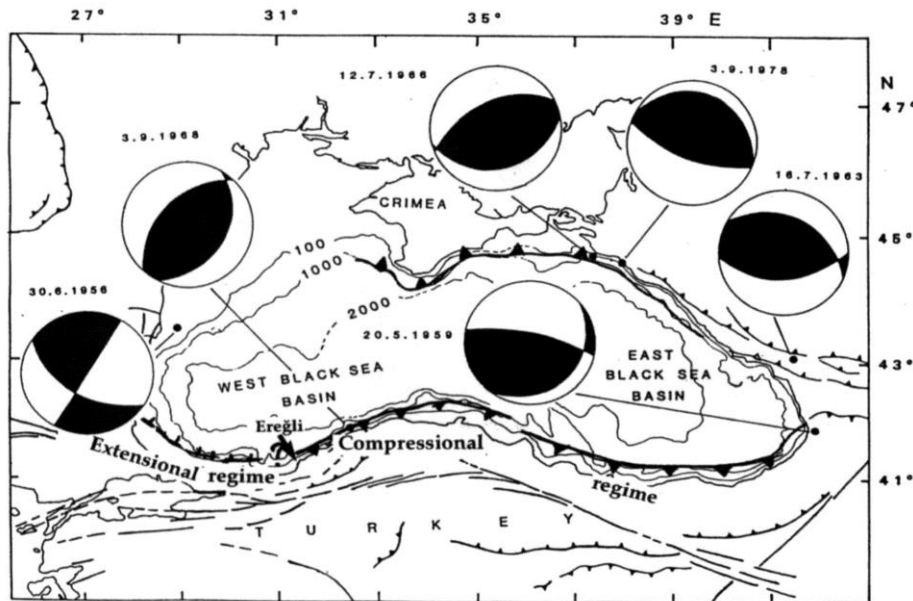


Fig 57. Tectonics of the Black Sea (from Barka and Reilinger, 1997)

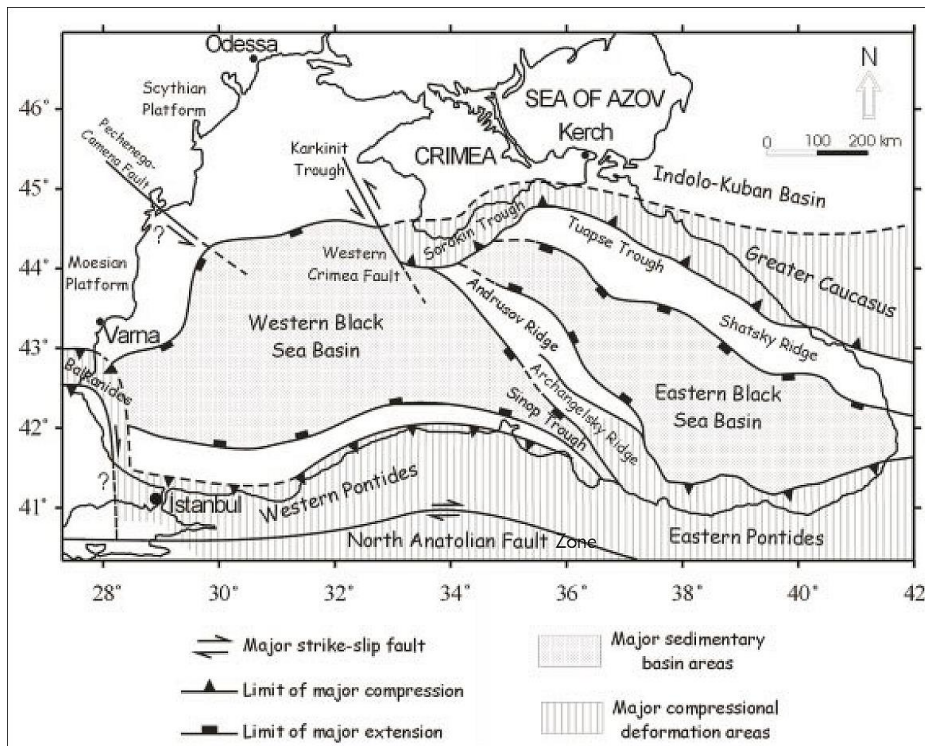


Fig 58. Tectonic framework of the Black Sea region (after Temel and Ciftci, 2002)

The Black Sea region is known to be an area of active tectonics and seismicity (Fig 59) after Chekunov *et al.*, 1994). The central, deepest part of the Black Sea depression is believed to be relatively aseismic. Thus, when estimating seismic hazard, only continental slope and on-shore tectonic structures are considered as zones of strong earthquake generation (Medvedev, 1968). The seismic activity within the circum Black Sea is assumed as low-moderate for this century. The seismic activity is influenced by the extensional tectonics in the Western Anatolia. There is also a speculation that the lithosphere of the Black Sea and Caspian Sea form a resistant “backstop” diverting the impinging Anatolian Plate to the west and “funneling” the continental lithosphere of Eastern Turkey and the Caucasus around the eastern side of the Black Sea (McClusky *et al.*, 2000).

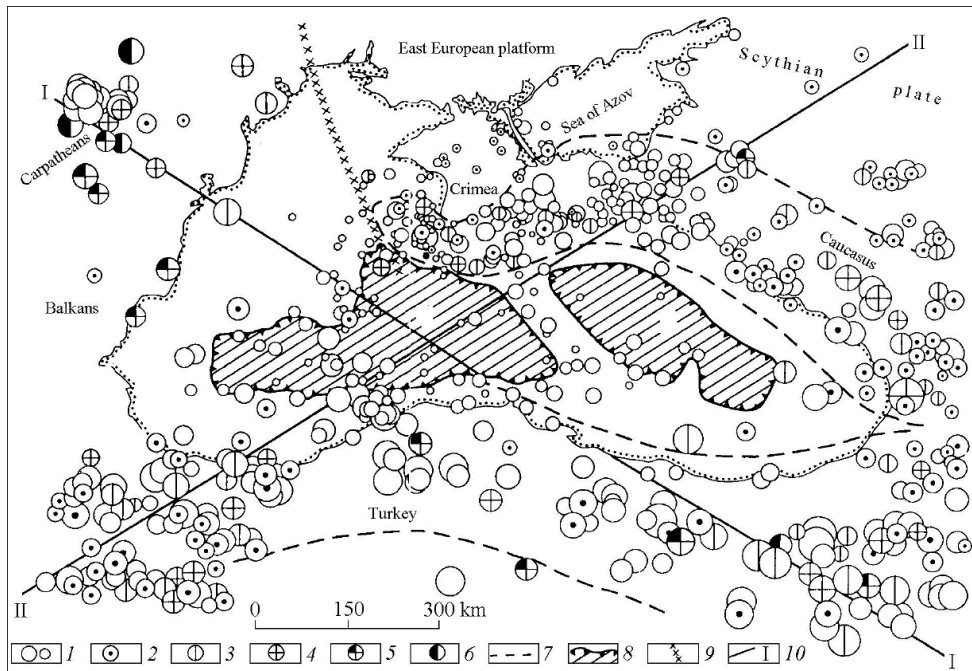


Fig 59. Map of the Black Sea region and seismic zones (after Chekunov, 1994).

Meredith and Egan (2002) showed that deeper parts of southern margin of the Black Sea are dominated by extensional faults (fig 60). The Sinop Basin is located between the Archangelsky Ridge and the Turkish coastline and has been affected by normal faults along the Turkish margin and the Archangelsky Ridge (Rangin *et al.*, 2002).

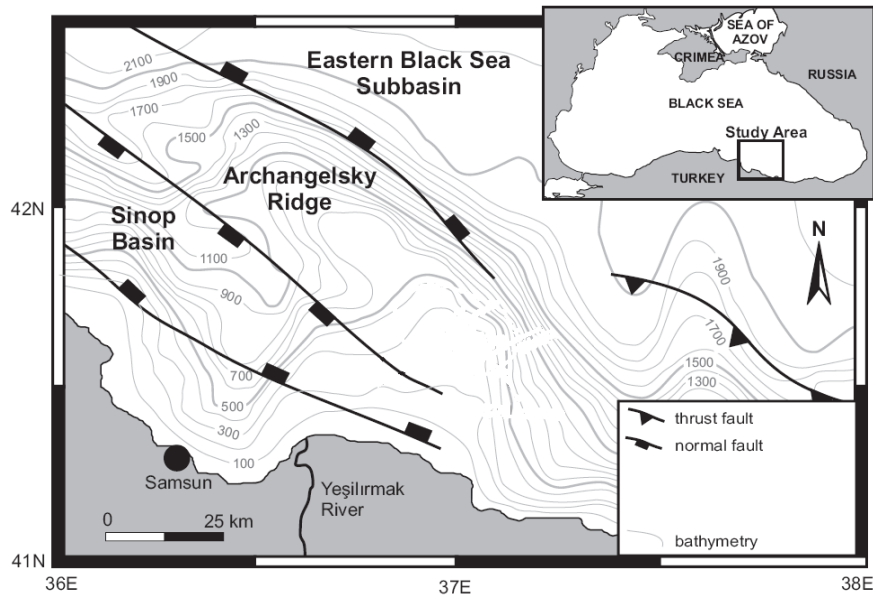


Fig 60. Offshore faulting associated with the Black Sea Escarpment (after Dondurur, 2009).

4.2.6 Seismic Source Zonation

The first step in seismic hazard assessment (probabilistic and/or deterministic) is the identification and the delineation of earthquake sources (seismic source zonation) where the future events will take place. The seismicity-related source zone parameters are the appropriate earthquake recurrence model, recurrence rate (the so-called b value) and the maximum earthquake size.

The earthquake sources may be characterized as discrete faults in tectonically active regions (fault sources) or as areal zones with uniform seismicity (areal sources). The geometric source zone parameters for areal and fault sources include the location, geometry, and for faults dip and width. Fault sources can be line sources (two dimensional) or planar sources (three dimensional) modeling the distribution of seismicity over the fault plane. Areal source zones are used to model spatial distribution of seismicity that cannot be specifically associated with major faults, background seismicity areas or in regions with unspecified faults. An areal seismic source zone is defined as a seismically homogenous area, in which every point within the source zone is assumed to have the same probability of being the epicenter of a future earthquake. Background seismic zones are areal sources that can be defined to account for floating earthquakes not accounted by these sources and also to delineate zones where no significant earthquake has taken place for centuries.

4.2.7 Seismic Source Zonation for Istanbul and Tekirdag (Marmara Region)

The earthquake hazard in the region is assumed to be the result of the contributions, computed in following two steps:

- (1) Ground motions that would result from the earthquakes in the magnitude range from 5.0 to 6.9
- (2) Ground motion that would result from larger events in the magnitude range 7.0 and higher.

Step (1) is termed as ‘background source activity’, i.e. the activity not associated with the main segmented tectonic entities. In this study, undelineated fault sources and small areal sources based on spatially smoothed historic seismicity are used as the background earthquake source.

Step (2) is related to the seismic energy release along well-defined and segmented faults. For this part the fault segmentation model that we used in the paper of Erdik et al. (2004), Figure 61.

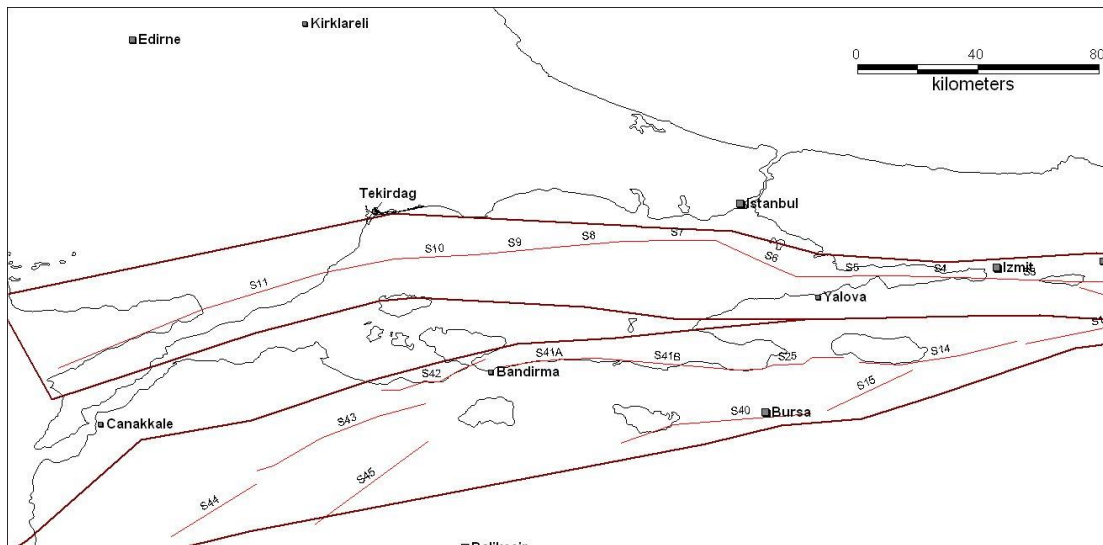


Fig 61. Fault segmentation model proposed for the Marmara region (Erdik et al., 2004)

4.2.8 Seismic Source Zonation for Samsun Province (Turkey)

The seismic source zonation for Samsun province (Turkey) used in this study is essentially based on the seismic source zonation model of Turkey developed within the context of a project conducted for the Ministry of Transportation Turkey, DLH, aiming for the preparation of an earthquake resistant design code for the construction of railways, seaports and airports. The main improvement of this model when compared to previous studies (e.g., GHSAP, TEFER, Baku-Ceyhan Crude Oil Pipeline Projects) is the representation of main fault traces (such as the North Anatolian and the East Anatolian Faults) with linear sources. Previous models used only areal zones to define seismic sources. In order to account for the

spatially more diffuse moderate size seismicity around these faults, widths of at least several kilometers were assigned to the zones even if the associated faults were well expressed on the surface. In the new model however, earthquakes with magnitude > 6.5 are assumed to take place on the linear zones, whereas the smaller magnitude events associated with the same fault are allowed to take place in the surrounding larger areal zone. In addition to linear and areal source zones background seismicity zones are defined to model the floating earthquakes that are located outside these distinctly defined source zones and to delineate zones where no significant earthquake has taken place (Fig 62).

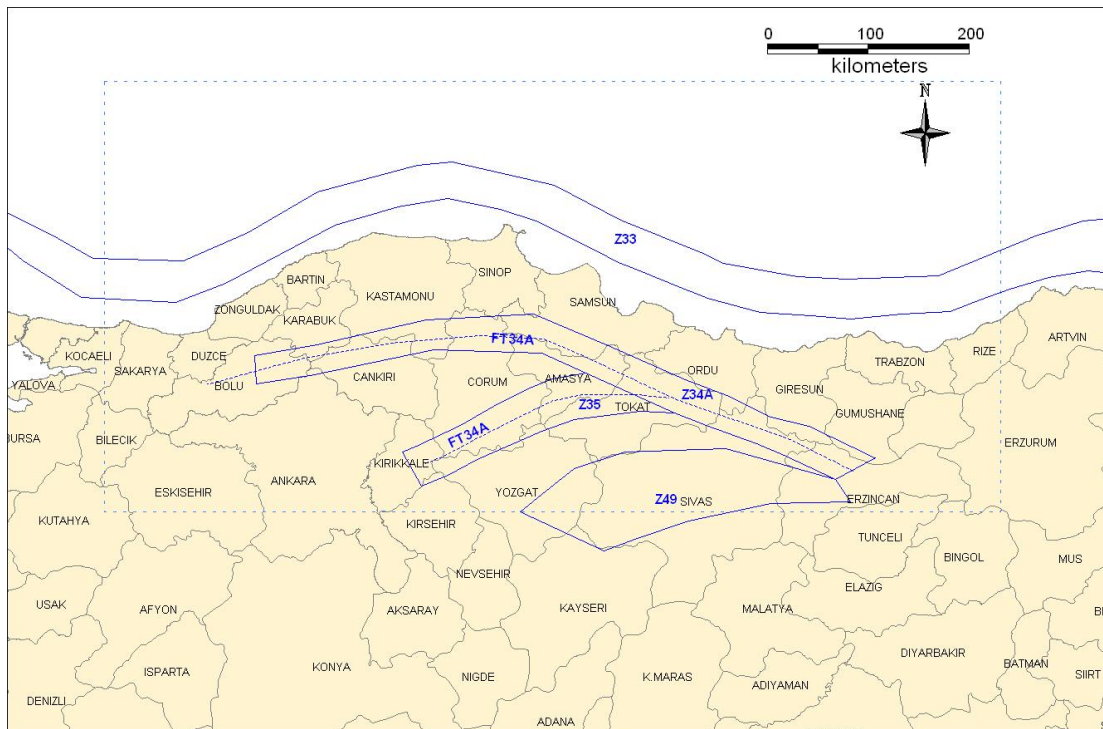


Fig 62. A seismic source zonation for Samsun province (Turkey)

4.2.9 Methodology of Probabilistic Seismic Hazard Assessment

Two different methodologies have been used to compute the probabilistic hazard for Samsun (Turkey), and Istanbul, Tekirdag (Marmara Region). These are:

1. Time-dependent and Poisson approaches for the Marmara region
2. Poisson approach for Samsun Province (Turkey)

The study of Erdik et al (2004) forms the basis of the time dependent hazard model for the Marmara region. Earthquake occurrence and fault segmentation data in the Marmara region are adequate to constrain a time dependent characteristic model for the region. The results of the study indicate a lower



future hazard for the region of the 1999 earthquake and a higher hazard for the Central Marmara Sea region corresponding to the unruptured segments of the Main Marmara Fault in the Marmara Sea, when compared to Poisson, so-called memory-less models. This finding is also in accordance with (Parsons et al, 2000) indicating heightened probabilities for a major earthquake in the Marmara Sea region based on stress transfer approach.

4.2.10 Time-Dependent Approach Used for Marmara Region

The use of a time-dependent probabilistic seismic-hazard model is felt to be needed for the assessment of probabilistic hazard in the Marmara region. In time-dependent models, the probability of earthquake occurrence increases with the elapsed time since the last major (or characteristic) earthquake on the fault that controls the regional earthquake hazard. In the case of the main Marmara Fault this earthquake is the 1999 Kocaeli event. This model is characterized by the recurrence-interval probability-density function of the characteristic earthquakes. Extensive paleoseismic and historical seismicity investigations on individual strike-slip faults (especially in California and Northwestern Turkey) indicate a quasi-periodic occurrence of characteristic earthquakes favoring the use of “time dependent” (or “renewal”) stochastic models.

The methodology, elaborated in Erdik et al. (2003), is essentially very similar to the one developed and used by United States Geological Survey - WGCEP (<http://geohazards.cr.usgs.gov/eq/index.html>) for the preparation of US National Seismic Hazard Maps. The main physical ingredients of seismic hazard assessment are the tectonic setting of the region, the earthquake occurrences and the local site conditions. These regional physical features, the applicable attenuation relationships and the appropriate stochastic model for probabilistic hazard analysis will be discussed in the following sections

The time-dependent (renewal) model

While the Poisson process seems to be applicable in a global sense in a regional scale, extensive paleoseismic and historical seismicity investigations on individual faults indicate a somewhat periodic occurrence of large (characteristic) magnitude earthquakes that necessitate the use of “time dependent” (or “renewal”) stochastic models (Schwartz and Coppersmith, 1984). The time dependent model is based on the assumption that the occurrence of large (characteristic) earthquakes has some periodicity. The conditional probability that an earthquake occurs in the next ΔT years, given that it has not occurred in the last T years is given by:



$$P(T, \Delta T) = \frac{\int_T^{T+\Delta T} f(t) dt}{\int_T^{\infty} f(t) dt} \quad (1)$$

where $f(t)$ is the probability density function for the earthquake recurrence intervals, T is the elapsed time since the last major earthquake and ΔT is the exposure period (taken as 50 years). Various statistical models have been proposed for the computation of the probability density function, such as Gaussian, log-normal, Weibull, Gamma and Brownian. Among those, the log-normal distribution is the most commonly used in the engineering practice. The Brownian Passage Time model is a more recently proposed model and is also assumed to adequately represent the earthquake distribution (Ellsworth et al., 1999). The log-normal and Brownian Passage Time models are compared in the following sections.

For the renewal model, the conditional probabilities for each fault segment are calculated. These probabilities are said to be conditional since they change as a function of the time elapsed since the last earthquake. A lognormal distribution with a covariance of 0.5 is assumed to represent the earthquake probability density distribution. The 50 year conditional probabilities thus calculated are converted to effective Poissonian annual probabilities by the use of the following expression (WGCEP, 1995):

$$R_{\text{eff}} = -\ln(1 - P_{\text{cond}}) / T \quad (2)$$

Earthquake recurrence parameters for the fault segmentation model

The association of historical earthquakes with the segments of the model is accomplished by a critical review of the literature on the historical seismicity of the Marmara region. The seismicity information from two of these studies, Ambraseys and Finkel (1991) and Hubert-Ferrari (2000) are presented in Figure 63 and Figure 64 respectively.

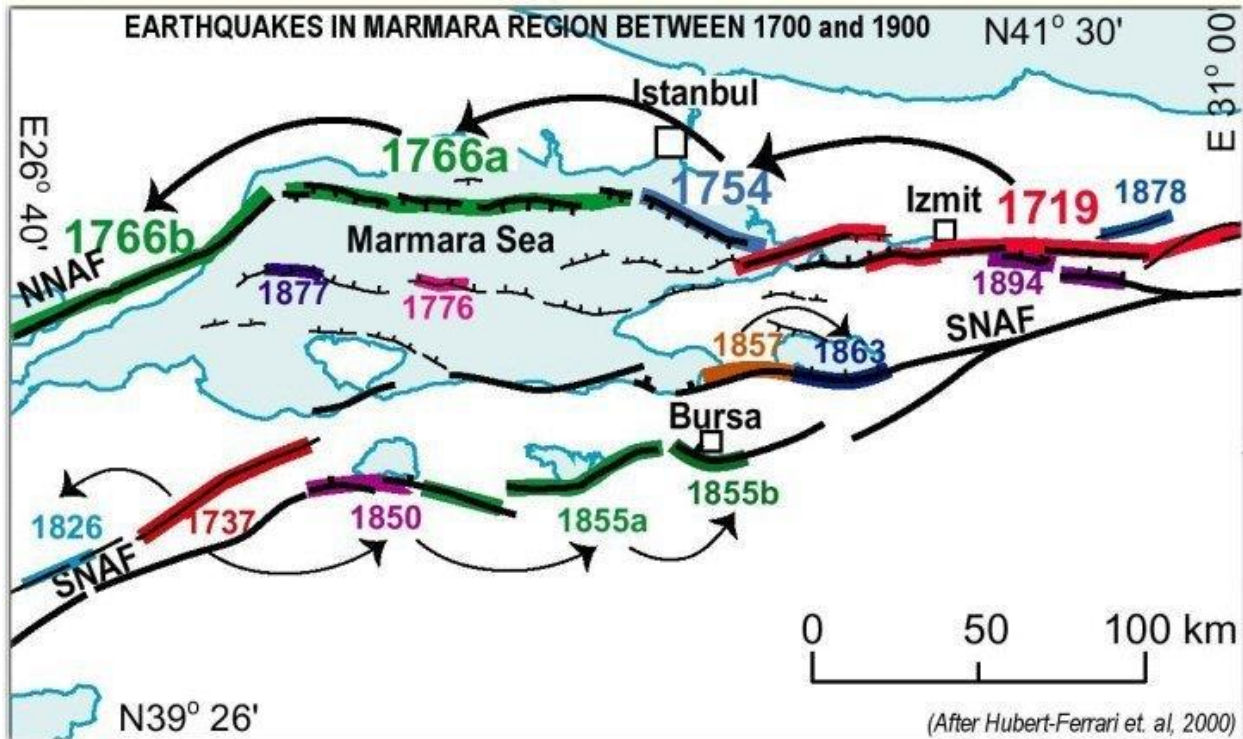


Fig 64. The sequence of earthquakes in the 18th century around Marmara region (after Hubert-Ferrari, 2000).

4.2.11 The Time-Independent (Poisson) Approach Used for Samsun Province (Turkey)

The time-independent probabilistic (simple Homogeneous Poissonian) model was used to assess the seismic hazard in the remaining regions of the Turkish territory. For the earthquake events to follow that model, the following assumptions are in order:

1. Earthquakes are spatially independent;
2. Earthquakes are temporally independent;
3. Probability that two seismic events will take place at the same time and at the same place approaches zero.

The historical and instrumental seismicity, tectonic models and the known slip rates along the faults constitute the main ingredients of the hazard analysis. Seismic zonation has been implemented in three levels. The first level consists of linear faults representing the North Anatolian Fault (NAF), the north and east branches of NAF in the Marmara region, Bitlis – Zagros Suture Zone, Hatay Fault, Ezinepazari Fault, East-Anatolian Fault, Goksun Fault, Ecemis Fault, Tuzgolü Fault, Eskisehir Fault Zone, Simav-Sultandağ Fault Zone, Fethiye-Burdur Fault Zone, Gokova Fault Zone, Menderes Fault Zone, Gediz Fault Zone and



Bergama Fault Zone. It is assumed that seismic energy along the line-segments is released by characteristic earthquakes, therefore the earthquakes with magnitude $M_w \geq 6.5$ are associated with these line sources. The second level consists of limited areal zones around these linear segments assuming that earthquakes with magnitude $M_w < 6.5$ may take place within this zone. Smaller en-echelon and/or diffused faults were assumed to be encompassed in these zones. The third level considers the background seismicity, which represents the diffused seismicity that cannot be associated with known faults.

The recurrence relationship of the events is expressed with the help of the empirical relationship first defined by Gutenberg - Richter: $\log N = A - bM$ where N is the number of shocks with magnitude greater or equal to M per unit time and unit area, and A and b are constants for any given region. The source regions may be described as lines representing the known faults or areas of diffuse seismicity, so that M may be related to unit length or unit area. The value of N will also generally be found assuming that M has upper and lower bounds M_1 and M_0 .

Using an application of the total probability theorem the probability per unit time that that ground motion amplitude a^* is exceeded can be expressed as follows (McGuire, 1993):

$$P[A > a^* \text{ in time } t] / t = \sum_i v_i \iint G_A |_{m,r} (a^*) f_m(m) f_r(r|m) dm dr \quad (3)$$

where $P[I \leq i | m, r]$ is the probability that the maximum effect I is less than i . Given m and r , $f_m(m)$ is the probability density function for magnitude, and $f_r(r|m)$ is the probability distribution function for distance. $f_r(r|m)$ is dependent on the geometric nature of the source.

The seismic zonation model developed in accordance with the Poisson approach is given in Figure 62.

4.2.12 Earthquake Recurrence Models for Marmara Region

The earthquake recurrence parameters for each fault segment (Fig 61) are calculated by the procedures described in the previous section and presented in Table 4.2.1. All these parameters that used in the paper of Erdik et al, (2004) are updated based on the current year.

Table 4.2.1 Poisson and renewal model characteristic earthquake parameters associated with the segments

Time dependent (Renewal)	Poissonian
-----------------------------	------------

Segment	Last Char. Eq.	“COV”	Mean Recurrence Time	Char. Magnitude	Time since Last Char. Eq.	50year Prob.	Annual Rate	Annual Rate
1	1999	0.5	140	7.2	15	0.08260	0.00172	0.0071
2	1999	0.5	140	7.2	15	0.08260	0.00172	0.0071
3	1999	0.5	140	7.2	15	0.08260	0.00172	0.0071
4	1999	0.5	140	7.2	15	0.08260	0.00172	0.0071
5	1894	0.5	175	7.2	120	0.39620	0.01009	0.0057
6	1754	0.5	210	7.2	260	0.41200	0.01062	0.0048
7	1766	0.5	250	7.2	248	0.34280	0.00840	0.0040
8	1766	0.5	250	7.2	248	0.34280	0.00840	0.0040
9	1556	0.5	200	7.2	458	0.41730	0.01080	0.0050
10	-	0.5	200	7.2	1012	0.33250	0.00808	0.0050
11	1912	0.5	150	7.5	102	0.44960	0.01194	0.0067
12	1967	0.5	250	7.2	47	0.03810	0.00078	0.0040
13	-	0.5	600	7.2	1012	0.17200	0.00377	0.0017
14	-	0.5	600	7.2	1012	0.17200	0.00377	0.0017
15	-	0.5	1000	7.2	1012	0.09790	0.00206	0.0010
19	1944	0.5	250	7.5	70	0.08750	0.00183	0.0040
21	1999	0.5	250	7.2	15	0.00450	0.00009	0.0040
22	1957	0.5	250	7.2	57	0.05750	0.00118	0.0040
25	-	0.5	1000	7.2	1012	0.09790	0.00206	0.0010
40	1855	0.5	1000	7.2	159	0.00092	0.00002	0.0010
41	-	0.5	1000	7.2	1012	0.09790	0.00206	0.0010
42	-	0.5	1000	7.2	1012	0.09790	0.00206	0.0010
43	1737	0.5	1000	7.2	277	0.01010	0.00020	0.0010
44	-	0.5	1000	7.2	1012	0.09790	0.00206	0.0010
45	1953	0.5	1000	7.2	61	-	-	0.0010
				Mmin - Mmax	alpha	Beta		
BCK	-	-	-	5.0 - 6.9	1.2078	1.767	-	
Z16								
Z17	-	-	-	5.0-6.6	1.5136	2.0954	-	

4.2.13 Earthquake Recurrence Model for Turkey

The earthquake recurrence parameters for each fault segment (Fig 62) are calculated by the procedures described in the previous section and presented in Table 4.2.2. computed recurrence parameters as well as the maximum magnitudes associated with the source zones are presented in Table 4.2.2

Table 4.2.2 Poisson model earthquake parameters associated with the segments

Source Zone No	Associated Fault	a	b	$M_{\min} - M_{\max}$
Z33	Black Sea Fault	3.8	0.9	5.0 - 7.3
Z34 Outside Zone	North Anatolian Fault Zone (NAF)	5	0.8	5.0 - 6.7
Z34 Inside Zone				6.8 - 7.9
Z35 Outside Zone	Alaca Ezine Pazari Fault	3.2	0.8	5.0 - 6.7
Z35 Inside Zone				6.8 - 7.9
Z49	Deliler Fault Zone	4.4	1	5.0 - 7.3
ZBK1	Background	5.13	1	5.0-6.5

4.2.14 Ground Motion Prediction Equations

For the PSHA investigations, we have considered the following GMPEs for “active shallow region” with equal weights in the fault tree combination:

Ground motion models for active shallow regions:

- Akkar and Bommer (2009, rev:2010)
- Boore and Atkinson (2008)
- Chiou and Youngs (2008)
- Campbell and Bozorgnia (2008)
- Abrahamson and Silva (2008)

The reason for this selection limited to global and pan-european and most recent GMPEs was simply the broad database to fully account the aleatoric variability. Various characteristics of the selected GMPEs are given in Table 4.2.3 (Delavaud et al., 2012).

Akkar and Bommer (2010) predicts spectral ordinates at response periods of up to 3 seconds as a function of moment magnitudes from M_w 5 to 7.6, style-of-faulting, R_{JB} distances up to 100 km, and site class, the



geometric mean values of 5%-damped horizontal pseudo-spectral acceleration, PSA (in cm/s^2) in Europe and the Middle East.

Boore and Atkinson (2008) used data from the PEER Next Generation Attenuation (NGA) Flatfile supplemented with additional data from three small events (2001 Anza M4.92, 2003 Big Bear City M4.92 and 2002 Yorba Linda M4.27) and the 2004 Parkfield earthquake, which were used only for a study of distance attenuation function but not the final regression (due to rules of NGA project); three faulting mechanism using P and T axes; focal depths between 2 and 31 km. This paper excludes singly-recorded earthquakes and aftershock records.

Chiou and Youngs (2008) model is based on PEER Next Generation Attenuation (NGA) database; characterizes sites using V_{s30} ; 1 is applicable for $150 \leq V_{s30} \leq 1500$ m/s; is included data from aftershocks; is excluded data from more than 70 km to remove the effects of bias in sample.

Campbell and Bozorgnia (2008) used data from PEER NGA Flatfile and three faulting mechanism types based on rake angle; characterize sites using V_{s30} ; included dip of rupture plane.

Abrahamson and Silva (2008) model is applicable for $5 \leq M_w \leq 8.5$ (strike-slip) and $5 \leq M_w \leq 8.0$ (dip-slip) and $0 \leq d_r \leq 200$ km; selected data from the Next Generation Attenuation (NGA) database and included data from all earthquakes, including aftershocks, from shallow crustal earthquakes in active tectonic regions under assumption that median ground motions from shallow crustal earthquakes at $d_r < 100$ km are similar. This assumes that median stress-drops are similar between shallow crustal events in: California, Alaska, Taiwan, Japan, Turkey, Italy, Greece, New Zealand and NW China.

Table 4.2.3 Characteristics of the selected GMPEs for active shallow regions (Delavaud et al., 2012)

Model	Area	Magnitude Range	Distance Range (km)	Period Range (s)	Site	Mechanism	Component
Abrahamson and Silva (2008)	California, Taiwan and other regions	$M_w=5.0-8.0$	$R_{rup} = 0 - 200$	$0.01 - 10.0$, PGA, PGV	Function of V_{s30}	N, R/T, S	GMRot150
Boore and Atkinson (2008)	California, Taiwan and other regions	$M_w=4.27 - 7.9$	$R_{jb} = 0 - 280$	$0.01 - 10.0$, PGA, PGV	Function of V_{s30}	N, R, S, U	GMRot150
Chiou and Youngs (2008)	California, Taiwan and other regions	$M_w=4.27 - 7.9$	$R_{rup} = 0.2 - 70$	$0.01 - 10.0$, PGA, PGV	Function of V_{s30}	N, R, S	GMRot150
Campbell and Bozorgnia	California, Taiwan and other	$M_w=4.27 - 7.9$	$R_{rup} = 0.07 - 199.27$	$0.01 - 10.0$, PGA, PGV	Function of V_{s30}	N, R, S	GMRot150



Project funded by the
EUROPEAN UNION



Model	Area	Magnitude Range	Distance Range (km)	Period Range (s)	Site	Mechanism	Component
(2008)	regions						
Akkar and Bommer (2010)	European and Middle East	Mw=5.0-7.6	Rrup = 0 – 99	0.05-3.0, PGA,PGV	3 classes	N,R/T,S	GMEAN

4.2.15 Hazard Maps for Marmara Region

For regional hazard maps it becomes essential to quantify seismic hazard associated with a certain ground condition, so-called the “reference ground”, from which the ground motion for other types of ground condition can be inferred. In this study NEHRP B/C Boundary (characterized with a 30m average shear wave propagation velocity of 760m/s) is used as the reference ground, similar to the seismic hazard maps prepared by USGS. The results obtained for 40%, 10%, 5% and 2% probabilities of exceedence in 50 years for PGA for the Poisson and renewal models are presented in Figure 65 through **Σφάλμα! Το αρχείο προέλευσης της αναφοράς δεν βρέθηκε.** 72, respectively.

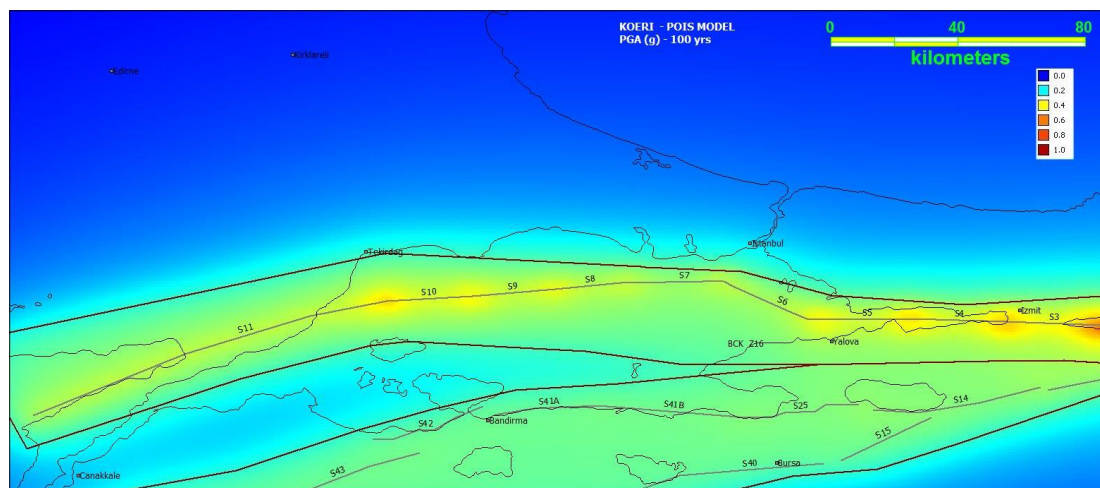


Fig 65. PGA map at NEHRP B/C boundary site class for 40% probability of exceedence in 50 yr (poisson model).

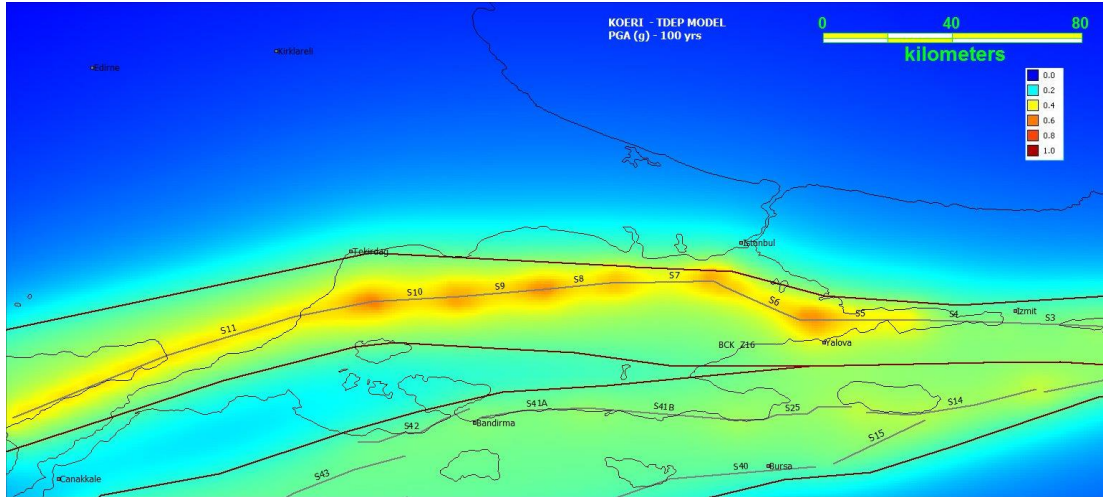


Fig 66. PGA map at NEHRP B/C boundary site class for 40% probability of exceedence in 50 yr (renewal model).

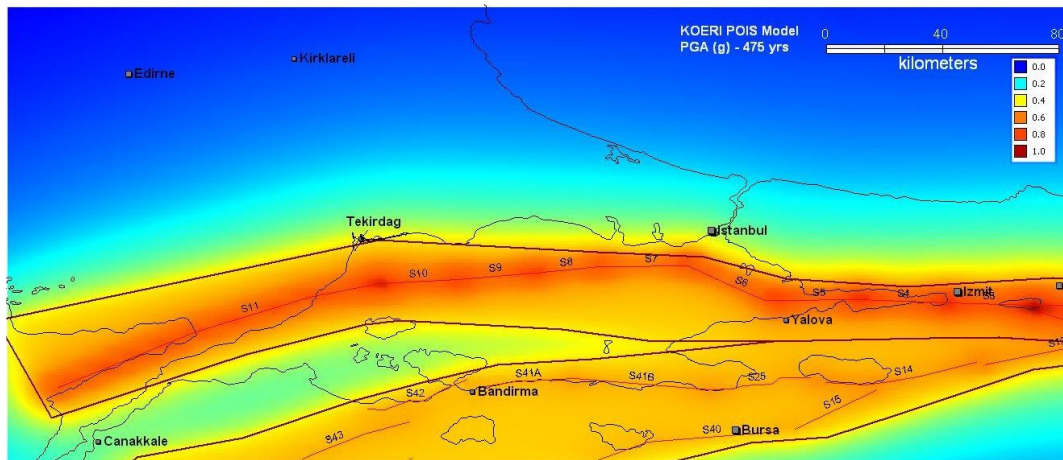


Fig 67. PGA map at NEHRP B/C boundary site class for 10% probability of exceedence in 50 yr (poisson model).



Project funded by the EUROPEAN UNION

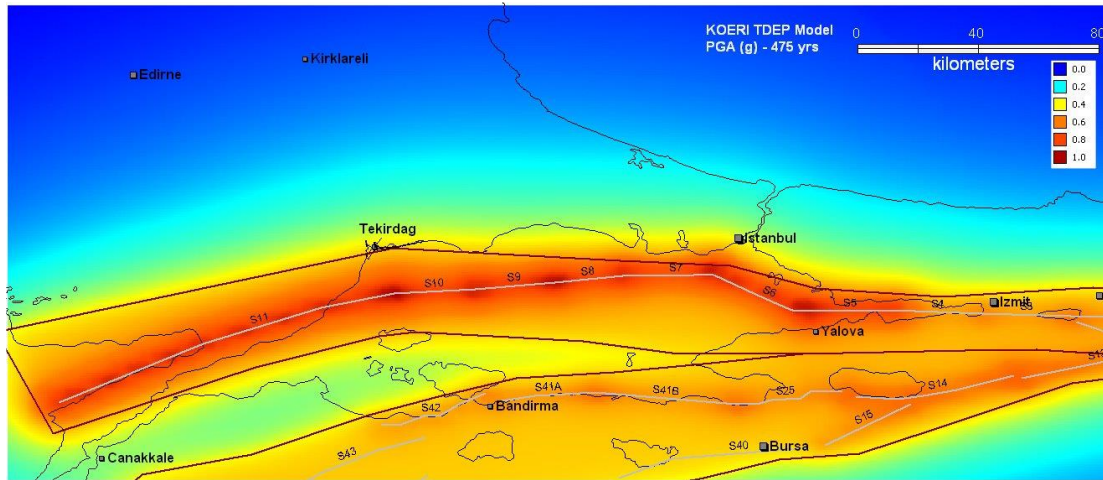


Fig 68. PGA map at NEHRP B/C boundary site class for 10% probability of exceedence in 50 yr (renewal model).

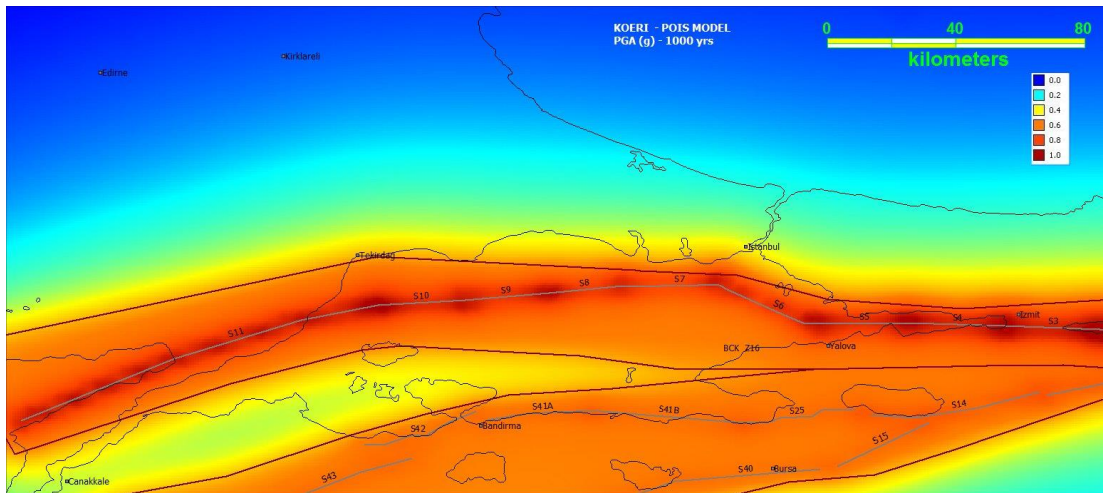


Fig 69. PGA map at NEHRP B/C boundary site class for 5% probability of exceedence in 50 yr (poisson model).



Project funded by the
EUROPEAN UNION

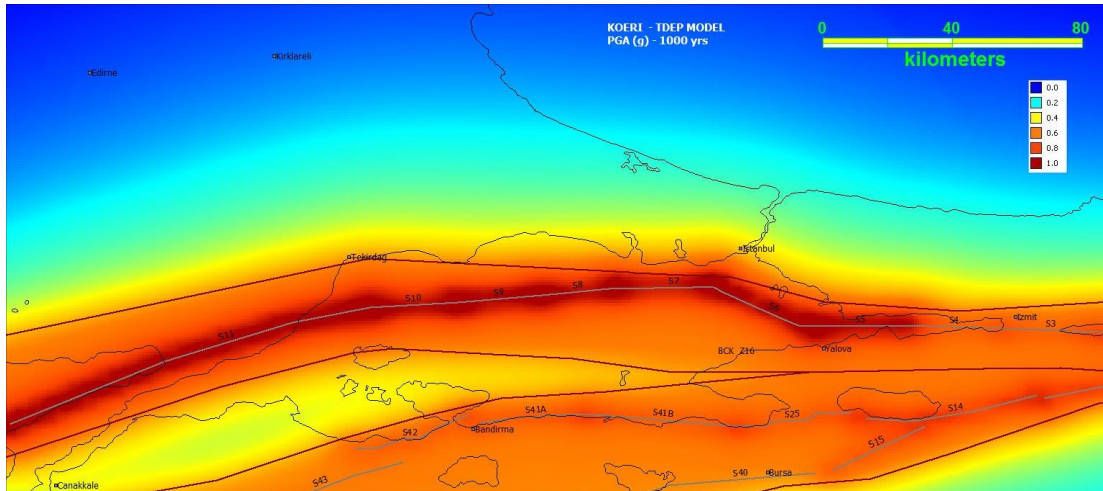


Fig 70. PGA map at NEHRP B/C boundary site class for 5% probability of exceedence in 50 yr (renewal model).

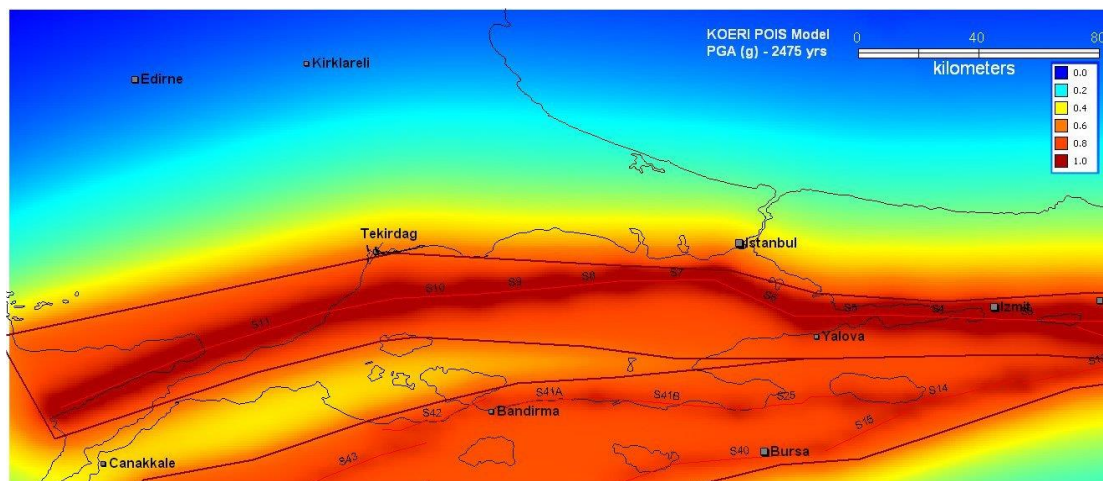


Fig 71. PGA map at NEHRP B/C boundary site class for 2% probability of exceedence in 50 yr (poisson model)



Project funded by the
EUROPEAN UNION

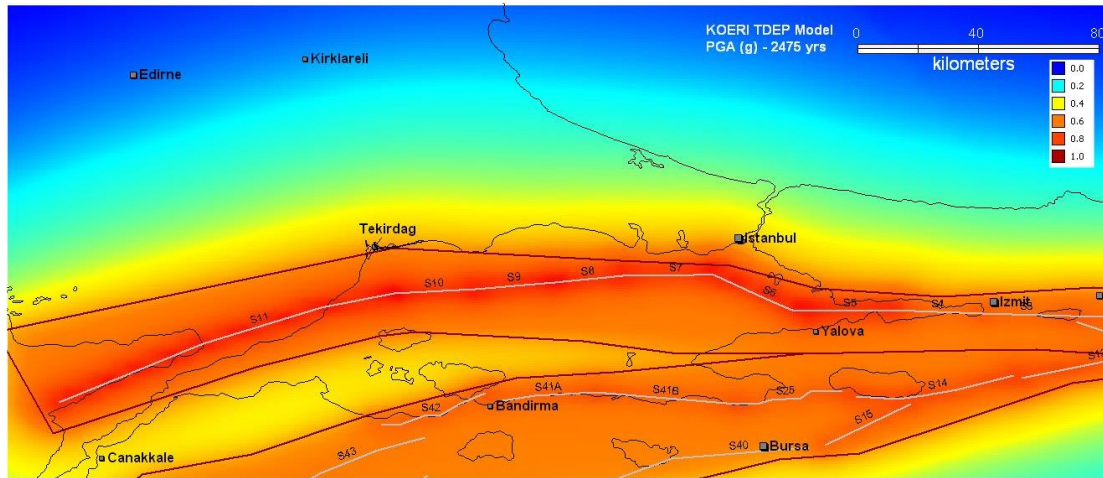


Fig 72. PGA map at NEHRP B/C boundary site class for 2% probability of exceedence in 50 yr (renewal model).

4.2.16 Hazard Maps for the Samsun Province (Turkey)

The results obtained for 40%, 10%, 5% and 2% probabilities of exceedence in 50 years for PGA for the Poisson

The results for Samsun province obtained for 40%, 10%, 5% and 2% probabilities of exceedence in 50 years for PGA for the Poisson model are presented in Figure 73 through Figure 76 respectively.

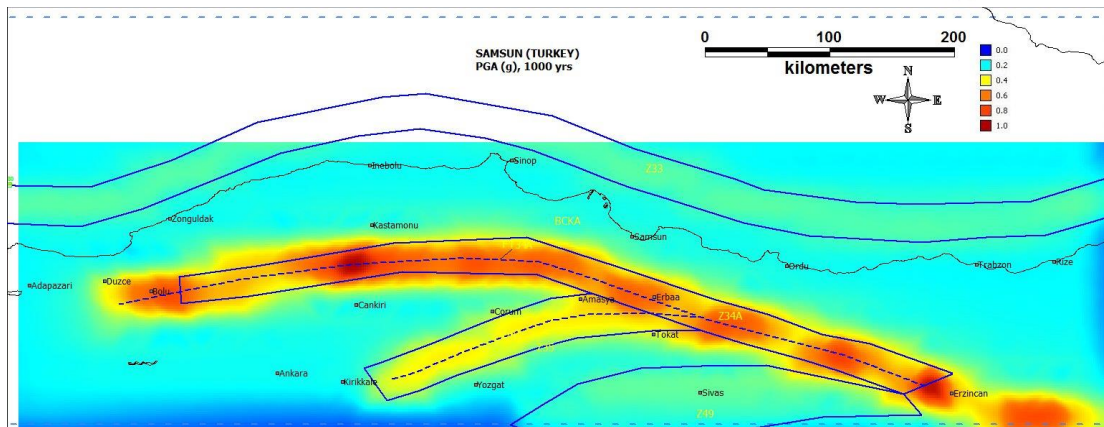


Fig 75. PGA map at NEHRP B/C boundary site class for 5% probability of exceedence in 50 yr (poisson model).

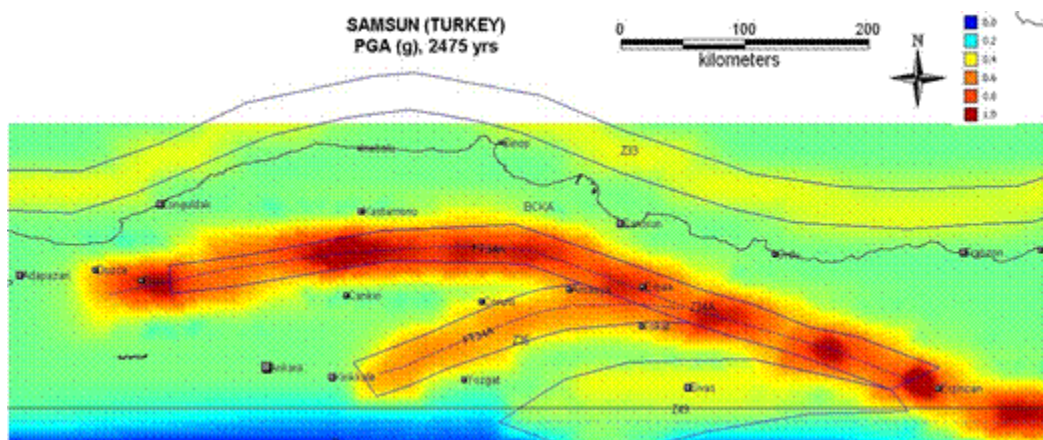


Fig 76. PGA map at NEHRP B/C boundary site class for 2% probability of exceedence in 50 yr (poisson model).

REFERENCES

Abrahamson, N. A., and W. J. Silva (2008), Summary of the Abrahamson & Silva NGA Ground-Motion Relations, *Earthquake Spectra*, 24(1), 67-97.

Akkar, S. and Bommer, J.J., 2010. Empirical equations for the prediction of PGA, PGV and spectral accelerations in Europe, the Mediterranean region and the Middle East, *Seismological Research Letters* 81, 195-206.



Aksu, A. E., T. J. Calon, R. N. Hiscott, and D. Yasar, 2000, “Anatomy of the North Anatolian Fault Zone in the Marmara Sea, Western Turkey: Extensional Basins above a Continental Transform”, *Geological Society of America (GSA Today)*, June 3-7.

Akyuz, H. S., E. Altunel, E. V. Karabacak, and C.C. Yalciner, 2006, “Historical Earthquake Activity of the Northern Part of the Dead Sea Fault Zone, Southern Turkey”, *Tectonophysics*, Vol. 426, pp.281–93

Alpar B. and C. Yaltirak, 2002, “Characteristic Features of the North Anatolian Fault in the Eastern Marmara Region and its Tectonic Evolution”, *Marine Geology*, Vol. 190, pp. 329-350.

Ambraseys N.N. and Finkel C.F., 1987, Seismicity of the Northeast Mediterranean region during early 20th century, *Annal. Geophys.* 5B, 701-726.

Armijo R., B. Meyer, A. Hubert, and A. Barka (1999), *Westwards Propagation of the North Anatolian Fault into the Northern Aegean: Timing and kinematics*, *Geology*, Vol. 27-3, pp. 267-270.

Armijo, R. N. Pondard, B. Meyer, B. Mercier de Lepinay, G. Uçarkus, J. Malavieille, S. Dominguez, M-A Beck Gustcher, M-A. Beck, N. Çagatay, Z. Cakir, C. Imren, E. Kadir and Natalin, and MARMARASCARPS cruise party, 2005, “Submarine Fault Scarps in the Sea of Marmara Pull-apart (North Anatolian Fault): Implications for Seismic Hazard in Istanbul”, *Geochemistry Geophysics Geosystems*, pp. 1-29.

Barka, A. (1992), *The North Anatolian Fault Zone*, *Annales Tectonicae*, Special Issue – Supplement to Vol. VI, pp: 164-195.

Barka, A. and K. Kadinsky-Cade (1988), Strike-slip fault geometry in Turkey and its influence on earthquake activity, *Tectonics*, Vol. 7, No. 3, pp. 663-684.

Barka, A. and R. Reilinger (1997), *Active tectonics of the Eastern Mediterranean: Deduced from GPS, neotectonic and seismicity data*, *Annali di Geofisica*, 1997.

Barka, A., 1996, Slip distribution along the North Anatolian Fault associated with the large earthquakes of the period 1939 to 1967: *Bulletin of the Seismological Society of America*, v. 86, pp. 1238-1254.

Belousov V. V. and B.S. Volvovsky, Editors, 1989, *Structure and Evolution of the Earth's Crust and Upper Mantle of the Black Sea*, Nauka, Moscow, Russia

Boore, D. M., and G. M. Atkinson, 2008, “Ground Motion Prediction Equations for the Average Horizontal Component of PGA, PGV, and 5% - damped PSA at Spectral Periods between 0.01 s and 10.0 s”, *Earthquake Spectra*, Vol. 24, pp. 99 –138.

Campbell, K. W., and Y. Bozorgnia, 2008, “Campbell-Bozorgnia NGA Horizontal Ground Motion Model for PGA, PGV, PGD and 5% Damped Linear Elastic Response Spectra”, *Earthquake Spectra*, Vol. 24, pp.139–171.

Chekunov A. V., B. G. Pustovitenko, and V. E. Kul’chitskiy, 1994, “Seismicity and Deep Tectonic of the Black Sea Depression and its Margins”, *Geotectonics*, Vol. 28, No.3, pp. 221- 225.



- Chiou, B., and R. R. Youngs, 2008, “An NGA Model for the Average Horizontal Component of Peak Ground Motion and Response Spectra”, *Earthquake Spectra*, Vol. 24, pp.173–215
- Cornell, A. (1968) Engineering Seismic Risk Analysis, Bulletin of Seismological Society of America, Vol. 58, No. 5, 1583-1606, October 1968.
- Delavaud, E., Cotton, F., Akkar, S., Scherbaum F., Danciu, L., Beuval, C., Drouet, S., Douglas, J., Basili, R., Sandikkaya, M.A, Segou, M., Faccioli, E., and Theodilidis, N., 2012. “Toward a ground-motion logic tree for probabilistic seismic hazard assessment in Europe,” *Journal of Seismology*, 16: 451-473
- Demirbag E., C. Rangin, X. Le Pichon, A.M.C. Sengor, 2003, “Investigation of the Tectonics of the Main Marmara Fault by Means of Deep-towed Seismic Data”, *Tectonophysics*, Vol. 361, pp.1-19.
- Erdik M., E. Durukal, B. Siyahi, Y. Fahjan, K. Şeşetyan, M. B. Demircioğlu, H. Akman, 2003, *Earthquake Risk Mitigation in Istanbul*, Chapter 7, in *Earthquake Science and Seismic Risk Reduction*, Ed. by F. Mulargia and R.J. Geller, Kluwer
- Erdik, M, Durukal, E., Siyahi B., Biro Y. and Birgoren G., 2001, “Earthquake Hazard Assessment For Baku-Tbilisi-Ceyhan Crude Oil Pipeline”, Prepared by Bogazici University
- Erdik, M. M. B. Demircioğlu, K. Şeşetyan, E. Durukal ve B.Siyahi, 2004, “Assessment of Probabilistic Earthquake Hazard in the Marmara Region”, *Soil Dynamics and Earthquake Engineering*, Vol: 24, pp. 605–631.
- Finetti, I., G. Bricchi, G., A. Del Ben, M. Pipan, and Z. Xuan, 1988, “Geophysical Study of the Black Sea”, *Bulletino di Geofisica Teorica ed Applicata*, Vol. 30, pp.197-324.
- Flerit F., R. Armijo, G.C.P. King, B. Meyer A. Barka, 2003, “Slip Partitioning in the Sea of Marmara Pull-apart Determined from GPS Velocity Vectors”, *Geophysics Journal International*, Vol.154, pp.1-7
- Giardini, D. and P. Basham, “The Global Seismic Hazard Assessment Program (GSHAP)”, *Ann. di Geofisica*, 36, 3-14, 1993
- Gutenberg, B. and C. F. Richter (1954), *Seismicity of the Earth and Associated Phenomena*, Princeton University Press, 2nd edition.
- Hubert-Ferrari A, R. Armijo, G. King, B. Meyer and A. Barka, 2002, “Morphology, Displacement, and Slip Rates along the North Anatolian Fault, Turkey”, *Journal of Geophysical Research*, Vol. 107, No. B10, pp. 2235.
- Idriss, I. M., 2008, “A NGA Empirical Model for Estimating the Horizontal Spectral Values Generated by Shallow Crustal Earthquakes”, *Earthquake Spectra*, Vol. 24, pp. 217 – 242
- Imren C., X. Le Pichon, C. Rangin, E. Demirbag, B. Ecevitoglu N. Gorur, 2001, “The North Anatolian Fault within the Sea of Marmara: a New Interpretation Based on Multi-channel Seismic and Multibeam Bathymetry Data”, *Earth and Planetary Science Letters*, Vol.186, pp.143-158.



Kusku, M., H. Okamura, Y. Matsuoka, Y. Awata, 2002, “Active Faults in the Gulf of Izmit on the North Anatolian Fault, NW Turkey: a High-resolution Shallow Seismic Study”, *Marine Geology*, Vol. 190, pp.421-443.

Le Pichon X., A. M. C. Sengor, E. Demirbag, C. Rangin, C. Imren, R. Armijo, N. Gorur, N. Cagatay, B.M. de Lepinay, B. Meyer, R. Saatchilar, B. Tok, 2001, “The Active Main Marmara Fault”, *Earth and Planetary Sc.Letters*, Vol.192, pp. 595-616.

Le Pichon X., N. Chamot - Rooke, C. Rangin, A. M. C. Sengor, 2003, “The North Anatolian Fault in the Sea of Marmara”, *Journal of Geophysical Research*, Vol. 108, pp. 2170-2179.

Le Pichon, *MARMARA SURVEY, 11 Sep - 4 Oct 2000, Cruise Report Web site*, www.cdf.u-3mrs.fr/lepichon/marmara/

McClusky, S., S. Bassalanian, A. Barka, C. Demir, S. Ergintav, I. Georgiev, O. Gurkan, M. Hamburger, K. Hurst, H.-G. Hans-Gert, K. Karstens, G. Kekelidze, R. King, V. Kotzev, O. Lenk, S. Mahmoud, A. Mishin, M. Nadariya, A. Ouzounis, D. Paradissis, Y. Peter, M. Prilepin, R. Relinger, I. Sanli, H. Seeger, A. Tealeb, M.N. Toksaz, G. Veis, 2002, “Global Positioning System Constraints on Plate Kinematics and Dynamics in the Eastern Mediterranean and Caucasus”, *Journal of Geophysical Research*, Vol. 105 (B3), pp. 5695-5719.

McKenzie, D. P. (1970), *Plate Tectonics of the Mediterranean Region*, *Nature*, 226, pp. 239-243.

Nikishin A., P. A. Ziegler, D. I. Panov, B. P. Nazarevich, M.-F. Brunet, R. A. Stephenson, S. N. Bolotov, M. V. Korotaev and P. L. Tikhomirov, 2001, “Mesozoic and Cenozoic Evolution of the Scythian Platform–Black Sea–Caucasus Domain”, in: P. A. Ziegler, W. Cavazza, A. H. F. Robertson and S. Crasquin-Soleau, Editors, *Peri-Tethys Memoir 6: Peri-Tethyan Rift/Wrench Basins and Passive Margins Mémoires du Muséum National d'Histoire naturelle*, Paris , Vol. 186, pp. 295–346

Okay, A. I., O. Tuysuz, S. Kaya, 2004, “From Transpression to Transtension: Changes in Morphology and Structure around a Bend on the North Anatolian Fault in the Marmara Region”, *Tectonophysics*, Vol. 391, pp. 259-282.

Okay, A.I., A. Kaslilar-Ozcan, C. Imren, A. Boztepe-Guney, E. Demirbag, I. Kuscu, 2000, “Active Faults and Evolving Strike-slip Basins in the Marmara Sea, Northwest Turkey: a Multichannel Seismic Reflection Study”, *Tectonophysics*, Vol. 321, pp. 189-218.

Parke, J. R., R. S. White, D. McKenzie, T. A. Minshull, J. M. Bull, I. Kuşçu, N. Görür, and C. Şengör (2002), Interaction between faulting and sedimentation in the Sea of Marmara, western Turkey, *J. Geophys. Res.*, 107(B11), 2286, doi:10.1029/2001JB000450.

Polonia, A., L. Gasperini, A. Amorosi, E. Bonatti, N. Çağatay, L. Capotondi, M.-H. Cormier, N. Gorur, C. McHugh, and L. Seeber (2004), Holocene slip rate of the North Anatolian Fault beneath the Sea of Marmara, *Earth Planet. Sci. Lett.*, **227**, 411–426



Rangin, C., A. G Bader, G. Pascal, B. Ecevitoglu, N. Görür, 2002, “Deep Structure of the Mid Black Sea High (offshore Turkey) Imaged by Multi-channel Seismic Survey (BLACKSIS cruise)”, *Marine Geology*, Vol.182, pp.265–278.

Reilinger, R., S. Ergintav, R. B`urgmann, *et al.*, Coseismic and postseismic fault slip for the 17 august 1999, $m = 7.5$, izmit, turkey earthquake., *Science*, 289, 1519–1524, 2000.

Reilinger, R., S. McClusky, P. Vernant, S. Lawrence, S. Ergintav, R. Cakmak, H. Ozener, F. Kadirov, I. Guliev, R. Stepanyan, M. Nadariya, G. Hahubia, S. Mahmoud, K. Sakr, A. ArRajehi, D. Paradissis, A. Al-Aydrus, M. Prilepin, T. Guseva, E. Evren, A. Dmitrotsa, S. V. Filikov, F. Gomez, R. Al-Ghazzi, 17 and G. Karam (2006), "GPS constraints on continental deformation in the Africa-Arabia-Eurasia continental collision zone and implications for the dynamics of plate interactions", *JOURNAL OF GEOPHYSICAL RESEARCH*, VOL. 111, B05411, doi:10.1029/2005JB004051

Robinson A.G., Editor, 1997, *Regional and Petroleum Geology of the Black Sea and Surrounding Region American Association of Petroleum Geologists, Memoir*, Vol. 68, pp. 385, Tulsa.

Sarođlu, F., O. Emre and I. Kuscı, 1992, *Active Fault Map of Turkey*, Mineral Res. Explor. Inst., Turkey.

Schwartz, D. P., and K.J. Coppersmith, 1984, “Fault Behavior and Characteristic Earthquakes from the Wasatch and San Andreas Faults,” *Journal of Geophysical Research*, Vol 89, pp 5681 - 5698.

Stein, R. S. and A. A. Barka, 1995, “Stress Triggering of Progressive Earthquake Failure on the North Anatolian Fault, Turkey, Since 1939: Implications for the Interaction of Faults and the Forecast of Hazard”, *Proc.11th Course: Active Faulting Studies for Seismic Hazard Assessment, Int. School of Solid Earth Geophysics*, Italy

TEFER (Turkey Emergency Flood and Earthquake Recovery), 2000, *A Probabilistic Seismic Hazard Assessment For Turkey*, Report prepared in connection with the Improvement Of Natural Hazard Insurance And Disaster Funding Strategy Project, Bařbakanlık Hazine ve Dıř ticaret Mısteřarlıđı - Sigortacılık Genel Mıdurluđu

Temel ˆ. and ˆiftˆci, 2002, “Gelibolu Yarımada ları, Gˆkˆeada ve Bozcaada Tersiyer ˆokellerinin Stratigrafisi ve Ortamsal ˆzellikleri”, *TPJD Bulletin* , Vol. 14, No.2, pp. 1740 (in Turkish).

Tugolesov, T. A, A. S Gorshkov, L. B. Meisner, V. V. Soloviev, E. M. Khakalev, 1985, “Tectonics of the Black Sea Basin”, *Geotectonika*, Vol.6, pp. 3–20 (in Russian)

Yaltırak, C., B. Alpar, H. Yuce, 1998, “Tectonic Elements Controlling the Evolution of the Gulf of Saros (Northeastern Aegean Sea)”, *Tectonophysics*, Vol. 300, pp. 227-248.



4.3 BULGARIA

4.3.1 Country, Project Area in the Country

Bulgaria is situated in the eastern part of the Balkan Peninsula and is bounded on the east with Black sea. The Bulgarian project area includes North-East and South-East regions (Severoiztochen and Yugoiztochen) of the country. These two regions consist of 8 districts (Fig. 77) – Burgas, Sliven, Yambol, Stara Zagora, Varna, Dobrich, Shumen and Targoviste. The total area of the these two regions is 33678 km² or more of 30% of the territory of Bulgaria. The population is 2131570 or more than 25% of the population of Bulgaria.

Economy

South-East region (Yugoiztochen - districts Burgas, Sliven, Yambol, Stara Zagora) is the second richest Bulgarian region. Most important are tourism, electric power generation, services. Burgas is the second largest Bulgarian port, big tourist centers are Sunny beach, Sozopol, Pomorie, Primorsko, Ravda and Kiten. Main industrial centers are the big cities and towns of Radnevo and Galabovo - electric power generation and mining.

One of richest regions of Bulgaria is North-East region (Severoiztochen - districts Varna, Dobrich, Shumen and Targoviste. It is important for the national economy. Its economy is service-oriented and includes tourism. Severoiztochen is the second most-visited region by foreign tourists after Yugoiztochen. Notable resorts include Golden Sands, Albena, SS Constantine and Helena. Interesting places are the towns of Balchik, Kavarna, Cape Kaliakra - on the sea, Madara - nearby Shumen; Shumen boasts the Monument to 1300 Years of Bulgaria. Dobrich Province form Southern Dobruja - the Bulgarian breadbasket. The port of Varna is the largest port in Bulgaria and the third largest on the Black Sea. The port of Balchik is a small fishing town. Varna is Bulgaria's second financial capital after Sofia; the city produces electronics, ships, food and other goods. Other important industrial centers in the region are Shumen - production and repair of trucks; Dobrich - big food-producing city, unofficial capital of Dobruja; Devnya - big chemical center (cement and nitric fertilizer).

4.3.2 Seismic Activity, Strong Earthquakes now and Historic Ones

Earthquakes are the most deadly of the natural disasters affecting the human environment, indeed catastrophic earthquakes have marked the whole human history, accounting for 60% of worldwide

casualties associated with natural disasters. Earthquakes are the expression of the continuing evolution of the Earth planet and its surface. Earthquakes adversely affect large parts of the Earth. Global seismic hazard and vulnerability to earthquakes are increasing steadily as urbanization and development occupy more areas that a prone to effects of strong earthquakes; the uncontrolled growth of megacities in highly seismic areas around the world is often associated with the construction of seismically unsafe buildings and infrastructures, and undertaken with an insufficient knowledge of the regional seismicity peculiarities and seismic hazard. The assessment of seismic hazard is the first link in the prevention chain and the first step in the evaluation of the seismic risk. The implementation of the seismic hazard estimates into the policies for seismic risk reduction will allow focusing on the prevention of earthquake effects rather than on intervention following the disasters.



Fig 77. Bulgarian eligible area

The territory of Bulgaria represents a typical example of high seismic risk area in the eastern part of the Balkan Peninsula. The Balkan Peninsula, from plate-tectonic point of view, is an element of the continental margin of Eurasia that is located between the stable part of the European continent to the north and ophiolitic sutures (Vardar and Izmir-Ankara) to the South. South of the sutures, fragments of the passive continental margin of Africa crop out (Boyanov et al., 1989). The neotectonic movements on the Balkan Peninsula were controlled by extensional collapse of the Late Alpin orogen, and were influenced by extension behind the Aegean arc and by the complicated vertical and horizontal movements in the Pannonian region (Zagorcev, 1992).

Bulgaria contains important industrial areas that face considerable earthquake risk, though less than its neighboring countries: Greece, Turkey and Romania. Over the past centuries, Bulgaria has experienced



strong earthquakes. The first well documented earthquake on the territory of Bulgaria is the 1 c BC quake occurred in the Black Sea near the town of Kavarna. In historical aspect, it is worth to mention the 1818 (VIII-IX MSK) and the 1858 ($M_S=6.3$, $I_0=IX$ MSK) earthquakes occurred near the town of Sofia. The 1858 earthquake caused heavy destruction to the city of Sofia and the appearance of thermal springs in the western part of the town. Some of the Europe's strongest earthquakes 20-th century occurred in Bulgaria (at the beginning of the 20th century from 1901 to 1928 on the territory of Bulgaria occurred 5 earthquakes with magnitude larger than or equal to 7.0). Impressive seismic activity developed in the SW Bulgaria during 1904-1906. The seismic sequence started on 4 of April 1904 with two catastrophic earthquakes within 23 minutes (the first quake at 10^h 05^{min} with $M_S=7.1$ considered as a foreshock and the second one at 10^h 26^{min} with $M_S=7.8$ and $I_0=X$ -the main shock). The main shock was felt in a very large are (up to Budapest, Hungary) and some eye-witnesses have seen waves on the surface in the town of Sofia. The surface outcrop caused by the 1904 earthquake still can be seen in the Kresna gorge. This earthquake was followed by a well expressed long-lasting aftershock activity. Along the Maritca valley (central part of Bulgaria), in 1928 a sequence of three destructive earthquakes occurred. The towns Plovdiv, Chirpan, Parvomay suffered great damage. Many other towns and villages were strongly affected. 74000 buildings were completely destroyed and 114 people killed. They caused two surface coseismic ruptures, each of them several tens of kilometers in length. That is the one of few cases (quoted in Richter, 1958) when before and after a strong earthquake detailed geodetic surveys have been performed (presented in Yankov, 1935). On some places the ground displacement reaches up to 1.5-2 m.

Moreover, the seismicity of the neighboring countries, like Greece, Turkey, former Yugoslavia and Romania (especially Vrancea-Romania intermediate earthquakes involving the non-crustal lithosphere), influences the seismic hazard in Bulgaria.

The strongest and most destructive earthquakes in Bulgarian occurred after 1900 are listed in Table 4.3.1.

The thickness of the earth crust varies from 30 km close to the Black sea up to 51 km in the southwestern part of Bulgaria. From the analysis of the depth distribution (as for example Sokerova et al., 1992; Dacev et al., 1995; Simeonova et al., 2006) it was recognized that most of earthquakes in Bulgaria and near surroundings occurred in the Earth's crust up to 50 km. The hypocenters are mainly located in the upper crust, and only a few events are related to the lower crust. The maximum density of seismicity involves the layer between 5 and 25 km.

Table 4.3.1 Strong and destructive earthquakes occurred in Bulgaria after 1900 year. (Bold and red – earthquakes in or close to eligible area)

Date	Time GMT	Epicenter	h	M	I_0
d. m. y.	h. m. s.	coordinates	km		
		$\varphi^\circ N$ $\lambda^\circ E$			

31.03.1901	07 10 22	43.37	28.70	14	7.2	10
04 04 1904	10 02 34	41.77	23.05	15	7.3	9-10
04 04 1904	10 25 55	41.85	23.08	18	7.8	10
08 10 1905	07 27 30	41.86	23.08	19	6.4	8-9
15 02 1909	09 33 40	42.52	26.48	4-8	6.0	8
23 02 1910	07 52 14	41.70	23.55	10	5.4	7-8
14 06 1913	09 33 13	43.10	25.70	15	7.0	9-10
18 10 1917	18 57 40	42.70	23.33	6	5.2	7-8
14 04 1928	09 00 01	42.21	25.36	10	6.8	9
18 04 1928	19 22 48	42.20	25.06	16	7.1	9-10
25 04 1928	09 25 46	42.08	25.89	13	5.7	8
23 08 1942	15 41 25	43.47	26.60	10	5.1	7
30 06 1956	01 50 22	43.55	28.68	20	5.5	7
03 11 1977	02 22 58	42.08	24.08	8	5.3	7
21 02 1986	05 39 56	43.21	26.01	8	5.1	7-8
07 12 1986	14 17 09	43.19	26.01	10	5.7	8
22 05 2012	00 00 32	42.58	23.00	9	5.8	7-8

The spatial pattern of seismicity in and near Bulgaria is shown in Fig.2. The figure represents the epicentral map of the earthquakes with magnitude: larger than or equal to 6.0 ($M \geq 6.0$) occurred before 1900; $M \geq 4.0$ after 1900; and with $M \geq 3.0$ occurred after 1980 in and near Bulgaria. Seismicity (all instrumentally recorded seismic events after 1980) in and near the country project area is presented in Fig.3.

Both epicentral maps (Fig.78 and Fig.79) show that seismicity is not uniformly distributed in space. Therefore the seismicity is described in distributed geographical zones (seismic source zones). Each source is characterized by its own specific seismicity, geological and tectonic development.



Project funded by the
EUROPEAN UNION

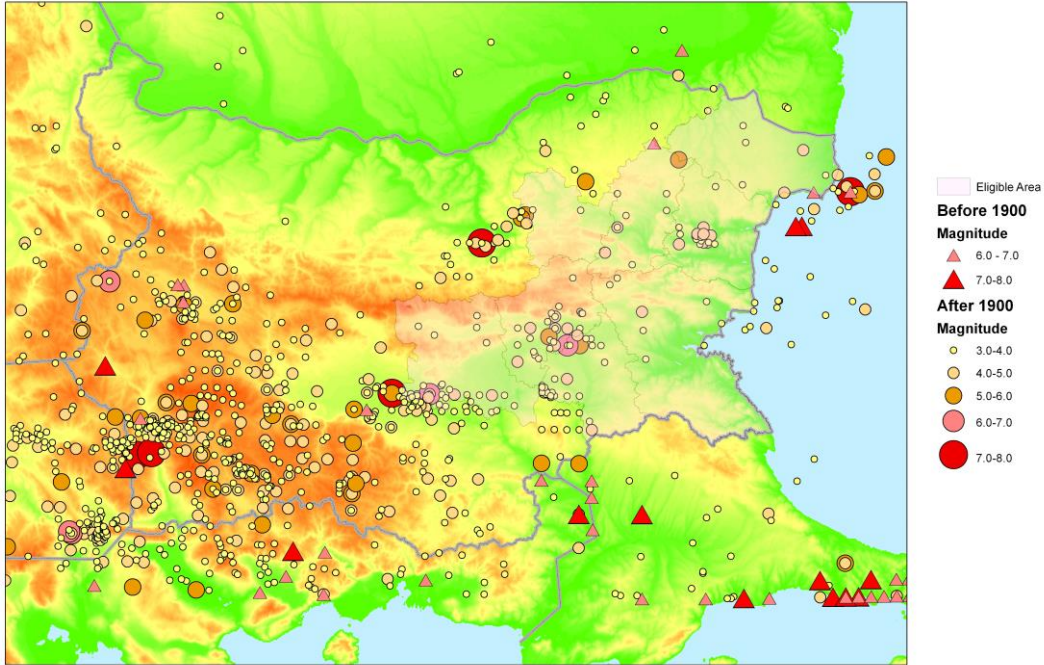


Fig 78. Epicentral map for Bulgaria and surroundings ($M \geq 3.0$)



Project funded by the
EUROPEAN UNION

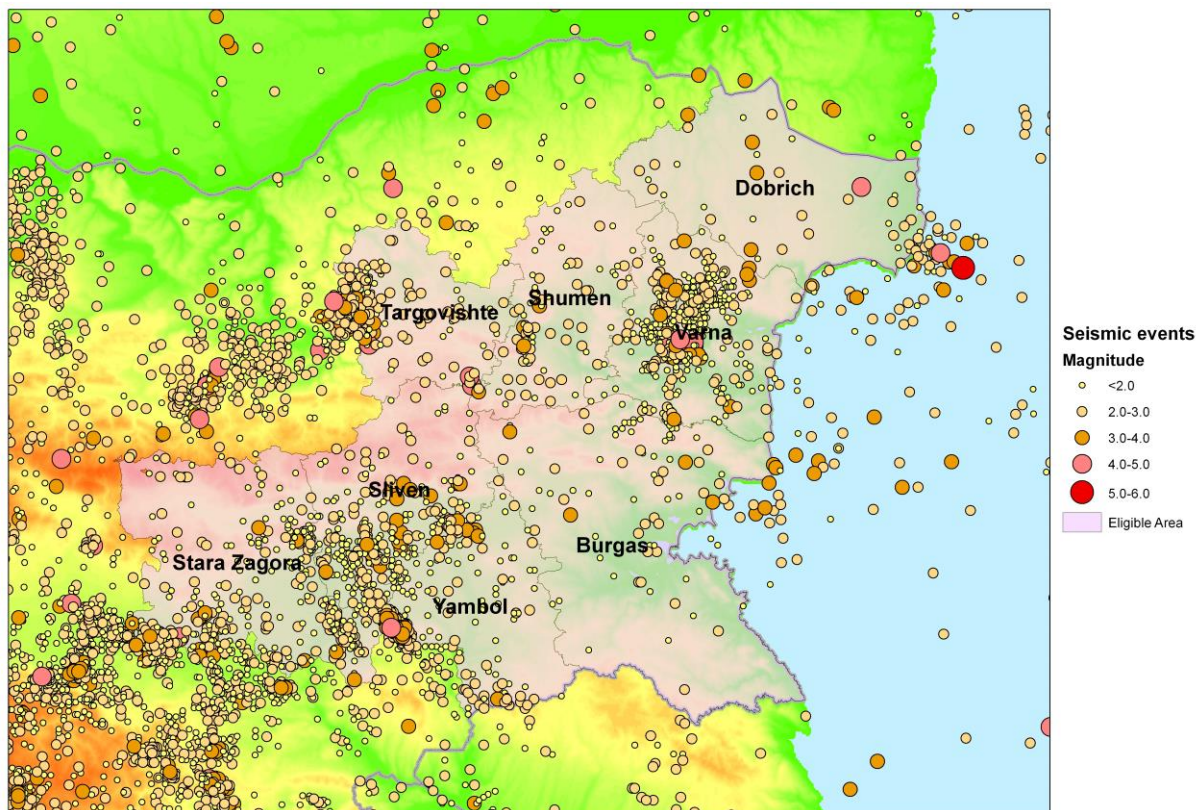


Fig 79. Epicentral map for Bulgaria and surroundings (after 1980, all recorded events)

From the seismotectonics analysis of the considered parts of the Balkans this modeling seems more appropriate than to use specific linear fault structures or three-dimensional fault planes. The main seismic source zones that are defined (as presented in Sokerova et al., 1992; Dachev et al. 1995; Simeonova et al., 2006; Solakov et al., 2009) within and near the country project area are as follows:

Shabla seismic zone The eastern periphery of the Moesian platform is marked by a fault system in NNE-SSW direction, separating the platform from deep part of the West Black Sea back-arch marginal riftogenic basin. Strong earthquakes manifest the Neotectonic/Quaternary activity of this fault system. The strongest seismic events (543 earthquake with $M=7.6$, 1444 earthquake with $M=7.5$, 1901 earthquake with $M=7.2$) are associated with Kaliakra fault system defined by numerous seismic profiling undertaken in the Black Sea. The hypocentre distribution involves the surficial 20 km. The maximum earthquake potential M_{max} associated with Shabla seismic zone is $M_{max}=8.0$ (Boncev et al., 1982).

North-East Bulgaria seismic zone The seismic source is situated in the broad transitional zone where the Moesian platform succession has been down faulted to the east during the Middle Cretaceous opening



of the Western Black Sea Basin (Tari et al. 1997). That is an area with not expressed contemporary tectonic activity. The southern part of the seismic source zone is characterized with low to moderate seismic activity while in the northern part sporadic moderate to strong earthquakes occurred. The strongest earthquakes generated in the zone is the 1892 Dulovo quake ($I_0=8$, $M_S \approx 7.0$) located in the northern part of the zone.

Close to the eligible area are located two active seismic zones Gorna Orjahovitca (North Bulgaria) and Marica (South Bulgaria). These zones have significant impact to the seismic hazard in the area. In these zones have been realized earthquakes with magnitudes of 7.0 at the beginning of previous century. The macroseismic intensities from these earthquakes reach VIII-IX for some parts of eligible area.

Gorna Orjahovitza seismic zone The main tectonic structure in this area is the E-W extended Resenski trough, which is formed during the Quaternary period. Two sublatitudinal faults, which are reactivated segments of the Fore Balkan fault, and an oblique fault in NE-SW direction marks the boundaries of the Resenski trough. The strongest event here occurred in 1913 ($M_S=7.0$), followed by seismic quiescence until 1986 when the two moderate Strazhitza earthquakes occurred ($M_S=5.3$ on February 21 and $M_S=5.7$ on December 7). The macroseismic effects caused by 1986 earthquakes are of intensity VII-VIII (MSK) in the western part of Targoviste district. The seismicity in the zone is shallow, concentrated mainly in the surficial 15 km, with rare events down to the 25-30 km depth. The maximum 7.0 earthquake is expected in Gorna Orjahovitza seismic zone ($M_{max}=7.0$, Boncev et al., 1982).

Maritsa seismic zone The contemporary tectonic activity of the area is associated with Maritsa fault system with WNW-ESE direction. The Maritsa fault with its satellites belongs to structures with a longlasting development, which continues in the neotectonic period. The largest of its segments, which is with well-expressed Neogene-Quaternary activity, reaches the length of about 70 km (Dachev et al., 1995). The strongest earthquakes occurred on the fault system are those in 1928 (the Chirpan earthquake of April 14, 1928 with $M_S=6.8$ and the Plovdiv earthquake of April 18, 1928 with $M_S=7.0$, $I=9-10$ MSK). 74000 buildings were completely destroyed and 114 people killed. The earthquakes caused two surface coseismic ruptures, each of them several tens of kilometers in length. Ground displacement reached the length of 1.5-2 m (Yankov, 1935). The hypocenter distribution involves the surficial 20 km, with sporadic events down to 45 km. The highest density of foci is observed at 5-10 km depth. The maximum 7.5 earthquake is expected in Maritsatza seismic zone ($M_{max}=7.5$, Boncev et al., 1982).

The Northern part of the region is strongly influenced by the intermediate Vrancea earthquakes. The Southern part is influenced by strongest earthquakes on Turkish and Greece territory.

In the region of Provadia are located a lot of earthquakes with magnitudes between 4.0 and 5.0 last 30 years with maximal macroseismic intensity up to VI-VII (MSK). Several earthquakes with magnitudes between 5 and 6 have been realized near the town of Yambol. The maximal observed intensity from these earthquakes is VIII (MSK).



4.3.3 Seismic Monitoring Network

The beginning of Bulgarian seismology dates back to 1891. At that time Spas Watzof, the director of Central Meteorological Station in Sofia, organized network of correspondents for observation of felt earthquakes in Bulgaria (Watzof, 1902). Watzof formed a proto-type of macroseismic bulletin containing: time of perceived shaking, locality, intensity, direction of impact, and observed effects. The first bulletin including data for Central Balkan earthquakes occurred in the 19th century was published in 1902 (Watzof, 1902). The initial data on earthquakes felt in Bulgaria were published in 17 volumes edited by Spas Watzof (1902-1923). Over more than 6 decades, reports on earthquakes affected the territory of Bulgaria (occurred in the Balkans) have been annually and/or periodically (at several years) published till 1964 (Glavcheva, 2004).

The period of Bulgarian historical era ends in 1905 when the seismograph of Omorri-Boch type was installed in the first Seismological Station in the town of Sofia. The same year four seismoscopes of Agamenonne type were installed in Sofia, Petrohan, Rila monastery and the town of Kazanlak.

The initial data on earthquakes felt in Bulgaria were published in 17 volumes edited by Watzof (1902-1923). Over more than 6 decades, reports on earthquakes affected the territory of Bulgaria (occurred in the Balkans) have been annually and/or periodically (at several years) published till 1964 (Glavcheva, 2004).

The period of Bulgarian historical era ends in 1905 when the seismograph of Omorri-Boch type was installed in the first Seismological Station in the town of Sofia. The same year four seismoscopes of Agamenonne type were installed in Sofia, Petrohan, Rila monastery and the town of Kazanlak.

At present NIGGG-BAS runs the Bulgarian seismological network-NOTSSI (National Operative Telemetric System for Seismological Information). NOTSSI was founded at the end of 1980. The overall objective for the NOTSSI is continuous monitoring of seismicity on the territory of Bulgaria and surroundings. NIGGG, respectively NOTSSI, is responsible for rapid earthquake determination, public information through media, and information of responsible governmental authorities if necessary urgent activities to be undertaken. The institute also operates two local seismic networks deployed around the Kozloduy Nuclear Power Plant and the town of Provadia in Northeastern Bulgaria. In 2005, the institute performed overall modernization of the NOTSSI. The upgraded Bulgarian National Digital Seismological Network (BNDSN) consists of a National Data Center (NDC), 15 stations equipped with RefTek High Resolution Broadband Seismic Recorders – model DAS 130-01/3. Configuration of BNDSN is presented in Figure 80.

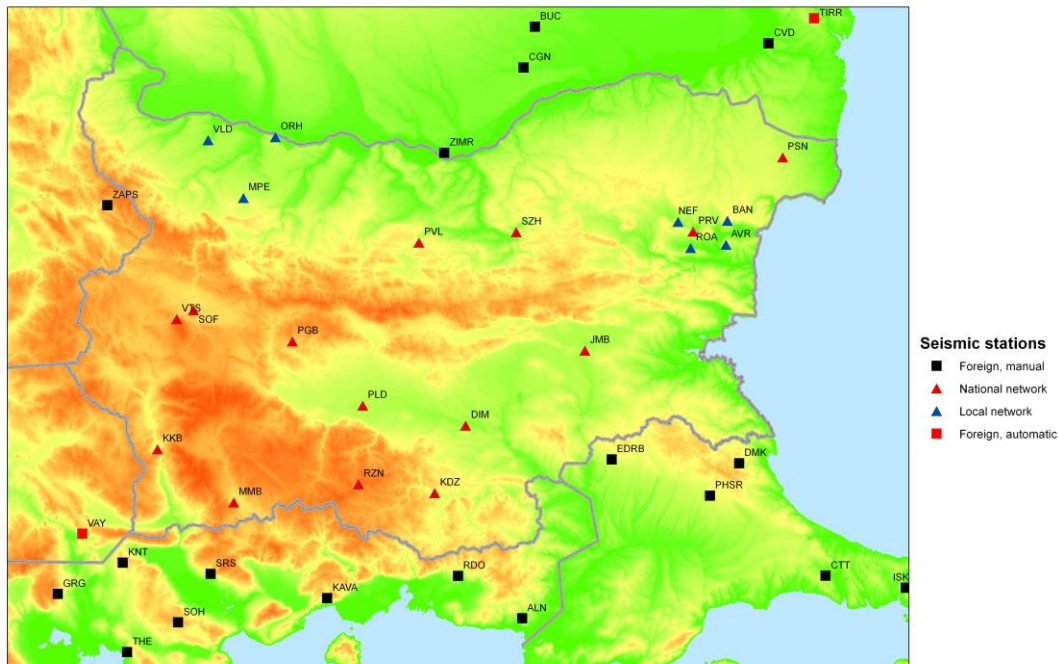


Fig 80. Bulgarian seismic network and foreign stations used in epicenter location

Real-time data transfer was realized via Virtual Private Network (VPN) of the Bulgarian Telecommunication Company (BTC). The data acquisition and processing hardware redundancy at the National Data Center was achieved by two clustered SUN Fire 5400 servers and two Blade 1500 Workstations. To secure the acquisition, processing and data storage processes a three layer network was designed at the NDC.

Real-time data acquisition was performed using REFTEK's full duplex errorcorrection protocol RTPD. For data archiving two formats are used: PASSCAL (PASSCAL Data Center) and widely used for seismological data miniSEED.

Data processing was performed by the Seismic Network Data Processor (SNDP) software package running on both Servers. SNDP includes two subsystems:

- *Real-time subsystem (RTS)* – for signal detection; evaluation of the signal parameters; phase identification and association; source estimation.
- *Seismic analysis subsystem (SNDA)* – for interactive data processing.

The signal detection process is performed by traditional STA/LTA detection algorithm. The filter parameters of the detectors are defined on the base of previously evaluated ambient noise at the seismic stations.



Currently, the BNDC and BNDSN allow reliable automatic localization of low magnitude events $MS > 1.5$ within the network, and $MS \geq 3.0$ at regional distances. Since 2005-2006, real-time data exchange between Bulgaria and Greece, Romania, Serbia, Macedonia, Slovakia, Slovenia, Austria and other regional and national seismological data centers was implemented.

4.3.4 Probabilistic Seismic Hazard Assessment (PSHA)

Seismic hazard is the probability that various levels of strong ground motion will be exceeded during a specified time period at a site. The ground motion levels may be expressed in terms of peak ground acceleration (velocity, displacement) and/or peak response spectral amplitudes for a range of frequencies.

PSHA was developed in the late 1960s and early 1970s at the Universidad Nacional Autonoma de Mexico (UNAM) and the Massachusetts Institute of Technology (MIT) and PSHA has now become the most widely used approach for estimating seismic-design loads (Bommer and Abrahamson, 2006). Probabilistic techniques utilize all the details and parameters of the seismotectonic model. Modern techniques allow uncertainties in the seismic input to be included in the analysis.

The main steps involved in the seismic hazard analysis are the following:

1. construction of seismic source model - each element of the model is represented as a seismic source (areal, volume, linear or point) with defined geometry and depth;
2. determination of the seismicity parameters such as magnitude frequency relationship, minimum magnitude, maximum magnitude and their uncertainties for each seismic source;
3. designation of a ground motion attenuation relationship for each seismic source;
4. Selection of appropriate stochastic model of earthquake occurrence (Poisson, Markov, etc.);
5. computation of seismic hazard curves with appropriate confidence levels such as to demonstrate the scatter of data.
6. Sensitive analysis

In Figure 81 a Flow Chart for main stages in probabilistic seismic hazard analysis is presented.

Mathematical Formulation

The formal procedure for probabilistic calculations taking account of spatial and temporal uncertainty in the future seismicity was presented by Esteva (1967, 1968) and Cornell (1968). The probabilistic method of seismic hazard analysis, as it is currently understood, was presented by Cornell (1971), and by Merz and Cornell (1973).

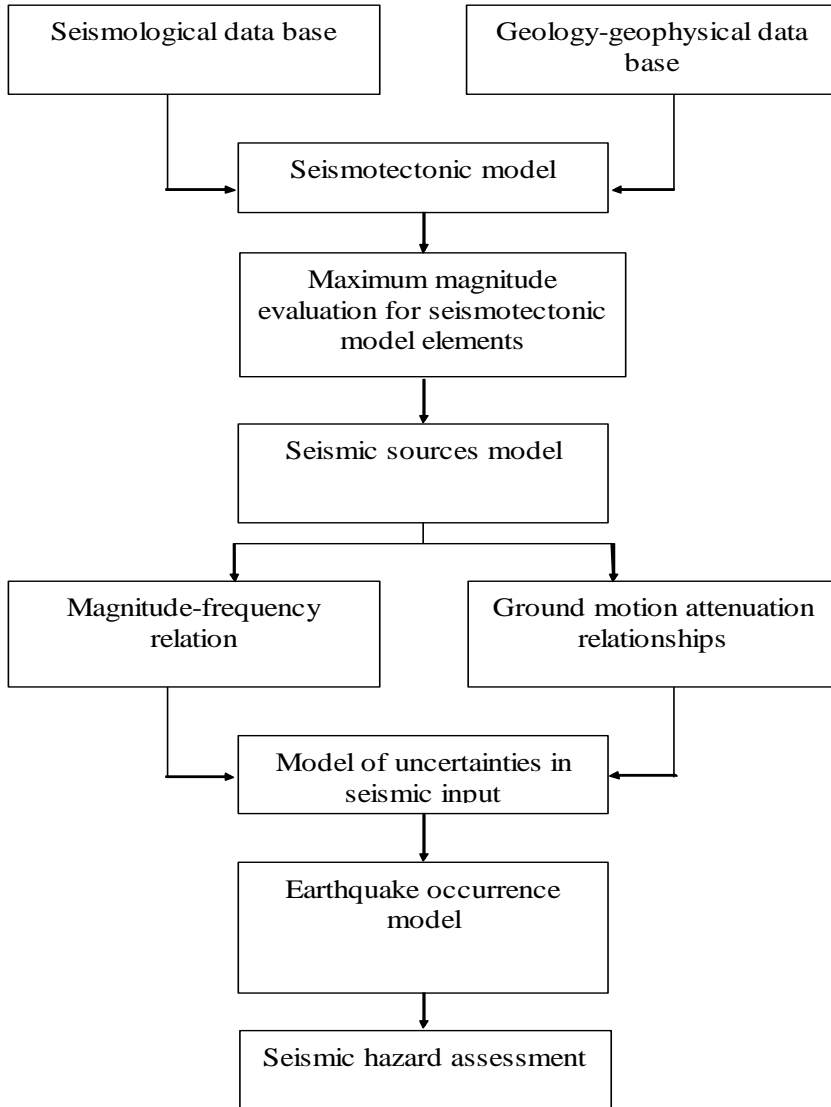


Fig 81. Flow chart for seismic hazard assessment

It is commonly assumed that the occurrence of individual event can be represented as a Poisson process. The probability that at a given site a ground motion parameter, Z , will exceed a specified level, z , during a given time period, t , is given by the expression:

$$P(Z \geq z | t) = 1 - e^{-v(z)t} \leq v(z)t \quad (1)$$

where $v(z)$ is the average frequency during time period t at which the level of ground motion parameter Z exceeds z at the site resulting from earthquakes in all sources in the region.



The “return period” of z is defined as:

$$R_z(z) = \frac{1}{v(Z \geq z)} = \frac{-t}{\ln(1 - P(Z \geq z))} \quad (2)$$

The inequality at the right side of above equation (4.1) is valid regardless of the appropriate probability model for earthquake occurrence and $v(z)t$ provides an accurate and slightly conservative estimate for probabilities less than 0.1.

The frequency of exceedance, $v(z)$, is a function of the uncertainty in the time, size and location of future earthquakes and uncertainty in the level of ground motions they may produce at the site.

It is computed by expression:

$$v(z) = \sum_n \alpha_n(m^0) \int_{m^0}^{m^u} \int_0^\infty f(m) f(r|m) P(Z \geq z | m, r) dr dm \quad (3)$$

where $\alpha_n(m^0)$ is the frequency of earthquakes on source n above a minimum magnitude of engineering significance m^0 ; $f(m)$ is the probability density function for event size between m^0 and maximal event for the source m^u ; $f(r|m)$ is the probability density function for distance to the earthquake rupture which is usually conditional on the earthquake size; and $P(Z < z | m, r)$ is the probability that for a given magnitude m earthquake at a distance r from the site, the ground motion exceeds level z . The average frequency $v(z)$ is evaluated by three probability functions: magnitude distribution, conditional distance distribution and conditional exceedance probability distribution.

Development of PSHA Models

The constituent models of the Probabilistic Seismic Hazard Methodology are models of: 1) seismic sources; 2) earthquake recurrence frequency; 3) ground motion attenuation; and 4) ground motion occurrence probability at a site (Thenhaus and Campbell, 2003).

Seismic sources

Description of the geometry of a seismic source is necessary for evaluation of site-source distances.

Seismic sources are identified on the base of geological, seismological and geophysical data. An understanding of the regional tectonics, local Quaternary history and seismicity of an area leads to the identification of geological structures that may be seismic sources. The association of geological structure with historic or instrumental seismicity clarifies their role in the present tectonic stress regime.

The limiting size earthquake that can occur on each seismic source is a very important parameter in seismic hazard analysis, especially at low probability levels. For sources defined as faults, the maximum



earthquake magnitude is related to the fault geometry and fault behavior through an assessment of the maximum dimensions of a single rupture. For area sources maximum magnitude is usually estimated to be the maximum historic event plus an increment.

Earthquake recurrence

Earthquake recurrence is represented in terms of the rate of the seismic activity and the relative frequency of various magnitude earthquakes. To determine earthquake recurrence frequency two sources of data are used: observed seismicity (historical and instrumental and geological (geology, geomorphology, tectonics and neotectonics)). For sources defined as individual faults historic seismicity and geological data can be used to characterize the earthquake recurrence. For large area sources, only historical seismicity is usually used to estimate the earthquake recurrence rate.

Ground motion attenuation

Ground motion attenuation relationships define the values of a ground motion parameter, such as peak ground acceleration or response spectral values, as a function of earthquake size (magnitude M) and the distance in terms of both the expected values and the dispersion of the expected values. Attenuation relationships are developed usually from statistical analysis of strong motion data or from peak ground motion parameters inferred from reported shaking intensity. The ground motion attenuation relationships and their uncertainties are of substantial importance in hazard analysis. Estimates of parameters (coefficients and standard deviation) of an attenuation equation depend on quantity and quality of input data (magnitude range, homogeneity of the available data sample etc.).

Ground motion probability

The probability model widely used in hazard analysis is that earthquakes occur as a Poisson process in a time. The probabilistic methodology quantifies the hazard at a site from all earthquakes of all possible magnitudes, at all distances from the site as probability of exceeding some amplitudes of shaking at a site in periods of interest (Thenhaus and Campbell, 2003).

4.3.5 Treatment of Uncertainties (Random & Epistemic)

Handling uncertainties is a key element of Probabilistic Seismic hazard Analysis. Two types of uncertainty are defined in seismic hazard analysis-random and modeling (McGuire, 1993).. Distinction between the two types of uncertainty has emerged as an important issue in the proper estimation of seismic hazard. The first type uncertainty (aleatory) represents the randomness inherent in the natural phenomena of earthquake generation and seismic wave propagation. The probability functions contained in the basic analysis model represent the random uncertainties. Specification of standard deviation (σ) of a mean ground attenuation relationship is a representation of aleatory variability. Aleatory variability is included directly in the PSHA calculations by means of mathematical formulation. Modeling (epistemic) uncertainties comes from statistical or modeling variations. The large uncertainties in seismic hazard



result from lack of knowledge about earthquake cause, characteristics, ground motions, i.e. from uncertainties in the inputs. There are many epistemic uncertainties in any seismic hazard assessment, including the configuration and characteristics of the seismic source zones, the model for earthquake recurrence frequency, and the maximum earthquake magnitude.

In PSHA, the established procedure is to incorporate the epistemic uncertainty into the calculation through the use of logic tree. Logic tree was first introduced into PSHA by Kulkarni et al, (1984) as a tool to model and quantify the uncertainties in the inputs required for such analysis, and they have since become a part of PSHA (Coppersmith & Youngs, 1986). The logic tree is to handle epistemic uncertainties and not random variabilities (aleatory) of known distribution (e.g. Bommer et al., 2005). The logic tree allows a formal characterization of uncertainty in the analysis by explicitly including alternative interpretations, models, and parameters that are weighted in the analysis according to their probability of being correct. Logic tree models may be evaluated, or adequately sampled through Monte Carlo simulation (introduced by Bungum et al., 1986), which is computationally a more efficient procedure (Thenhaus and Campbell, 2003). An important principle to follow in setting up a logic tree (as defined in Bommer et al., 2005), is that the options represented by the branches extending from a single node should encompass the complete range of physical possibilities that particular parameter could be expected to take. The branches should be set up so that, as knowledge improves revised estimates for the parameters should fall within the bounds expressed by the logic tree branches. However, physically unrealizable scenarios should not be included in the logic tree. The use of a logic tree does not relieve the analyst from the responsibility of judging if the specified value of a particular parameter could be expected to occur in nature (Bommer et al., 2005).

Nowadays it has become established practice that the ground motion variability is an integral and indispensable part of PSHA (McGuire, 2004; Bommer and Abrahamson, 2006). Modern methods of seismic hazard analysis incorporate uncertainties into the analysis to assess their impact on the estimate of the expected level of seismic hazard as well as the uncertainty in that estimate.

4.3.6 De-Aggregation of PSHA

Probabilistic seismic hazard analysis considers a multitude of earthquake occurrence and ground motion, and produces an integrated description on seismic hazard representing all events. The PSHA is able to quantify and account for the random uncertainties associated with estimation of the seismicity and the attenuation characteristics of the region. For physical interpretation of the results from PSHA and to take certain engineering decisions, it is desirable to have a representative earthquake which is compatible with the results of the PSHA method. This could be achieved through the de-aggregation of the probabilistic seismic hazard. A procedure called de-aggregation was applied to examine the spatial and magnitude dependence of PSHA results.



For physical interpretation of the PSHA results and to take certain engineering decisions, it is desirable to have a representative earthquake which is compatible with the results of the PSHA method. This could be achieved through the de-aggregation of the probabilistic seismic hazard (McGuire, 1995). A procedure called de-aggregation (or disaggregation) has been developed to examine the spatial and magnitude dependence of PSHA results. The aim is to determine the magnitudes and distances that contribute to the calculated exceedance frequencies at a given return period and at a structural period of engineering interest (Thenhaus and Campbell, 2003). De-aggregating PSHA results two important goals are achieved (McGuire, 1995): 1) a relation between the calculated hazard and the specified seismic sources; 2) the loop between scientists performing hazard assessment and users of hazard studies is closed. As a result the seismic hazard philosophy is better understood and more reliable decisions on seismic design, analysis, and retrofit are undertaken.

4.3.7 PSHA Results for Eligible Area

A seismic source model is developed for PSHA for the territory of Bulgaria. The model is based on complex geodetic, geological, geophysical and seismological data and is presented in Figure 82. For each source are defined the all parameters describing the seismicity in the source. Two cases are considered:

1. All sources are areal sources – earthquakes are randomly distributed in the corresponding source
2. Smaller earthquakes are randomly distributed in the source while stronger earthquakes are happened only on the faults defined in the source.

The final result is a mean of the two considered cases.

Seismic sources map

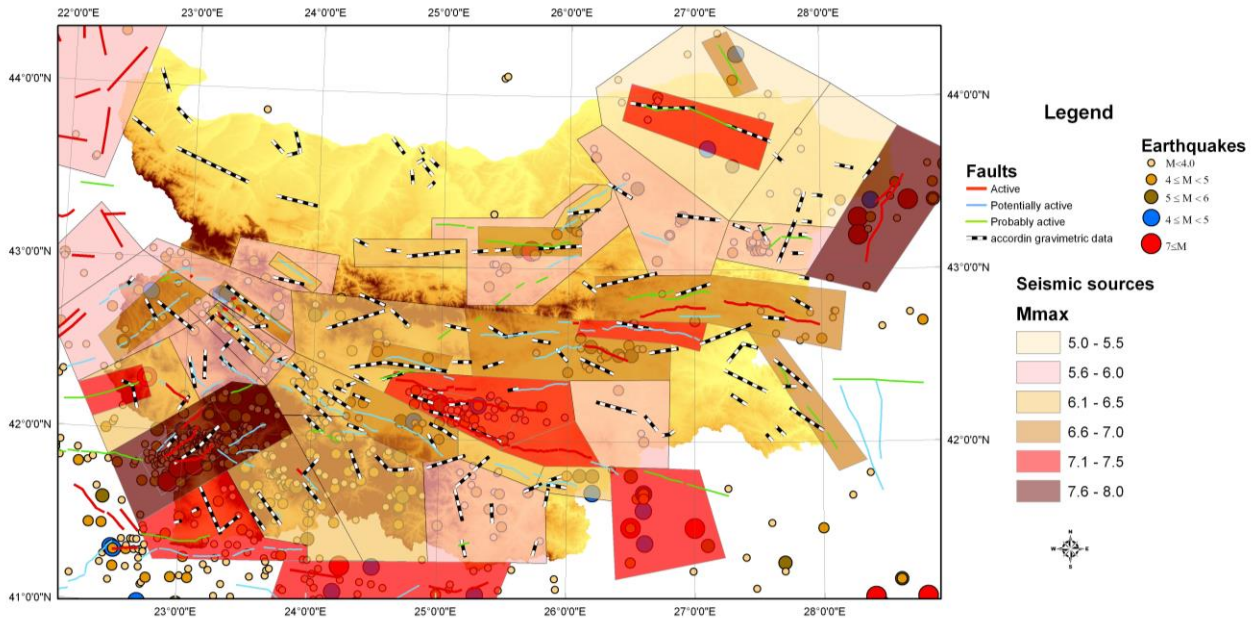


Fig 82. Map of seismic sources used for seismic hazard assessment

The ground motion attenuation relationship presented in Ambraseys et al. (1996) is used for hazard assessment.

The seismic hazard for the country in different return periods have been evaluated applying the above described methodology, the compiled seismic source model and selected attenuation model. In Fig. 83 are presented the obtained results for the eligible area for return period of 475 years (probability of exceedance of 10% in 50 years).

Large parts of the area are with expected acceleration between 0.09g and 0.13g and between 0.13g and 0.18g. Small parts (North-East and South-West) fall in territories with expected acceleration between 0.18g and 0.26g and larger than 0.26g.

In Fig. 84 is presented the influence of the intermediate Vrancea earthquakes on the seismic hazard. As seen in the figure almost all Northern part of the eligible area is strongly (more than 50 %) influenced by intermediate Vrancea earthquakes.



Project funded by the
EUROPEAN UNION



Seismic hazard (475 years return period)

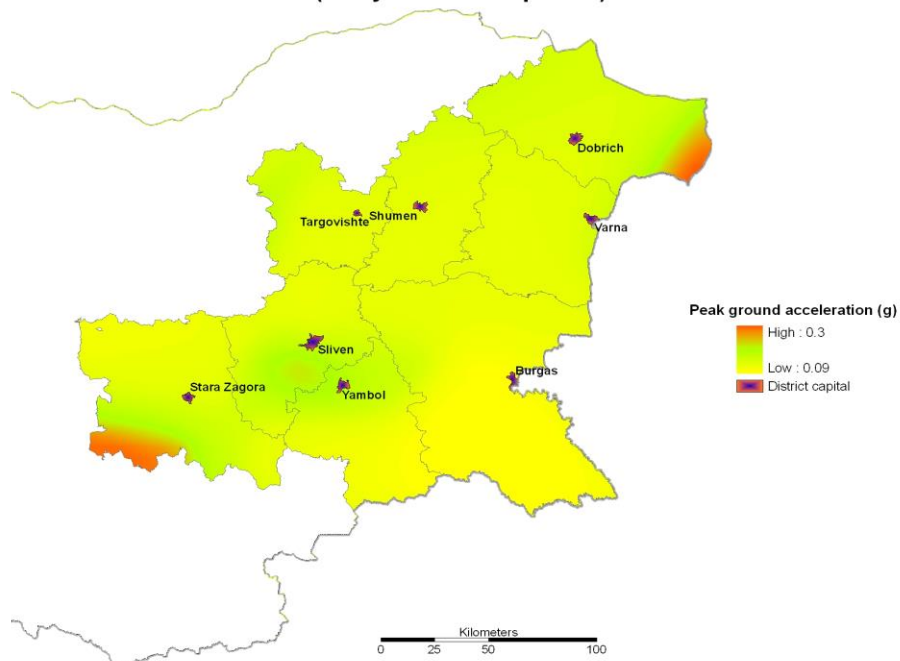


Fig 83. Proposed map for seismic code (eligible area)

Seismic hazard (475 years return period)

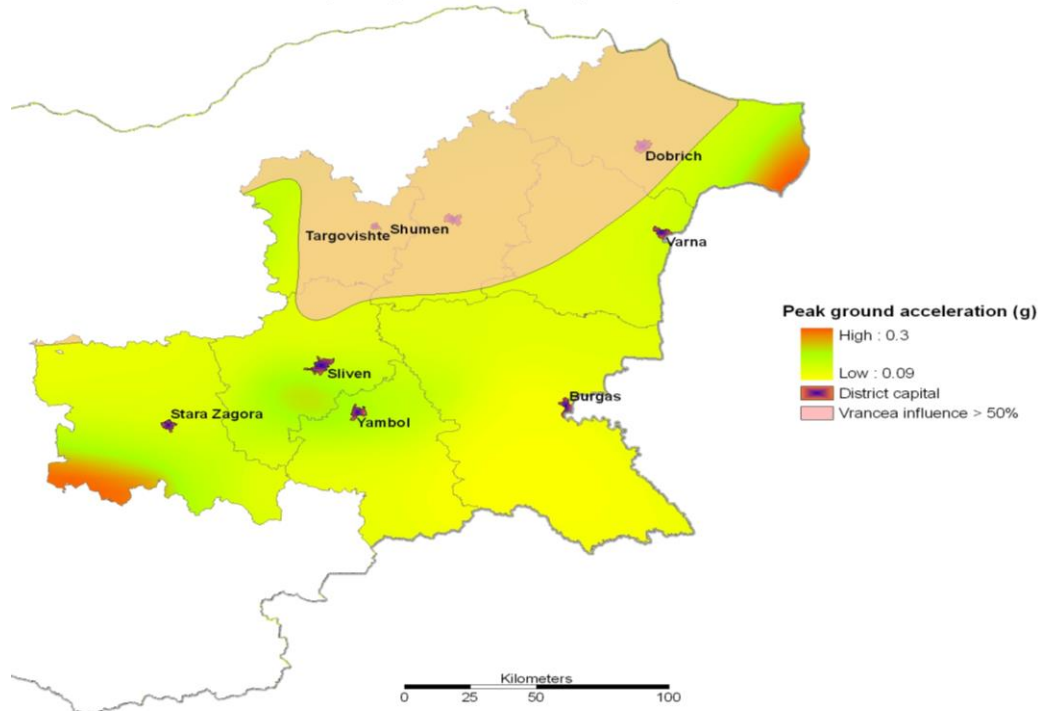


Fig 84. Influence of the intermediate Vrancea earthquakes on the seismic hazard

4.3.8 De-Aggregation of Probabilistic Seismic Hazard Assessment for Bulgarian Eligible Area (Main District Towns)

De-aggregation of the seismic hazard for a return period of 475 years (probability of exceedance of 10% in 50 years) for PGA was performed for 8 cities (administrative centres) on the territory of ESNET Bulgarian eligible area (Figs. 85 – 88)

The de-aggregation results show existence of both unimodal and bimodal distribution of earthquake magnitude and distance to ground motion exceedance frequency for PGA.

PSHA de-aggregation plots for PGA show the following peculiarities:

1. Unimodal distribution of earthquake magnitude and distance to ground motion exceedance frequency is observed. The mode of the distribution is for magnitude 5.0-7.5 earthquake at a distance of 5 to 20 km from the city of Yambol. The strongest contributor to the hazard is the near regional seismicity (Fig.85).
2. PSHA disaggregation plots show a slight bimodal distribution of earthquake magnitude and distance to ground motion exceedance frequency is observed for PGA (Fig.86). The primary mode in Fig.86 (well



expressed) is a magnitude 5.0 to 6.0 earthquake at 10 to 20 km from the cities of Sliven and Stara Zagora (effect of the near regional seismicity). The secondary mode (not well expressed) is for magnitude greater or equal to 7.5 earthquakes at a large distance (effect of Vrancea intermediate earthquakes). The strongest contributor to the hazard is the near regional seismicity.

3. PSHA disaggregation plots show a slight bimodal distribution of earthquake magnitude and distance to ground motion exceedance frequency is observed for PGA (Fig.87). The primary mode in Fig.11 is for magnitude greater or equal to 7.5 earthquakes at a distance of more than 200 km from the cities of Targovishte, Shumen, Dobrich and Burgas (effect of Vrancea intermediate earthquakes). The secondary mode is a magnitude 5.0 to 6.0 earthquake at 10 to 20 km from the cities (effect of the near regional seismicity). The strongest contributor to the hazard is the Vrancea intermediate source.

4. PSHA disaggregation plots show a bimodal distribution of earthquake magnitude and distance to ground motion exceedance frequency (Fig.88). The primary mode of the distribution is for magnitude greater or equal to 7.0 earthquakes at a distance 10 to 20 km from the city of Varna (effect of the near regional seismicity). The secondary mode is a magnitude 7.5 or larger earthquake at a distance of more than 250 km from the city of Varna (effect of Vrancea intermediate earthquakes).

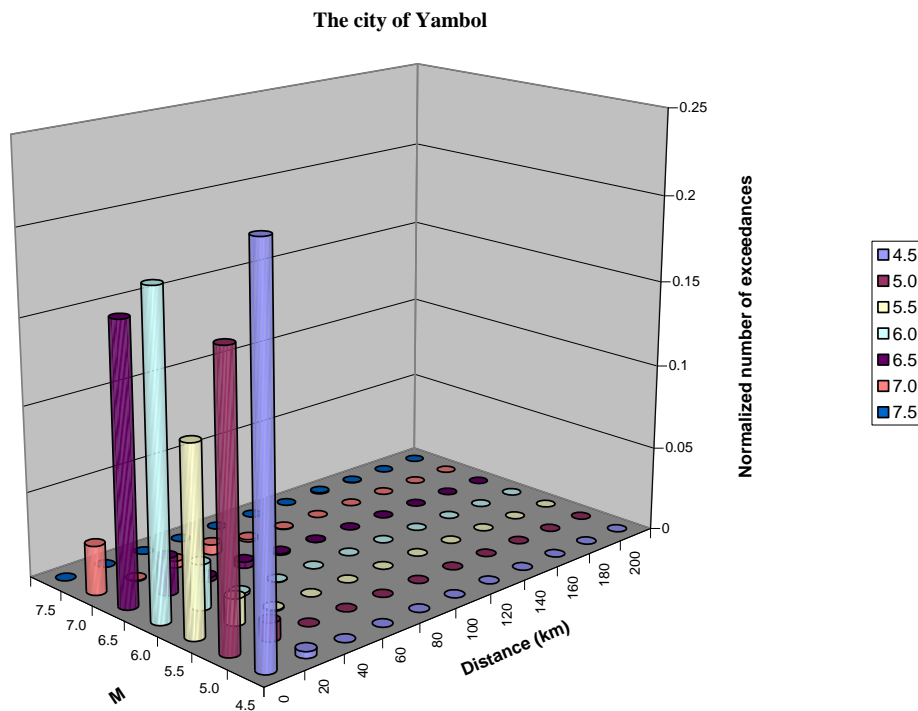




Fig 85. Unimodal distribution of earthquake magnitude and distance to ground motion exceedance frequency - the strongest contributor to the hazard for the cities is the near regional seismicity

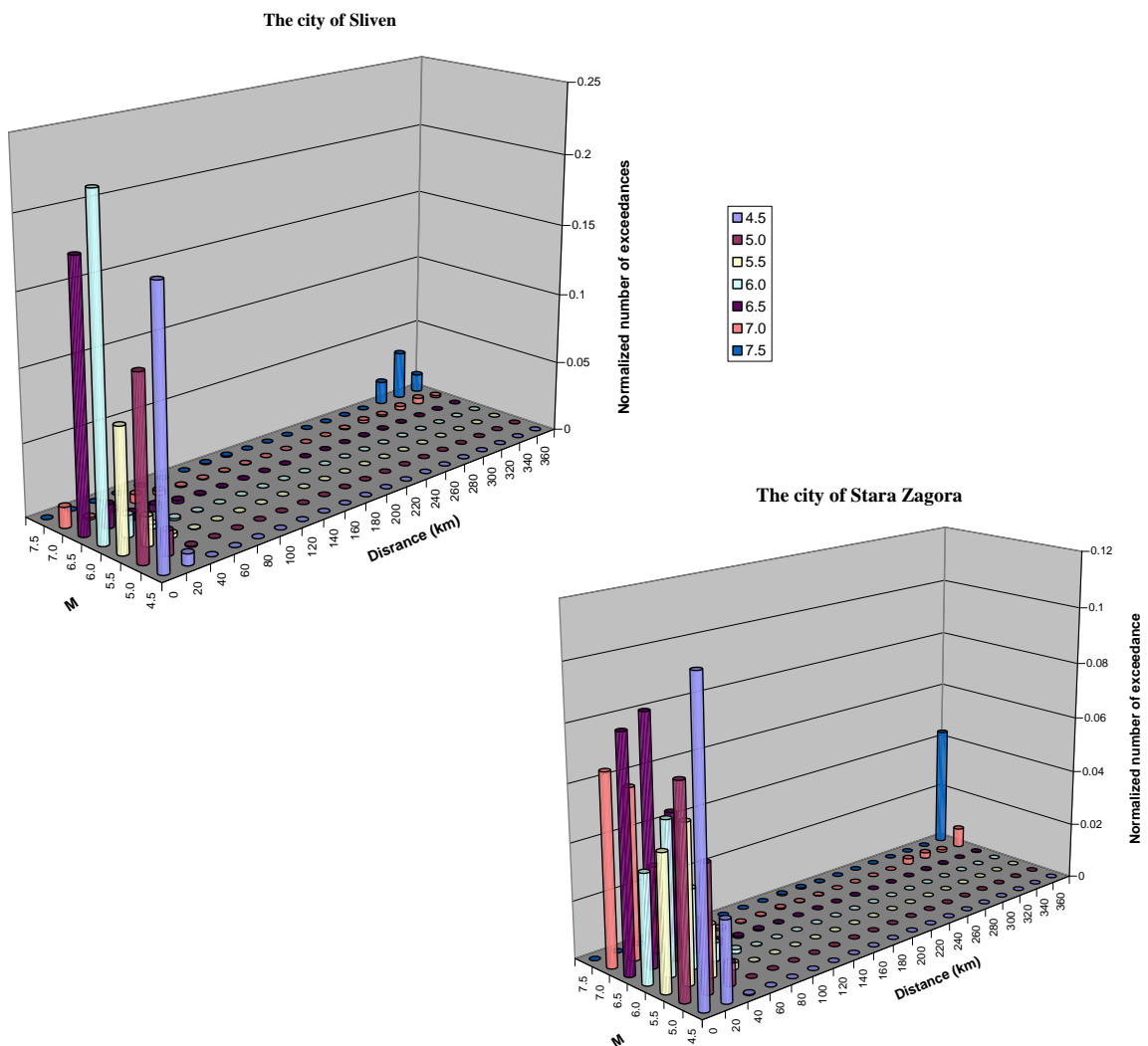


Fig 86. Slight bimodal distribution of earthquake magnitude and distance - stronger contributor to the hazard for the cities is the near regional seismicity

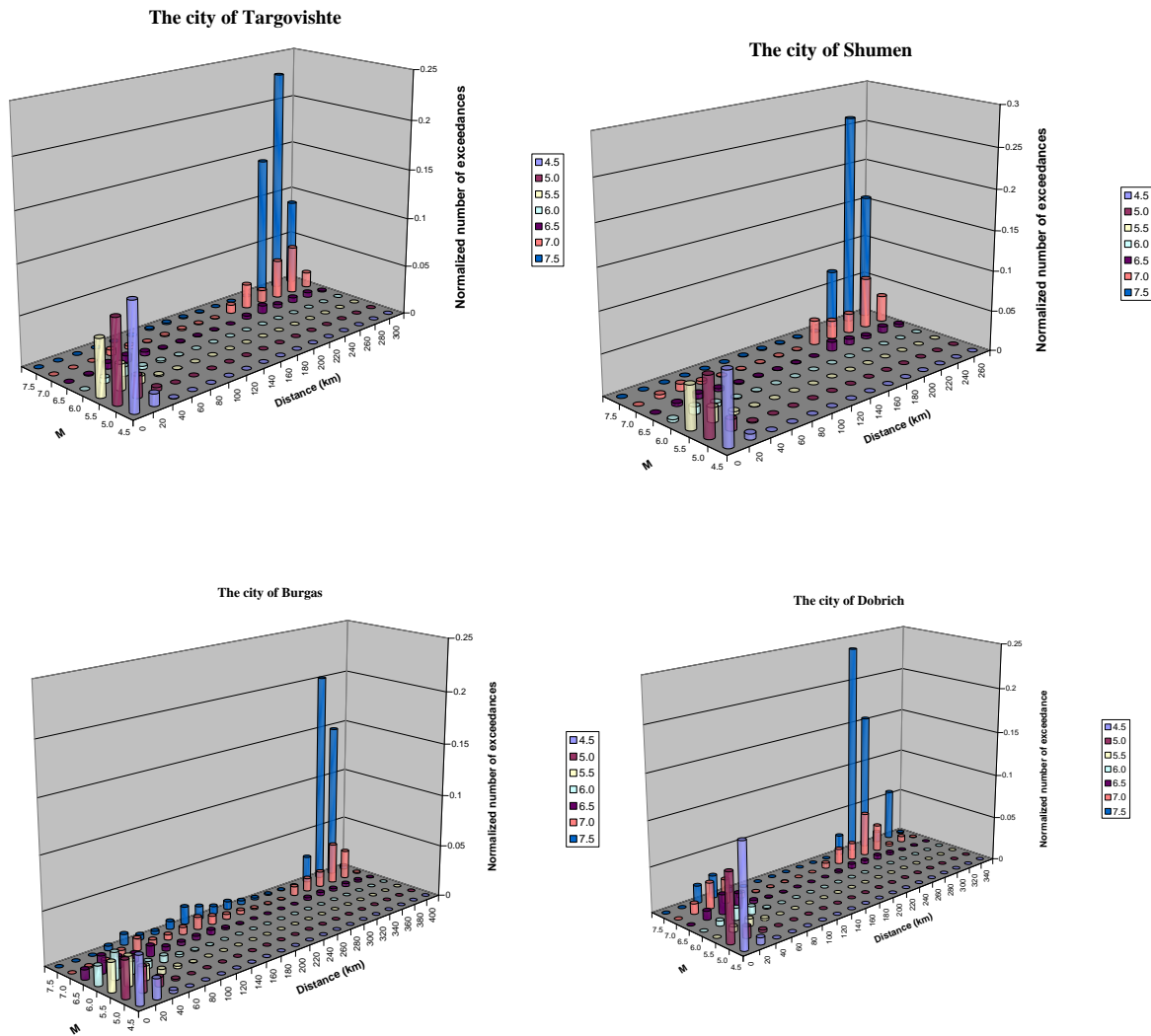


Fig 87. Slight bimodal distribution of earthquake magnitude and distance - stronger contributor to the hazard for the cities is the Vrancea intermediate source

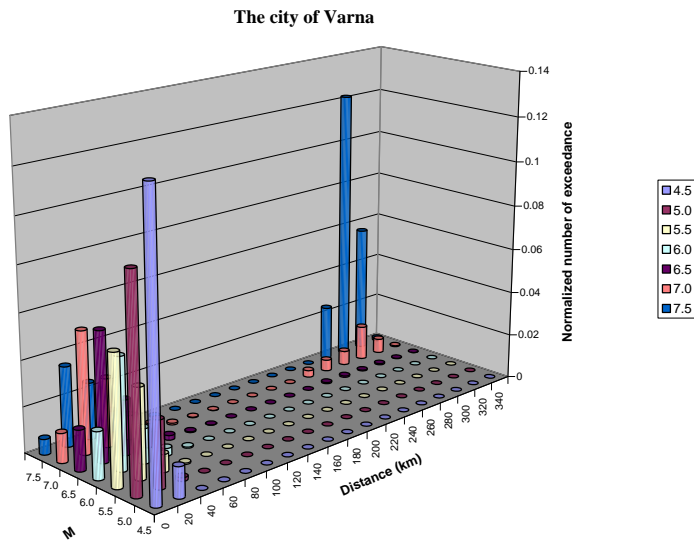


Fig 88. A bimodal distribution of earthquake magnitude and distance to ground motion exceedance frequency

4.3.9 Deterministic Hazard

For the largest cities in the eligible area, Bourgas and Varna was performed deterministic hazard evaluation. In Fig. 89 are presented the active faults near the two cities. Five GMPE's were used for evaluation:

Abrahamson and Silva (2008) - Abrahamson, N. and W. Silva (2008) "Summary of the Abrahamson & Silva NGA Ground-Motion Relations" Earthquake Spectra, Volume 24, No. 1, pp. 67–97

Akkar and Bommer (2009, rev:2010) - Akkar S, Bommer JJ (2010) Empirical Equations for the Prediction of PGA, PGV, and Spectral Accelerations in Europe, the Mediterranean Region, and the Middle East. Seismological Research Letters 81 (2): 195-206.

Boore and Atkinson (2008) - Boore, D.M. and Atkinson G. M. (2008), "Ground-Motion Prediction Equations for the Average Horizontal Component of PGA, PGV, and 5%-Damped PSA at Spectral Periods between 0.01 s and 10.0 s" Earthquake Spectra, Vol. 24, No. 1, pp: 99–138



Campbell and Bozorgnia (2008) - Campbell, K. W. and Y. Bozorgnia (2008) “NGA Ground Motion Model for the Geometric Mean Horizontal Component of PGA, PGV, PGD and 5% Damped Linear Elastic Response Spectra for Periods Ranging from 0.01 to 10 s” Earthquake Spectra, Vol. 24, No. 1, pp: 139–171

Chiou and Youngs (2008) - Chiou, B.S.J. and R.R. Youngs (2008) “An NGA Model for the Average Horizontal Component of Peak Ground Motion and Response Spectra” Earthquake Spectra, Vol. 24, No. 1, pp: 173–215

In Fig. 90 are presented the 5% damped mean and mean $+1\sigma$ hazard spectra for the cities of Bourgas and Varna.



Project funded by the
EUROPEAN UNION

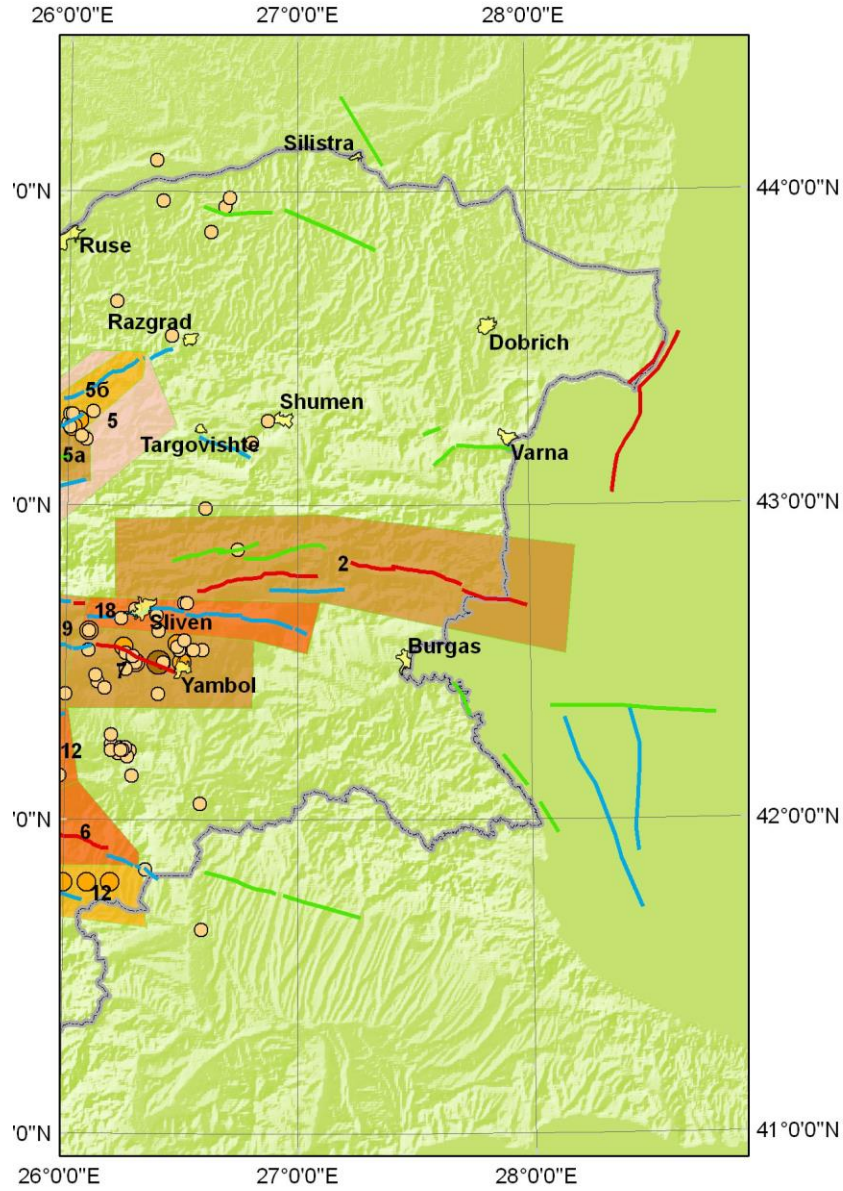
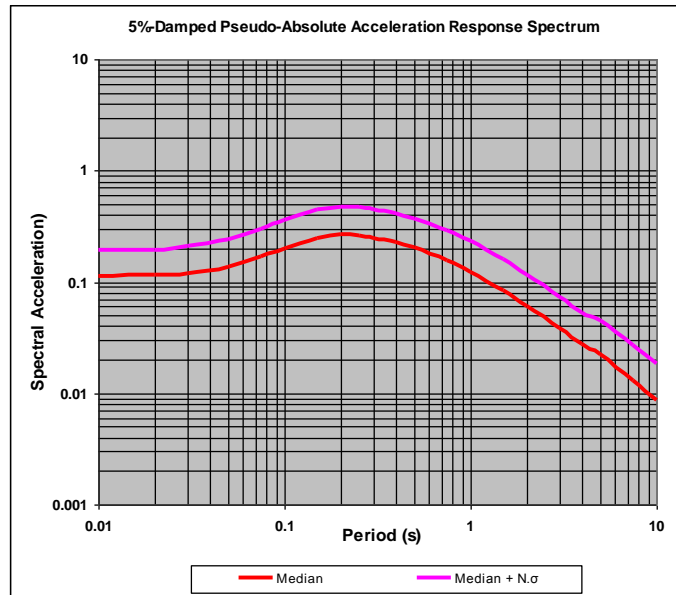
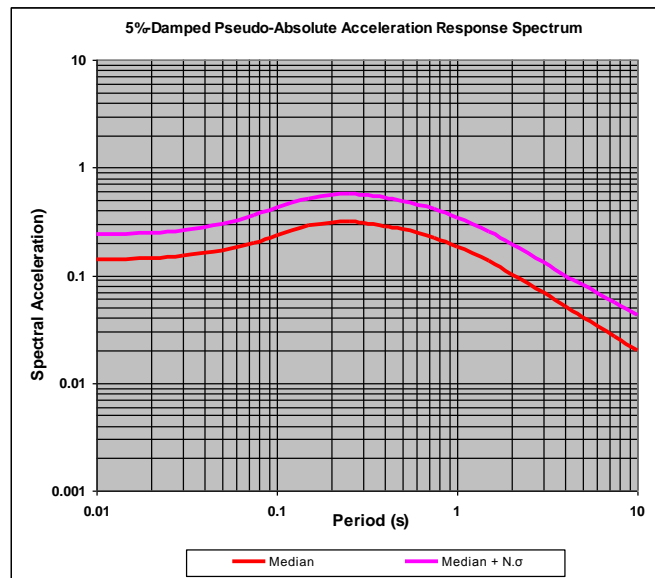


Fig 89. Active faults



Bourgas,

Fault length=64 km, $M=7.2$, distance=31km



Varna,

$M=8$, distance=39km

Fig 90. 5% damped mean and mean + 1σ hazard spectra



REFERENCES

- Abrahamson, N. and W. Silva (2008) “Summary of the Abrahamson & Silva NGA Ground-Motion Relations” *Earthquake Spectra*, Volume 24, No. 1, pp. 67–97
- Akkar S, Bommer JJ (2010) Empirical Equations for the Prediction of PGA, PGV, and Spectral Accelerations in Europe, the Mediterranean Region, and the Middle East. *Seismological Research Letters* 81 (2): 195-206.
- Ambraseys, N. N., Simpson, K. A., & Bommer, J. J. 1996. Prediction of horizontal response spectra in Europe. *Earthquake Engineering and Structural Dynamics*, 25(4), 371–400.
- Bender, B., D. Perkins, 1982. SEISRISK II: A computer program for seismic hazard estimation, Open file report, USGS, pp 82-293.
- Bender, B., D. Perkins, 1987. SEISRISK III: A computer program for seismic hazard estimation, USGS Bull. 1772.
- Bommer, J. J., F. Scherbaum, H. Bungum, F. Cotton, F. Sabetta, and N. A. Abrahamson, 2005. On the use of logic trees for ground-motion prediction equations in seismic hazard assessment, *Bull. Seism. Soc. Am* 95, no. 2, 377–389.
- Bommer, J., N. Abrahamson, 2006. Why Do Modern Probabilistic Seismic-Hazard Analyses Often Lead to Increased Hazard Estimates?. *Bulletin of the Seismological Society of America*, Vol. 96, No. 6, pp. 1967–1977.
- Boncev E., V.Bune, L.Christoskov, J.Karagjuleva, V.Kostadinov, G.Reisner, S.Rizhikova, N.Shebalin, V.Sholpo, D.Sokerova, 1982. A method for compilation of seismic zoning prognostic maps for the territory of Bulgaria. *Geologica Balcanica*, 12(2), 2-48.
- Boore, D.M. and Atkinson G. M. (2008), “Ground-Motion Prediction Equations for the Average Horizontal Component of PGA, PGV, and 5%-Damped PSA at Spectral Periods between 0.01 s and 10.0 s” *Earthquake Spectra*, Vol. 24, No. 1, pp: 99–138
- Boyanov I, C. Dabovski, P. Gocev, A. Harkovska, V. Kostadinov, TZ. Tzankov, I. Zagorcrv, 1989. A new view of the Alpine tectonic evolution of Bulgaria, *Geologica Rhodopica*, vol. I, pp 107-121.
- Bungum, H., P. Swearingen, G. Woo, 1986. Earthquake hazard assessment in the North Sea. *Phys. Earth Planet. Inter.*, 44, 201-210.
- Campbell, K. W. and Y. Bozorgnia (2008) “NGA Ground Motion Model for the Geometric Mean Horizontal Component of PGA, PGV, PGD and 5% Damped Linear Elastic Response Spectra for Periods Ranging from 0.01 to 10 s” *Earthquake Spectra*, Vol. 24, No. 1, pp: 139–171



- Chiou, B.S.J. and R.R. Youngs (2008) “An NGA Model for the Average Horizontal Component of Peak Ground Motion and Response Spectra” *Earthquake Spectra*, Vol. 24, No. 1, pp: 173–215
- Coppersmith K., and R. Youngs, 1986. Capturing uncertainty in probabilistic seismic hazard assessments within intraplate environments: in *Proceedings of the 3rd National Conference on Earthquake Engineering*, Charleston, August 24-28, v. I, pp 301.
- Cornell C., 1968. *Engineering Seismic Risk Analysis*. BSSA, v.5, pp 1583.
- Cornell C., 1971. Probabilistic analysis of damage to structures under seismic loads, in *Dynamic Waves in Civil Engineering*, D.A.Howells, I.P.Haigh, and C.Taylor (Editors), John Wiley&Sons, New York, 473-488.
- Dachev H., I. Vaptzarov, L. Filipov, D. Solakov, S. Simeonova, S. Nikolova, P. Sokolova, E. Botev, Tz. Georgiev, 1995. Seismology, geology, neotectonics, seismotectonics and seismic hazard assessment for the PNPP Belene site, Report of Project: Investigations and activities for increasing of the seismic safety of the PNPP Belene site, Geoph. Inst., BAS, S, I, pp 250.
- Esteva, L, 1967. Criteria for the construction of spectra for seismic design, presented at Third Panamerican Symposium on Structures, Caracas, Venezuela.
- Esteva, L, 1968. Bases para la formulaci3n de decisiones de dise1o s3smico, Ph.D. Thesis, Universidad Nacional Auto3noma de Me3xico, Mexico City.
- Glavcheva R., 2004. State of the art of historical earthquake investigation in Bulgaria. *Annals of Geophysics*, 47, 2/3, 705-721.
- Joyner, W. B., and D. M. Boore, 1981. Peak horizontal acceleration and velocity from strong-motion records including records from the 1979 Imperial Valley, California, earthquake, *Bull. Seism. Soc. Am.* 71, no. 6, 2011–2038.
- Kulkarni R., R. Youngs, and K. Coppersmith, 1984. Assessment of confidence dintervals for results of seismic hazard analysis: in *Proceedings of the 8 World Conference on Earthquake Engineering*, San Francisco, California, v I, pp 263.
- McGuire, R., 1976. FORTRAN Computer Program for Seismic Risk Analysis, U.S. Geol.Surv. Open-File Rep. 76-67, U.S., Rep. 1-90.
- McGuire, R., 1978, FRISK: Computer Program for Seismic Risk Analysis using faults as earthquake sources, U.S. Geol.Surv. Open-File Rep. 76-67, U.S., Rep. 78-1007.
- McGuire, R., 1993. Computations of seismic hazard, *Annali di Geofisica*, XXXVI, 3-4, 181-200.
- McGuire, R. K., 2004. *Seismic Hazard and Risk Analysis*, EERI Monograph MNO-10, Earthquake Engineering Research Institute, Oakland, California.



- Merz, H. A., and C.A. Cornell, 1973. Seismic risk based on a quadratic magnitude-frequency law. *Bull.Seism.Soc.Am.*, 63, 6, 1999-2006.
- Richter Ch., 1958. *Elementary Seismology*. W. H. Freeman and Company, San Francisco, pp 670.
- Simeonova, S.D., Solakov, D.E., Leydecker, G., Busche, H., Schmitt, T., Kaiser, D., 2006. Probabilistic seismic hazard map for Bulgaria as a basis for a new building code. *Natural Hazards and Earth System Science*, v. 6, 6, 2006, 881-887.
- Sokerova, D., S. Simeonova, S. Nikolova, D. Solakov, E. Botev, R. Glavcheva, S. Dineva, B. Babachkova, S. Velichkova, S. Maslinkova, K. Donkova, S. Rizikova, M. Arsovski, M. Matova, I. Vaptzarov, L. Filipov, 1992. Geomorphology, neotectonic, seismicity and seismotectonic of NPP Kozloduy, Final Report (Summary) on IAEA Mission: Design basis earthquake for seismic upgrading of NPP Kozloduy, Sofia, pp 200.
- Solakov, D. Simeonova S, Christoskov L., Alexandrova I., Trifonova P., Dimitrova L., 2009. Project report: "Microseismic zoning of Bulgaria according to EC8", *Geophysical Inst.-BAS, S.*, pp 79.
- Tari, G., O. Dicea, J. Faulkerson, G. Georgiev, S. Popov, M. Stefanescu, G. Weir. 1997. Cimmerian and Alpine Stratigraphy and Structural Evolution of the Moesian Platform (Romania/Bulgaria). In: - Robinson A. G. (Ed.) *Regional and Petroleum geology of the Black Sea and surrounded region: AAPG Memoir 68*, 63-90.
- Thenhaus P., K. Campbell, 2003. Seismic hazard analysis, In: *Earthquake engineering handbook*, W.Chen and C.Scawthorn (Editors), CRC Press, Boca Raton, Fl., 8-1–8-50.
- Watzof Sp., 1902, 1903, 1904...1923. *Earthquakes in Bulgaria*. Report on earthquakes felt during 1901, 1902,..., 1913-1916. CMI, S. (in Bulgarian and French)
- Yankov, Y., 1935. Regional deformations caused by the 14 and 18 April 1928 earthquakes. *Earthquakes in Bulgaria No.20-21*, Central Meteorological Station, Imprimerie de l'Etat, Sofia, pp 93. (in Bulgarian and French).
- Zagorcev, I., 1992. Neotectonics of the central parts of the Balkan Peninsula: basic features and concepts, *Geologische Rundschau*, 81/3, 635-654.



4.4 UKRAINE

Seismic risk of the Odessa region.

Alexander Kendzera¹ Konstantin Yegupov² Vyacheslav Yegupov³

¹ Associate Professor, Ph. D., S. Subbotin Institute of Geophysics of NAS of the Ukraine, Kiev, kendzera@igph.kiev.ua

² Dr. of Science, Odessa State Academy of Construction and Architecture, Odessa, k_yegupov@eurocom.od.ua

³ Engineer, S. Subbotin Institute of Geophysics of NAS of the Ukraine, Odessa, slava.yegupov@gmail.com

4.4.1 Seismic hazard

City of Odessa is located in a seismically dangerous and seismically active zone of Ukraine. The strongest earthquakes are located at a distance of 300 kilometers from Odessa in the Vrancea area and the area of Dobrogea (Fig. 91). [1] In addition, as seen from Fig. 92, near Odessa has several major faults, for which several methods confirmed by tectonic activity in the Neogene-Quaternary period [2]. In this connection, the presence of seismic hazard in the city is not in doubt.

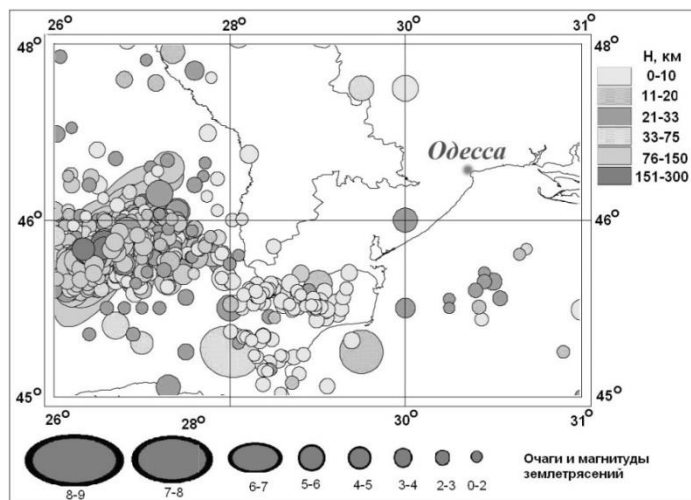


Fig 91. Map of earthquake epicenters in Odessa region and surrounding areas (B. Pustovitenko, 2004)

¹ Associate Professor, Ph. D., S. Subbotin Institute of Geophysics of NAS of the Ukraine, Kiev, kendzera@igph.kiev.ua

² Dr. of Science, Odessa State Academy of Construction and Architecture, Odessa, k_yegupov@eurocom.od.ua

³ Engineer, S. Subbotin Institute of Geophysics of NAS of the Ukraine, Odessa, slava.yegupov@gmail.com

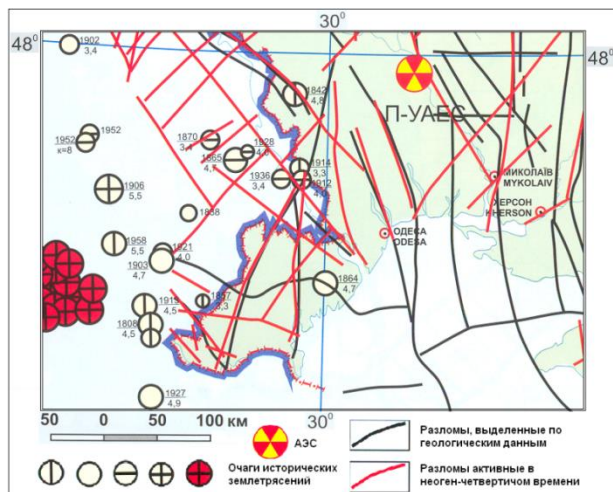


Fig 92. The fault structure and pockets of historical earthquakes near Odessa [2].

Potentially dangerous for investigated territory is an earthquake zone Vrancea region Dobrogea and local tectonic structures within a radius of 100 km with respect to the city (Fig. 91 and Fig. 92).

Vrancea zone earthquakes. The greatest seismic hazard for Odessa is shaking from the Vrancea zone of deep earthquakes. Only in the last 200 years, the city of Odessa 7 times subjected to seismic actions with $I = 6$ twice in 1802 and 1940. with $I = 7$ [3, 4] (Fig. 93).

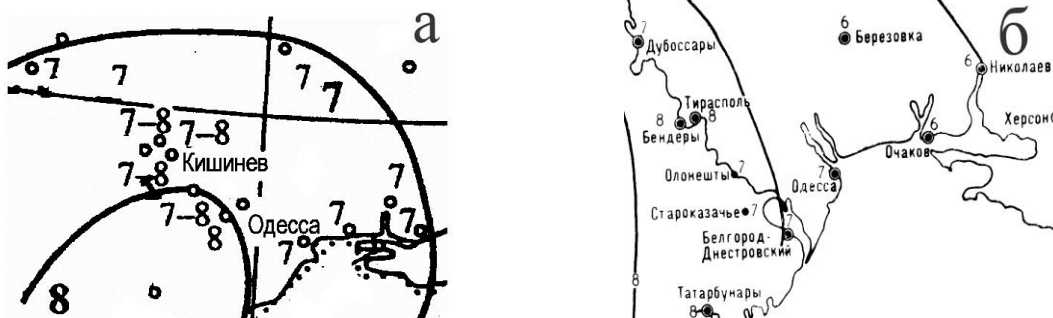


Fig 93. Schematic map isoseismals Vrancea earthquake in 1802 (a) [3] and 1940. (б) [4].
The numbers near the name means the observed seismic rating.

According to the published data in historical times there are known cases of local earthquakes near Odessa. For example, work [5] (S. Evseev, 1969) provides a reference to the earthquake of July 9, 1857 with an intensity $I = 5$ points, which was displayed as "... a local short jerk with a buzz." Another

earthquake with the magnitude of 4.7 occurred at a distance 50 km from Odessa in 1864.[5] (S. Evseev , 1969).

The graph repeatability [9] concluded that an earthquake with a magnitude of $M = 7 \pm 0.25$ average realized 1 time in 15 years. Extrapolating the dependence towards the maximum magnitudes get that once in a $T \approx 500$ years is possible to realize an earthquake with $M = 8$ [1]. The same value of the maximum possible earthquake magnitude given by the authors of [10]. Thus, in the region of Vrancea forecast maximum possible earthquake magnitude will correspond to $M = 8$.

Dobrogea zone earthquakes. In contrast to the area of Vrancea region Dobrogea seismically studied poorly. About earthquakes of this region is known mainly only macroseismic information [11]. There have been two groups of epicenters [6].

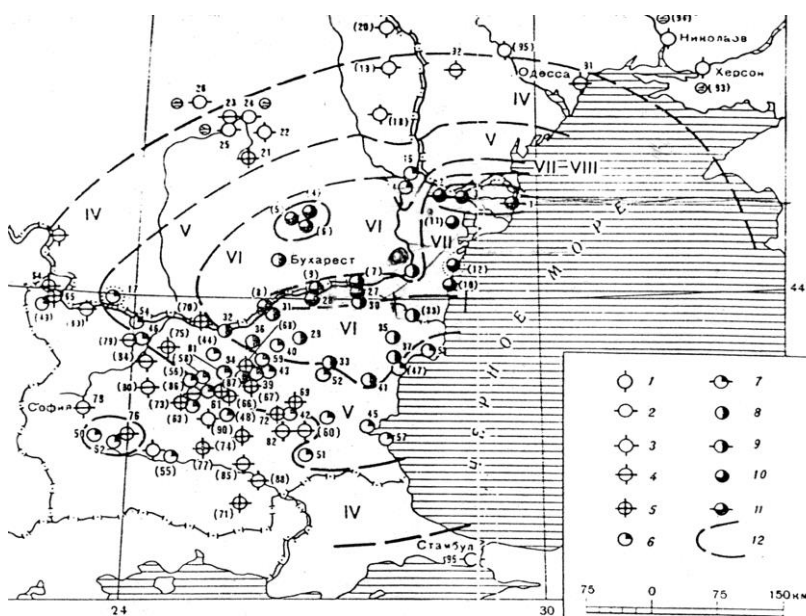


Fig 94. A schematic map of the earthquake isoseismals Dobrogea region October 14, 1892. Legend: 1 - 2-3 points, 2 - 3 points, 3 - 3-4 score 4 - 4 points, 5 - 4-5, 6 - 5 points, 7 - 5-6, 8 - 6 points, 9 - 6-7, 10 - 7 points, 11 7-8, 12 field isoseismals (from [11]).

The northern part of Dobrogea (near the city of Reni, Isakcha, Tulcha, Kilia) observed intensity tremors from local earthquakes reached 6 points. The most recent earthquake in this group was 13 November 1981 in the delta of the Dunay River and has been registered in many seismic stations. Seismic effects in the south of the Odessa region reached 6 points. The earthquakes of this group marked shift type motions.

Earthquake foci of the second group are located in central and southern Dobrogea (Kyrshelag area of the city, Babadag, Hyrshov). Probably, to this group belongs destructive earthquake October 14, 1892



(magnitude 7.2, intensity at the epicenter of 7-8 points) (Fig. 94). [11] Seven-point tremors were covered area with an area of about 4500 square meters. km, including in Odessa not more than 4 points.

Location of earthquake zones coincide with major tectonic disturbances. Thus, the Dobrogea region should be regarded as potentially seismic hazard for the territory of Odessa region. During historical times there are several earthquakes of magnitude $M = 3.5 \square 7.0$ with intensity at the epicenter $I \square 5$ points [11].

Local seismicity

Local seismic activity is connected with tectonic faults in the basement of the East European platform and by faults the shelf and continental slope of the western part of the Black Sea.

Total near Odessa in a radius of 250 km it is known about 30 local earthquakes with calculated and observed intensities from 2 to 5 points. Examples of such earthquakes are given in [6, 9, 13, 14].

The last of the perceptible earthquakes occurred in the Black Sea May 7, 2008 in Odessa and demonstrated the intensity of 3 points, and in the south of the Odessa region - with an intensity of 4 points.

4.4.2 Seismic events in Odessa region

Odessa's first seismic station "Odessa city" was founded in Odessa State Academy of Construction and Architecture to study the level of seismic danger in Odessa region. Before that such observations were conducted in the two nearby seismic stations *Stepanovka* and *Zmeinyi Island* (Snake Island). The latter station worked only from time to time due to intrinsic maintenance and operation difficulty on a remote island.

Since its work the seismic station "Odessa city" has recorded more than 100 seismic events, including 8 earthquakes with the magnitude of $4,5 \div 5,3$ (K.Yegupov, 2013). Figure 95 shows the vertical component of earthquake records in the subcrust Vrancea zone recorded by the seismic station "Odessa-city" on 06.10.2013(K.Yegupov, 2013). Figure 96 shows the horizontal of oscillations calculated by recording the earthquake 22.11.2014, of the Vrancea zone, registered by the seismic station "Odessa-city": a - acceleration, b - speed I c – offset.

Figure 97 shows soil conditions of the location of the seismic station "Odessa-city" in the basement housing of Odessa Academy of Civil Engineering and Architecture. Apparently, the seismic detection sensors are located on relatively hard soil, which may be considered as soil of the second category as for seismic properties, according to the table 1.1. DBN B.1.1-12: 2006.



Project funded by the
EUROPEAN UNION

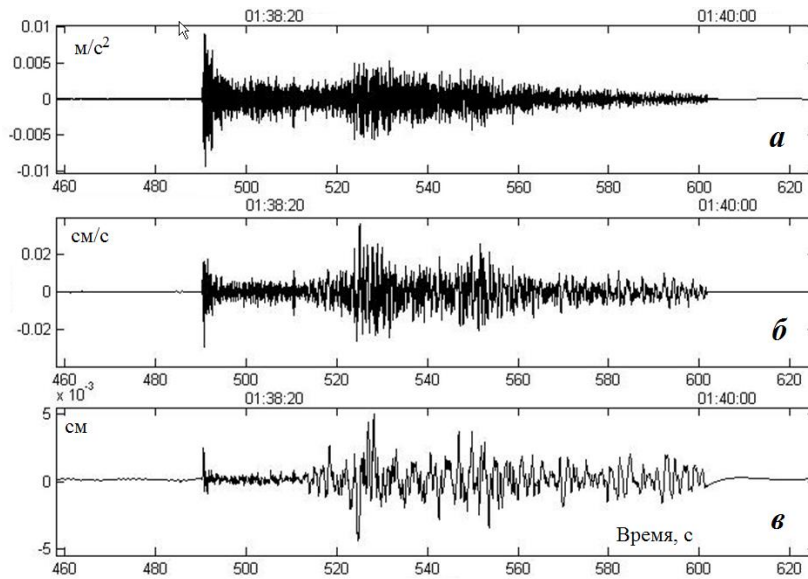


Fig 95. The vertical component of oscillations calculated by recording the earthquake 06.10.2013, of the Vrancea zone, registered by the seismic station "Odessa-city": a - acceleration, b - speed | c - offset. (Mag 4.7)

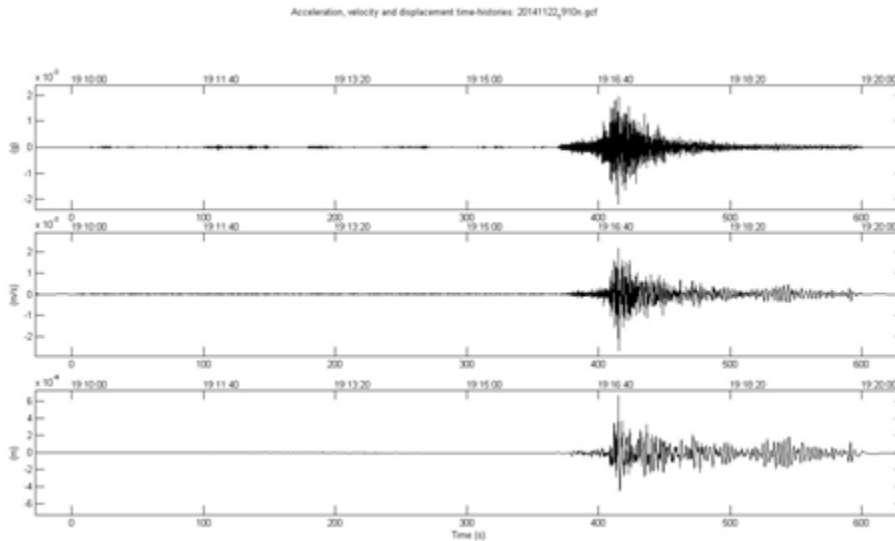


Fig 96. The horizontal of oscillations calculated by recording the earthquake 22.11.2014, of the Vrancea zone, registered by the seismic station "Odessa-city": a - acceleration, b - speed | c - offset. (Mag 6.3)

Information shown in figure 97 is used to determine the relative increase (decrease) of the parameters of seismic effects on the construction and operation stages of the city with other types of soil conditions.

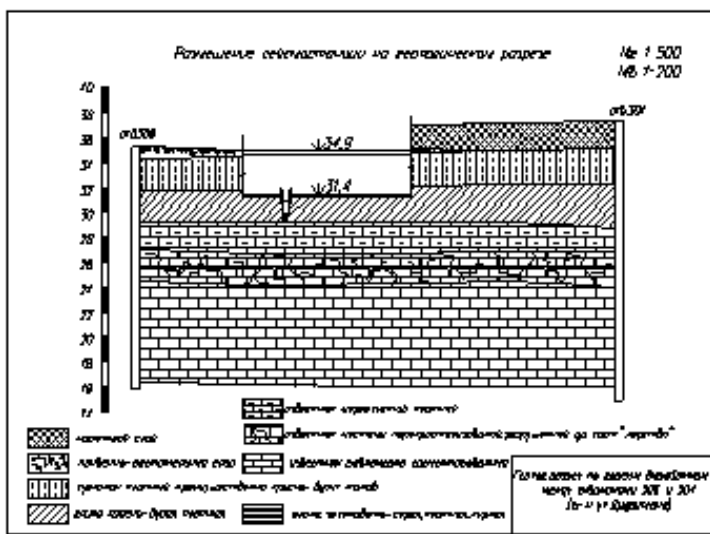


Fig 97. Seismic layout in the basement housing of Odessa Academy of Civil Engineering and Architecture.

During the work of the seismic station "Odessa-city" a series of earthquakes imperceptible to the public, which are the most dangerous for the parts of the city of Odessa and Odessa region, local source zones and the Vrancea zone was registered. Their list indicating the parameters of foci is shown in the table 4.3.1.

Table 4.4.1 Seismic events with magnitude >4 of 2008 to 2014year

Year	2008	2009	2010	2011	2012	2013	2014	2015
Mag	4.0-5.0	4.0-5.3	4.5	4.0-4.8	4.0-4.6	4.0-5.3	4.0-5.6	4.0-5.0
Number of events	8	8	2	8	14	15	18	10



4.4.3 Seismic microzoning

Seismic micro zoning represents the section of the engineering seismology which subject is the specification of the data of seismic zoning for territories or sites under construction taking into consideration the local ground, hydrological conditions and the landscape. Seismic micro zoning became a regular practice of engineering research in the Ukraine according to the requirements of the Ukrainian national construction regulation B.1.1.-12:2006. [16].

Main objective of the research using seismic micro zoning is the quantitative assessment of rated seismicity in terms of seismic force and physical parameters of eventual seismic effects, taking into account the influence of local geotechnical conditions of a project construction site.

For mass civil and industrial engineering venues, that make the majority of the project buildings in Odessa and Odessa region, the background seismicity according to the 1.1.1 of the Ukrainian national construction regulation has to be accepted with a tolerant seismic risk of 10% (frequency of 500 years). However, the maps of the general seismic zoning do not take into account local soil conditions, although it is known that geotechnological, geomorphological, hydrogeological and geotectonic features of a building site can significantly influence the size of local seismic manifestations that have to be taken into consideration according to the 1.1.2 of the requirements of the Ukrainian national construction regulation [16].

Works on seismic micro zoning of building and operational sites in Odessa and Odessa region actualizes the data base organization of geotechnological and seismological data for the region, and also the method development of obtaining quantitative assessment of rated seismicity, focused on the use of empirical regularities of the field of seismic fluctuations under the conditions of the city of Odessa, obtained according to the data of the instrumental surveys.

Records of strong earthquakes of hazardous for the site of seismogenic zones registered directly on it can provide the most complete information about the magnitude and the nature of the ground motion on the test site during potentially possible maximal earthquakes. However, because large earthquakes are rare, one usually fails to get their records in such a limited period of time for geological and geophysical studies of construction sites. Therefore, synthetic rated accelerograms were calculated for modeling of seismic ground motion calculated on the construction site.

A semi-empirical approach based on the use of the theoretical calculation of the amplitude spectra of the accelerograms and their empirical phase spectra (A.Kendzera, 2008) was used. The spectral density of the resulting impact was calculated on regional (for the Vrancea zone) and the world average (for local source zones) dependencies between the position of the characteristic points of the amplitude spectrum of acceleration, the magnitude of a rated earthquake magnitude and the epicentral distance. Influence of soil conditions on the site was taken into account by using generalized theoretical models of the frequency characteristics of the geological environment under the platform.



For each construction site three rated three-component accelerograms were provided, which were modelling predicted seismic oscillations of the free surface of the ground during earthquakes in the Vrancea zone and three ones – in the local reservoir zones. While generating there were used different combinations of theoretical spectra envelopes of the rated accelerograms, normed frequency characteristics of the medium and phase spectra obtained for various posts of real earthquakes.

In the course of work on seismic microzoning "Seysmobud " and the Subbotin Institute of Geophysics studied about 30 construction sites in Odessa region to clarify the calculation of seismicity. In the course of research three-component rated accelerograms (Fig 98) present time functions, modelling the components of acceleration of seismic movements in the surface soil at the construction site during earthquakes, which can be realized on it once in 500 years. For practical use we propose two types of rated accelerograms corresponding earthquake focal zone of Vrancea and local focal zones of possible occurrence of earthquakes (A.Kendzera, 2008).

Figure 99 shows the three dimensional orientation of the vector components of the total seismic oscillations shown in Fig 98: vertical - Z, «North-South» - NS, «East-West» - EW, radial - R (facing away from the construction site towards the reservoir) and tangential - T (perpendicular to the radial).

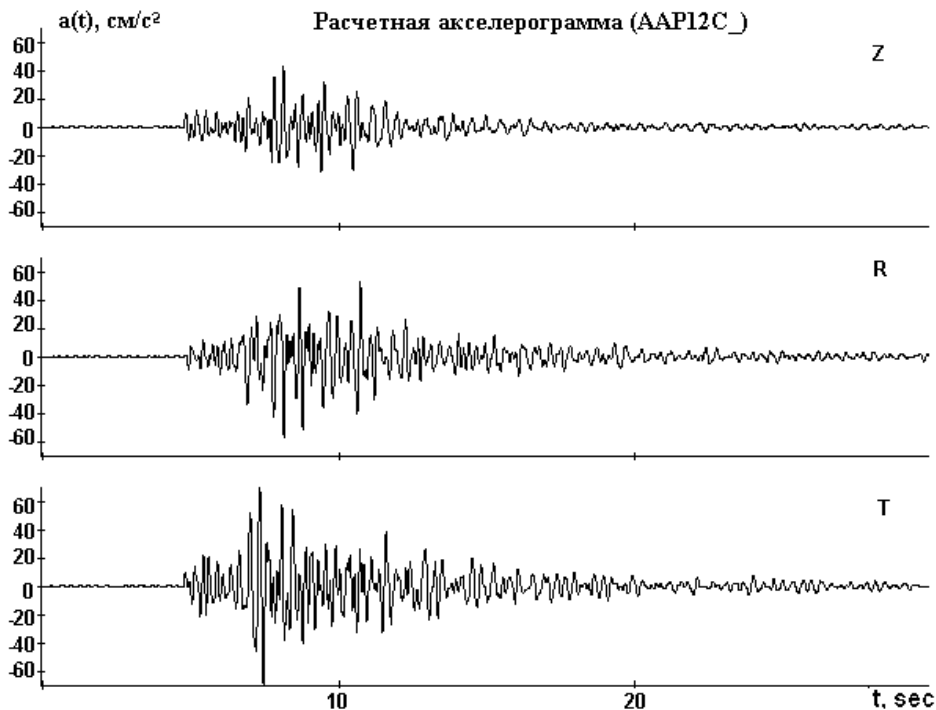


Fig 98. Example of the three-component rated accelerograms, modelling rated earthquake of local focal zone on the free surface of the ground one of the sites in the city of Odessa.

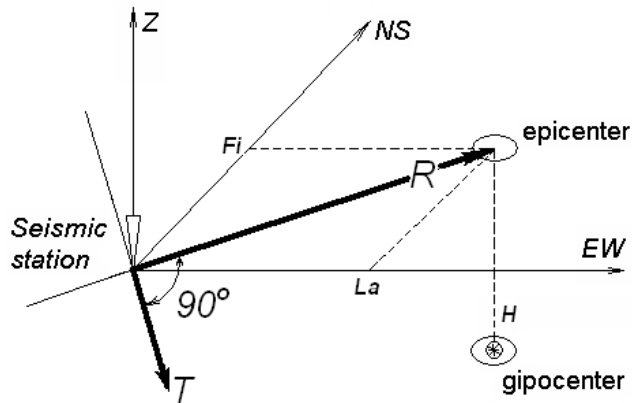


Fig 99. Direction of vector components of the total seismic vibrations.

Figure 100 shows the response spectra of individual oscillators T - component of the rated accelerograms shown in Figure 98.

The dominant oscillation frequency oscillators with 2, 5 and 10 percent level of intrinsic attenuation were determined according to the spectra of the reaction. Under the predominant frequencies we understand oscillation frequency, at which response spectra have the intensity greater than half of its maximum value.

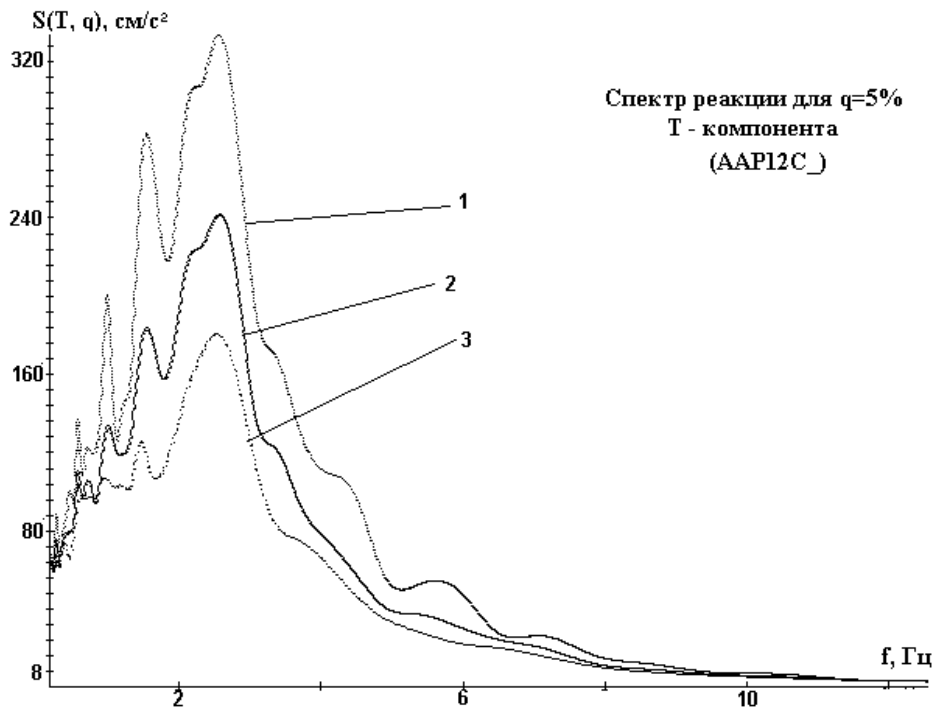




Fig 100. Linear response spectra of individual oscillators accelerogram shown in figure 4. Figures 1, 2, 3 correspond with intrinsic attenuation of single oscillators: 2, 5 and 10 percent of critical, f - the angular frequency and $T = 1 / f$.

In the course of construction works the base of engineering and geological information and the basic parameters of the synthesized accelerograms (see table 4.4.5) have been formed. The set of accelerograms is supplemented by a computer program for visualizing of the accelerograms and their preprocessing. The program allows to plot accelerogram charts, analyse in detail their individual plots, calculate the spectra, build response spectra, graphics oscillation frequency and duration of different intensity (A.Kendzera, 2008).

Table 4.4.2 Example of the basic parameters of the synthesized ternary rated accelerograms shown in figure 98.

Component	Acceleration, a, cm/c ²	Dominant frequency, Hz	Oscillation time	
			a > 0,9a	a > 0,5
T	69.5	1.8- 5.6	4	2.5
R	57.0	1.6- 6.1	8	4.1
Z	43.1	1.9- 6.1	4	2.9

A map of the location of the studied sites in Odessa and the Odessa region was prepared, their classification according to soil conditions was made, the data describing the frequency parameters, the predominant periods and amplitudes of the three-component accelerograms synthesized for modelling seismic waves from earthquakes of the Vrancea zone and local focal zones was collected.

Addresses of the construction sites are shown in table 4.4.3, where the research the seismic zoning, indicating an updated seismic hazard - I_{RN} , obtained seismic intensity increments - Δ_{IM} and totals calculated intensities I_R , was conducted.

Table 4.4.3 List of works performed by seismic microzoning.

№	Coordinates of the construction site	IR intensity rated value for site

1	46.617016, 31.099141.	$I_R = I_{RN} + \Delta I_M = 6.12 + 0.34 = 6.46 \text{ points.}$
2	46.471814, 30.706389	$I_R = I_{RN} + \Delta I_M = 6.51 + 0.31 = 6.82 \text{ points}$
3	46.556782, 30.767741	$I_R = I_{RN} + \Delta I_M = 6.51 + 1.03 = 7.54 \text{ points}$

Table 4.4.4 PGA Model (46.617016, 31.099141)

№№	lithological composition	depth interval <i>H, m</i>	Seismic wave velocity		Decrements the absorption of seismic waves		$\rho, \text{g/cm}^3$
			transverse $V_P, \text{m/sec}$	transverse $V_S, \text{m/sec}$	longitudinal ν_P	Longitudinal ν_S	
1	Top soil	0-0,5	320	150	1,5	1,7	1,4
2	loam solid	0,5-3,0	470	280	0,09	0,15	1,67
3	Sandy loam semisolid	3,0-6,9	400	220	0,1	0,12	1,540
4	loam solid	6,9-10,4	480	320	0,09	0,12	1,61
5	Sandy loam solid, loam, clay, hard	10,4-15,8	560	360	0,08	0,1	1,75
6	Clay dense	15,8-21,0	780	500	0,06	0,08	1,91
7	limestone - coquina	21,0-25,0	1250	800	0,05	0,06	2,0
8	Clay gray-green, sand	25,0-38,0	1400	750	0,06	0,07	2,1
9	Clay, limestone - coquina	38,0-80,0	1800	900	0,06	0,07	2,2
10*	limestone, Clay	80,0-171,0	2300	1000	0,05	0,06	2,2
11*	limestone, Clay	171,0-871,0	2600	1200	0,04	0,05	2,4
12*	Sandstones, clay	871,0-	3600	1500	0,01	0,03	2,6

		1471,0					
13*	Granites, biotite gneisses	1471,0 - ∞	5000	2300	0,01	0,03	2,9

note: * parameters taken on the areas of the Odessa region.

Table 4.4.5 PGA Model (46.471814, 30.706389)

№ №	lithological composition	depth interval <i>H, m</i>	Seismic wave velocity		Decrements the absorption of seismic waves		$\rho, \text{g/cm}^3$
			transverse $V_P, \text{m/sec}$	transverse $V_S, \text{m/sec}$	longitudinal ν_P	Longitudinal ν_S	
1	Top soil	0-0,7	300	120	1,5	1,5	1,4
2	limestone - coquina	0,7-3,0	490	320	0,09	0,15	1,8
3	Limestone, coquina recrystallized	3,0-5,0	760	480	0,06	0,08	2,0
4	Limestone, coquina	5,0-8,5	600	380	0,09	0,1	1,8
5	Limestone, coquina recrystallized	8,5-12,0	1400	850	0,05	0,07	2,2
6	Clay dense	12,0-26,0	1100	600	0,1	0,2	1,9
7	Clay	26,0-38,0	1200	700	0,1	0,15	2,1
8	Clay, Limestone – coquina	38,0-80,0	1800	900	0,08	0,1	2,2
9*	Limestone, Clay	80,0-171,0	1400	1000	0,06	0,12	2,2



Project funded by the
EUROPEAN UNION



10 *	marl, chalk	171,0- 871,0	1800	1200	0,06	0,06	2,4
11 *	Sandstones, clay	871,0- 1471,0	3000	1600	0,01	0,03	2,6
12 *	Granites, biotite gneisses	1471,0 - ∞	5000	3200	0,01	0,03	2,9

note: * parameters taken on the areas of the Odessa region.

Table 4.4.6 PGA Model (46.556782, 30.767741)

№№	lithological composition	depth interval <i>H, m</i>	Seismic wave velocity		Decrements the absorption of seismic waves		$\rho, \text{g/cm}^3$
			transverse $V_P, \text{m/sec}$	transverse $V_S, \text{m/sec}$	longitudinal ν_P	Longitudinal ν_S	
1	Top soil	0	120	100	0,1	0,2	1,90
2	Silt	0,5	150	120	0,09	0,15	1,82
3	Silt loamy	2,5	280	140	0,08	0,12	1,91
4	Silt loamy	4,2	400	160	0,08	0,10	1,90
5	Silt loamy	5,8	460	160	0,07	0,10	1,86
6	Silt loamy	7	480	185	0,08	0,09	1,86
7	Clay, silt	9	520	220	0,07	0,08	1,94
8	Clay, silt	12	520	260	0,06	0,07	1,94
9	Clay, silt	14,4	520	320	0,06	0,06	1,89
10	Limestone, clay	18	1200	820	0,04	0,05	1,90
11	Sandy loam, clay	23	1000	680	0,05	0,06	1,93



Project funded by the
EUROPEAN UNION



12	Clay, sand	29	1100	640	0,05	0,07	1,90
13*	Limestone	35	1200	800	0,05	0,05	1,80
14*	Limestone	45	1400	900	0,04	0,05	1,85
15*	loam solid	50	1500	1100	0,04	0,04	2,1
16*	Clay, sand	60	1600	1200	0,04	0,04	2,1
17*	clay, Limestone	70	2300	1300	0,02	0,03	2,1
18*	Limestone, clay	80,0	2600	1400	0,02	0,03	2,2
19*	marl	171,0	3000	1900	0,03	0,02	2,4
20*	Sandstones, mudstones, clays	871,0	3600	2300	0,01	0,01	2,6
21*	Granites, biotite gneisses	1471,0	5000	3000	0,01	0,01	2,9

note: * parameters taken on the areas of the Odessa region.

Above (free) records of the accelerograms of the ground were introduced, but the data on the oscillations of the buildings during an earthquake indicate that additional pressure on the ground from the weight of buildings and structures also significantly affect the intensity of seismic ground motion base and the degree of transmission of seismic effects from soil towards the construction (A.Tamrazan, 2003). In this respects many scientists have been recently paying attention to taking into consideration the effect of pressure of constructions on the maximum amplitude of the accelerograms of the ground work oscillations (Ju.Nemchynov, 2008)

Currently, a seismometric station is being founded to assess the response of real buildings (building of Odessa State Academy of Building and Architecture) on seismic effects, taking into account soil conditions. The equipment for recording vibrations on the free surface of the soil is being installed in the basement of the building on the isolated pedestal on the ground work, as well as on the second and eighth floors. Seismic equipment will record the time-synchronized oscillations.



4.4.4 Maps of general seismic zoning

Supplement contains maps of general seismic zoning (GSZ) in Ukraine and Odessa region with periods of recurrence of once every 500 years (Map GSZ-2004-A, Figure 101), 1000 years (Map GSZ-2004-B, Figure 102) and 5000 years (Map GSZ -2004-C, Figure 103) for medium soil conditions and the probability of exceeding the calculated intensity for 50 s 10%, 5% and 1%, respectively.

General seismic zoning map of Odessa region, except maps A, B, C, supplemented maps GSZ-2004-A0 (Figure 104 - 107) for the average return period of 100 years, and the probability of exceeding a given intensity of 39% for 50 years.

Note. Marked on the map OCP 2004 points for the scale that according to macro-seismic MSK-64 scale and DSTU -B - B.1.1 -28:2010 "Scale of seismic intensity".



Project funded by the
EUROPEAN UNION

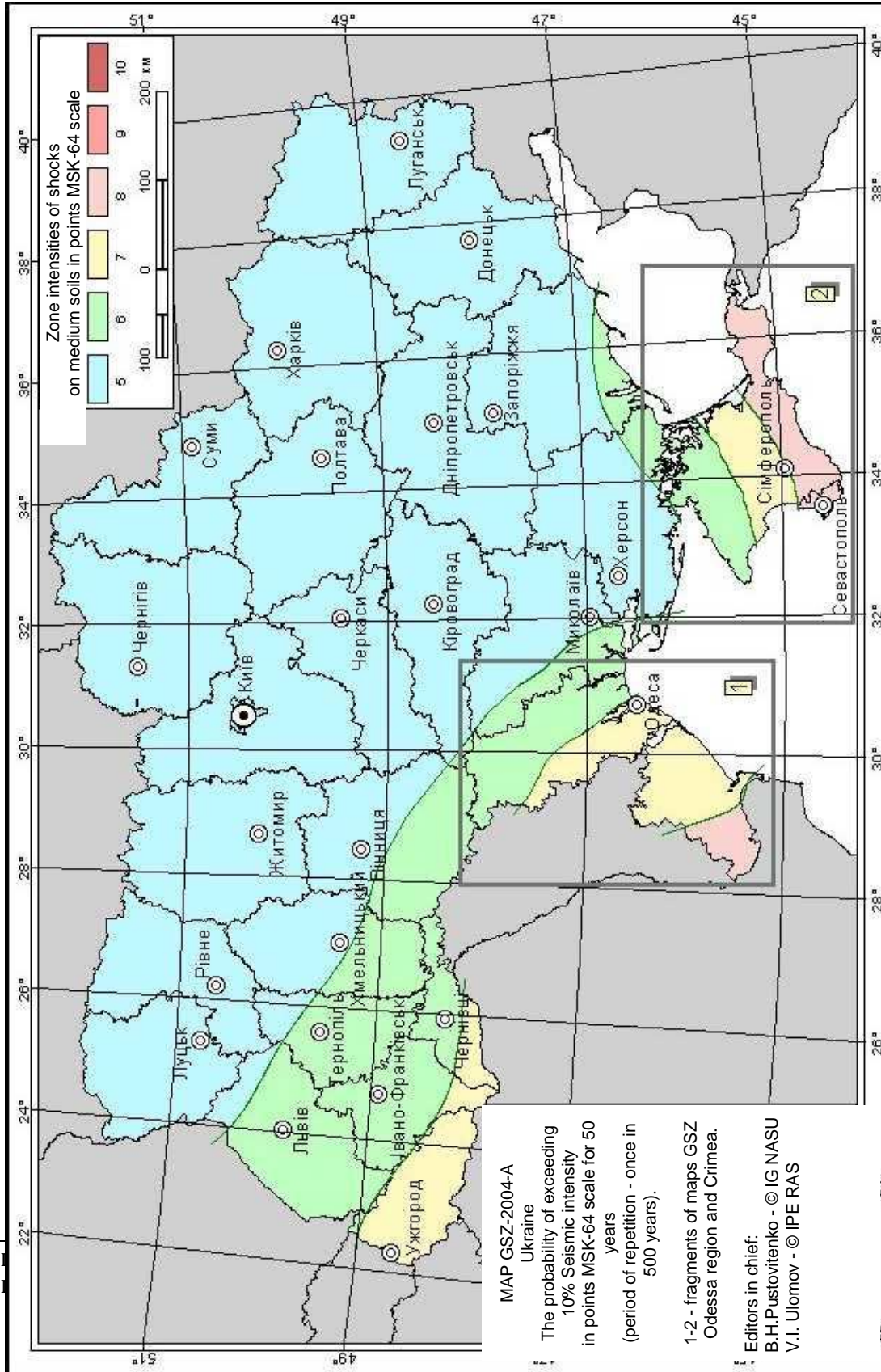


Fig 101– General seismic zoning map GSZ-2004-A in Ukraine



Project funded by the
EUROPEAN UNION

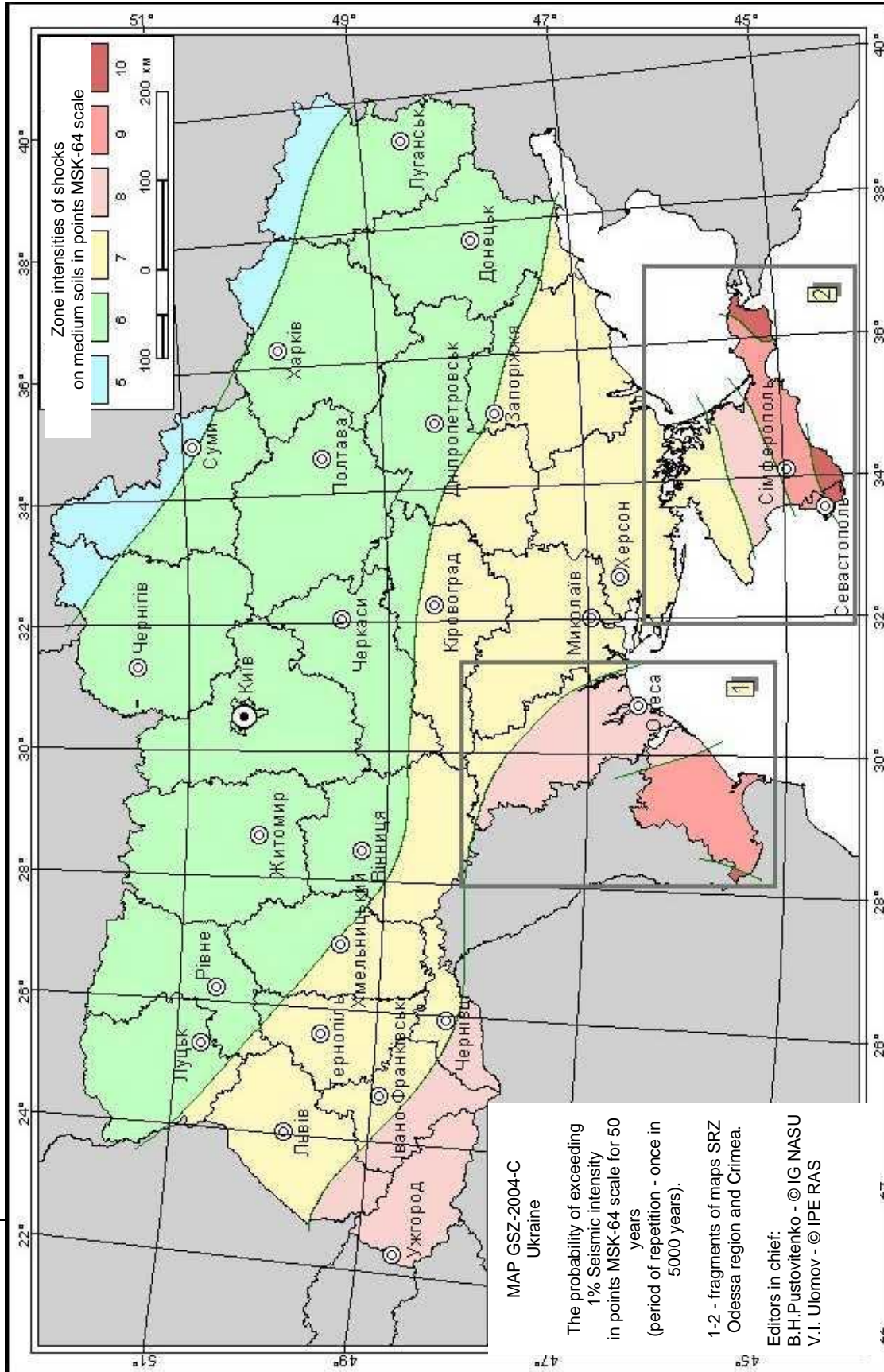


Fig 103– General seismic zoning map GSZ-2004-C in Ukraine



Project funded by the
EUROPEAN UNION

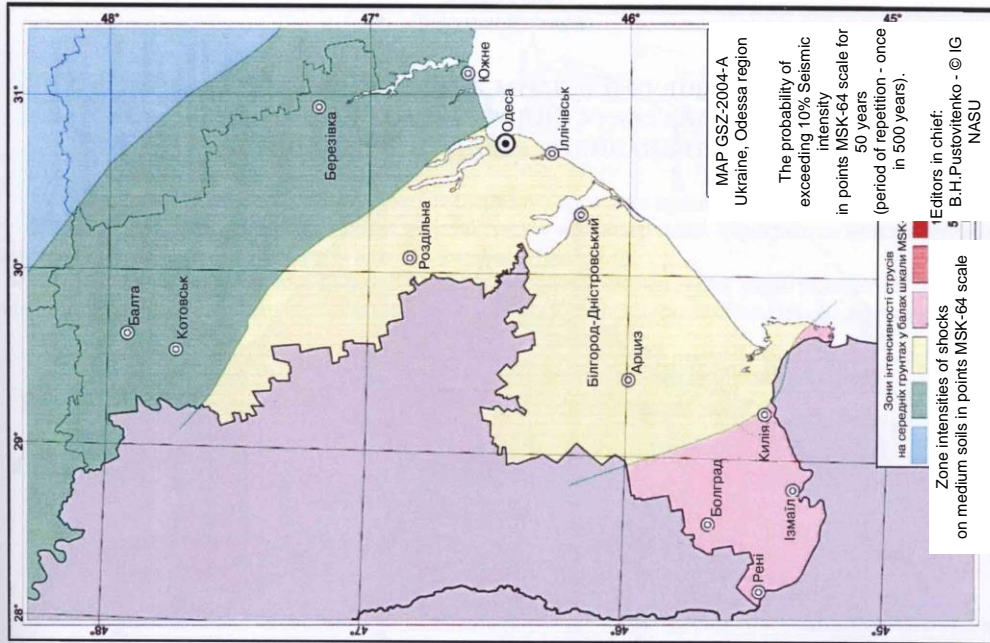


Fig 105– Detail maps GSZ-2004-A.
Odessa region

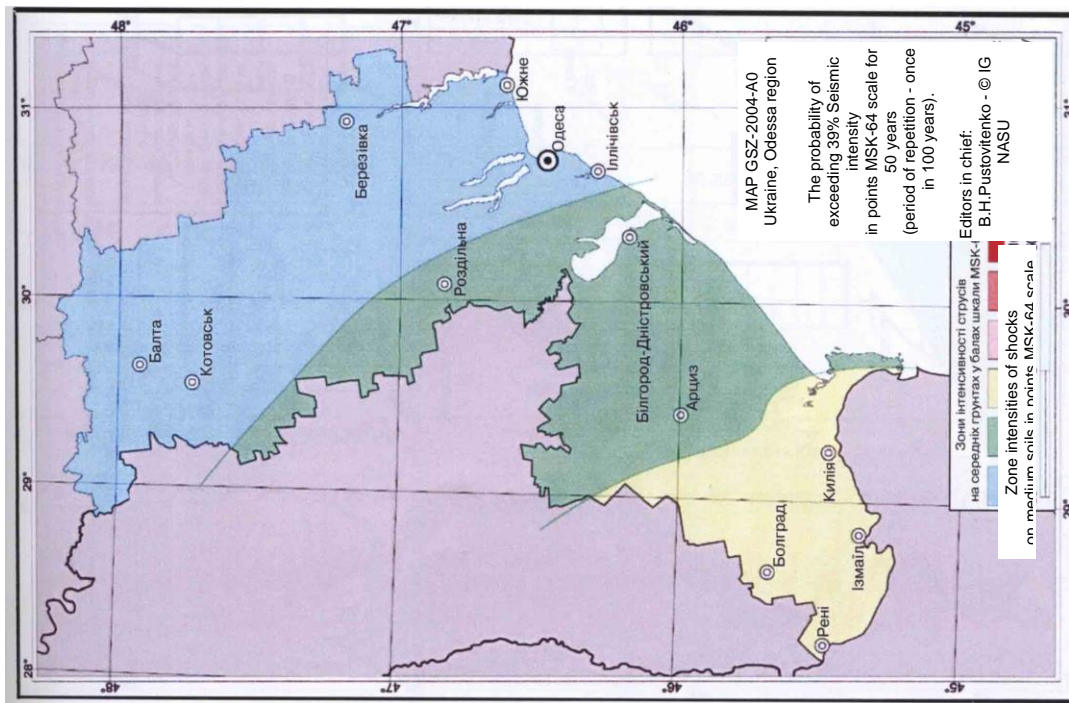
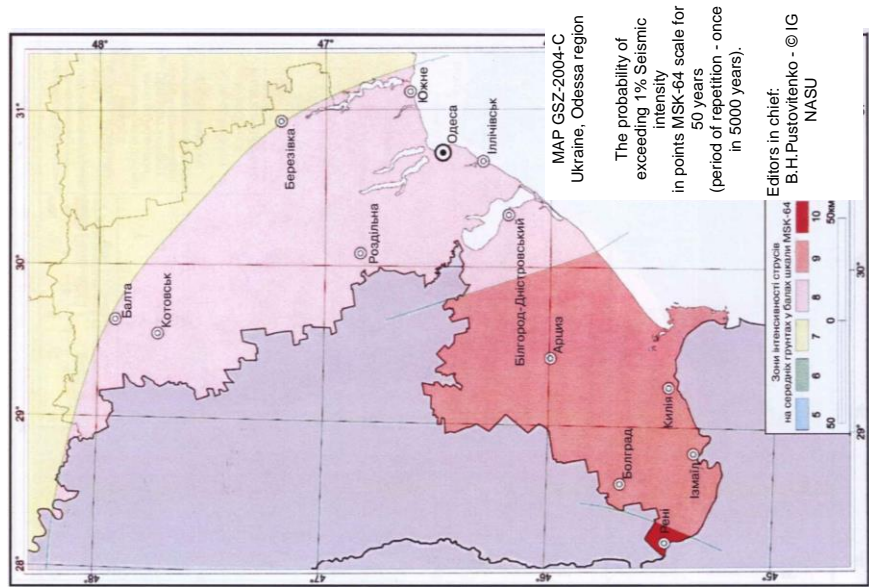


Fig 104– Detail maps GSZ-2004-A0.
Odessa region



Project funded by the
EUROPEAN UNION



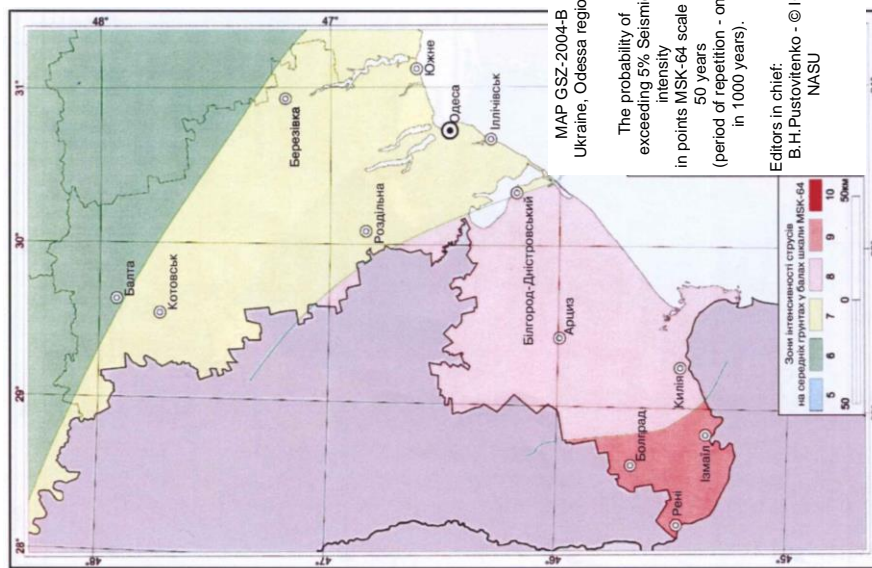
Zone intensities of shocks
on medium soils in points MSK-64 scale

Fig 107– Detail maps GSZ-2004-C.
Odessa region

Fig
106–
Detail
I
man



Project funded by the
EUROPEAN UNION



Zone intensities of shocks
on medium scale in points MSK-64 scale

Title cities of Ukraine	MAP GSZ-2004			Title cities of Ukraine	MAP GSZ-2004		
	A	B	C		A	B	C
Odessa region							
Ananyiv	6	7	8	Krasni Okni	6	7	8
Arciz	7	8	9	Limanske	7	8	8
Balta	6	6 ^{*)}	8	Lubashovka	6	6	7
Berezino	7	8	9	Nikoloevka	6	6	7
Berizovka	6	7	7	Novie Bilyari	6	7	8
Bilgorod-Dnistrovskii	7	7 ^{*)}	8	Ovidiopol	7	7	8
Bilyaivka	7	7	8	Odessa	7 ^{*)}	7	8

Title cities of Ukraine	MAP GSZ-2004			Title cities of Ukraine	MAP GSZ-2004		
	A	B	C		A	B	C
Bolgrad	8	9	9	Radosnoe	6	7	8
Borodino	7	8	9	Reni	8	9	10
Veliko Mykhailivka	7	7	8	Rozdilna	7	7	8
Velikodolinskoe	7	7	8	Savran	6	6	7
Vilkovo	7	8	9	Sarata	7	8	9
Zatishya	6	7	8	Serpneve	7	8	9
Zatoka	7	7	8	Slobodka	6	7	8
Zelinogirske	6	6	7	Suvorove	8	8	9
Ivanivka	6	7	8	Tairove	7	7	8
Izmail	8	9	9	Tarutine	7	8	9
Ilichivsk	7	7	8	Tatarbunari	7	8	9
Kiliya	8 [*])	8	9	Teplodar	7	7	8
Kodima	6	6	7	Frunzivka	7	7	8
kominternivske	6	7	8	Shiryaeve	6	7	8
Kotovsk	6	7	8	Ugne	6	7	8

4.4.5 Potential losses

Research results Ukrainian seismologists convincing evidence that seismic hazard in the Odessa region substantially understated. The probability of occurrence of earthquakes with an intensity of 7 points is quite high.

Table 4.4.7 is a list of destructive earthquakes of Vrancea and the intensity of their manifestations in the major cities of Moldova, Ukraine and Russia.[18]

Table 4.4.7 Destructive earthquakes Romanian Carpathians (Vrancea zone)



Date	Magnitude	Intensity at the epicenter	The intensity of the earthquake in the city					
			Kishinev	Lviv	Chernovtsy	Odessa	Kiev	Moscow
26.10.1802	7,5	9-10	7	4	7	7	5	3
26.11.1829	6,5	8	7		6	6	4-5	-
23.01.1838	7,0	9	7	4-5	6	6	4-5	-
6.10.1908	6,75	8	6	5	6	6	5	-
10.11.1940	7,3	9	7-8	5	6	7	5	4
4.03.1977	7,2	9	6-7	4	5-6	5-6	4-5	3
30.08.1986	7,0	8-9	6	4	5	5	4	-
30.05.1990	6,7	8-9	6	4	5	5	4	3

The risk is also increased, due to the sharp rise in the groundwater, the presence of extensive underground mines, and others.

According to current data, displayed on the new maps of general seismic zoning of Ukraine GSZ-2004, the real seismic risk in some areas of the country is higher than was indicated in the previous regulatory maps of CP-78 and CP-68. With this in mind, some of the buildings and structures in seismic zones may appear insufficiently resistant to earthquakes

Interdepartmental Committee on Scientific and Technological Security of the Council of National Security and Defense of Ukraine, April 3, 2008 decided « **About a condition of seismic safety and development problems of earthquake engineering in Ukraine** ».

There is an urgent need to improve the reliability of life support systems of the population and reduce the risk of emergency situations at the seismic influences. You need to specify the design parameters of seismic risk based on local seismic conditions.

Black Sea shelf, the creation of environmentally hazardous proizvodstv- neteprovodov oil terminals and, against the background of a sharp jump in seismic coast. This makes it necessary to ensure the reliability of offshore structures under the influence of earthquakes and sea.



Project funded by the
EUROPEAN UNION



Commission on technogenic and ecological safety and emergencies at the Odessa oblastnoygosudarstvennoy administration submitted a table 7.

Table 4.4.8 Prediction of possible losses among the population of the Odessa region in the residential sector in the earthquake 01.01.2006.

№	Name of cities and regions	Intensive in points on the MSK-64 scale	Total population.	Number of residential buildings	The total number of destroyed buildings	The degree of the destruction of residential buildings			Losses among the population	
						of them:			common ones	
						completely destroyed	strong	medium	Irreversible	sanitary
								number of people	number of people	
1	Odessa	VI-VII	1002,048	25983	2600	52	468	416	16315	48944
2	Izmail	VIII-IX	79,663	12845	3211	257	385	541	6099	6099
3	Ilichevsk	VI-VII	67,492	937	239	5	41	39	3292	3292
4	Kotovsk	VI-VII	10,263	4455	1899	100	400	560	657	3665
5	Bilgorod-Dnistrovskii	VII-VIII	57,433	6330	950	38	152	304	937	2811
6	Tepلودar	VI-VII	9,484	43					154	463
7	Ugne	VI-VII	25,775						140	419
8	Ananiv region	VI-VII	30,690	18706	2348	94	374	752	503	1509
9	Arciz region	VII-VIII	48,581	14490	2477	277	417	670	1242	3726



Project funded by the
EUROPEAN UNION



10	Balta region	VI-VII	46,059	21982	2740	110	438	876	755	2264
11	Belyaivka region	VI-VII	98,812	30783	3340	67	601	535	1619	4858
12	Berezovski region	VI-VII	34,771	12848	1280	-	-	256	190	570
13	Bolgrad region	VIII-IX	70,968	25606	1890 0	792	1188	1015 2	1809	5428
14	Bilgorod-Dnistrovskii	VII-VIII	60,563	26280	3940	157	631	1261	991	2974
15	Veliko Mykhailivka	VI-VII	31,456	12315	1840	74	294	588	516	1547
16	Ivonovka region	VI-VII	27,885	11283	1273	-	-	254	457	1371
17	Izmail region	VIII-IX	52,979	18238	4560	364	548	2189	1347	4040
18	Kiliya region	VIII-IX	56,031	22049	4100	164	656	1312	1429	4286
19	Kominternov region	VI-VII	67,924	14350	1400	28	252	224	369	1108
20	Kodima region	VI-VII	32,493	17274	2590	104	416	828	534	1602
21	Kotovsk region	VI-VII	29,108	11455	5320	100	400	1928	478	1433
22	Krasni Okni region	VI-VII	21,522	12108	1804	72	290	577	355	1064
23	Ovidiopol region	VI-VII	63,759	11279	1200	25	215	192	1033	3099
24	Lubashovka region	VI-VII	32,088	15530	1550	-	-	310	175	526
25	Nikolaev region	VI-VII	18,501	8302	830	-	-	166	101	304
26	Razdelnaya region	VI-VII	55,846	12589	1250	50	200	400	912	2736

27	<i>Reni region</i>	<i>VIII-IX</i>	38,611	11347	5482	258	387	2902	985	2956
28	<i>Savransk region</i>	<i>VI-VII</i>	21,015	11265	1120	22	202	179	115	345
29	<i>Sarata region</i>	<i>VII-VIII</i>	48,074	16309	2400	96	384	768	1225	3676
30	<i>Tarutin region</i>	<i>VII-VIII</i>	43,201	15143	3700	296	444	1775	1103	3309
31	<i>Tatarbunari region</i>	<i>VII-VIII</i>	40,262	14866	2220	89	355	710	660	1980
32	<i>Frunzjvka region</i>	<i>VI-VII</i>	20,348	9238	1300	52	208	416	334	1002
33	<i>Shiryaeve region</i>	<i>VI-VII</i>	28,535	11854	1300	58	202	426	468	1405
34	Total in regions		2372,2 4	45808 2	8916 3	380 1	1054 8	3250 6	4729 9	12481 1

REFERENCES

1. B. Pustovitenko , V. Kulchitsky, A. Pustovitenko “New data on seismic danger of the city of Odessa and Odessa region”, *Construction designs. Mechanics of soil, geotechnics, foundation engineering.* – 2004 .vol. 61. – pp. 388-397
2. M. Baysarovich, O. Kendzera, B. Pustovitenko, O. Safronov, V. Tregubenko, geodynamics and seismicity (maps) // Atlas “ The deep structure of the lithosphere and environment Ukraine ”. – Kyiv: IGS of Ukraine, "Heohrafika", 2002. - P. 36-42.
3. A. Nikonov Stronger in eastern Europe Carpathian earthquake October 26, 1802 - new materials and evaluation. // Reports of the Russian Academy of Sciences. - №1, t. 347, 1996. - S.99-102.
4. E. Sagalova “To a question of seismic micro zoning of the territory of Bukovina” - Seismicity of Ukraine.– 1969.–pp.70–81.
5. S. Evseev “Intensity of earthquakes of Ukraine” - Seismicity of Ukraine– 1969.– pp. 32-55.
6. A. Drumea, T. Ustinova, J.Shchukin Problems of tectonics and Seismology Moldova. - Vol. 2. Chisinau: Map Moldoveniaske, 1964. - 119
7. Earthquakes in the USSR in 1977. - M .: Nauka, 1979 - 360c.



8. Earthquakes in the USSR in 1986 . - M.: Nauka, 1989. - 364 c.
9. B. Pustovitenko , V. Kulchitsky, A. Pustovitenko “New data on seismic danger of the city of Odessa and Odessa region”, *Construction designs. Mechanics of soil, geotechnics, foundation engineering.* –2004 .vol. 61. – pp. 388-397
10. A.Kendzera, S. Verbytskyy, Ju. Verbytskyy, O. Verbytska, K.Yegupov, V.Yegupov, S. Kovalchuk, R. Prokopec “ Implementation of requirements of DBN B.1.1-12:2006 concerning parameters of seismic influences for aseismic design in Odessa” - *Construction designs.*- - 2008.- vol.69.-pp. 45-55
11. A. Nikonov , K. Nikonov About seismic hazard of Delta Dunai river according to the historical earthquakes. // *Problems of engineering seismology.* - 1990, vyp.31. - S.127-134.
12. N. Stepanenko, N.Simonov, I. Alekseev Macroseismic date of earthquakes Carpathian region in 2004. *Seismological Bulletin of Ukraine for 2004. SPC "ECOS-Hydrophysics."* - Sevastopol. - 2006. - S.114-119.
13. The natural conditions of the Dunai River and seaside Snake Island: the current state of the ecosystem (edited by V. Ivanov, SV Goshovsky) NASU. - Sevastopol, 1999 - 268 p.
14. B. Pustovitenko, L.Dubinko “Macroseismic effect manifestation of strong earthquakes”, UKRNIITI №1764, Yk87, 1987, 23 c
15. K.Yegupov, A. Bondarenko, V.Yegupov “Instumentalny records for an assessment of seismic danger of the Odessa region” - - *Bulletin of OSACA – Odessa* 2013.- vol.49.- pp.143-149
16. DBN B.1.1-12:2006. Construction in seismic regions oa Ukraine. The official version . – The Ministry of regional development, construction and housing of Ukraine, 2006. – 82 p.
17. A.Tamrazan, R.Atabekjan “Influence of external pressure of constructions on extent of transfer of seismic influences” - *Researches and experience. Housing construction* № 6/2003.
18. Ju.Nemchynov “Seismic stability of buildings and constructions”. - 2008. –P. 480.



4.5 ROMANIA

4.5.1 Seismic zonation

For probabilistic hazard assessment purposes we used the seismic zonation represented in the Figure 108 that includes both normal and intermediate-depth earthquakes from the Black Sea and the South Eastern part of Romania.

In order to have the most reliable and homogeneous seismic dataset, we compiled the catalogues available at the European scale covering historical and modern instrumental seismicity until present days (ANSS-Advanced National Seismic System-USA, NEIC - National Earthquake Information Centre, World Data for Seismology Denver-USA, ISC-International Seismological Centre-UK) and the catalog of the National Institute for Earth Physics (Romplus catalogue, Oncescu et al., 1999, updated)

The seismic zonation of the Eastern part of Romania and the Black Sea Area was obtained using the distribution map of earthquakes and the map of the zones with active tectonics (Radulian et al., 2000;



Moldovan, 2008, 2013). We took into consideration various past seismic zonation studies carried out in the framework of different projects (SHARE project - www.share-eu.org, MARINEGEOHAZARD project - www.geohazard-blacksea.eu, BIGSEES project - infp.infp.ro/bigsees/default.htm). The seismic source configuration in the Figure 1 is a synthesis of all the previous approaches.

The present configuration of the potential seismic sources contains fifteen crustal and one intermediate-depth seismic sources: Vrancea intermediate-depth (VRI), Vrancea normal (VN), Barlad Depression (BD), Predobrogean Depression (PD), Intramoesian Fault (IMF), North Dobrogea (BS1), Central Dobrogea (BS2), Shabla (BS3), Istanbul (BS4), North Anatolian Fault (BS5), Georgia (BS6), Novorossjsk (BS7), Crimea (BS8), West Black Sea (BS9) and Mid Black Sea (BS10).

The input parameters describing the seismic sources requested for a probabilistic evaluation of seismic hazard are given in Table 4.5.1. The attenuation relations of ground motion parameters (PGA and macroseismic intensities) obtained by Moldovan et al. in a series of studies (1999, 2007, 2008) were adopted for our investigation.



Project funded by the
EUROPEAN UNION

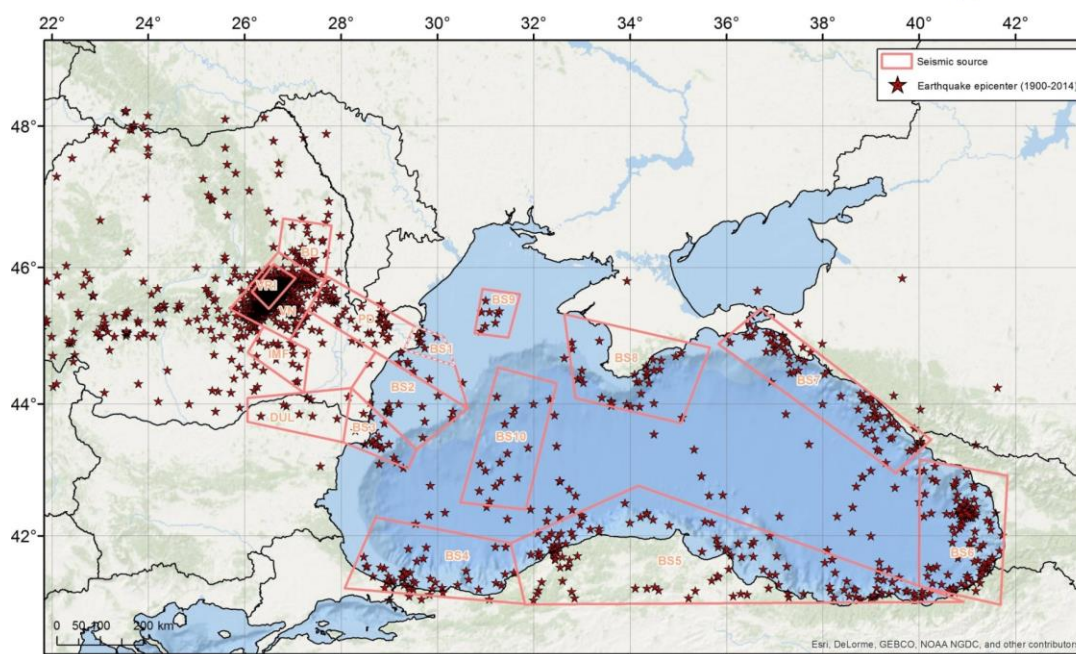


Fig 108. The seismic zonation of the Eastern part of Romania and the Black Sea Area

Table 4.5.1 Parameters needed for a probabilistic hazard assessment: geographical distribution, average depth, activity rate and Gutenberg Richter parameters, etc.

Seismic Sources	Coordinates		Average depth (km)	M min (Mw)	M max (Mw)	b	I min	I max	bi	$\beta_{i=}$ $=b \ln 10$	Seismic activity rate
VRI	45.65	26.15	130	5.0	7.9	0.85	4.0	10	0.48	1.12183	1.762380
	45.4	26.5									
	45.85	27.05									
	46.05	26.6									
VN	45.44	25.65	30	3.0	5.9	0.95	2.5	7.0	0.6	1.38155	0.514526
	46.22	26.70									
	45.75	27.90									
	44.90	27.00									
BD	46.22	26.70	10	2.5	5.5	0.75	2.0	6.5	0.49	1.12826	1.534712
	46.7	26.8									
	45.79	27.66									
PD	45.23	27.60	10	3.0	5.5	0.81	3.0	6.5	0.53	1.22405	0.360254
	45.75	27.90									
	45.2	29.3									
	44.67	28.74									
IMF	44.76	26.06	15	3.0	5.4	0.46	3.0	6.5	0.3	0.69077	0.034600
	44	27.36									



Project funded by the
EUROPEAN UNION



	45.14	26.39									
	44.8	27.33									
DUL	44.24	28.22	15	3.0	7.2	0.46	3.0	9.0	0.3	0.69077	0.028000
	43.42	28.05									
	44.00	26.00									
	43.75	26.20									
	45.11	30.55									
BS1	44.56	30.36	33	3.0	3.5 Mb=4.7	0.81	2.5	3.5	0.53	1.22405	0.386363
	44.9	29									
	45.55	29.6									
	44.24	28.22									
BS2	44.9	29	11	3.0	5.0	0.65	2.5	5.5	0.43	0.99011	0.118644
	44.48	30.69									
	43.77	30.57									
	43.32	29.56									
	44.24	28.22									
BS3	43.32	29.56	16.4	3.0	7.2	0.32	2.5	9.0	0.21	0.48354	0.165137
	43.03	29.39									
	43.42	28.05									
	41.19	28.07									
BS4	42.28	28.72	22.1	3.0	6.7	0.53	2.5	8.0	0.35	0.8059	0.47761
	41.89	31.52									
	40.94	31.82									
	40.93	31.82									
BS5	41.89	31.52	14.8	3.0	6.1	0.61	2.5	7.5	0.40	0.92103	0.740741
	42.77	34.17									
	40.97	40.92									
	41.22	39.99									
BS6	43.17	40.01	13.5	3.0	5.5	0.59	2.5	6.5	0.39	0.89800	1.039215
	42.92	41.83									
	40.93	41.69									
	44.89	35.83									
BS7	45.40	36.70	20.8	3.0	5.2	0.75	2.5	6.0	0.50	1.15129	0.59091
	43.46	40.24									
	42.96	39.52									
	44.09	32.86									
BS8	45.32	32.63	22.8	3.0	6.5	0.38	2.5	8.0	0.25	0.57564	0.25301
	44.83	35.65									
	43.72	35.06									
	45.05	30.77									
BS9	45.69	30.94	14.8	3.0	4.9	0.61	2.5	5.5	0.40	0.9163	0.19512
	45.62	31.71									
	44.98	31.47									
	42.51	30.48									
BS10	44.54	31.26	26.9	3.0	3.9	0.72	2.5	4.0	0.48	1.10524	0.25581
	44.30	32.48									
	42.40	31.84									

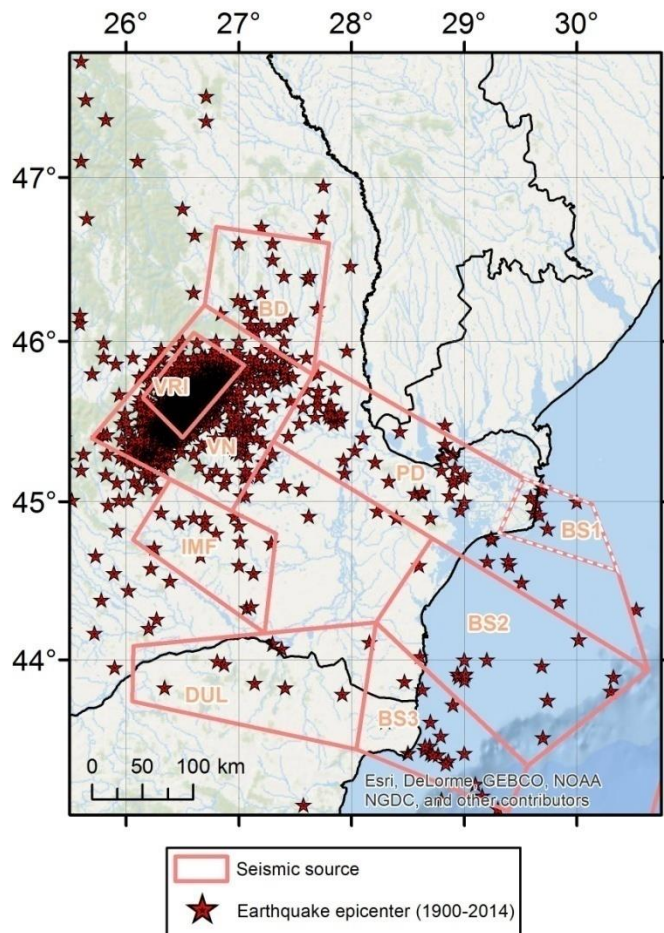


Fig 109 Seismic sources selected for this study together with the associated seismicity. We plotted epicenters for $M_w > 3.5$ for the inland sources and $M_w > 3.0$ for the marine sources.

From the total number of seismic sources we selected for hazard estimations nine sources (marked with red and blue in Table 1 and presented in Figure 109) since the effects produced by the other seven sources in our study area are negligible (Figure 110).

The parameters of the Gutenberg-Richter distribution (a, b) are compiled for each source. Also we mapped the b values to emphasize the zones with low and high stress, for different time intervals.



Fig 110. The SciNetNatHaz implementation area for the Romanian Partner is marked with a black rectangle

Vrancea intermediate source - vi

Vrancea subcrustal zone represents a complex and particular seismic source, situated in a region of continental convergence of at least three major tectonic units: East-European Plate, Intra-Alpine Plate and Moesian Plate (Constantinescu et al., 1976). The highest seismic activity recorded in Romania is concentrated in a depth range between 60 and 180 km, in a narrow vertically descending high-velocity body. The focal volume of the Vrancea zone is particularly restraint in horizontal plane, where 3-5 major earthquakes ($M_w > 7.0$) are recorded per century. The seismic moment rate is high, approximately 1.2×10^{19} Nm/year, what makes the Vrancea to be the most concentrated seismic source in Europe.

The focal mechanisms of all the major intermediate-depth earthquakes are of reverse fault type, with T axis (tension) almost vertical and P axis (compression) almost horizontal. For the largest events the rupture plane is quasi-similar, NE-SW oriented. The reverse faulting mechanism is characteristic for about 90% of the Vrancea events, independent of magnitude. A second type of mechanism which is observed in Vrancea is characterized still by reverse faulting, but with the rupture plane oriented perpendicularly relative to the previous case, NW-SE respectively (Enescu, 1980; Enescu și Zugarăvescu, 1990; Oncescu și Trifu, 1987; Radulian et al., 2000).

The maximum instrumental magnitude is $M_w = 7.7$ ($M_{GR}=7.5$) for the event of 10.11.1940. The maximum estimated magnitude is attributed to the historical earthquake of 14.10.1802: $M_w = 7.9$ ($M_{GR}=7.7$). The computation in the present study are performed for the catalogue starting in 1900. Therefore, we prefer to consider as maximum magnitude (Table 1) the instrumental magnitude $M_w = 7.7$ recorded in 1940. **The seismic activity rate for earthquakes with $5.0 < M_w < 7.7$ is $\nu_0 = 1.762380$ events/year.**

The frequency-magnitude distribution for VI, determined from the 1900-2014 earthquake catalogue, for different magnitude intervals, is plotted in the Figure 111.

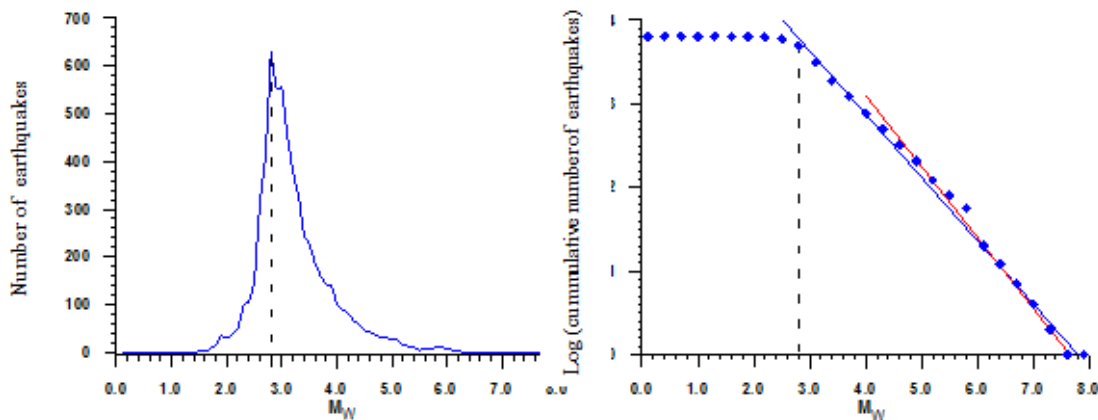


Fig 111. The frequency-magnitude distribution for VI zone: a) non-cumulative; b) cumulative; $M_w \geq 2.8$ -blue line, $M_w \geq 5.0$ -red line

Two regression lines are computed for the decay of the cumulative distribution, for two threshold magnitudes, $M_w = 2.8$ and $M_w = 5.0$:

$$VRI-1900, M_c=2.8, \quad \log N_c = -(0.76 \pm 0.01)M_w + (5.90 \pm 0.08), \quad \text{blue line} \quad (1)$$

$$R=0.997, \sigma=0.09$$

$$VRI-1900, M_c=5.0, \quad \log N_c = -(0.85 \pm 0.02)M_w + (6.49 \pm 0.14), \quad \text{red line} \quad (2)$$



$$R=0.997, \sigma=0.06$$

The frequency-epicentral intensity distribution (needed in the hazard assessment program) was obtained from equation (2) and $M_w = 0.58I_0 + 2.08$ (Radu, 1979):

$$\lg N_{cum} = -0.493 \cdot I_0 + 4.722 \quad (3)$$

The used intensity interval is [5.0, 10.0] and $a= 4.722$, $b=0.4872$. The β_i value was computed from the intensity - frequency distribution, using the relation:

$$\beta_i = b \ln 10 \quad (4)$$

We obtained: $\beta=0.4872 \cdot 2.3026= 1.12183$.

Vrancea crustal earthquakes (vn)

The seismic activity in the Vrancea in the crustal domain (VN) is located in front of the South-Eastern Carpathians arc, spread over a stripe area delimited to the north by the Peceneaga-Camena fault and to the south by the Intramoesian fault. The seismicity is more diffuse than for the subcrustal source and consists only of moderate-magnitude earthquakes ($M_w < 6.0$) generated frequently in clusters, localized in the eastern part (seismic sequences of Râmnicu Sarat area) and in the northern part (seismic swarms in the Vrincioaia area and seismic sequences north of Focșani). The catalogue contains only two earthquakes with magnitude above 5.0: one occurred on March 1, 1894 of $M_w = 5.9$, with magnitude estimated from historical information (possibly overestimated), and the most recent one, of November 22, 2014, with $M_w = 5.7$.

The rate of the seismic moment release, $M_o = 5.3 \times 10^{15}$ Nm/year, is four orders of magnitude less than the moment rate characteristic for the Vrancea intermediate-depth domain. The analysis of the fault plane solutions shows a complex stress field in the Vrancea crust, like a transition zone from the compressional regime at subcrustal depths to extensional regime characteristic for the entire Moesian platform. The largest earthquakes, for which the fault plane solutions could be relatively well constrained, are the main shocks of the sequences occurred between 1983 and 2014.

The frequency-magnitude distribution for VN, determined from the 1900-2014 earthquake catalogue, for different magnitude intervals, is plotted in the Figure 112 and the equations for the regression lines are given below (equations 5 and 6).

$$EV- 1900, M_c=2.2-5.5, \quad \log N_c=-(1.02 \pm 0.04)M_w + (5.45 \pm 0.23), \quad \text{green line} \quad (5)$$

$$R=0.99, \sigma=0.16$$

$$EV- 1900, M_c=3.0-5.5, \quad \log N_c=-(0.95 \pm 0.05)M_w + (5.10 \pm 0.21), \quad \text{blue line} \quad (6)$$

$$R=0.98, \sigma=0.14$$

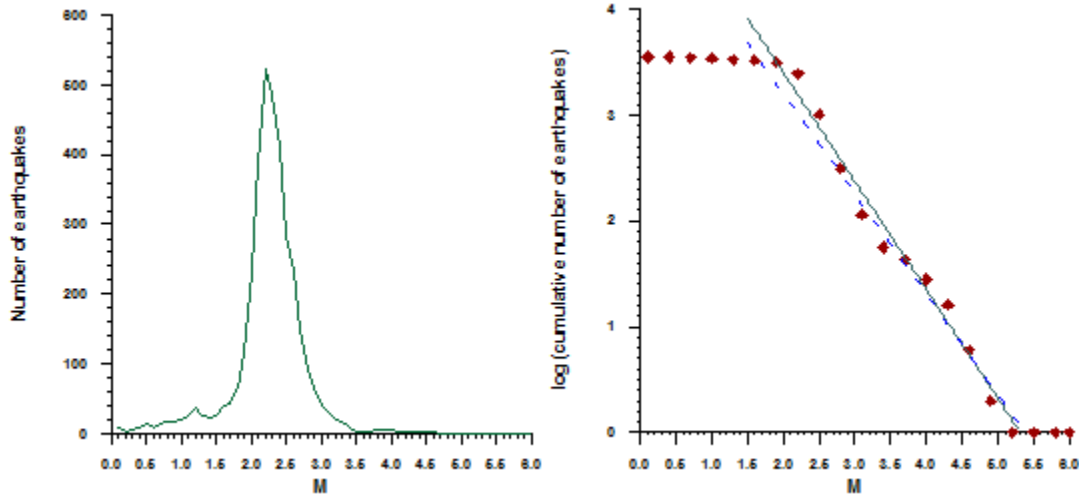


Fig 112. The frequency-magnitude distribution for VN zone: a) non-cumulative; b) cumulative

The frequency-epicentral intensity distribution obtained from Eq. 6 and $M_w = 0.66 I_0 + 1.23$ (Radu, 1979) is: $\lg N_{cum} = -0.6 * I_0 + 3.98$. From the above equations we obtain: $a_1 = 3.98$ and $b_1 = 0.6$ and $\beta = 1.38155$.

Barlad depression (bd)

Barlad Depression (BD), situated NE of the Vrancea zone, is characterized only by moderate size events (only four shocks with $M_w > 5.0$, but not exceeding $M_w = 5.6$). Having in mind that from seismotectonic point of view the Barlad Depression belongs to the Scythian platform as well as the Predobrogean Depression (Mutihac and Ionesi, 1974), we considered for both zones the same maximum magnitude, respectively the maximum observed one, $M_w = 5.6$.

The frequency-magnitude distribution for **BD**, determined from the 1900-2014 earthquake catalogue, for different magnitude intervals, is plotted in Figure 113, and equations of the regression lines are given below (relations 7 and 8).

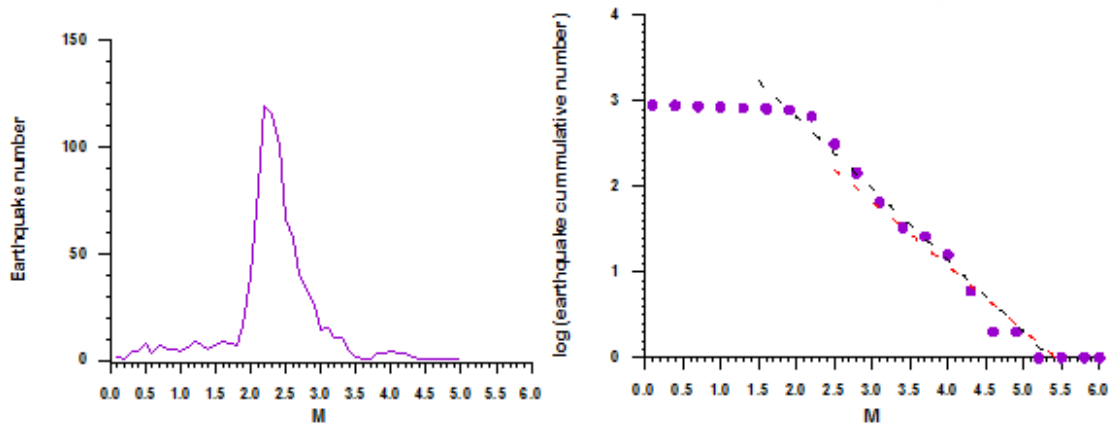


Fig 113. The frequency-magnitude distribution for BD zone: (a) non-cumulative; (b) cumulative

$$BD-1900 \quad M_c=2.2-5.8, \quad \log N_c=-(0.84 \pm 0.05)M_w + (4.49 \pm 0.19) \quad (\text{black line}) \quad (7)$$

$$R=0.98, \quad \sigma=0.18$$

$$BD-1900 \quad M_c=3.1-5.8, \quad \log N_c=-(0.75 \pm 0.07)M_w + (4.08 \pm 0.30) \quad (\text{red line}) \quad (8)$$

$$R=0.97, \quad \sigma=0.18$$

The frequency-epicentral intensity distribution obtained from Eq. 8 and $M_w=0.66 I_o+1.23$ (Radu, 1979) is: $\lg N_{cum} = -0.495 \cdot I_o + 3.227$. From the above equations we obtain: $a = 3.227$ and $b = 0.495$ and $\beta = 1.12826$.

Predobrogean depression – pd

Predobrogean Depression (PD) zone belongs to the southern margin of Predobrogean Depression. It follows the alignment of the Sfantul Gheorghe fault. Only moderate-size events are observed ($M_w < 5.3$) clustered especially along Sfantul Gheorghe fault. The fault plane solutions reflect the existence of the extensional regime of the deformation field. In our opinion this consistently reflects the affiliation of the Predobrogean Depression to the Scythian platform tectonic unit.

The rate of the seismic moment release is $M_o = 1.8 \cdot 10^{15} \text{ Nm/year}$. The maximum observed magnitude for the Predobrogean Depression crustal zone is $M_w = 5.3$, assigned to the event occurred on *February 11, 1871*. The seismic activity for events with $M_w > 3.0$ is $v_0 = \text{no. of seismic events}/T(\text{years}) = 0.36$ seismic events/year. Considering that from seismotectonic point of view the Predobrogean Depression belongs to the Scythian platform as well as Barlad Depression we considered the observed maximum magnitude for both zones, $M_w = 5.5$

For **Predobrogean Depression** zone the frequency-magnitude distributions, estimated for different magnitude intervals are presented in Figure 114, and relations (9 - 12):

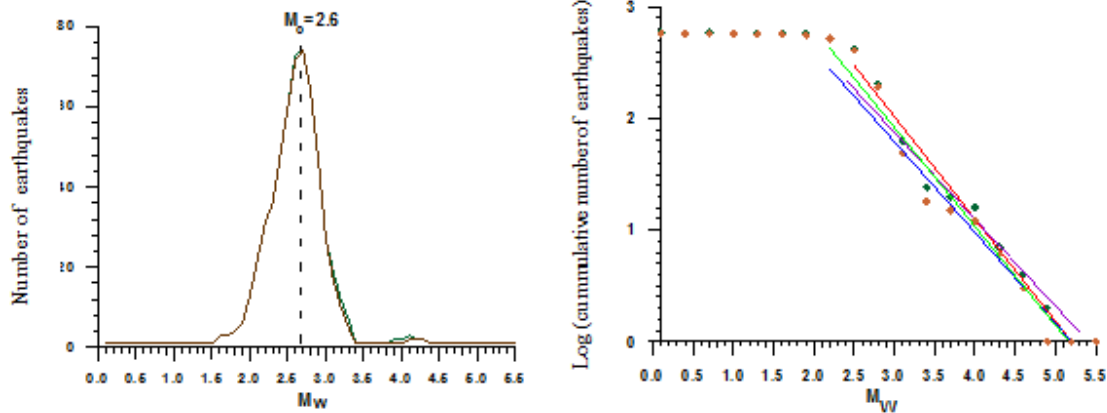


Fig 114. The frequency-magnitude distribution for PD zone: (a) non-cumulative; (b) cumulative

$$PD\text{-all catalogue } M_c=2.5, \quad \log N_c = -(0.92 \pm 0.05)M_w + (4.76 \pm 0.20) \text{ red line} \quad (10)$$

$$R=0.98, \sigma=0.13$$

$$PD\text{-all catalogue } M_c=2.9, \quad \log N_c = -(0.78 \pm 0.05)M_w + (4.21 \pm 0.19) \text{ purple line} \quad (11)$$

$$R=0.98, \sigma=0.12$$

$$PD\text{-1900 } M_c=2.5, \quad \log N_c = -(0.89 \pm 0.06)M_w + (4.57 \pm 0.27) \text{ green line} \quad (12)$$

$$R=0.97, \sigma=0.2$$

$$PD\text{-1900 } M_c=2.9, \quad \log N_c = -(0.81 \pm 0.05)M_w + (4.23 \pm 0.25) \text{ blue line} \quad (13)$$

$$R=0.97, \sigma=0.16$$

The **frequency-epicentral intensity distribution** obtained from equation (13) and $M_w=0.66 I_o+1.23$ (Radu, 1979) is: $\lg N_{cum} = -0.5346 \cdot I_o + 3.234$. The resulted Gutenberg-Richter parameters are: $a = 3.234$ and $b = 0.5346$ and $\beta = 1.22405$ (Table 1).

Intramoesian fault and dulovo zone- imf-dul



The Intramoesian fault (IMF) crosses the Moesian platform in a SE-NW direction, separating two distinct sectors with different constitution and structure of the basement. Although it is a well-defined deep fault, reaching the base of the lithosphere (Enescu and Enescu, 1993), and extends southeast to the Anatolian fault region (Sandulescu, 1984), the associated seismic activity is scarce and weak. Geological and geotectonic data indicate only a relatively small active sector in the Romanian Plain, situated to the NE from Bucharest.

The geometry of the Intramoesian fault source and the distribution of the earthquakes with $M_w \geq 3.0$ occurred between 1892 and 2001 (30 events) are presented in Fig. 108. The magnitude domain of earthquakes is $M_w \in [3.0, 5.4]$. The maximum magnitude was recorded in *January 4, 1960* ($M_w = 5.4$) in the central part of the Romanian Plain.

The seismic activity for events with $M_w > 3.0$ is $v_0 = \text{no. of seismic events}/T(\text{years}) = 0.034600$ seismic events/year.

A significant increase of seismicity is observed in the *Dulovo* (DU) zone and *Shabla* zone (BS3, NE Bulgaria), where an earthquake with an estimated magnitude of $M_w = 7.2$ occurred in 1901. The focal depth, whenever it can be constrained, has relatively large values ($h \sim 35$ km), suggesting active processes in the lower crust or in the upper lithosphere.

Fig. 108 presents the geometry of these two sources located in Bulgaria and the distribution of the earthquakes with $M_w \geq 3.0$ occurred between 1892 and 2001 (20 events). The magnitude domain of earthquakes is $M_w \in [3.0, 7.2]$. We assumed the same maximum magnitude ($M_w = 7.2$) for both sources. The greatest magnitudes are attributed to the historical earthquakes of October, 14, 1892 ($M_w = 6.5$) and March, 31, 1901 ($M_w = 7.2$), while no event with magnitude greater than 5 was reported after 1950 since the instrumental earthquake monitoring has become operational.

The seismic activity for events with $M_w > 3.0$ is $v_0 = \text{no. of seismic events}/T(\text{years}) = 0.028000$ seismic events/year for Dulovo.

The frequency-magnitude distribution for **Intramoesian fault - Dulovo crustal sources**, determined for the magnitude interval [4.5, 7.2], is presented in relation (14) and plotted in Figure 115, with red line. The green and blue lines are for smaller threshold magnitudes (2.6 and 3.0).

$$\text{DULIMF-1900 } M_c=4.5, \quad \log N_c = -(0.46 \pm 0.02)M_w + (3.21 \pm 0.10) \text{ red line} \quad (14)$$

$$R=0.98, \sigma=0.07$$

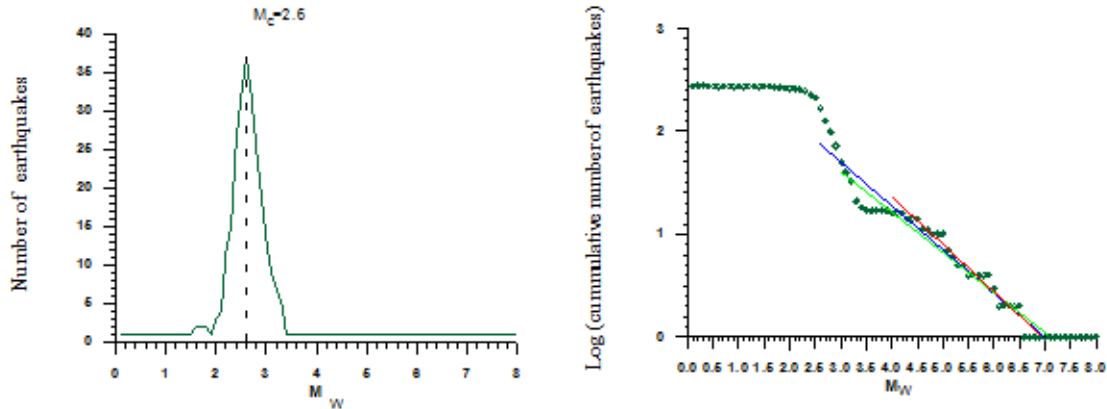


Fig 115. The frequency-magnitude distribution for IMF and DUL zone: (a) non-cumulative; (b) cumulative.

The frequency-epicentral intensity distribution obtained from Eq. 14 and $M_w = 0.66 I_0 + 1.23$ (Radu, 1979) is: $\lg N_{cum} = -0.3 \cdot I_0 + 2.6442$. From the above equations we obtain: $a_i = 2.6442$ and $b_i = 0.3$ and $\beta = 0.69078$ (Table 4.5.1).

Black sea seismic source no.1. north dobrogea – bs1

The earthquakes in the North Dobrogea are associated to the prolongation of Peceneaga-Camena, Sf. Gheorghe and Sulina Faults. Some of the earthquakes belong to the Lacu Rosu fault as well. The maximum observed magnitude for 1967-2007 period in North Dobrogea was $m_b = 4.7$ (7 July 2005). Applying the practice of increment on the maximum observed magnitude we obtain the expected value of the maximum possible magnitude to be $m_b = 5.2 / M_w = 4.0$ with an error value of ± 0.1 . The average depth is **33 km**. For seismic hazard purposes the minimum magnitude was considered $m_0 = 3.0$ (M_w). The seismic activity $v_0 = \text{no. of seismic events} / T(\text{years}) = 0.425$ seismic events/year. The Gutenberg-Richter values are assumed to be the same as the values of PD zone, because BS1 is included in PD.

Black sea seismic source no. 2. central dobrogea – bs2

Seismic source cover all the seismic events occurred within 543-2014 time interval. The earthquakes in this area are associated to the prolongations of Capidava – Ovidiu fault and Horia – Pantelimonul de Sus fault in the Black sea shelf. The 118 years catalogue (1892-2010), contains 336 earthquakes with $M_w > 0.5$, but only 14 events with $M_w \geq 3$. In this area there are numerous active quarries which disturb in a way the local seismicity caused by tectonic events in the low magnitude range (M_w below 2). The maximum observed magnitude in Central Dobrogea was $M_w = 5$ (12.12.1986). Applying the practice of increment on the maximum observed magnitude, the expected value of the maximum possible magnitude is considered to be $M_{w,max} = 5.2$ with an error value of ± 0.1 . For Central Dobrogea, the minimum magnitude was considered $m_0 = 3.0$ (M_w). The seismic activity $v_0 = \text{no. of seismic events} / T(\text{years}) = 14$ seismic events / 118 years = **0.118644** seismic events/year. The average depth is **11km**.

The Gutenberg-Richter frequency-magnitude distribution for S2, determined for magnitudes M_w between 3.0 and 5.0 intervals, is presented in relation 15 and plotted in Figure 119.

$$\log N_c = -(0.65 \pm 0.06)M + (3.15 \pm 0.25), \quad 3.0 < M < 5.0 \quad (15)$$

$$R=0.98, \sigma=0.10$$

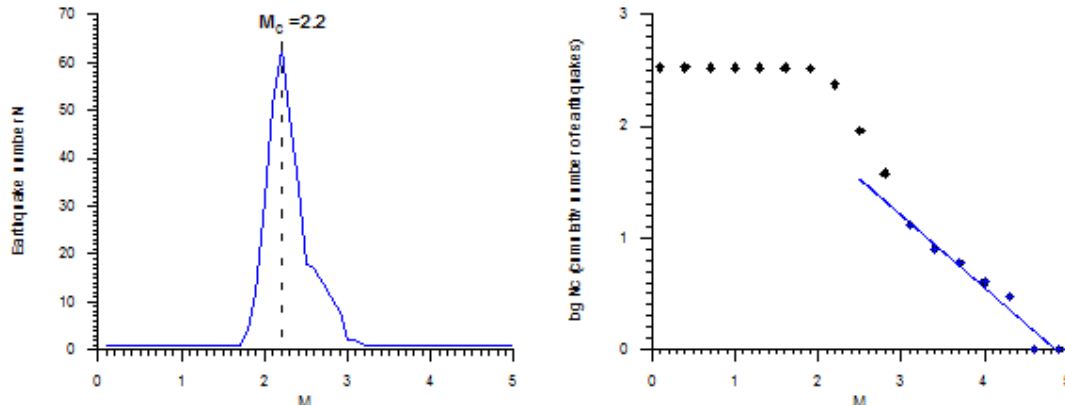


Fig 116. The frequency-magnitude relations for BS2 with $M_w \geq 3.0$; a) non-cumulative; b) cumulative

The frequency-epicentral intensity distribution obtained from Eq. 2 and $M_w = 0.66 I_0 + 1.23$ (Radu, 1979) is: $\lg N_{cum} = -0.5346 I_0 + 3.234$. From the above equations we obtain: $a_i = 2.3505$ and $b_i = 0.429$ and $\beta = 0.99011$ (Table 4.5.1).

Black sea seismic source no.3. – shabla – bs3

The Shabla seismic area, located in Bulgaria, belongs from tectonic point of view to the south edge of Moesian Platform. The earthquakes recorded in the Shabla – Cap Kaliakra area have the foci located along a NE-SW alignment. This active tectonic area is the north-east border of major crustal foci which is developed collateral by Black Sea, with NE-SW direction and which sinks in Burgas area. The foci of Shabla source have limited development, the active sector having 20-25 km length with 15 earthquakes of $M_w \geq 4$. The distribution of epicenters marks the coupling between existent structural lines in the Shabla area, where the powerful earthquake of magnitude 7.2 occurred on 31.03.1901. For seismic hazard assessment we used from a 113-year catalogue (1901-2014), containing 37 earthquakes with $M_w > 1.1$, only 19 events with $M_w > 3.0$ (Table 4). The average depth is **16.4 km**. The minimum magnitude was considered $m_0 = 3.0$ (M_w). Seismic activity $v_0 = \text{no. of seismic events}/T$ (years) = **0.165137** seismic events/year.

The Gutenberg-Richter frequency-magnitude distribution for S3, determined for magnitudes M_w between 3.0 and 7.2, is presented in relation 16 and plotted in Figure 117.

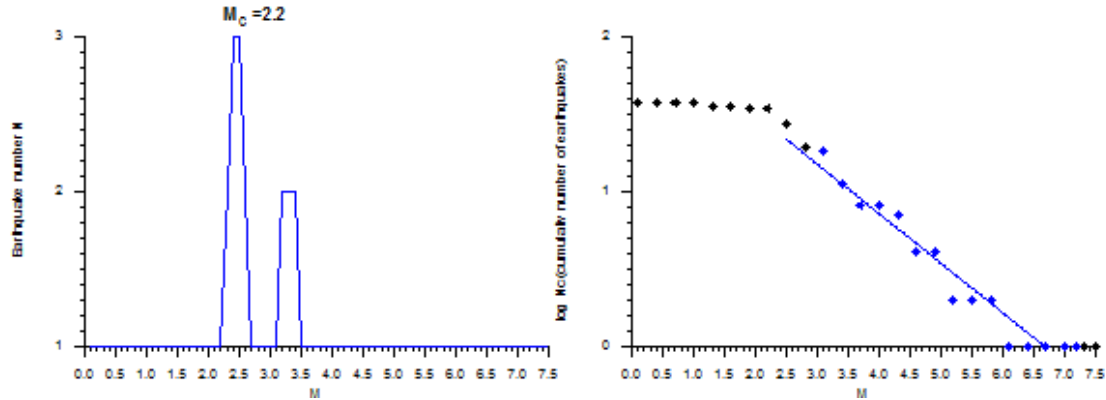


Fig 117. The frequency-magnitude distribution for BS3 zone. The frequency-magnitude relations for with $MW \geq 3.0$; a) non-cumulative; b) cumulative

$$\log N_c = -(0.32 \pm 0.02)M + (2.13 \pm 0.11), \quad 3.0 < M < 7.2 \quad (16)$$

$$R = 0.97, \sigma = 0.11$$

The frequency-epicentral intensity distribution obtained from Eq. 16 and $M_w = 0.66 I_o + 1.23$ (Radu, 1979) is: $\lg N_{cum} = -0.2112 * I_o + 1.7364$. From the above equations we obtain: $a_1 = 1.7364$ and $b_1 = 0.2112$ and $\beta = 0.48631$ (Table 4.5.1).

4.5.2 The assessment of seismic hazard using the probabilistic approach

The theoretical fundamentals of the deductive procedure for probabilistic seismic hazard analyses were formulated in the reference paper of Cornell (1968). The paper develops a method which produces relationships between the parameters describing the ground motion – macroseismic intensity, peak ground acceleration, peak ground velocity – and their average return period for a given site. The input data needed are the estimates of the average activity levels of the various potential seismic sources. The technique integrates the individual influences of potential earthquake sources, near and far, more active or less, into the probability distribution of maximum annual values of the ground motion parameters (intensity, peak ground acceleration, etc.).

Ground motion probability

The assumption widely used in the probability model for hazard analysis is that earthquakes occur as a Poisson process in time. The probabilistic methodology quantifies the hazard at a site from all earthquakes of all possible magnitudes, at all significant distances from the site as probability of exceeding some amplitude of shaking at a site in periods of interest (Thenhaus and Campbell, 2003).



Mathematical formulation

The formal procedure for probabilistic calculations taking account of spatial and temporal uncertainty in the future seismicity was presented by Esteva (1967, 1968) and Cornell (1968). The probabilistic method of seismic hazard analysis, as it is currently understood, was presented by Cornell (1971), and by Merz and Cornell (1973).

It is commonly assumed that the occurrence of individual event can be represented as a Poisson process. The probability that at a given site a ground motion parameter, Z , will exceed a specified level, z , during a given time period, t , is given by the expression:

$$P(Z \geq z | t) = 1 - e^{-v(z)t} \approx v(z)t$$

where $v(z)$ is the average frequency during time period t at which the level of ground motion parameter Z exceeds z at the site resulting from earthquakes in all sources in the region.

The “return period” of z is defined as:

$$R_z(z) = \frac{1}{v(Z \geq z)} = \frac{-t}{\ln(1 - P(Z \geq z))}$$

The inequality at the right side of above equation is valid regardless of the appropriate probability model for earthquake occurrence and $v(z)t$ provides an accurate and slightly conservative estimate for probabilities less than 0.1.

The frequency of exceedance, $v(z)$, is a function of the uncertainty in the occurrence time, size and location of future earthquakes and uncertainty in the level of ground motions they may produce at the site. It is computed by expression

$$v(z) = \sum_n \alpha_n(m_0) \int_{m_0}^{m_n} \int_0^{\infty} f(m) f(r|m) P(Z \geq z | m, r) dr dm$$

where $\alpha_n(m_0)$ is the frequency of earthquakes in the source n above a minimum magnitude of engineering significance m_0 ; $f(m)$ is the probability density function for event size between m_0 and maximal event for the source m_n ; $f(r|m)$ is the probability density function for distance to the earthquake rupture which is usually conditional on the earthquake size; and $P(Z < z | m, r)$ is the probability that for a given magnitude m earthquake at a distance r from the site, the ground motion exceeds level z . The average frequency $v(z)$ is evaluated by three probability functions: magnitude distribution, conditional distance distribution and conditional exceedance probability distribution.

PSHA software



A key milestone in the development of PSHA was the computer program EQRISK, written by McGuire (1976). Nowadays there are a number of PSHA computer codes available to the analyst, but the most widely used in practice are those developed by McGuire (1976, 1978) and Bender and Perkins (1982, 1987). A version of machine code EQRISK (McGuire, 1976) improved by Leideker et al (2001) was formerly used in practice for probabilistic hazard assessment in Romania (Moldovan, 2007 and Moldovan et al, 2008). The code is widely distributed, and today is still the most frequently used hazard software. The PSHA output is often referred to as Cornell- McGuire method (Bommer and Abrahamson, 2006).

Work across boundaries

Seismic hazard is traditionally assessed at national scale and within national boundaries, to serve as input for various regulatory applications, making it impossible to achieve regional harmonization, for lack of data or limited geographical extent. In this project national experts have participated with their knowledge in building regional consensus models, transcending the traditional administrative and disciplinary boundaries.

Probabilistic hazard assessment (PSHA) for the south-eastern part of Romania using crustal inland and marine sources

With the input parameters as defined in Table 4.5.1 for the nine selected sources which likely affect the eligible area we computed seismic hazard values for three return periods (100, 475 and 1000 years) and for two hazard parameters, PGA (g) and Modified Mercalli Intensity (IMM). The computations were performed on a grid of 0.25⁰ x 0.25⁰ cell, covering the whole eligible area.

The hazard maps obtained when considering only the seismic sources in the crust, in terms of PGA/IMM are presented in the Figure 118 for 100 years return period, Figure 119 for 475 years return period and Figure 120 for 1000 years return period. In Figures 121 and 122 are highlighted the hazard values for the Romanian eligible area.

The conversion between macroseismic intensities and peak ground motion is given by STAS 3684-71 in Table 4.5.2

Table 4.5.2 *Macroseismic intensity based on instrumental recordings (STAS 3684-71)*

IMM (degrees)	a (cm.s ⁻²)	v (cm.s ⁻¹)	x ₀ (mm)
V	12...25	1,0...2,0	0,5...1,0
VI	26...50	2,1...4,0	1,1...2,0
VII	51...100	4,1...8,0	2,1...4,0

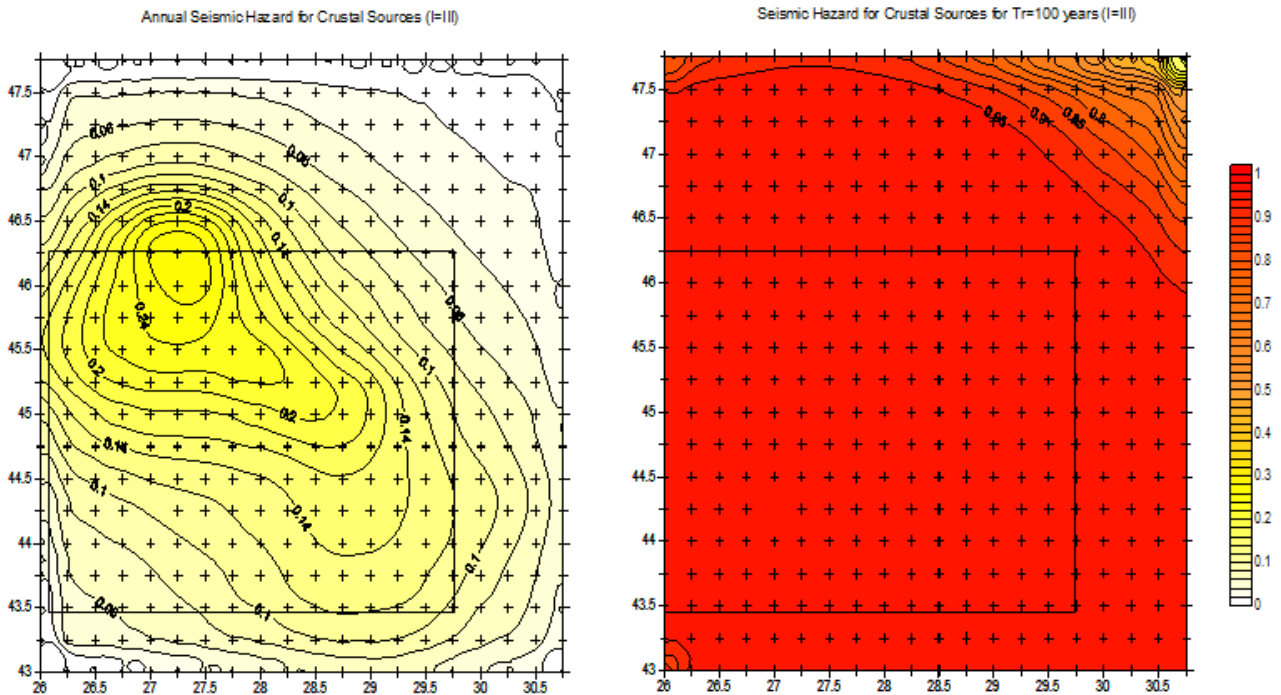
VIII	101...200	8,1...16	4,1...8,0
IX	201...400	16,1...32,0	8,1...16,0
X	401...800	32,1...64,0	16,1...32,0

a – peak ground motion for periods of 0,1...0,5 s;

v – peak ground velocity for periods of 0,5...2,0 s;

x_0 - amplitude of the relative displacement of a pendulum with natural period of 0,25 s and damping of 0,5.

In Figures 123 - 127 are presented the macroseismic intensity curves for different exposure/return periods: 50, 100, 475, 1000 and 2000 years using only crustal sources.



A comparison between the annual hazard and the seismic hazard for 100 years for I=III (using only crustal sources)

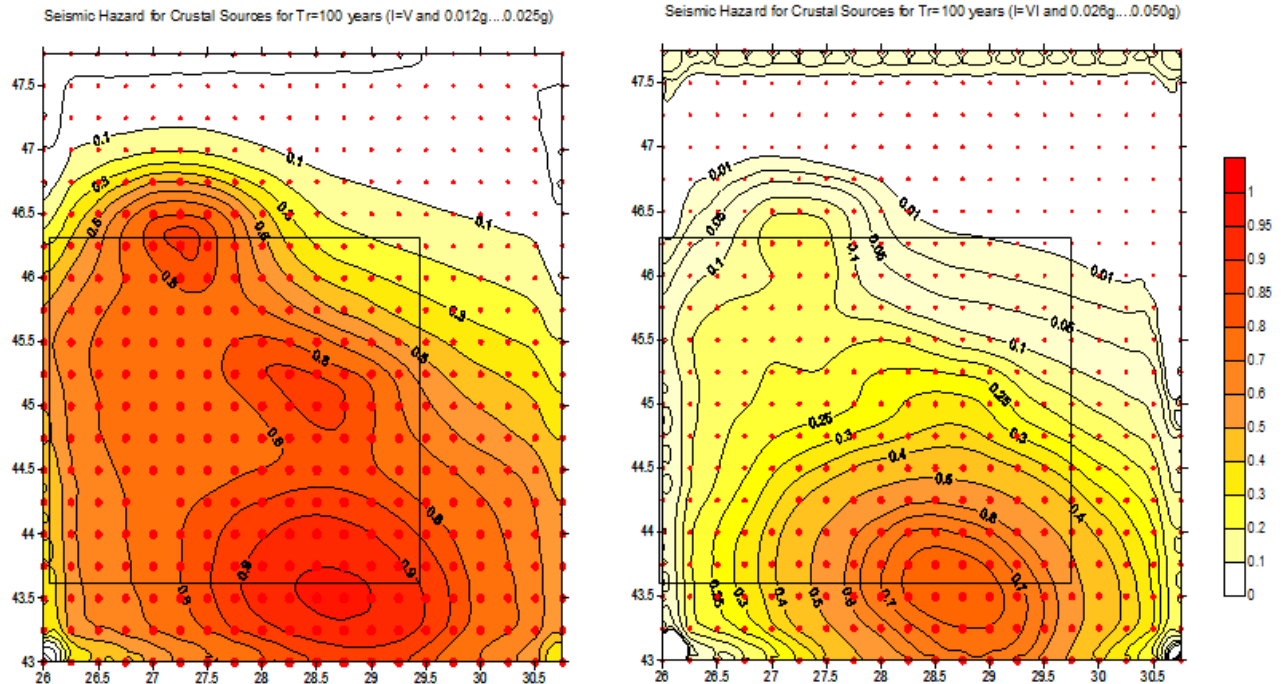


Fig 118. Seismic hazard for $T_r=100$ years for $I=V$ and $I=VI$ (using only crustal sources)



Project funded by the
EUROPEAN UNION

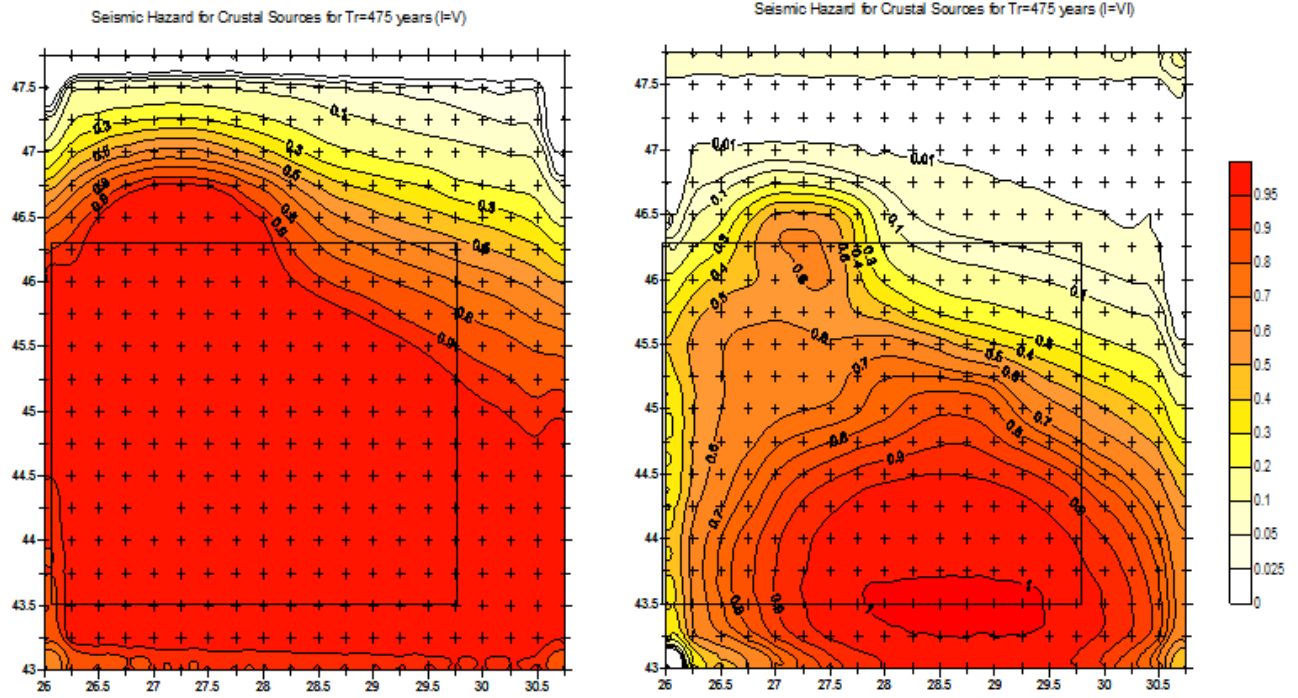
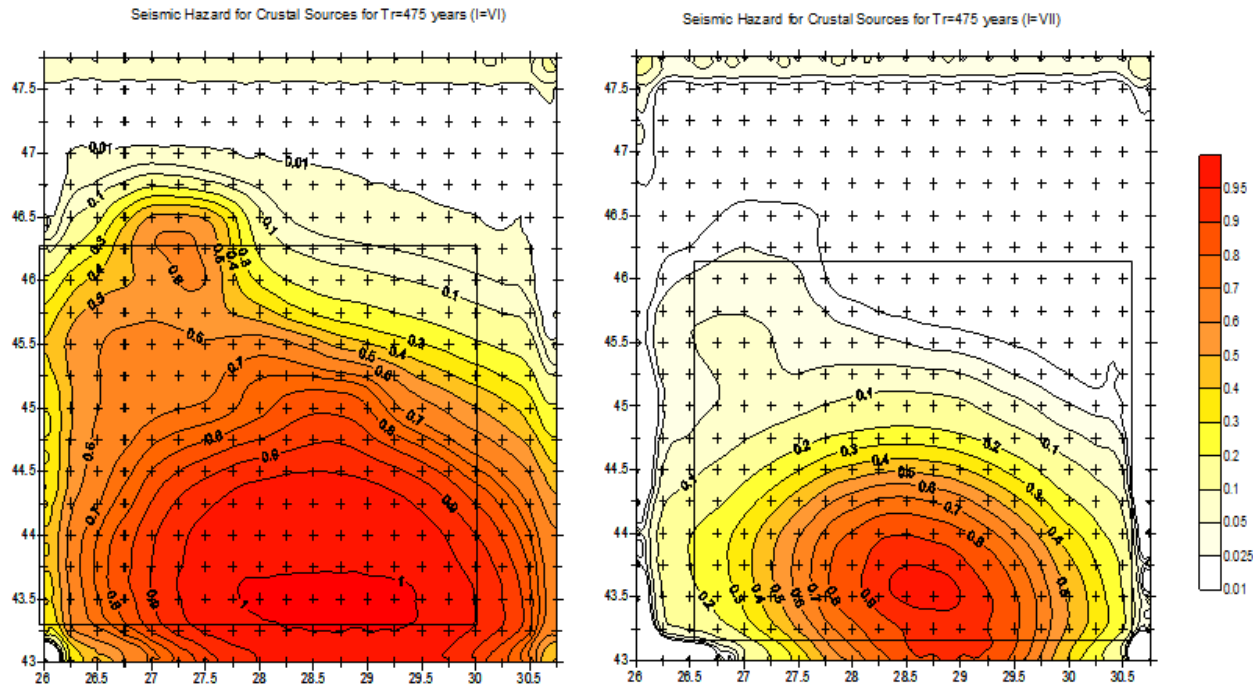


Fig 119a. Seismic hazard for $T_r=475$ years for $I=V/ a=0.012g...0.025g$ and $I=VI/ a=0.026g...0.050g$ (using only crustal sources)





Project funded by the
EUROPEAN UNION



Fig 119b. Seismic hazard for $T_r=475$ years for $I=VI/ a=0.026g \dots 0.050g$ and $I=VII / a=0.051g \dots 0.100g$ (using only crustal sources)

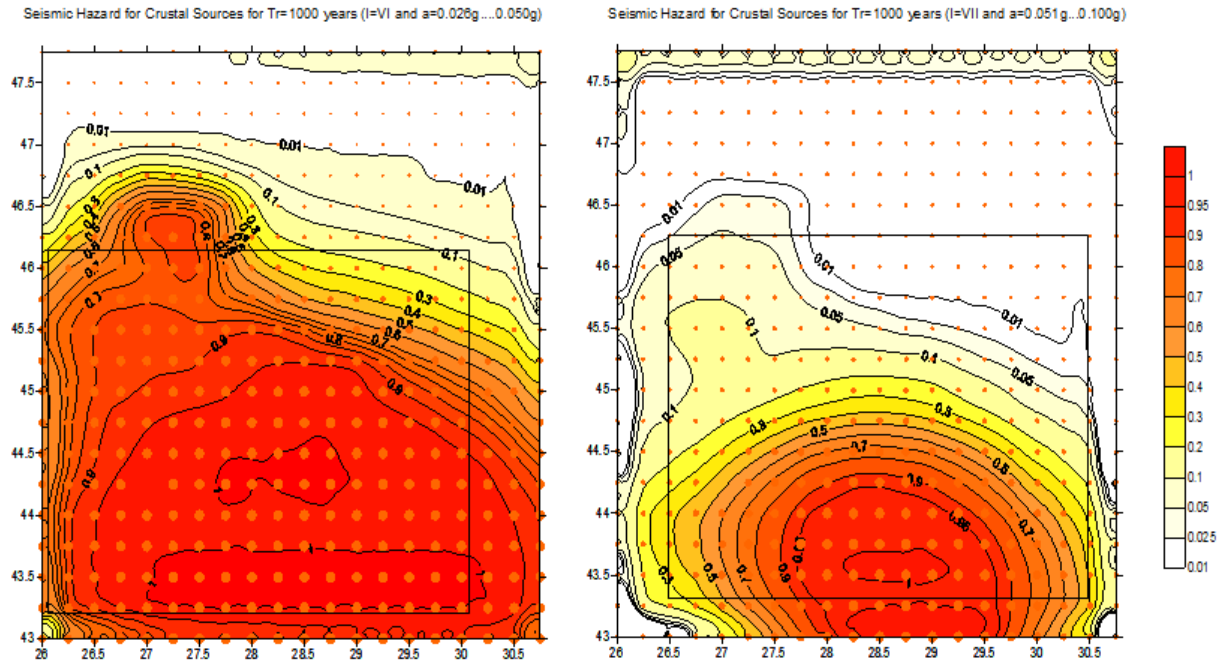


Fig 120. Seismic hazard for $T_r=1000$ years for $I=VI/ a=0.026g \dots 0.050g$ and $I=VII / a=0.051g \dots 0.100g$ (using only crustal sources)

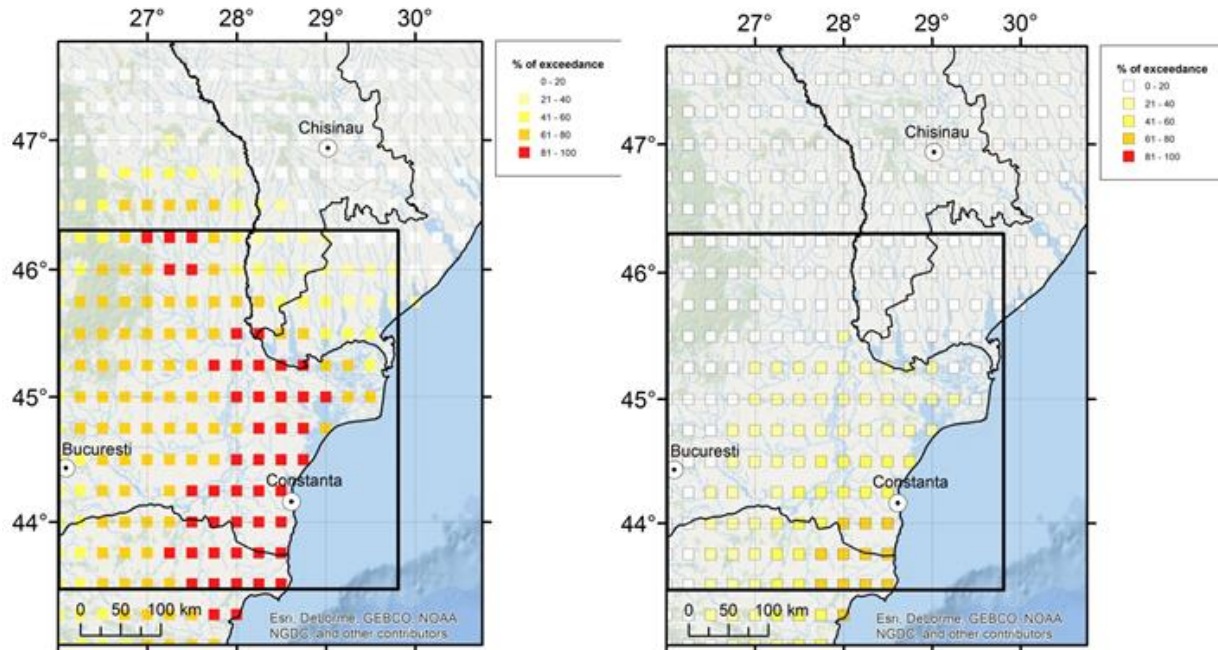


Fig 121. Exceedance probability (%) of I=V and I=VI in an 100 years return period (using only crustal sources)

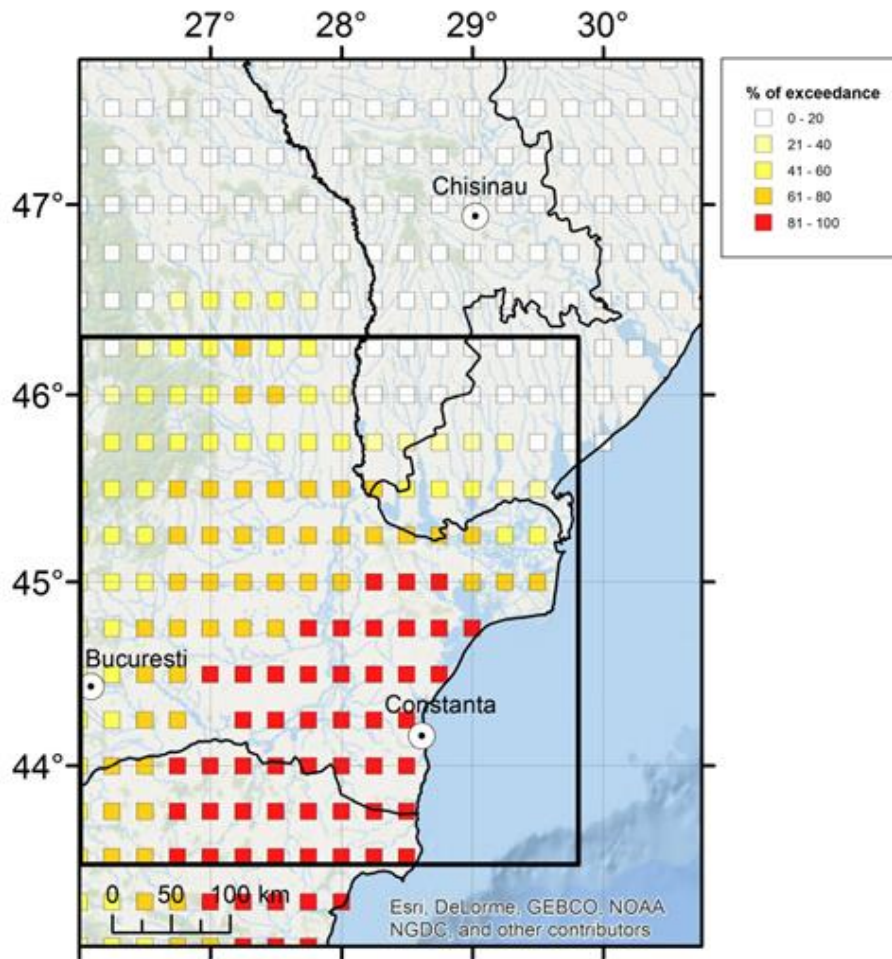


Fig 122. Exceedance probability (%) of I=VI in 475 years return period (using only crustal sources)

The hazard values are also given in the attached xls tables, consisting in a grid of examined points every 0.25 of degree covering the whole eligible area, presenting the geographical coordinates of each examined point and the results of seismic hazard assessment for different return periods (1 year, 50 years, 100 years, 475 years and 1000 years) and for the macroseismic intensity. The studies have been made in two different cases: (i) using only crustal sources and (ii) using both crustal and intermediate depth seismic sources. This splitting of our studies was necessary because when using intermediate depth Vrancea earthquakes, the local influences of crustal sources are completely covered. Only BS3 - Shabla zone is an



Project funded by the
EUROPEAN UNION



exception. It's effects might be seen (together with those due to VI) on the maps from Figures 128-131 and Figures132-134.



Project funded by the
EUROPEAN UNION

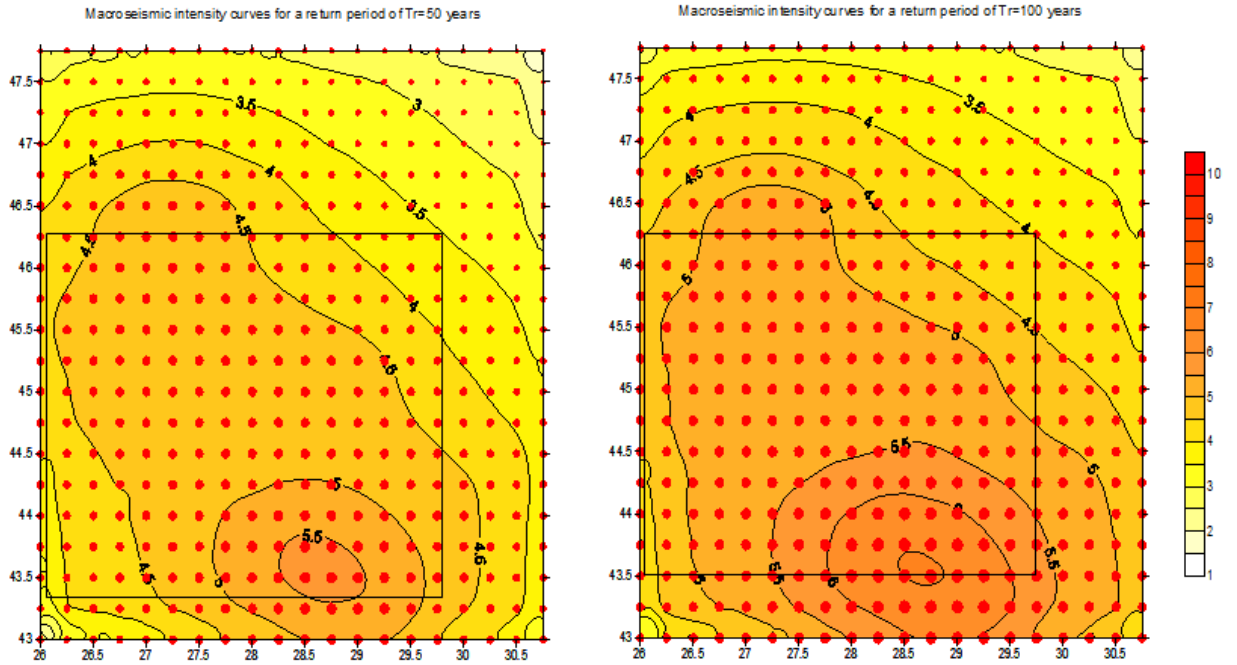


Fig 123. Macroseismic intensity curves for $T_r=50$ and 100 years (using only crustal sources)

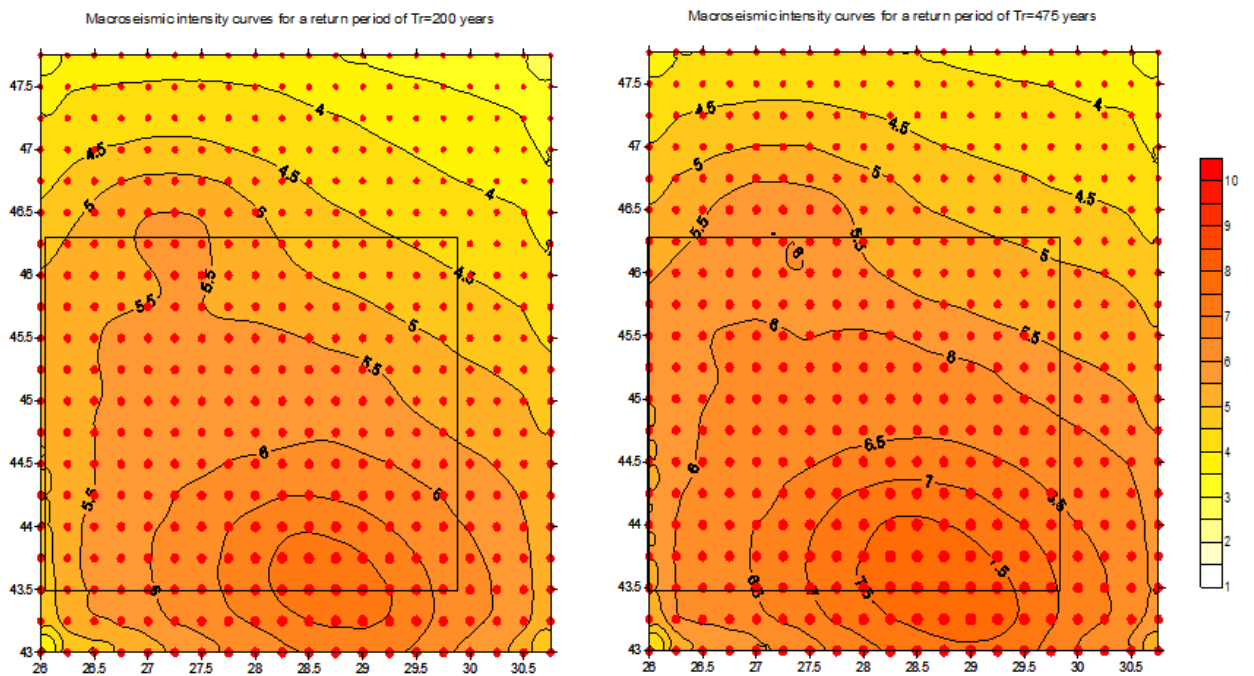


Fig 124. Macroseismic intensity curves for $T_r=200$ and 475 years (using only crustal sources)

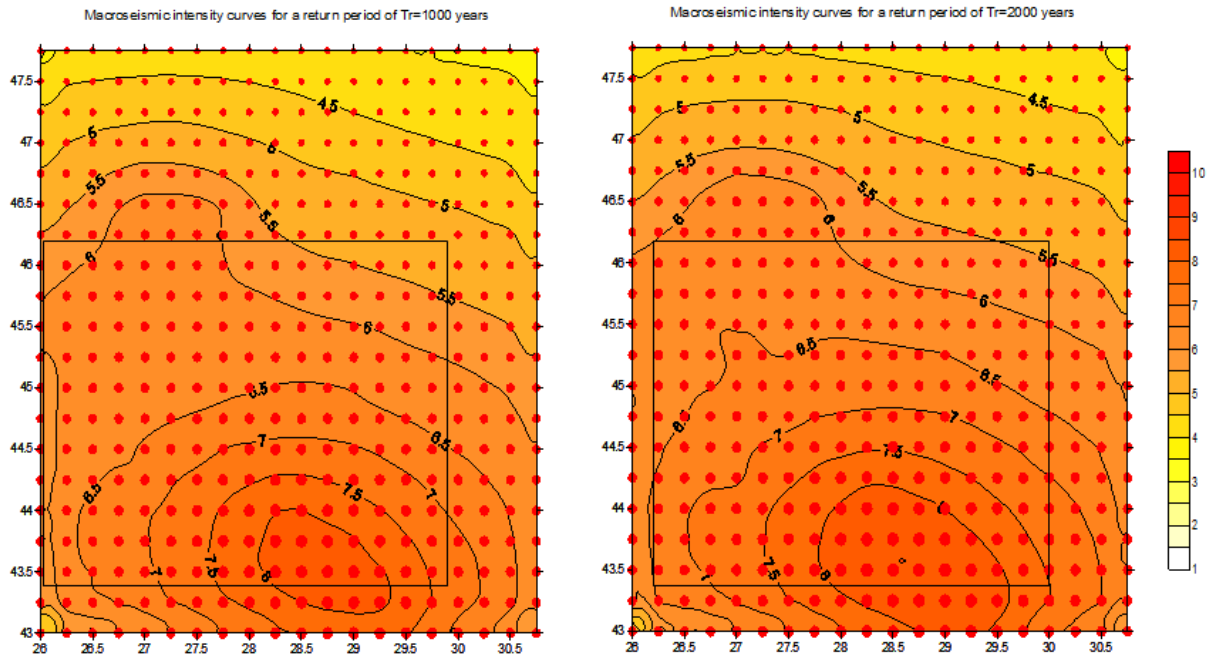


Fig 125. Macroseismic intensity curves for Tr=1000 and 2000 years (using only crustal sources)

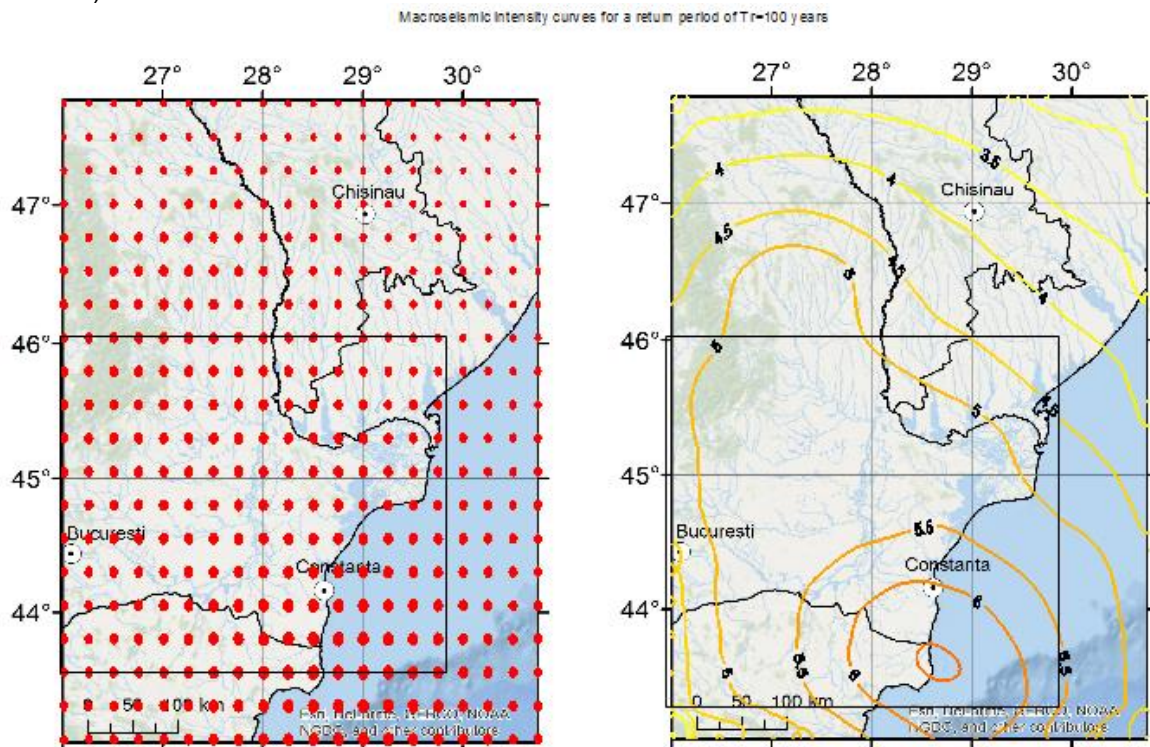


Fig 126. Macroseismic intensity values and curves for Tr=100 years (using only crustal sources)

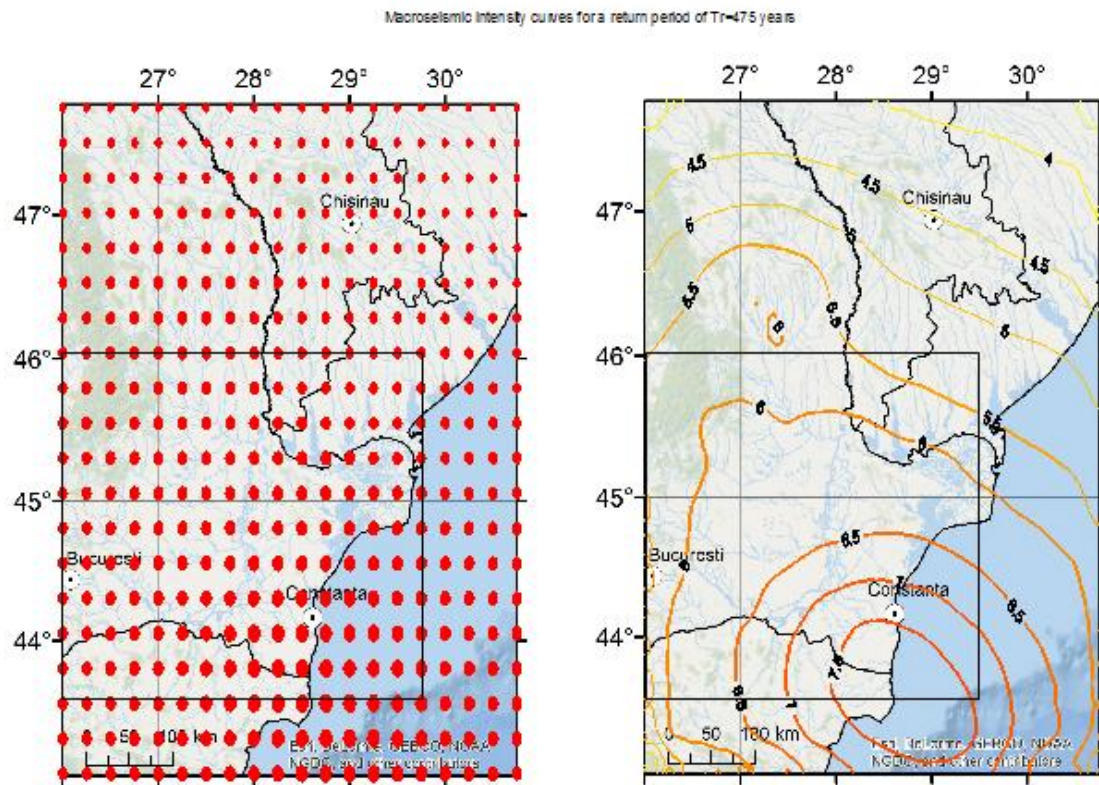


Fig 127. Macroseismic intensity values and curves for $T_r=475$ years (using only crustal sources)

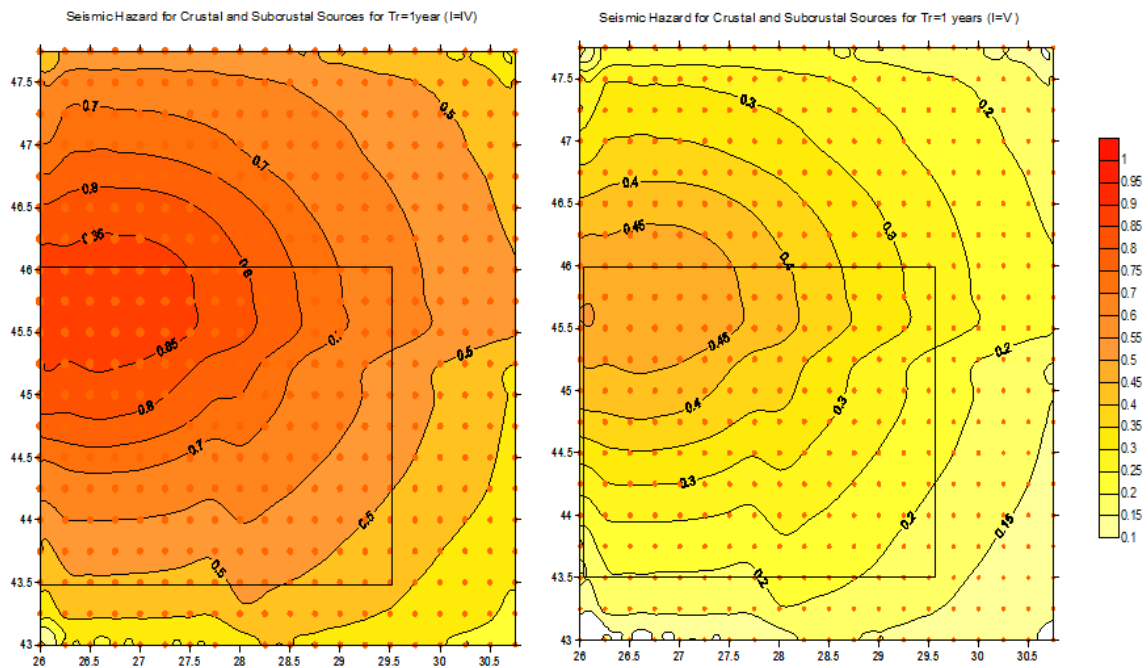


Fig 128. Annual Seismic hazard for $I=IV$ and $I=V$ (using both crustal and intermediate depth sources)

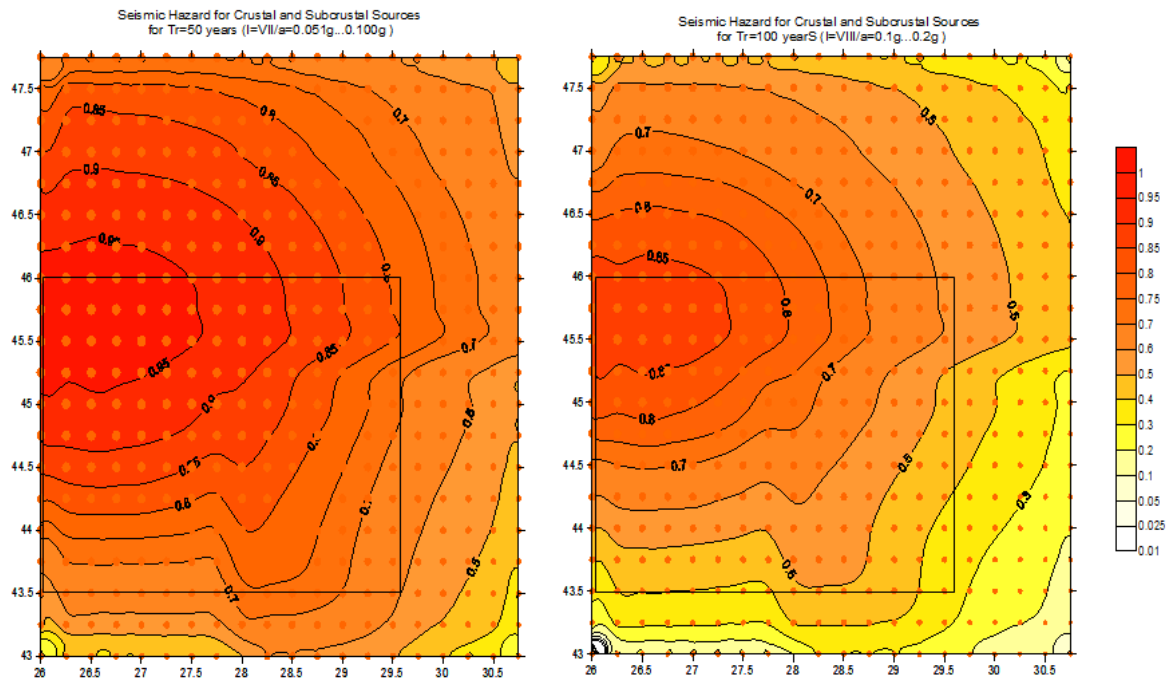


Fig 129. Seismic hazard for Tr=50 years for I=VII and Tr=100 years I=VIII (using both crustal and intermediate depth sources)

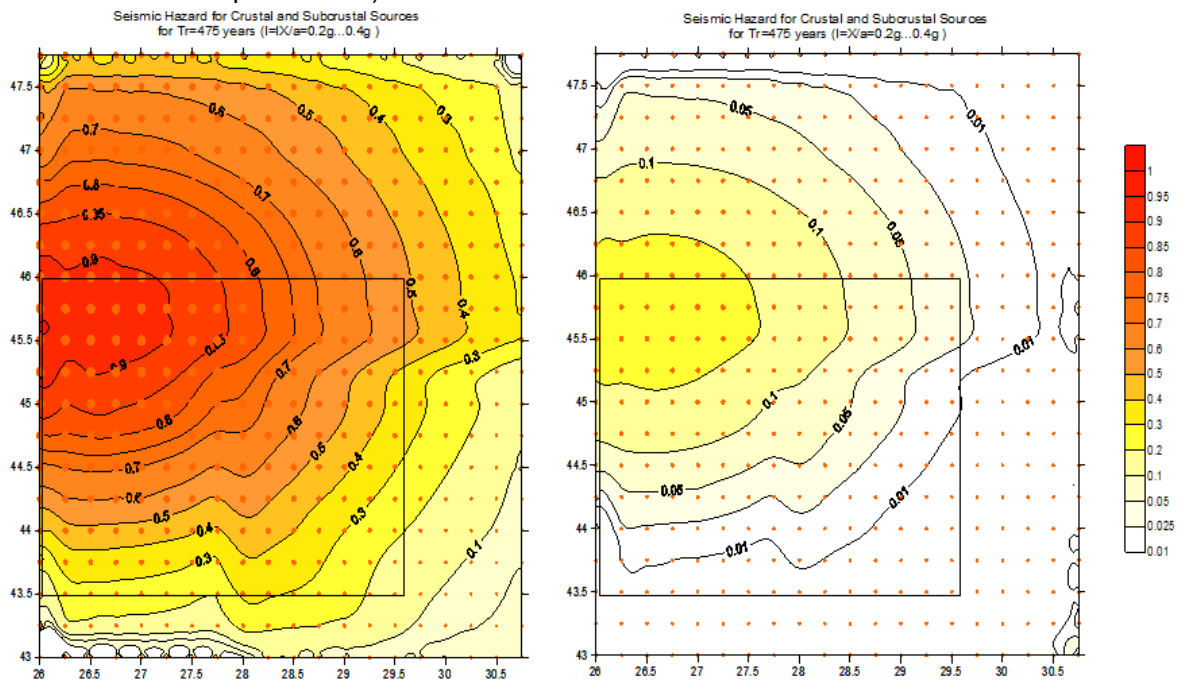


Fig 130. Seismic hazard for Tr=475 years for I=IX and I=X (using both crustal and intermediate depth sources)

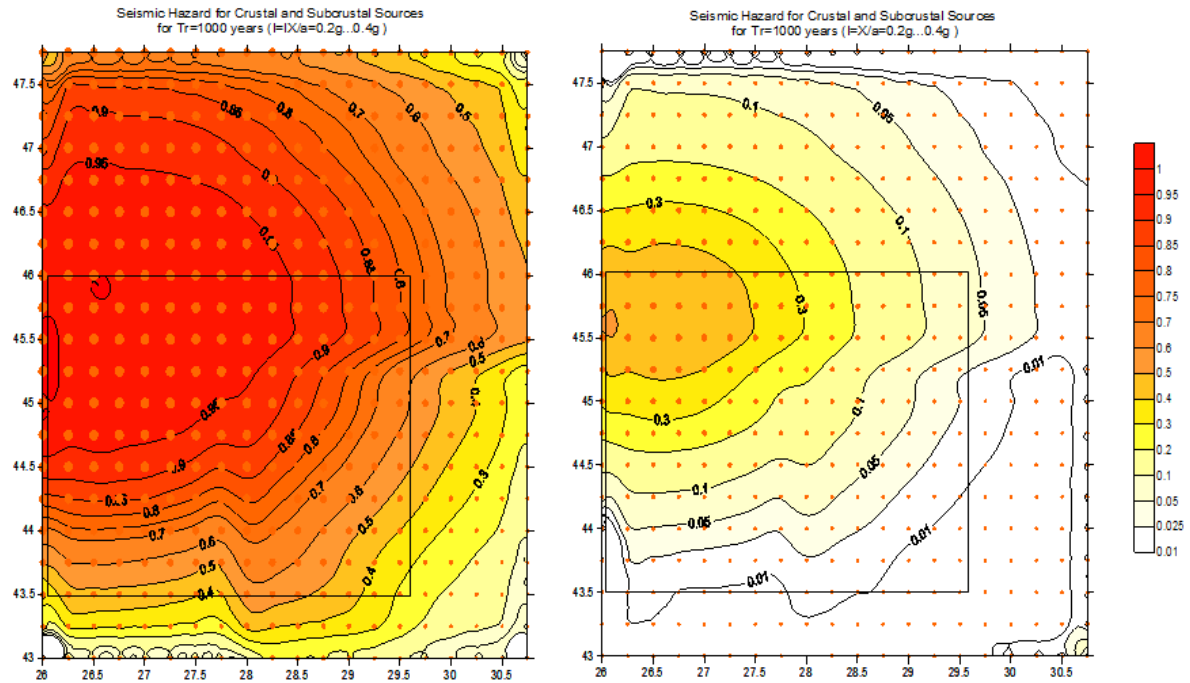


Fig 131. Seismic hazard for $T_r=1000$ years for $I=IX$ and $I=X$ (using both crustal and intermediate depth sources)

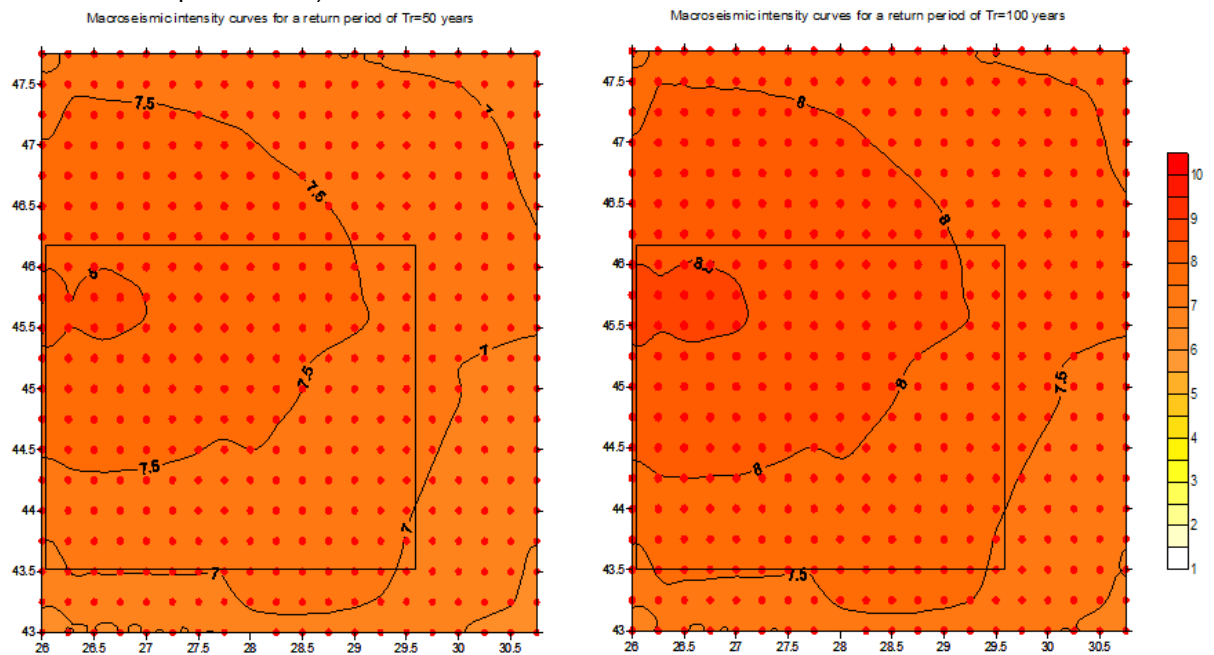


Fig 132. Macroseismic intensity curves for $T_r=50$ and 100 years (using both crustal and intermediate depth sources)

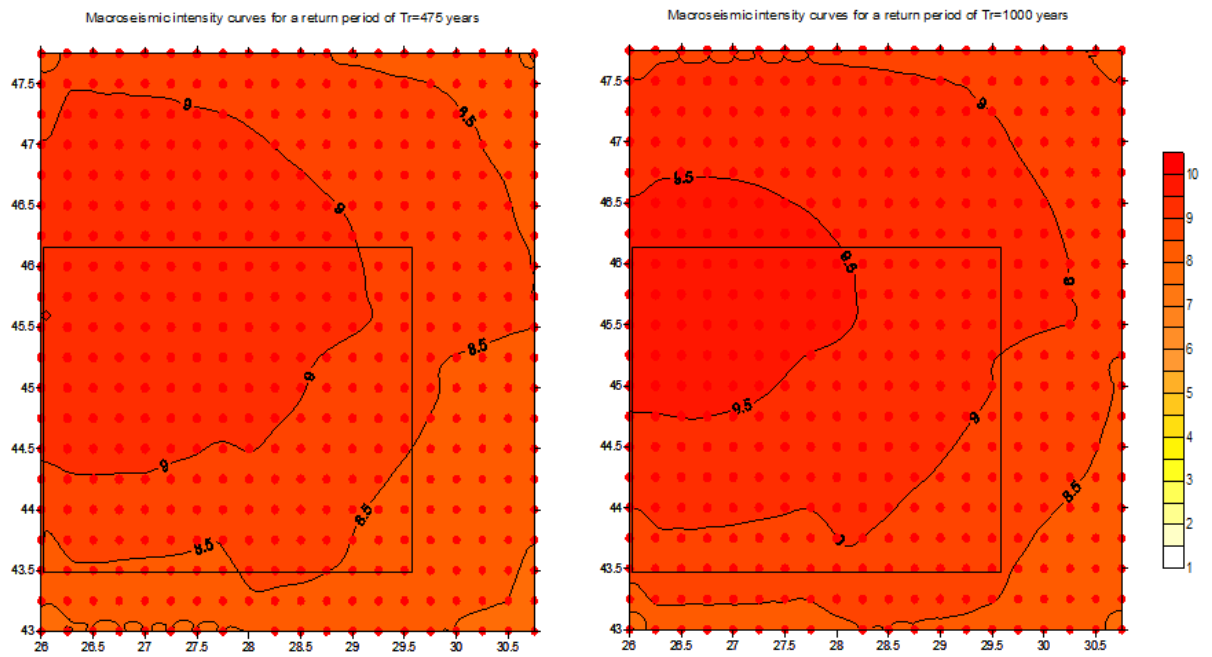


Fig 133. Macroseismic intensity curves for $Tr=50$ and 100 years (using both crustal and intermediate depth sources)

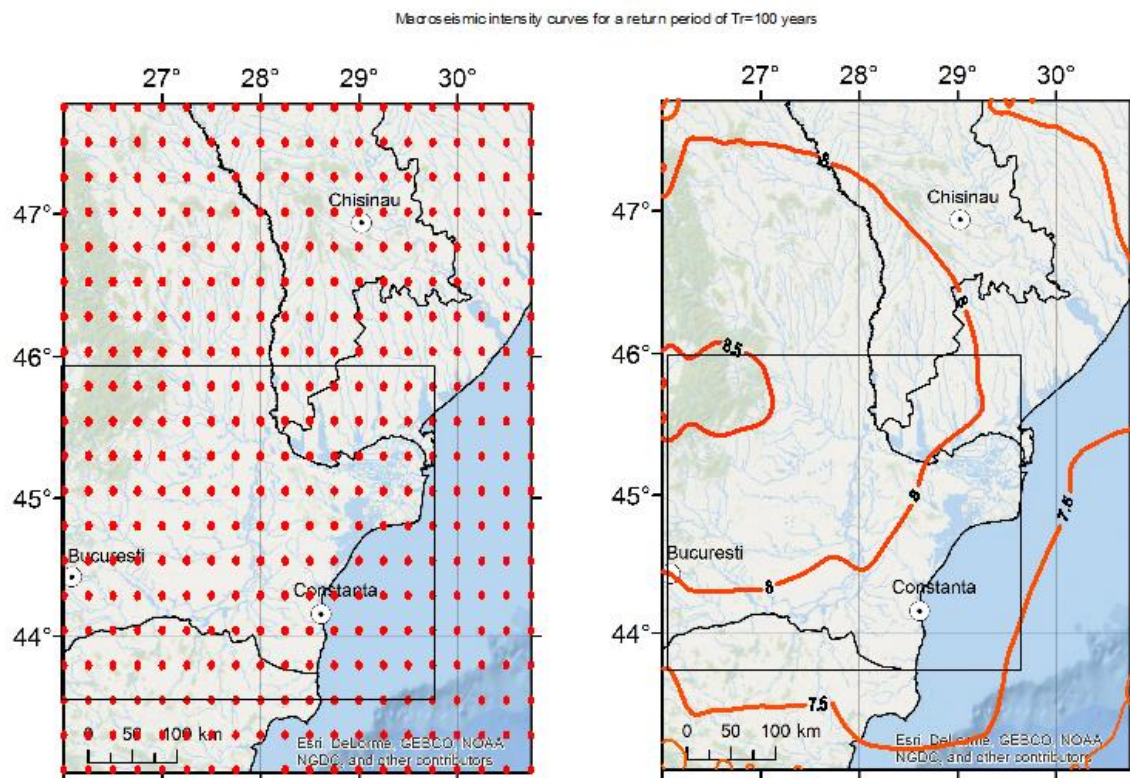


Fig 134. Macroseismic intensity curves for $Tr= 100$ years (using both crustal and intermediate depth sources)

REFERENCES

- Bender, B., and Perkins, D. M., 1982, SEISRISK II, A computer program for seismic hazard estimation: U.S. Geological Survey Open-File Report 82-293, 103 p.
- Bender, B. and Perkins, D. (1987). SEISRISK III: A computer program for seismic hazard estimation. Bulletin 1772, United States Geological Survey. 24 p.
- Bommer, J.J., Abrahamson, N.A. (2006). Why do modern probabilistic seismic-hazard analyses often lead to increased hazard estimates? Bull. Seismo. Soc. Am., 96, 1,976–1,977.
- Constantinescu, L., Constantinescu, P., Cornea, I., Lăzărescu, V. (1976), Recent seismic information on the lithosphere in Romania, Rev. Roum. Geol., Geophys., Geogr., Ser Geophys. 20, 33–40.
- Cornell, C.A. (1968). Engineering seismic risk analysis, Bull. Seism. Soc. Am., 58, 1583-1606.
- Cornell, C.A. (1971). Probabilistic analysis of damage to structures under seismic loads, in Howells, D.A., Haigh, I.P., and Taylor, C., eds., Dynamic waves in civil engineering. Proceedings of a conference organized by the Society for Earthquake and Civil Engineering Dynamics, New York, John Wiley, p. 473–493.
- Enescu D., Contributions to the knowledge of the focal mechanism of the Vrancea strong earthquake of March 4, 1977, *Rev. Roum. de Géoph.*, 24, 1, 3-18, 1980.
- Enescu, D., Zugrăvescu, D. (1990), Geodynamic considerations regarding the Eastern Carpathians Arc Bend, based on studies on Vrancea earthquakes, Rev. Roum. Geophysique 34, 17–34.
- Enescu, D., Enescu, B. D. (1993), Contributions to the Knowledge of the Genesis of the Vrancea (Romania) Earthquakes, Romanian Reports in Physics 45, 777–796.
- McGuire, R.: 1976, Fortran computer program for seismic risk analysis, Technical Report 76-77, US Geological Survey Open File Report.
- Moldovan I.A., Popescu E., Plăcintă A.O., Moldoveanu T., Moldavian dam's rating in seismic risk classes - A probabilistic approach, Proc. CRC-461 International Symposium on Strong Vrancea Earthquakes and Risk Mitigation, MATRIX ROM, Bucharest, p.383-388, 2007.
- Moldovan I.A., Popescu E., Constantin A., Probabilistic seismic hazard assessment in Romania: application for crustal seismic active zones, *Romanian Journal of Physics* 53, 575-591, 2008.
- Moldovan, I.A., Modeling the seismogenic process of earthquake occurrence in the Black Sea region using statistical methods, in Special volume in honor of Professor Emeritus M. E. Contadakis, Faculty of Rural and Surveying Engineering - Department of Geodesy and Surveying, Aristotle University of Thessaloniki, pp. 247-258, 2013.
- Mutihac, V., Ionesi, L., *Geology of Romania* (in Romanian) (Technical Press, Bucharest 1974).

- Oncescu M.C., Trifu C.I., Depth variation of moment tensor principal axes in Vrancea (Romania) seismic region, *Ann. Geophys.* 5B, 149-154, 1987.
- Oncescu M.C., Mârza V.I., Rizescu M., Popa M., The Romanian earthquake catalogue between 984-1997, "Vrancea Earthquakes: Tectonics, Hazard and Risk Mitigation", F. Wenzel, D. Lungu, O. Novak. (Eds.), Kluwer Academic Publishers, 43-47, 1999.
- Radu C., Catalogue of strong earthquakes originated on the Romanian territory. Part I- before 1901, Part II-1901-1979 (in Romanian) in “Seismological research on the earthquake of March 4, 1977 (Coordinators Cornea I., Radu C.)”, 723-752, ICEFIZ, Bucharest, 1979.
- Radulian, M., Mândrescu N., Popescu E., Utale A., Panza G., Characterization of Romanian seismic zones, *Pure and Applied Geophysics* 157, 57-77, 2000.
- Săndulescu, M., *Geotectonics of Romania* (in Romanian) (Technical Press, Bucharest 1984).
- Thenhaus, P. C., Campbell, K. W. (2003). Seismic Hazard Analysis. Earthquake Engineering Handbook, Chapter 8, Chen W. And Scawthorn C. ed., CRC Press.

4.6 MOLDOVA

4.6.1 Past Events and Their Consequences

Seismic observations in Moldova on a regular basis started in 1949, when, on December 20, the first seismogram was recorded at the seismic station Kishinev. The year 1963 could be considered the starting point of the scientific investigations into earthquake engineering, when the first volume of scientific publications was issued dedicated to problems of tectonics and seismology of Moldova, prepared by the group of young scientists of the Institute of Geology and Mineral Resources of the Academy of Sciences of Moldavian Soviet Socialist Republic (MSSR).

The Institute of Geophysics and Geology (IGG) was founded in 1967 on the basis of the Institute of Geology and Minerals and the regional seismic station "Kishinev." The research priorities of the Institute are monitoring of seismicity of the Vrancea zone, seismic hazard and risk assessment, microzonation, GIS technologies, and mathematical models in earthquake engineering. The present director is Dr. Vasiliu Alkaz. The staff has numbered from 100 to 120 in the 1970s and 1980s to 50 in the 1990s. Currently the staff consists of 22 seismologists (including staff of seismological stations), 8 of them with Ph.D. degrees. The seismological section consists of (1) Laboratory for Seismology, (2) Laboratory of Survey of Seismic Effects, and (3) the Center of Experimental Seismology.

The territory of the Republic of Moldova is influenced by earthquakes of intermediate depth from the Vrancea seismic zone, situated in Romania. The strongest of these earthquakes are distributed in the depth interval of 80-150 km, with maximum magnitude of 7.5-7.8. The most significant seismic effect, maximum intensity VIII-IX on the scale of XII, is observed in Romania and Moldova. Statistical information about seismic activity of the Vrancea zone is available since the year 1000. On average, strong earthquakes of magnitude $M > 6$ occur five times or more per century. Some of them (November 10, 1940, March 4, 1977, August 31, 1986) caused casualties and considerable damage.

The main mission of the seismological section is monitoring seismicity for the territory of Moldova, and conducting seismotectonic investigation, seismic hazard assessment, long-term earthquake prediction research, and engineering seismology. These investigations have resulted in maps of macro- and microzonation for seismic-resistant construction and are the basis for taking measures in reducing the consequences of strong earthquakes.

The seismic network of Moldova consists of five seismic stations, situated in Kishinev, Cahul, Leovo, Soroky, and Djurjuleshti. Kishinev is the base station for the network; the other four provide regional data. Station Kishinev was established in 1949 by the Institute for Earth Physics, USSR Academy of Sciences, to provide supplementary data on parameters of Carpathian earthquakes. Station Cahul started its observations in 1978 and provides additional information for studying of characteristics of earthquakes from the Vrancea zone. Stations Leovo (1982) and Soroki (1983) were established in connection with structural changes in the

Soviet network in 1979 for work on earthquake forecasts. Djurjuleshti was installed in 1988. Information about the location of the seismic stations is shown in Fig 135.

In the last twenty years the Laboratory of Seismology performed the investigation of the horizontal discontinuities of the upper mantle for Moldova and neighboring Romania by analysis of teleseismic P-wave propagation. A database of the seismological information has been created in the Institute, including the catalog of the earthquakes and focal mechanisms of the studied region, macroseismic information. The statistical algorithms for interpretation of seismic intensity and seismic impact and alternative models of its assessment are considered in probabilistic representation of seismic hazard.

The Laboratory of Survey of Seismic Effects has launched a projects aimed at utilizing GIS technology for storing and processing of the available information. These projects allow constructing of seismic macrozonation maps in digital format, and certain advances in seismic risk and seismic microzonation studies.

Some results of these projects are shown in Fig 136- Fig 140.

4.6.2 Existing legislation framework

Regulatory Documents which standardizes the activity in the domain of Seismology and Engineering Geology:

- Decision of Government of the Republic of Moldova on measures to optimize the infrastructure sphere of science and innovation no. 1326 of 14.12.2005, Official Monitor (Gazette) of the Republic of Moldova nr.168-171/1406 of 16.12.2005 regarding the reorganization and creation of organizations and institutions of science and innovation, including Institute of Geology and Seismology.
- SNIP 1.02.07-87. Engineering exploration for the construction. General definitions. (“Инженерные изыскания для строительства. Основные положения”).
- SNIP II-7-81. Construction in seismic regions („Строительство в сейсмических районах”).
- SNIP 2.01.15-90 Engineering protection of territories, buildings and construction from dangerous geological processes. Principal regulations of designing. (“Инженерная защита территорий, зданий и сооружений от опасных геологических процессов. основные положения проектирования”).



Fig 135. The location of the seismic stations in Republic of Moldova

- RSN 60-86 Engineering exploration for construction. Seismic microzoning. Norms of work realization (“Инженерные изыскания для строительства. Сейсмическое микрорайонирование. Нормы производства работ”).
- RSN 65-87 Engineering exploration for construction. Seismic microzoning. Technical requirements of work realization Инженерные изыскания для строительства. Сейсмическое микрорайонирование. Технические требования к производству работ
- СП 11-105-97 Part 1 Engineer-geological study for the construction. General requirements for work realization (“Часть 1 Инженерно-геологические изыскания для строительства. Общие правила производства работ”).

The Institute of Geology and Seismology made some special investigation in the field of seismic zonation and seismic microzonation which were adopted as normative documents in

Moldova Republic. Fig 136 illustrates a seismic zonation of Republic of Moldova. Fig 139 illustrates a seismic microzonation of Chisinau city with the consideration of the local geological condition and soil properties. The seismic risk map for Chisinau city was elaborated on the base of seismic microzonation (Fig 138).

Fig 139 and Fig 140 illustrate the seismic risk for Republic of Moldova in the damage and integral risks.

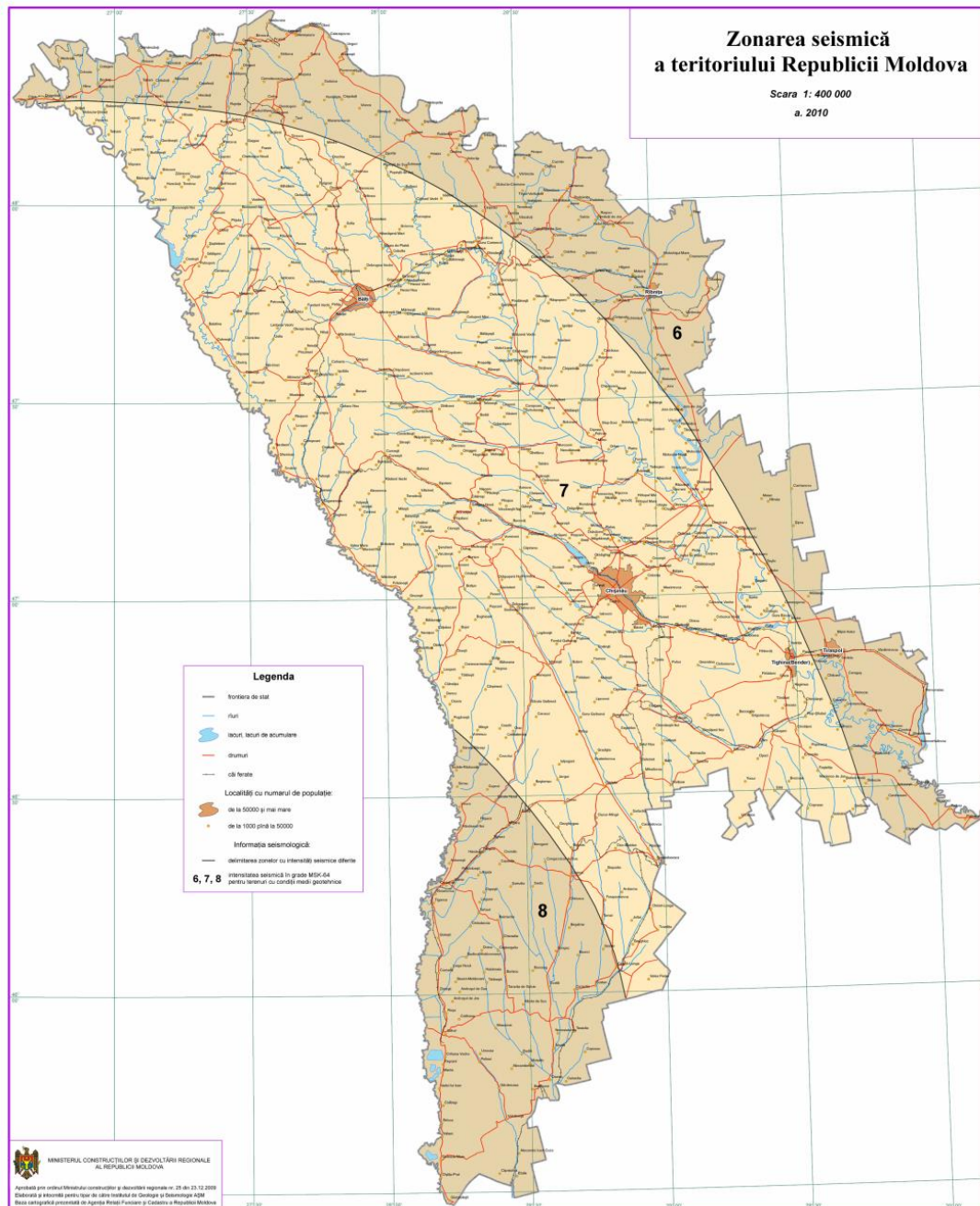


Fig 136. The new seismic zoning map of Moldova Republic.

It was adopted by the Ministry of Regional Development and Construction in 2010, and approved for practical use (aseismic design and construction).

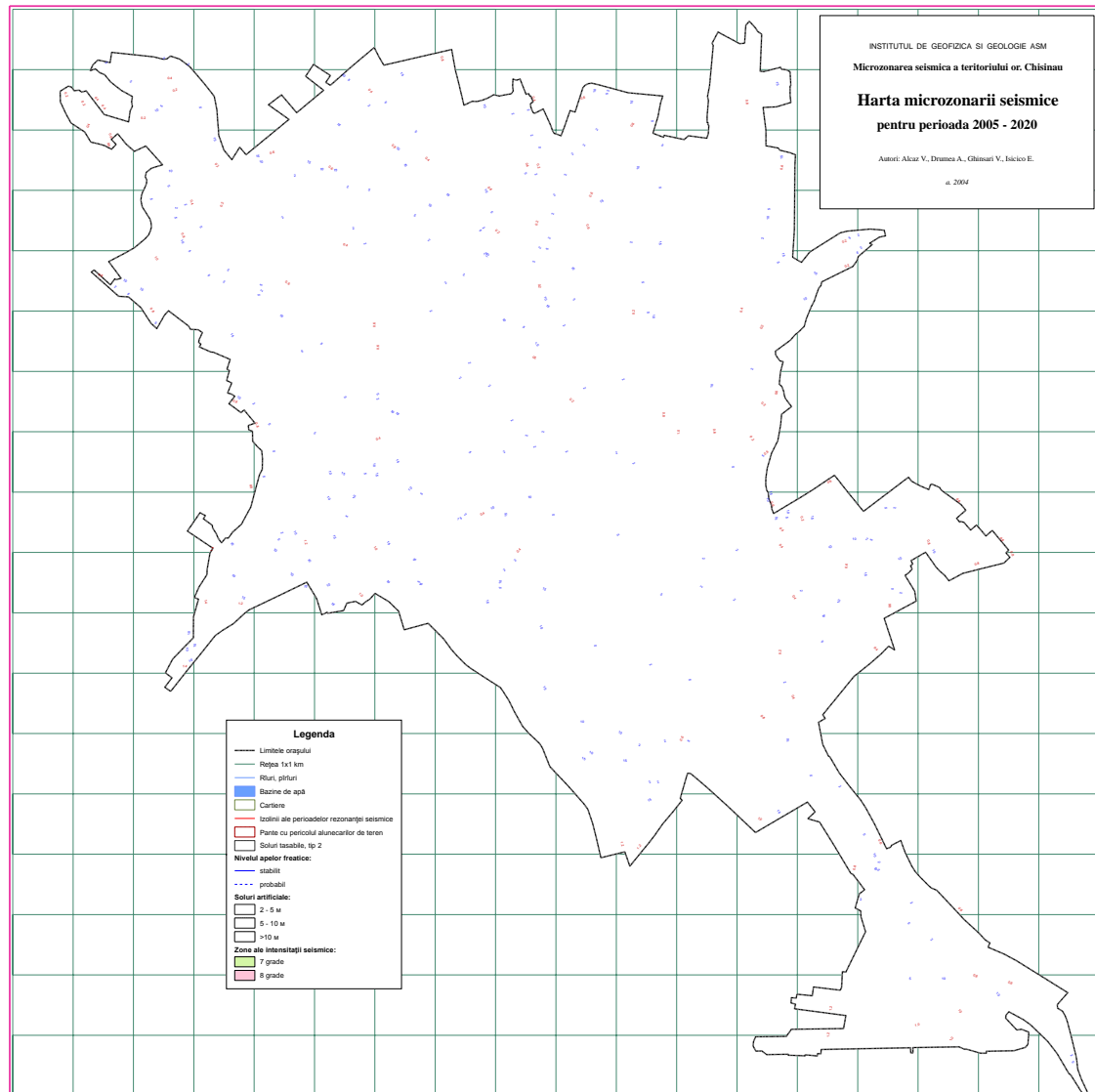


Fig 137. The new seismic microzonation map of Chisinau city.

It was adopted as normative document for the construction project design in Chisinau city by the Ministry of Regional Development and Construction in 2013.

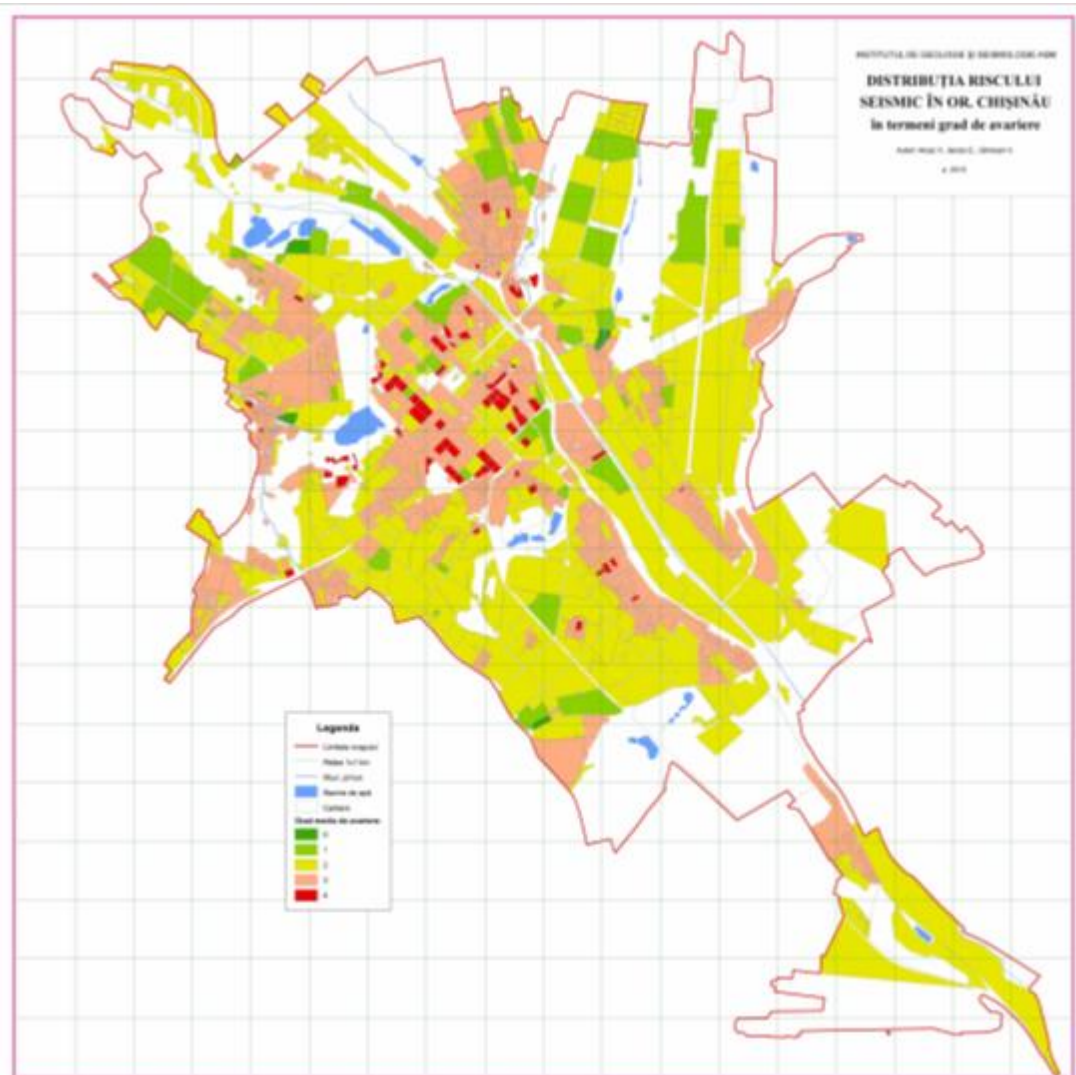


Fig 138. Seismic risk map of Kishinev city.

It was elaborated in 2009 for scenario earthquake (like 10.11.1940) in terms of the average degree of damage for each quarter of the city.

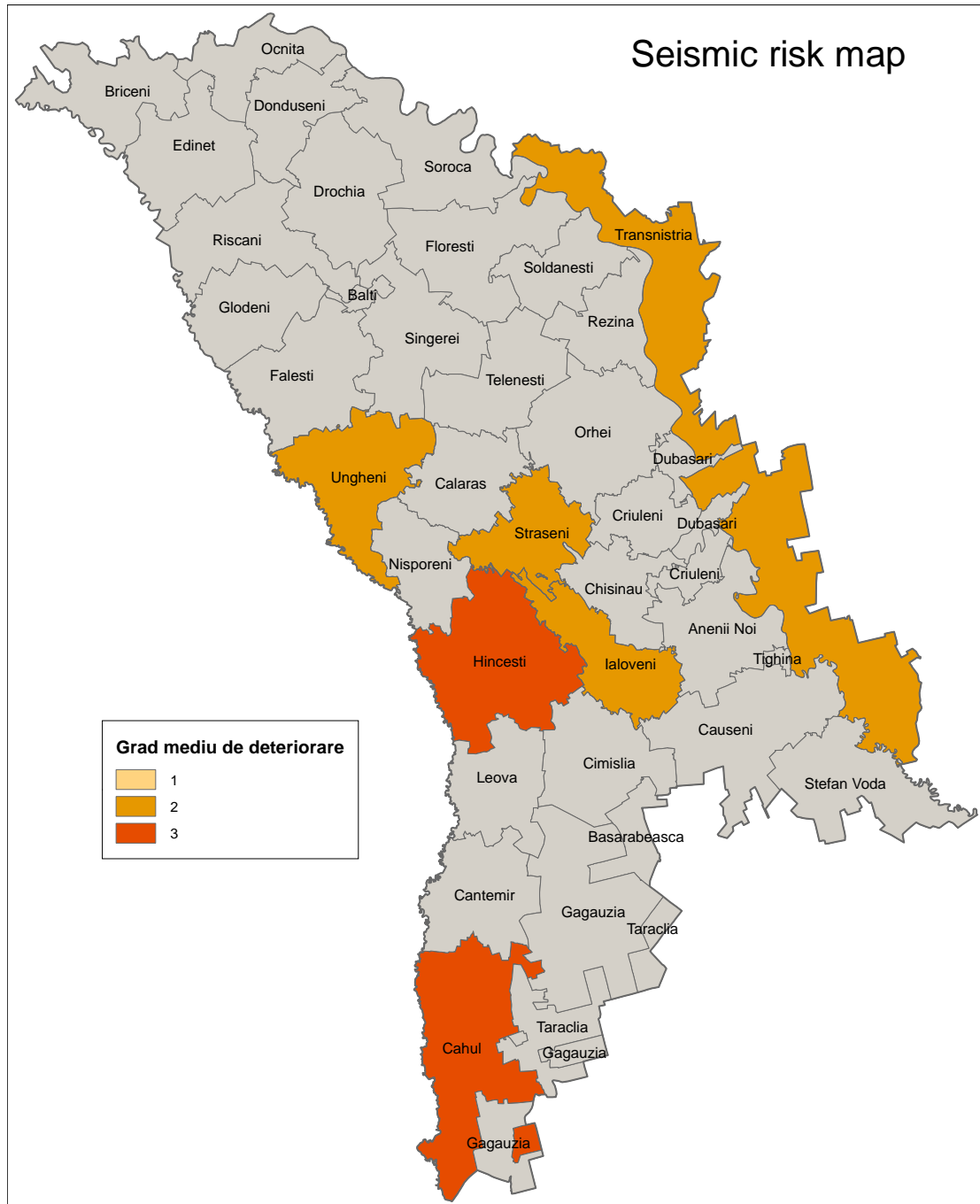


Fig 139. Seismic risk map of Moldova Republic.

It was elaborated in 2012 for scenario earthquake (like 10.11.1940) in terms of the average degree of damage for each district.

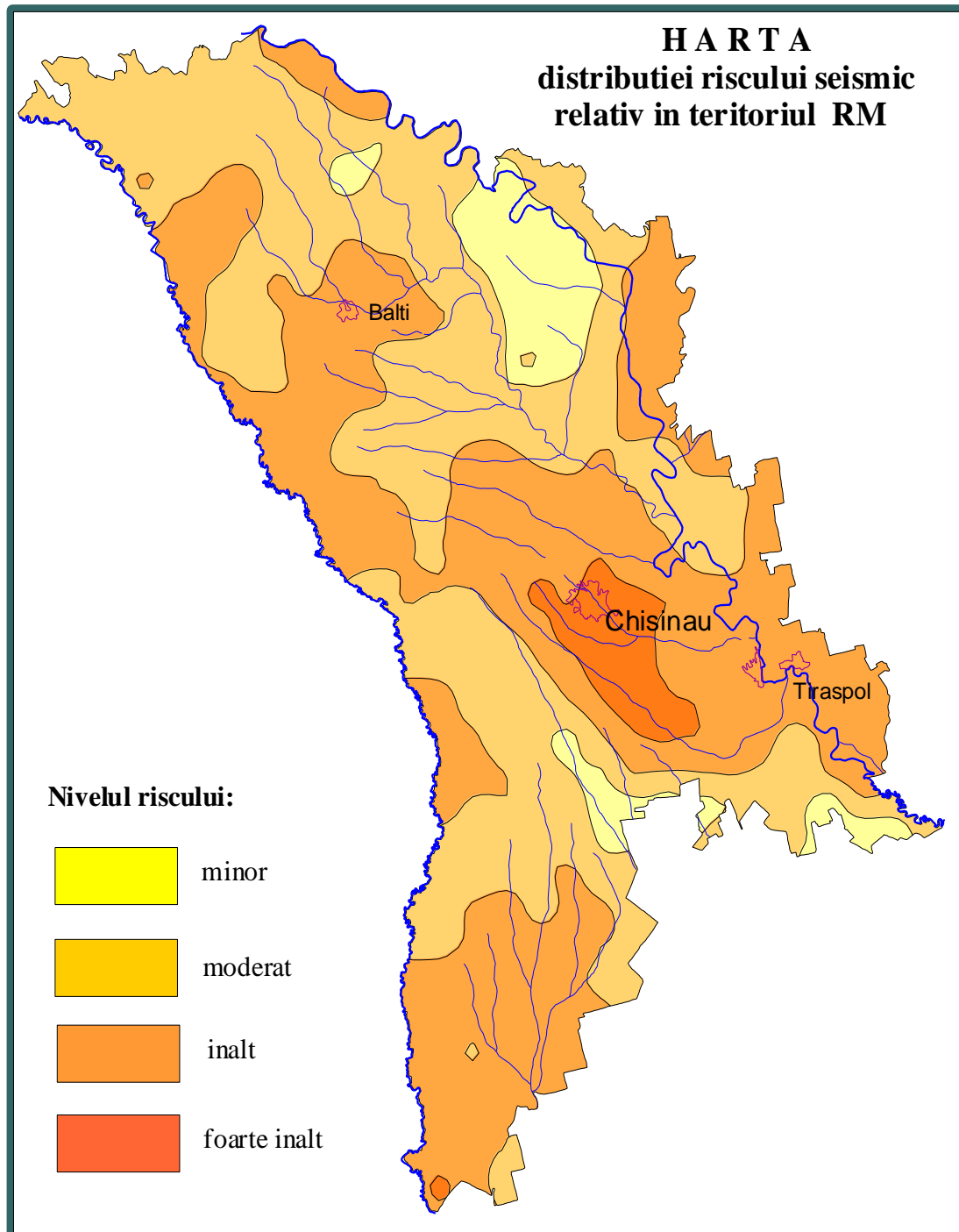


Fig 140. Relative seismic risk map of Moldova Republic.

REFERENCES

1. ALCAZ V. Potential Impact of Earthquakes on Built and Physical Environment: Republic of Moldova Case Study. Proceedings of the International Disaster Reduction Conference, Davos, Switzerland, August, 2008, p. 29-31.
2. Alcaz V., (1999). Influence of Local Soil Conditions on Earthquake Motion in the Territory of Moldova Republic. In: Vrancea Earthquakers: Tectonics, Hazard and Risk Mitigation. Ed.: F.Wenzel, D.Lungu, Kluwer Academic Publishers, Dordrecht/ Boston/ London, p.187-195.
3. Alcaz V., A.Zaicenco, (1999). Spatial Correlation Between Level of Water Table and Damage of Buildings After 1986 Vrancea Earthquake in Kishinev Using GIS. Proceedings of DACH-tagging Conference, Berlin, pp.145-150.
4. Alcaz V., A.Zaicenco, (2002) Project of Seismic Risk Estimation and Disaster Mitigation of Kishinev City. "Geology", v.23, Kiev, pp.17-19.
5. ALCAZ V., ZAICENCO A., ISICIKO E. Instrumental and Macroseismic Database for Regional Seismic Hazard and Risk Studies. Proceedings of the 31 st General Assembly of European Seismological Commission, Hersonissos, Crete, Greece, September 2008, p. 17-20.
6. Alcaz V.. Основы прогноза сейсмической опасности и сейсмического риска территории РМ. Chisinau, "Elena", 2007.
7. Alcaz V.. Studiul influentei conditiilor locale de teren prin modelari numerice. Tezele Conferintei Fizicienilor din Moldova, Chisinau, 2007.
8. Alcaz V.G.,Drumea A.V., Numerical and experimental site effects study: Republic of Moldova. (Abstract for conference). Proceedings of International conference in Yalta (Ukraine), september, 2007.
9. ALKAZ V., A. ZAICENCO, E. ISICIKO. Microzonation of Chisinau: a Tool for Reducing Seismic Risk. Harmonization of Seismic Hazard in Vrancea Zone. NATO Science for Peace and Security Series, C: Environmental Security, Springer, 2008, p.117-132.
10. Alkaz V., A. Zaicenco, E. Isicko and I. Sandu. Loss Estimation from Scenario Earthquakes in the Republic of Moldova. Proceedings of the International Symposium on Seismic Risk Reduction, , Editura "Orizonturi Universitare", Timisoara, Romania, 2007.
11. АРТИКАЕВ F., BORCEA I.S., ERTELEVA O., SANDI H., ALCAZ V. Development of instrumental criteria for intensity estimate. Revue. Roumaine de Geophysique. 2008-2009, 52-53, pp.3-10. ISSN 1220-5303
12. Алказ В.Г., Капустян Н.К., Марченков А.Ю. К оценке проектируемого сейсмического воздействия на высотные здания в Москве. Buletinul Institutului de Geofizica si Geologie al Academiei de Stiinte a Moldovei, N1, 2007.

13. BURTIEV R. Статистическая связь между сейсмическими зонами Балкан. Buletinul Institutului de Geologie si Seismologie al Academiei de Stiinte a Moldovei, Chisinau, nr. 1, 2008, p. 31-34.
14. Drumea A. "Moldova" - Encyclopedia of European Regional Geology. U.K. London, 1997.
15. DRUMEA A., Alcaz V. E posibil oare astazi predictia unui cutremur de pamant puternic? Chisinau, Academos, N 1-2 (9), 2008, 3 p.
16. Drumea A., V.Alcaz, A.Zaicenco, (2001). Behavior During Strong Vrancea Earthquakes of Vulnerable Buildings in Republic of Moldova. In: Lungu, T Saito (editors). Earthquake Hazard and Countermeasures for Existing Fragile Buildings. Bucharest, Romania, 2001, pp.267-270.
17. Drumea A.V., Ginsar V.N., Poiata I.A., Stepanenco N.Ya., Shebalin N.V., Shumila V.I., "International Geological-Geophysical Atlas of the Atlantic Ocean". Part "Seismicity". Published in accordance with a decision of the Intergovernmental Oceanographic Commission of UNESCO. Moscow, 1989-1990, pp. 95, 101-107, 152-153 (in English and Russian).
18. G. KOLEVA, I. SANDU, S. AKKAR. An Estimation of the Maximum Interstory Drift Ratio for Shear-wall Type Structure. NATO Science for Peace and Security Series, C: Environmental Security, Springer, 2008, p.225-240.
19. GINSARI V. Estimation of the Recurrence and Probability of Vrancea Intermediate Depth Earthquakes. Harmonization of Seismic Hazard in Vrancea Zone. NATO Science for Peace and Security Series - C: Environmental Security, Springer, 2008, 85-99.
20. SANDU, A. ZAICENCO. Focal Mechanism Solutions for Vrancea Seismic Area. Harmonization of Seismic Hazard in Vrancea Zone. NATO Science for Peace and Security Series, C: Environmental Security, Springer, 2008, p.17-46.
21. I.Sandu. A.Zaicenco. Focal Mechanism Solution for SE Carpatian Region. Proceedings of the International Simposium "Thirty Years from the Romania Earthquake of March 4, 1977", Bucharest, Romania, 2007.
22. ILIES I., Ionescu C. Monitorizarea seismica a teritoriului Republicii Moldova: starea actuala si de perspectiva, Buletinul Institutului de Geologie si Seismologie al Academiei de Stiinte a Moldovei, 2008, Nr. 1, p.24 - 30.
23. Ilies I., Borodatii I. The Moldavian Seismic Network: Current State in 2007, (poster). ORFEUS-NERIES Observatory coordination workshop, Sinaia, Romania, May 7-11, 2007.
24. OLONTIR N., ILIES I., Capitolul II, Hazardurile geologice si geomorfologice, p.20-61, Vol.3: HAZARDURILE NATURALE din colectia in 4 vol.MEDIUL GEOGRAFIC AL REPUBLICII MOLDOVA, Intreprinderea Editorial-Poligrafica Stiinta, 2008.
25. PANZA, G.F., KOUTEVA, M., VACCARI, F., PERESAN A., CIOFLAN, C.O., ROMANELLI, F., PASKALEVA, I., RADULIAN, M., GRIBOVSKY, K., HERAK,

- M., ZAICHENCO, A., MARMUREANU, G., VARGA, P. , ZIVCIC, M. Recent Achievements of the Neo-Deterministic Seismic Hazard Assessment in the CEI Region, Proc. of the 2008 seismic Engineering Conference, Reggio Calabria, Italy 8-11.07.2008, Editors: A. Santini and N. Moraci, American Institute of Physics, Melville, New York, AIP Conf. Proc., Vol. 1020, p. 402-413.
26. R. MOHNIUC, A. ZAICENCO, C. KUENDING, T. KURMANN. MEMS-based Data Logger for Seismic Arrays and Structural Health Monitoring. NATO Science for Peace and Security Series, C: Environmental Security, Springer, 2008, p.309-318.
27. R.Burtiev, VI. Cherniy. Seismic Hazard Assessment for the Territory Influenced by Earthquakes from Romania and Bulgaria. Proceedings of the International Symposium "Thirty Years from the Romania Earthquake of March 4, 1977", Bucharest, Romania, 2007.
28. Sandi H., F. Apticaev, V. Alcaz, I. Borcia, A. Drumea, O. Erteleva, A. Roman A NATO Project on deriving Improved (Instrumental) Criteria for Seismic Intensity Assessment Proceedings of the First European Conference on Earthquake Engineering and Seismology, Geneva, Switzerland
29. SANDI, H., APTICAEV, F., BORCIA, I., ERTELEVA, O., **ALCAZ, V.** Quantification of Seismic Actions on Structures. *AGIR Publishing House*, Bucharest, 2010, 211p. ISBN 978-973-720-319-9
30. Sandu I. Composite fault plane solution for Republic of Moldova Proceedings of the First European Conference on Earthquake Engineering and Seismology, Geneva, Switzerland
31. SANDU I. Cronologia evoluției conceptuale asupra seismelor. Buletinul Institutului de Geologie și Seismologie ASM, N 1. 2012, pp.47-62. ISSN 1857-0046.
32. Sandu I. Relocation of Hypocenters and Composite Fault Plane Solutions for Earthquakes in Republic of Moldova Individual Studies by Participants at the International Institute of Seismology and Earthquake Engineering, 2006, vol. 41, ISSN 0074-6606, Tsucuba, Japan
33. Sandu I., Hurukawa N. Relocation of hypocenters and focal mechanism for earthquakes in Republic of Moldova Buletinul Institutului de Geofizica și Geologie al Academiei de Științe a Moldovei, 2006, N1
34. SANDU I., LA MURA C., PANZA G.F., ALCAZ V. Parametric test for the impact of May 30, 1990 Vrancea earthquake on Cahul area. Buletinul Institutului de Geologie și Seismologie ASM, N 1. 2012, pp. 33-46. ISSN 1857-0046.
35. Sandu, A. Zaicenco, The Focal Mechanism Solutions Catalogue for SE-Carpathian Region. Proceedings of the International Symposium "Thirty Years from the Romania Earthquake of March 4, 1977", Bucharest, Romania, 2007.
36. SANDU, I., ZAICHENCO, A.. Azimutul, distanța epicentrală și eroarea acestor parametri în contextul mecanismului focal. *Buletinul Institutului de Geologie și Seismologie al AȘM*, Nr. 1., Chișinău, 2010, p. 89-93. ISSN 1857-0046.

37. TELESCA L., ALCAZ V., SANDU I. Analysis the 1978–2008 crustal and sub-crustal earthquake catalog of Vrancea region. *Journal Natural Hazards and Earth System Sciences*, 2012, pp.1321-1325. ISSN: 1561-8633, (IF: 1,983)
38. TELESCA Luciano, ALCAZ Vasile, BURTIEV Raşid, SANDU Ilie. The stress field of Vrancea region from fault plane solution (FPS). *Natural Hazards and Earth System Sciences*, 2011, pp.2817-2820. ISSN: 1561-8633, (IF: 1,792)
39. TELESCA Luciano, ALCAZ Vasile, BURTIEV Raşid, SANDU Ilie. Time-clustering analysis of the 1978-2008 sub-crustal seismicity of Vrancea region. *Journal Natural Hazards and Earth System Sciences*, 2011, pp.2335-2340. ISSN: 1561-8633, (IF: 1,792)
40. V.Alkaz, A.Zaicenco, E.Isicko. Earthquake loss modelling for seismic risk Management. Conferinta Internationala NATO "Risk Assessment as a Basis for Elaboration of Recommendations for Forecast and Prevention of Catastrophes", Chisinau, 2007.
41. V.Alkaz, A.Zaicenco, E.Isicko. Site Effect Evaluation in Kishinev City, Republic of Moldova. Proceedings of the International Symposium "Thirty Years from the Romania Earthquake of March 4, 1977", Bucharest, Romania, 2007.
42. V.Alkaz, A.Zaicenco, E.Isicko. Site Response Assessment via a Multidisciplinary Approach: Kishinev City, Republic of Moldova. Proceedings of the International Symposium on Strong Vrancea Earthquakes and Risk Mitigation, Bucharest, Romania, 2007.
43. V.Alkaz, E.Isicko, A.Zaicenco. Numerical and Experimental Site Effects Study: Kishinev city, Republic of Moldova. Proceedings of the 3rd International Conference on Science and Technologz for Safe Develop-ment of Lifeline SistemNatural Risks. Bucha-rest, Romania, 2007.
44. Vasile Alcaz, Ioan Sorin Borgia, Anatol Drumea, Horea Sandi, Dorel Zugravescu. Cooperarea stiintifica Romania-Republica Moldova in domeniul ttiintelor tehnice, pe teme de protectie antiseismica. Materialele conferintei "10 ani de la constituirea Academiei de Stiinte Tehnice din Romania". Bucuresti. 2007.
45. Zaicenco A. & V.Alcaz, (2001). Seismic Test On a 16-Storez Cast in Place R/C Building, and Stochastic Simulation Results. *The Structural Design of Tall Buildings*, 10, pp.69-77.
46. Zaicenco A. & V.Alkaz A wavelet-based analytical model accounting for near-field effects of Vrancea earthquakes Proceedings of the First European Conference on Earthquake Engineering and Seismology, Geneva, Switzerland
47. Zaicenco A. Influence of local soil condition on spectral content of seismic ground motion. *Buletinul Institutului de Geofizica si Geologie al Academiei de Stiinte a Moldovei*, N1, 2007.
48. ZAICENCO A., N.P. GAVIN, B.W. DISKINSON. A Parametric Model for the August 30, 1986 Vrancea Earthquake. Harmonization of Seismic Hazard in Vrancea Zone. NATO Science for Peace and Security Series, C: Environmental Security, Springer, 2008, p.63-84.

49. Zaicenco A., Performance and Reliability of Semi-active Equipment isolation. Journal of Sound and Vibration, v. 306, 2007, Elsevier, USA
50. Zaicenco A., Performance and Reliability of Semi-active Equipment isolation. Journal of Sound and Vibration, v. 306, 2007, Elsevier, USA.
51. Zaicenco A., V. Alkaz I. Sandu. 2D FEM simulation of earthquake ground motion in sedimentary basin. Proceedings of the International Symposium on Seismic Risk Reduction, Editura "Orizonturi Universitare", Timisoara, Romania, 2007.
52. Zaicenco A., V. ALKAZ. Numerical Solution of an Elastic Wave Equation Using the Spectral Methods. Harmonization of Seismic Hazard in Vrancea Zone. NATO Science for Peace and Security Series, C: Environmental Security, Springer, 2008, p.319-327.
53. Zaicenco A., V.ALCAZ. Analysis of SSI from Instrumented Building Response. The Structural Design of Tall and Special Buildings. V. 17, Issue 2, p. 387-399.
54. Zaicenco A., V.Alcaz. Soil-Structure Interaction Effects on an Instrumented Building. Bulletin of Earthquake Engineering. V.5, No 4, Springer, 2007.
55. Алексеев И.В., Симонова Н.А. Об определениях магнитуд землетрясений Карпатской зоны по наблюдениям на сейсмических станциях Молдовы. *Buletinul Institutului de geologie si seismologie al ASM*, N1. Chisinau, 2007.
56. АЛКАЗ В. Г. Актуальные проблемы оценки сейсмической опасности территории Республики Молдова. Сейсмичность Северной Евразии, ГС РАН, Обнинск, 2008, с. 15-18.
57. АЛКАЗ В. Г., ИЛИЕШ И.И. Мониторинг вариации динамических параметров зданий и сооружений г. Кишинева. Будівельні конструкції. Випуск 69, Київ, НДІБК, 2008. стр. 646-652.
58. АЛКАЗ, В., ИСИЧКО, Е., ГИНСАРЬ, В. Методические аспекты и результаты оценки сейсмического риска на территории г. Кишинева. *Buletinul Institutului de Geologie și Seismologie al AȘM*. Nr. 1., Chișinău, 2010, p. 16-24. ISSN 1857-0046.
59. БУРТИЕВ Р. З. О статистической связи сейсмической активности Балканских сейсмических зон. *Buletinul Institutului de Geologie și Seismologie al AȘM*, Nr. 1., Chișinău, 2010, p. 5-15. ISSN 1857-0046.
60. Буртиев Р.З. О применении статистики экстремальных значений к оценке M_{max} . *Buletinul Institutului de Geofizica si Geologie al ASM*, N2, 2007.
61. Гинсарь В.Н. Анализ информативности возможных сейсмологических предвестников землетрясений для зоны Вранча. (Тезисы). Conferinta Fizicienilor din Moldova (CFM-2007).
62. Гинсарь В.Н. Анализ информативности ряда среднесрочных предвестников сильных землетрясений зоны Вранча. *Buletinul Institutului de Geologie si Seismologie al Academiei de Stiinte a Moldovei*, 2007, N2.
63. Гинсарь В.Н. Анализ пред- и постсейсмических стадий сейсмического процесса при сильных землетрясениях зоны Вранча. *Buletinul Institutului de Geofizica si Geologie al Academiei de Stiinte a Moldovei*, 2006, N2 (in presa)

64. Гинсарь В.Н. Пространственно-временные вариации суммарного сейсмического момента в зоне Вранча. *Buletinul Institutului de Geofizica si Geologie al Academiei de Stiinte a Moldovei*, 2006, N2 (in presa)
65. ГИНСАРЬ В.Н. Статистическая оценка максимальной возможной магнитуды подкорковых землетрясений зоны Вранча. *Buletinul Institutului de Geologie si Seismologie al Academiei de Stiinte a Moldovei*, 2008, N2.
66. ДРУМЯ А.В. , СТЕПАНЕНКО Н.Я., ИЛИЕШ И.И., АЛЕКСЕЕВ И.В., СИМОНОВА Н.А. Сейсмический режим области Вранча за период 1991-2001гг. Сейсмичность Северной Евразии, ГС РАН, Обнинск, 2008, с. 73-77.
67. Друмя А.В., Степаненко Н.Я. К вопросу о сейсмичности дельты реки Дунай *Buletinul Institutului de Geofizica si Geologie al Academiei de Stiinte a Moldovei*, 2006, N1
68. Измайлова Д., Богдевич О. Оценка неопределенности при анализе природных объектов методом атомной абсорбции *Buletin Institutului de Geologie si Seismologie*, Nr 1, 2006, pp. 127-135
69. ИЛИЕШ И.И. Сейсмическая сеть Республики Молдова: состояние и перспективы. Сейсмичность Северной Евразии. Материалы Международной конференции Обнинск,: ГС РАН, 2008, стр.87-92.
70. ИЛИЕШ, И.И., СТЕПАНЕНКО, Н.Я., СИМОНОВА, Н.А., АЛЕКСЕЕВ,И. Сейсмичность Карпат по наблюдениям на сейсмических станциях на территории Молдовы. *Buletinul Institutului de Geologie și Seismologie al AȘM*, Nr. 1., Chișinău, 2010, p. 32-40. ISSN 1857-0046.
71. Исичко Е.С. Методика расчета акселерограмм для конкретной строительной площадки. *Buletinul Institutului de Geofizica si Geologie al Academiei de Stiinte a Moldovei*, N1, 2007.
72. Исичко Е.С., Богдевич О.П., Гинсарь В.Н. Моделирование геометрических и упругих свойств среды на стадии сейсмического микрорайонирования г. Кишинева *Buletinul Institutului de Geofizica si Geologie al Academiei de Stiinte a Moldovei*, 2006, N1
73. Павлов П.П. Расчетный анализ влияния рельефа территории г. Кишинева на интенсивность сейсмических колебаний. *Buletinul Institutului de Geofizica si Geologie al Academiei de Stiinte a Moldovei*, 2006, N1
74. Роман А.А., Алексеев И.В., Cherniy V.I. Информационное содержание макросейсмического поля и его количественная характеристика *Buletinul Institutului de Geofizica si Geologie al Academiei de Stiinte a Moldovei*, 2006, N1
75. Скляр А.М., Степаненко Н.Я., Симонова Н.А. и др. Макросейсмический эффект Карпатского землетрясения 27 октября 2004 г. на территории Украины и Республики Молдова *Сейсмологический бюллетень Украины за 2004 год*. Севастополь, НАНУ, 2006
76. СКЛЯР, А.М., КНЯЗЕВА, В.С., СТЕПАНЕНКО, Н.Я., СИМОНОВА, Н.А., АЛЕКСЕЕВ, И.В., СТАСЮК, А.Ф., ЧУБА, М.В. Ощутимое на Украине и в

Молдове землетрясение 27 октября 2004 года с $K_p=15.4$, $M_w=5.8$, $I_0=6$ (Карпатский регион). *Землетрясения Северной Евразии 2004*. Обнинск: ГС РАН. 2010, с. 51-57. ISSN1818-6254.

77. СКЛЯР, А.М., КНЯЗЕВА, В.С., СТЕПАНЕНКО, Н.Я., СИМОНОВА, Н.А., АЛЕКСЕЕВ, И.В., СТАСЮК, А.Ф., ЧУБА, М.В. Распределение макросейсмического эффекта от карпатского землетрясения 27 октября 2004 года на территории Украины и Молдовы. *Землетрясения Северной Евразии 2004*. Обнинск: ГС РАН. 2010, с. 52-63. ISSN 1818-6254.
78. Степаненко Н.Я., Друмя А.В., Симонова Н.А. Сильнейшие землетрясения Карпатского региона в XVIII-XX веке Buletinul Institutului de Geofizica si Geologie al Academiei de Stiinte a Moldovei, 2006, N1
79. СТЕПАНЕНКО Н.Я., ПРОНИШИН Р.С., МИХАЙЛОВА Р.С. К вопросу об уточнении параметров землетрясений Карпат в каталоге 2002. *Землетрясения Северной Евразии в 2002 году*. Обнинск, ГС РАН, 2008, Раздел VIII, СД, 3 стр.
80. Степаненко Н.Я., Симонова Н.А., Алексеев И.В. Макросейсмические данные землетрясений Карпатского региона в 2004 году. *Сейсмологический бюллетень Украины за 2004 год*. Севастополь, НАНУ, 2006
81. Степаненко Н.Я., Симонова Н.А., Алексеев И.В. Макросейсмика и механизм землетрясений Карпат в 2005 году. *Сейсмологический бюллетень Украины за 2005 год*. Севастополь, НАНУ, 2007.
82. СТЕПАНЕНКО, Н.Я., СИМОНОВА, Н.А., АЛЕКСЕЕВ, И.В. Дунайское землетрясение 3 октября 2004 года с $K_p=13.0$, $M_w=4.8$, $I_0=5-6$ (Карпатский регион). *Землетрясения Северной Евразии 2004*. Обнинск: ГС РАН. 2010, с. 370-374. ISSN 1818-6254.
83. СТЕПАНЕНКО, Н.Я., СИМОНОВА, Н.А., АЛЕКСЕЕВ, И.В. Ощутимое в Молдове землетрясение 27 сентября 2004 года с $K_p=13.4$, $M_w=4.8$, $I_0=4-5$ (Карпатский регион). *Землетрясения Северной Евразии 2004*. Обнинск: ГС РАН. 2010, с. 43-50. ISSN1818-6254.
84. Чуба М.В., Степаненко Н.Я., Симонова Н.А. и др. Каталог и подробные данные о землетрясениях Карпатского региона за 2004 год. *Сейсмологический бюллетень Украины за 2004 год*. Севастополь, НАНУ, 2006
85. Чуба М.В., Степаненко Н.Я., Симонова Н.А. и др. Каталог и подробные данные о землетрясениях Карпатского региона за 2005 год. *Сейсмологический бюллетень Украины за 2005 год*. Севастополь, НАНУ, 2007.

5 CONCLUDING REMARKS

Summarizing the main conclusions based on the extended elaborated work we could deduce that a first objective of any seismic hazard analysis, either deterministic or probabilistic is to determine vibratory ground motion in various forms for a series of levels of probabilities of exceedance. Probabilistic (PSHA) or Deterministic (DSHA) seismic hazard assessment is used for making important risk mitigation decisions regarding building design, insurance rates, land use planning, and public policy issues that need to balance safety and economics. It is important that state-of-the-art science be incorporated in seismic hazard analysis that are used for public policy and safety. Generally seismic hazard products should be updated regularly as new information on earthquake recurrence and ground shaking becomes available from the scientific community. Research on such important hazard topics as recurrence time and rupture histories of prehistoric or historical earthquakes, magnitude-frequency distributions for individual faults, and the effects of shallow and deep site conditions on ground shaking will improve these assessments in the future.

An analytical description of the basic issues of seismic hazard assessment is presented in this work combining probabilistic and deterministic approaches. The Regional Seismic hazard is assessed combining seismic sources, active seismic faults and regional seismic zones in all eligible region in the various participating countries of the SCINETNATHAZ project. The contributing seismic sources and faults are described and presented in each National report which are included in the general presentation. Lastly, the surface faulting hazard needs to be taken into account, as was illustrated by the earthquakes. Simultaneously the Ground Motion Predictive Equations (GMPE) are given and their contribution in the seismic hazard assessment of the area is examined. GMPE's are then called on to calculate ground motion, taking into account the influence of superficial geological layers. Various recurrence models are examined by the partners of this project intending to improve the results of the seismic hazard assessment. A series of seismic hazard maps are depicted in the report covering different strong motion parameters (MMI, PGA etc) in terms of the various return periods (annual probability of exceedance). In countries with high seismic activity (Turkey and Greece) or moderate one (Bulgaria and Romania) advanced methods and seismic models are utilized deriving detailed and accurate results.

In Greece and Turkey, Seismic Hazard Assessment was carried out in a local scale, focusing the calculations in specific sites where they are extremely importance within

the framework of the project, taking into account all the available seismic sources and active faults which can affect the areas studied. Thus various seismic scenarios are proposed for the Greek region, Serres and Komotini sites eligible in the project, and seismic hazard results and design ground motion parameters are probabilistically and deterministically recommended. The obtained results are differentiated from the values come up from National Seismic Code and some special attention should be paid. On the other side, for Marmaras and Samsun areas in Turkey, local seismic hazard is probabilistically assessed, presented by hazard maps for various return periods. A very analytical work is accomplished in Bulgaria and Romania areas, adopting in their calculations the seismotectonic regime of the intermediate – depth seismic zones in Romania affecting a great part of the Bulgaria territory as well. The remainder National reports (Moldova and Ukraine) present the up-to date progress in seismology and seismic hazard giving the available data and results for the aforementioned countries.

Future needs for this part of the program.

1. Physical understanding of seismicity and geological setting of the common studied area within the framework of this project.
2. Adoption of updated earthquake –occurrence models and time dependent ones.
3. Strong motion seismological data in a common open-access database for any scientist, engineer, or decision maker for the whole eligible area as a continuation of the first attempt, achieved in this project.
4. PSHA and DSHA methodologies suitable adaptive for the whole region of study in order to develop site-specific applications and assessments.